STRENGTHENING OF HEAT DAMAGED REINFORCED CONCRETE ELEMENTS

Ph.D. THESIS

by

DANIE ROY A.B

DEPARTMENT OF CIVIL ENGINEERING
INDIAN INSTITUTE OF TECHNOLOGY ROORKEE
ROORKEE – 247 667 (INDIA)
DECEMBER, 2014

STRENGTHENING OF HEAT DAMAGED REINFORCED CONCRETE ELEMENTS

A THESIS

Submitted in partial fulfilment of the requirements for the award of the degree

of

DOCTOR OF PHILOSOPHY

in

CIVIL ENGINEERING

by

DANIE ROY A.B

DEPARTMENT OF CIVIL ENGINEERING
INDIAN INSTITUTE OF TECHNOLOGY ROORKEE
ROORKEE – 247 667 (INDIA)
DECEMBER, 2014

INDIAN INSTITUTE OF TECHNOLOGY ROORKEE
ROORKEE

<u>CANDIDATE'S DECLARATION</u>

I hereby certify that the work which is being presented in the thesis entitled "**STRENGTHENING OF HEAT DAMAGED REINFORCED CONCRETE ELEMENTS"** in partial fulfilment of the requirements for the award of the degree of Doctor of Philosophy and submitted in the Department of Civil Engineering, Indian Institute of Technology Roorkee is an authentic record of my own work carried out during a period from July, 2010 to December, 2014 under the supervision of Dr. Umesh Kumar Sharma, Associate Professor and Dr. Pradeep Bhargava, Professor, Department of Civil Engineering, Indian Institute of Technology Roorkee.

The matter presented in this thesis has not been submitted by me for the award of any other degree of this or any other Institute.

(DANIE ROY A.B)

This is to certify that the above statement made by the candidate is correct to the best of our knowledge.

(PRADEEP BHARGAVA)   (UMESH KUMAR SHARMA)
Supervisor   Supervisor

Date: , 2014

ABSTRACT

In the light of extreme events of natural disasters (earthquakes or hurricanes) and accidents (fire or explosion), repairing and strengthening of existing concrete structures has become more common during the last decade due to the increasing knowledge and confidence in the use of advanced composite repairing materials. The past experience from real fires shows that it is exceptional for a concrete building to collapse as a result of fire and most fire-damaged concrete structures can be repaired economically rather than completely replacing or demolishing them. In this connection an experimental study was carried out to evaluate the performance of different repair schemes, which included the use of fiber reinforced polymer (FRP), ferrocement (FC), high strength fiber reinforced concrete (HSFRC) and steel plate (SP) jackets, in restoring the heat damaged structural concrete elements.

A critical review of the literature shows that while tremendous amount of data is available on strengthening of reinforced concrete elements under normal ambient temperature condition, only limited studies have been carried out in the past on strengthening and restoring of heat damaged concrete elements. Previous researchers studied heat damaged reinforced concrete columns with one layer of wrapping of FRP and it has been reported that it does not provide much enhancement in the stiffness properties of strengthened reinforced concrete elements. Research on strengthening of heat damaged reinforced concrete elements with varying FRP parameters has not been attempted. Effectiveness of other available techniques of strengthening in restoring heat damaged concrete elements has not been investigated to best of knowledge. In the past strengthening of heat damaged RC elements has been studied by exposing the concrete elements to target temperatures of 500°C and 600°C only. However the influence of other temperatures of exposure has not been studied with respect to the behavior of strengthened heat damaged reinforced concrete elements. Earlier researchers have studied the effect of strengthening heat damaged RC elements, which were cooled under normal cooling conditions, but the rate of cooling in different cooling regimes like water sprinkling or water quenching was not studied. Influence of cyclic temperature conditions becomes important in some situations like cooling tower, cooling container,

nuclear container vessels. But strengthening of such cyclic heat damaged elements has not been studied in the past.

In view of the preceding discussion, the primary objective of the study undertaken in this research was to examine experimentally the effectiveness of various strengthening techniques in restoring structural performance of heat damaged RC elements. In this context, reinforced concrete columns and beams were constructed and then tested after grouping them into three main groups: un-heated, heat damaged and heat damaged & strengthened. The heat-damaged circular short columns, square short columns and T- Beams were initially damaged by heating to various temperatures and then were strengthened with different strengthening schemes. The variables of the study were type of strengthening scheme, heating temperature, number of heating cycles and type of cooling.

In the first phase of the research program, a total of sixty-three reinforced concrete short columns were constructed and then tested after grouping them into three main groups: un-heated, heat damaged and heat damaged strengthened. All the specimens were of cylindrical shape (150 mm x 450 mm). The specimens were initially damaged by heating to various temperatures ranging from 300^0C to 900^0C. After exposing to target temperature for certain duration the specimens were cooled. The heating rate was set at 10°C /min., which was considered to be realistic for structures exposed to fire. Two different cooling regimes were chosen namely natural cooling and sudden water quenching. Some specimens were also subjected to cycle of heating and cooling. The heat damaged columns were subsequently repaired using different schemes namely FRP wraps, high strength fiber reinforced concrete jacketing and ferrocement jackets. The effects of various variables of the study were investigated with respect to stiffness, ductility, ultimate strain and the ultimate strength. The columns were tested under axial compressive loading. It was observed that the reduction in residual stiffness of heat damaged circular columns was greater than the reduction in ultimate load. The strength of heated specimens repaired with HSFRC jacket was higher than the heat damaged unstrengthen specimens, but remained less than the strength of control specimens in all cases. In case of FC jacketed specimens also, the axial compressive strength was higher than that of unstrengthen heat damaged specimens, but remained less than the control specimens except for 300°C heat damaged specimens. However, the strength of GFRP jacketed specimens was considerably higher than both the heat

damaged unstrengthen specimen and the unheated control specimens. The stiffness of HSFRC and FC jacketed specimens was higher than both the control and heat damaged specimens exposed up to 600°C. However in the specimens heated to 900°C, though it was found to be higher than the heat damaged specimens but was less than that of control specimens. In case of GFRP, no significant improvement in stiffness of heat damaged specimens was noticed except in the specimen heated to 300°C. It was also observed that the specimens strengthened with GFRP, dissipated more energy compared to HSFRC and FC jacketed specimens.

In the second phase of the research program a total of fifty-one reinforced concrete square columns were constructed and then tested after grouping them into three different groups: un-heated, heat damaged and heat damaged & strengthened. The specimens were initially heated to various temperatures of 300°C, 600°C & 900°C. After exposing to target temperatures for certain duration the specimens were cooled. The heat damaged columns were subsequently repaired with fiber reinforced polymer wraps, high strength fiber reinforced concrete jackets, ferrocement jacketing and steel plate jackets (SP). The effects of various variables of the study were investigated with respect to stiffness, ductility, ultimate strain and the ultimate strength. The square short columns were tested under axial compressive loading. The results show that the reduction in residual stiffness of heat damaged specimens was greater than the reduction in ultimate load. The results indicate that the strength values of GFRP jacketed specimens were higher than both the heat damaged unstrengthen specimens as well as the control unheated specimens at all the considered temperatures. However the specimens heated at 900°C temperature and strengthened with GFRP was not able to regain its original strength of the control specimens. The strength of heat damaged & HSFRC jacketed specimens was higher than 300°C, 600°C and 900°C heat damaged unstrengthen specimen up to 8%, 12% and 150% respectively, but remained less than the corresponding control unheated specimen at all the considered temperatures. Similarly, in case of FC jacketed specimens though the axial compressive strength was higher than the heat damaged unstrengthen specimen, but it remained less than that of the corresponding control specimens, except in 300°C heat damaged specimen. The restoration of stiffness of the heated damaged specimen depends upon the confining action of HSFRC, FC, GFRP and SP jackets. The confining action of GFRP jackets takes effect when the heated concrete specimen approaches its ultimate unconfined

compressive strength. The GFRP and SP do not contribute in the initial structural response because it is not active in the elastic range of the heated specimens when loaded axially. However, on the other hand, the HSFRC and FC jackets increased the stiffness of the heat damaged specimens due to the increase in the cross-sectional area of the specimens improving the dimensional stability of square columns.

In the third phase of the research program a total of twenty-seven reinforced concrete T-Beams were constructed and then tested after grouping them into three main groups: un-heated, heat damaged and heat damaged strengthened. The beams were heated to temperatures of 600°C & 900°C. The beams were placed in the furnace upside down so that heat won't affect the flange directly, which simulates the real condition of the structure during fire. The rate of heating was set at 10°C/min, which has been shown to be reasonable for structures exposed to fire. Each target temperature was maintained for three hours to achieve a thermal steady state condition. After heating it was observed that some hairline cracks developed at 600°C. The number of cracks became relatively pronounced at 900°C; therefore the section of beam had to be restored with micro concrete to make the surface a feasible one for strengthening. Subsequently the heat damaged beams were strengthened using the Glass Fibre Reinforced Polymer (GFRP), or High Strength Fibre Reinforced Concrete (HSFRC) and or Ferrocement (FC). The beams were tested in loading frame under 4 point loading condition using a 200 Ton capacity hand operated jacks connected to a data acquisition system through load cells. The beams were tested under monotonically increasing load. The deflection of the beams was noted using linear variable differential transducers (LVDT), placed at five locations at the bottom of beams and strain gauges were mounted on bottom of web and side web on GFRP jackets. The recorded data from the LVDTs, strain gauges and load cell were fed into a data acquisition system and stored on a computer. The load-deflection curves for the beams were examined to evaluate the effect of strengthening. The beams exposed to different temperatures caused a reduction in ultimate load carrying capacity by about 14 % to 61% when compared with undamaged control beams. The secant stiffness and energy dissipation were reduced by 34% to 56% and 10% to 41% respectively. The strengthened beams showed significant improvement in flexural strength over the heat damaged unstrengthen beams and in some cases the strength enhancement was even more than the undamaged control beams. The study proved that GFRP is the best option for the strengthening of heat damaged beams. On the contrary FC and HSFRC jacketing

were mainly effective in improving ductility property but strength increase was minimal. The load corresponding to concrete cracking got increased considerably when the damaged beams were strengthened with different strengthening techniques.

The fourth phase of research program includes an experimental study to investigate the bond behavior between GFRP laminate and heated concrete. The specimens were initially heated to various temperatures of 200°C, 400°C, 600°C & 800°C. After exposing to target temperatures for certain duration the specimens were cooled. The heat damaged specimens were subsequently bonded with fiber reinforced polymer sheets with various bond lengths. The test variables were different bond length; bond width and different elevated temperatures. The specimens were tested in single shear in a universal testing machine by dragging the GFRP sheet upward from the specimen and the applied load was measured with the help of a pressure sensor. The load was applied in a monotonically increasing manner. The bond strength increased with increasing bond length and reduced noticeably as temperature exceeded 400°C. The thickness of the delaminated concrete layer with GFRP composite was less for the specimens subjected to temperatures less than 400°C. However thickness of delamination was more in 600°C and 800°C heat damaged specimens. The value of the ultimate bond stress was influenced by the bond length and got increased with the decrease in bonded length. The failure of the specimens was found to be sudden followed by debonding of GFRP strip from the concrete. For specimen with 100 and 150mm bond length the increase in GFRP strain was gradual until 90 percent of failure load, but with larger bond length (200mm) the increase of GFRP strain was found to be gradual until 70 percent of the failure load. The propagation of debonding was clearly reflected by the strain distribution. A model has been proposed to estimate the bond strength between GFRP laminate and heated concrete.

ACKNOWLEDGEMENT

(DANIE ROY A.B)

CONTENTS

LIST OF FIGURES

LIST OF TABLES

NOTATIONS

A_c	cross sectional area of concrete in the column specimen section
A_{cc}	cross sectional area of core concrete in the column specimen section
A_g	gross area of column cross section
A_{st}	gross sectional area of longitudinal steel
b_c	the width of the concrete member
b_p	the width of the FRP plate or sheet
c	core diameter centre to centre of parameter tie
E	Young's modulus of steel bars at ambient temperature
E_c	modulus of elasticity of concrete
E_p	modulus of elasticity of FRP sheet
f_c	any stress value on the stress strain curve
f'_c	standard cylinder compressive strength of plain concrete on the day of testing
f'_{cc}	peak stress of confined concrete
f_{co}	compressive strength of unconfined concrete
fp	tensile strength of GFRP
f_u	ultimate tensile strength of reinforcing bar
f_y	yield strength of reinforcing bar
fc'	the cylinder compressive strength of the concrete
fcT'	Compressive strength of the concrete at elevated Temperature
L	bonded length
L_e	effective bonding length
l_f	length of the fibres
P_u	maximum transferable load (bond capacity/bond strength)
r	correlation coefficient
s	centre to centre spacing of confining ties
t_p	thickness of FRP plate or sheet
T	exposed temperature (ºC)
w	moisture content of concrete
w_i	initial mass of the test specimen (cube) before drying

w_t	final mass of the test specimen (cube) after drying at 105ºC
Δm^T	loss of mass at a given temperature T
μ_Δ	deflection ductility
μ_E	energy ductility
βp	bond width factor
βL	bond length factor
ε'	axial strain corresponding to P_{max}
ε'_c	axial strain corresponding to the stress, f'_c, of standard plain concrete cylinder
ε_{c80c}	axial strain at which the load drops to 80% of the peak confined concrete load
ε_{cc}	axial strain at peak confined load P_{cc}
εp	ultimate strain in GFRP
σp	stress in GFRP
α	regression coefficient

CHAPTER - 1

INTRODUCTION

1.1 GENERAL

Rehabilitation and upgrading of existing civil engineering infrastructure has recently become a major issue that often requires immediate attention of asset managers. The primary reasons for strengthening of structures include upgrading of capacity to withstand under-estimated loads, increase the load carrying capacity for higher permit loads, eliminating premature failure due to inadequate detailing, restoration of lost load carrying capacity due to heat or fire, corrosion or other types of degradation caused by aging, etc. Heating or fire accidents in concrete structures often demand repair and rehabilitation. The concrete structures including turbo jet runways, launching pads, nuclear reactor vessels, clinker silos of cement plants, metallurgical and chemical industrial structures, glass making industrial structures, storage tanks for hot crude oils and hot water, coal gasification and liquefaction vessels, reinforced concrete chimneys and high rise buildings during an accidental fire are often subjected to elevated temperatures. In terms of structural performance after thermal damage, concrete structures normally perform very well due mainly to the concrete's low thermal conductivity which consequences in the increase in temperature at a slow rate during a fire. It is very infrequent for concrete structures to collapse during a fire and post-fire repair of concrete structures is typically an economical and viable option compared to demolition and reconstruction. However the verdict to renovate or demolish a structure must be established on the economic thoughts such as direct costs and time.

In fire damaged concrete structures, the knowledge of the residual properties of materials is required as a basis for designing suitable repair and retrofitting schemes. For the evaluation of residual strength in existing fire damaged concrete structures, there are number of in-situ and laboratory-based techniques available to diagnose the site condition of concrete. The in-situ techniques include visual inspection; non-destructive testing, testing on site and taking samples of concrete and reinforcement for testing in the laboratory. Therefore, it is necessary to obtain a direct relation between the residual compressive strength of fire damaged concrete and the different types of non-destructive testing methods to get reliable results of the residual compressive strength of fire

damaged reinforced concrete. In this investigation the ultrasonic pulse velocity was used to get an insight into the residual strength of the heat damaged concrete. A relationship between the ultrasonic pulse velocity and residual compressive strength of heat damaged concrete is investigated to predict the residual compressive strength of fire damaged concrete in existing reinforced concrete columns, beams and single shear test specimens.

It can be seen while enormous research has been carried out and huge data generated on the strengthening of reinforced concrete elements under normal ambient temperature conditions. However the literature database is lacking in terms of the research on the strengthening and restoring of heat damaged concrete elements. Studies have been carried out where in heat damaged reinforced concrete columns were strengthened by wrapping of one layer of FRP and the results suggest that it does not provide much enhancement in the stiffness properties of strengthened reinforced concrete elements. No research is available in literature where in the effect of varying FRP parameter has been studied. Another important factor i.e. the effect and effectiveness of the techniques of strengthening in restoring heat damaged concrete elements has not been investigated as of now. Some research has been carried out on the strengthening of the elements exposed to 500°C and 600°C only rendering the data base incomplete as the effect of the other lower temperatures and higher temperatures is missing in the literature. Although the studies have been carried on the specimens cooled naturally no such research is available where in the effect of the rate of cooling in different cooling regimes like water sprinkling or water quenching has been studied. Another important condition of cyclic heating and cooling has also been neglected in previous research. Influence of cyclic temperature conditions becomes important in some situations like cooling tower, cooling container, nuclear container vessels. However the research has not been carried out to study the strengthening of cyclic heat damaged elements.

In view of the preceding discussion, the primary objective of the study undertaken in this research was to examine experimentally the effectiveness of various strengthening techniques in restoring structural performance of heat damaged RC elements. In this context, reinforced concrete columns and beams were constructed and then tested after grouping them into three main groups: un-heated, heat damaged and heat damaged & strengthened. The heat-damaged circular short columns, square short columns and T- Beams were initially damaged by heating to various temperatures and

then were strengthened with different strengthening schemes. The variables of the study were type of strengthening scheme, heating temperature, number of heating cycles and type of cooling. A brief review of the existing literature under various relevant heads is presented in the following sections.

1.2 EFFECTS OF ELEVATED TEMPERATURES ON CONCRETE STRUCTURES

Temperatures more than 900°C remain common in fires within structures (TR68). Concrete and fire have a multifarious interaction, due to the structure of concrete and the acute thermal circumstances that exist in a fire. Concrete structures normally perform very well due primarily to the concrete's low thermal conductivity which consequences in increase in temperature at a relatively slow rate during a fire. Knowledge from real fires shows that it is infrequent for a concrete building to collapse due to fire and most fire-damaged concrete structures can be restored effectively. Lea and straddling (Lea 1920, Lea and Straddling 1922) were the first to initiate investigations into the influence of high temperature on the behaviour of concrete in RC structures. The drop in load-bearing capacity of the concrete structural members in fire is governed by numerous causes (Malhotra 1956, Abrams 1977, Hertz 2005, Fletcher et al. 2007, Lee 2008). They are type of aggregate, duration and the severity of fire exposure, conditions of testing, conditions of loading during heating of the specimens, amount of moisture content present in the concrete specimens at the time of heating, shape and dimensions of the structural member and concrete cover.

The initial studies mainly paid attention on the mechanical properties of concrete at elevated temperatures. It was reported that the mechanical properties of concrete such as compressive strength, tensile strength, Poisson's ratio and modulus of elasticity degrade with the increase of temperature. These changes are governed by the peak temperature, the rate of heating and cooling, the fire duration, the type of concrete and type of testing (Malhotra 1956). Three types of test settings; stressed, un-stressed, and un-stressed residual strength tests, have been used to investigate the performance of concrete subjected to elevated temperatures (Abrams 1971, Sullivan et al. 1992, Phan et al. 1996, Phan et al. 1998, Usmani 2001, Phan et al. 2002, Usmani 2008, Kim et al. 2009, Zaidi et al.2011, Kishor et al. 2011, Kumar et al. 2013). A schematic view of these three test methods is shown in Fig. 1.1 which clarifies the state of mechanical pre-loading and thermal loading during the testing process of the concrete specimens under uni-axial

compression. In a stressed test condition, a preload, generally in the range of 20 to 40 percent of the ultimate compressive strength at room temperature is applied to the concrete specimen subsequent to heating, and the load is maintained during the heating period. The specimen is heated continuously at a recommended rate until a definite temperature is reached, and the temperature is kept constant until a thermal steady state is achieved (Phan et al. 1996). After achieving uniform temperature, the load is then increased at a recommended rate until the specimen fails. In the un-stressed test method, the specimen is heated, without any loading, at a recommended rate to the specified temperature, and is maintained constant until a thermal steady state is reached within the specimen. After attaining the target temperature, the specimen is loaded at a recommended rate until failure occurs. The stressed and un-stressed test methods are performed to assess the properties of concrete at elevated temperature (Phan et al. 1996). In the un-stressed residual strength test, the specimen is heated without any load at a recommended heating degree. After attaining the target temperature, the temperature is kept constant until a thermal steady state is reached within the specimen. After heating, the specimen is then allowed to cool down to room temperature and loaded at room temperature up to the failure. This method is most suitable for assessing the post-fire or residual properties of concrete (Phan et al. 1996) for retrofitting purpose.
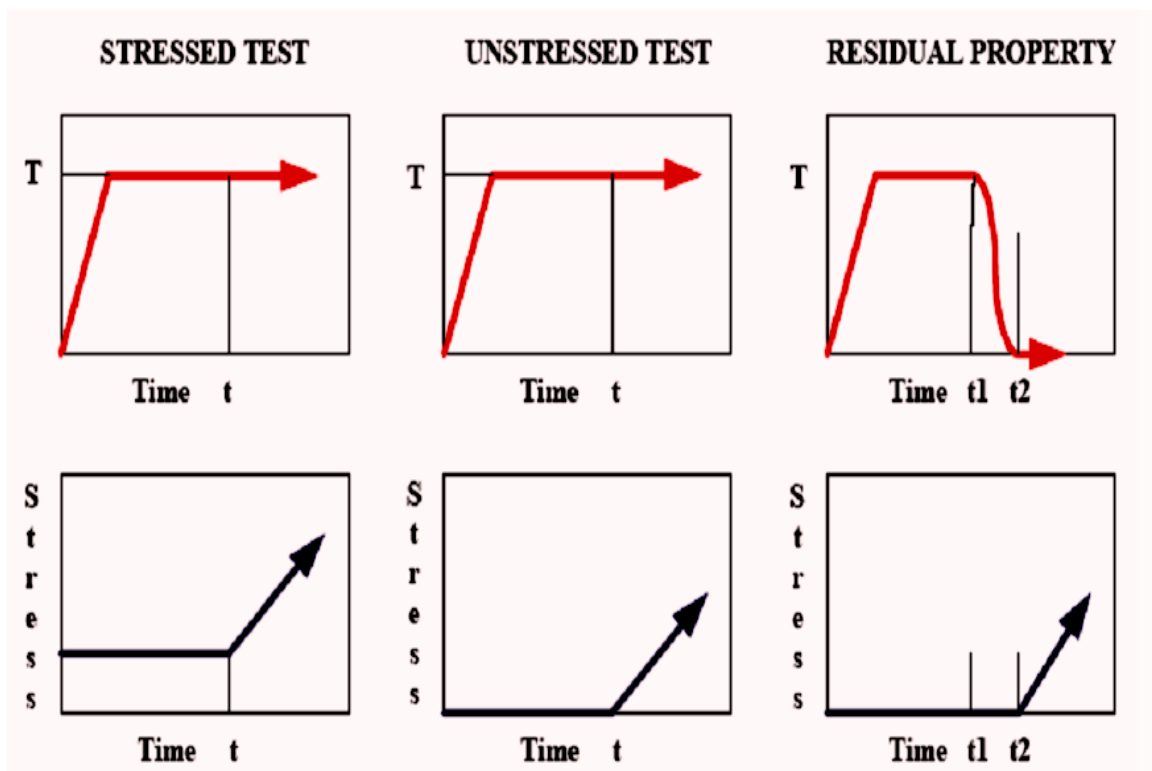
Fig.1. 1: Schematic of temperature and load histories for different test methods

4

1.2.1 Residual Compressive Strength of Concrete

Significant amount of research has been targeted in the past to study the effect of elevated temperature on the mechanical properties of concrete mainly involving compressive strength and thermal spalling (Lea and Straddling 1922, Malhotra 1956, 1982, Harmathy and Berndt 1966, Lankard et al. 1971, Abrahm 1971, 1978, Mohamedbhai et al.1986, Schneider 1985, Diederichs et.al. 1988, Kumar and Bhattacharjee 1995, Phan 1996, Chan et.al. 1999, Peng 2000, Suresh 2002, 2006, Poon et.al. 2004, Cheng et al. 2004, Lau and Anson 2006, Xiao et al. 2006, Baruah et al. 2007, Laskar et al. 2008, Raju et al. 2007, Kodur et al. 2008, Chowdhury et al. 2008, Noumowe et al. 2009, Demirel and Kelestemur 2010, Jeongwon et al. 2011, Ozawa et al. 2012, Vidya Sagar et al. 2013, Abdul Rahim 2013). These studies indicate that concrete strength decreases with increasing temperature and there is additional decrease in strength on cooling probably because of micro cracking during cooling. When concrete cools down, the quicklime (calcium oxide) absorbs moisture and converts to slaked lime (calcium hydroxide). When this happens, disintegration of the affected concrete will occur (Perkins 1986). Generally, the residual strength of concrete remains approximately in the range of 75% to 25% of the original room temperature strength when heated to temperatures in the range of 300°C to 600°C respectively. Hertz (Hertz 2005) investigated the behaviour of siliceous, limestone, granite, sea gravel, pumice and expanded clay aggregate concrete at elevated temperatures. It was found that the relative residual compressive strength of heated siliceous concrete was about 20% lesser than the hot strength for temperatures above 400°C. He found that concrete made with aggregates having lower thermal expansion suffers less damage than siliceous aggregate concrete during fire. It was found that the reduction in compressive strength and the standard deviation for this reduction was nearly the same for granite, basalt, limestone, and sea gravel. It was also confirmed in a study (Abrams 1997) that at temperatures above 430°C, siliceous aggregate concrete lost a greater proportion of its strength than concretes made with limestone or lightweight aggregates but when the temperature reached approximately 800°C the difference disappeared (Nassif 2006).

Malhotra (Malhotra 1956) used various mix proportions and water-cement ratios to determine the compressive strength of heated concrete. He found that at temperatures less than 200°C, the reduction in compressive strength was minor. At higher temperatures, the reductions were significant and depended on the test conditions. The

reduction in compressive strength at 500°C for stressed and, unstressed specimens was about 35% and 60% of the un-heated value respectively. The residual strength of unstressed specimens heated at 500°C and tested after cooling was reported to have reduced by up to about 80% of its initial strength. It was also found that the reduction in compressive strength for concrete made with an aggregate-cement mix ratio of 4.5:1 and water-cement ratio of 0.65 was larger than that of concrete made with an aggregate-cement mix ratio 6:1 and water-cement ratio of 0.5. It was reported that the residual strength of the heated and cooled concrete was less than the strength in heated condition and was approximately 20% less than the corresponding hot strength in the temperature range of 200°C to 450°C. Abrams (Abrams 1977) reported the results of compressive strength of cylindrical specimens heated to temperatures of 93-871°C. The results confirmed that the unstressed residual strength obtained after cooling showed the greater losses compared to unstressed and stressed strength tested at elevated temperature. The results of siliceous and expanded shale aggregate concretes showed that the specimens stressed during heating had smaller reductions in strength at high temperatures than unstressed specimens tested hot (Fig. 1.2). This may be due to the reduction of crack formation owing to the imposed stress. The siliceous aggregate concrete exhibited about 75% of the original strength at 450°C in unstressed conditions (Fig. 1.3)
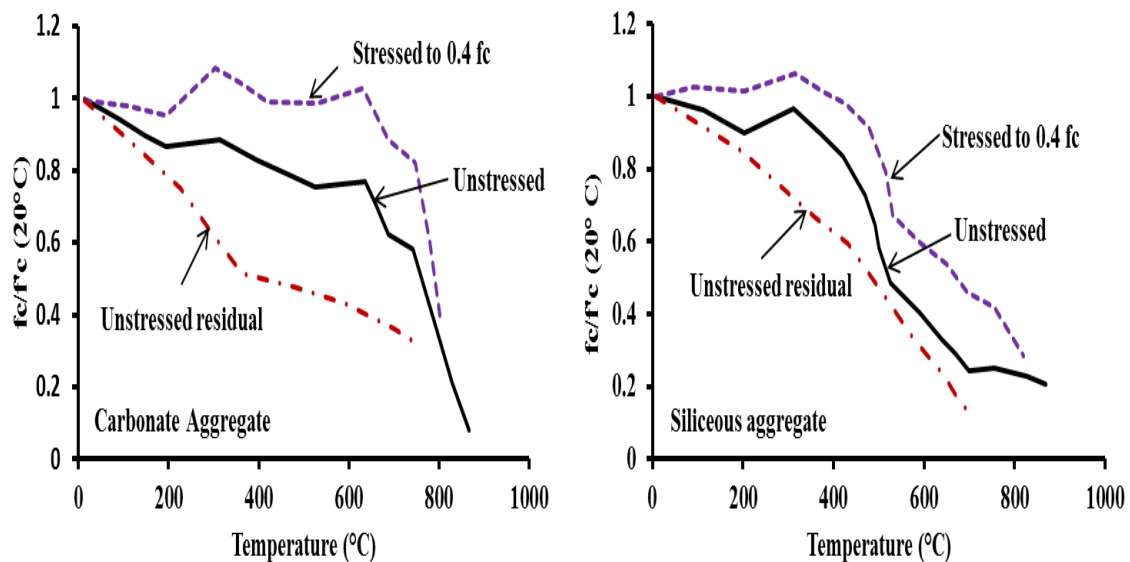
Fig.1. 2: Effect of temperature on compressive strength of carbonate aggregate concrete and siliceous aggregate concrete (Abrams 1971)

6
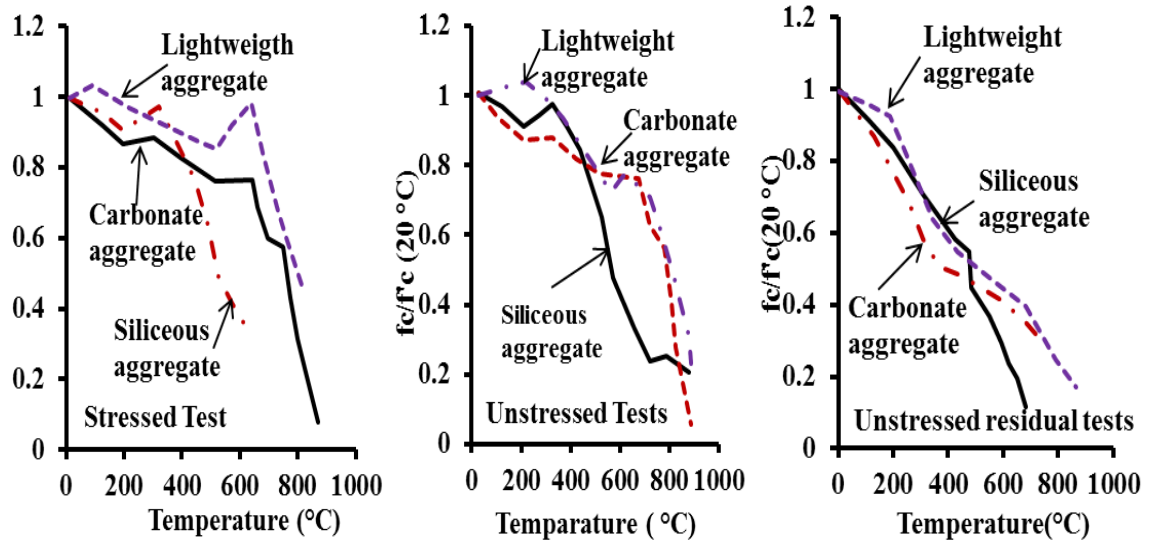
Fig.1. 3: The stressed, unstressed and residual properties test data of high temperatures (Abrams 1971)

In all types of aggregates, it was found that the loss of compressive strength was independent of the original level of strength but the sequence of heating and loading had a significant effect on the residual strength. The findings of Abrams (Abrams 1977) were very close to those from other studies (Malhotra 1956, Harmathy and Berndth 1966). However, the reduction in strength up to 600°C, as reported by Malhotra (Malhotra 1956) was larger compared with that reported by Abrams (Abrams 1977). Nassif (Nassif 2006) reported that heating to temperatures less than 220°C had no significant effect on the compressive strength of the river gravel aggregate concrete. But, the residual strength of concrete was found to be 70% and 42% of the original value at temperatures of 320°C and 470°C respectively. The findings of Nassif (Nassif 2006) were very close to the TR 33, and Hertz (Hertz 2005). Chang (Chang et al 2006) investigated the effect of temperatures on the properties of concrete subjected to temperatures in the range of 100-800°C. The residual strength at 200°C, 400°C, 600 °C and 800°C was found to be 90%, 65%, 40% and 15% of the original control value respectively. The findings of Chang (Chang et al 2006) were very close to the results of Abrams (1997).

Chan (Chan et al. 1999) investigated the effect of temperature on the residual compressive strength of concrete. The results indicated that, there were three temperatures ranges (20-400°C, 400-800°C, and 800-1200°C) in which the loss of compressive strength was noticeably different. Chan et al. 1999 found that up to a temperature of 400°C, the loss in strength was 25% and severe strength loss occurred

7

within the range of 400-800°C due to dehydration of C-S-H gel. Mohamed Bhai (Mohamed Bhai 1986) investigated the effect of varying the time of exposure and the rates of heating and cooling on the residual compressive strength of basalt aggregate concrete. The results demonstrated that the residual compressive strengths of concrete at temperatures, 20°C, 200°C, 400°C, 600°C and 800°C were 100, 50-92, 45-83, 38-69 and 20-36% of room temperature strength respectively.

1.2.1.1 Effect of cooling methods on the compressive strength of concrete

The literature shows that the residual compressive strength of heated concrete after various cooling regimes decreases. After cooling, the material takes time to come to equilibrium with its surroundings (Hertz 2005). It is reported by many researchers that the compressive strength of concrete measured after cooling is lower than that at high temperature (Malhotra 1956, Abrams 1977, Neville, Mohamedbhai 1986, Khoury 1992, Phan and Carino 2002, Lamont et al. 2004, Ali et al. 2004, Hertz 2005, Benmarce and Guenfound 2005, Franssen 2005, Purkiss 2007, Peng et al. 2008, Monal et al. 2012, Yaragal et al. 2012). There is further post-cooling variations in strength due to re-absorption of moisture in the concrete (Phan 1996). The above literature cites the post-cooling changes in strength that happens due to micro structural and by dimensional variations within a structure. These variations would cause further redistribution of stress and possibly additional damage during the period immediately after fire (Phan 1996). It is reported that the loss of strength of heated concrete by means of water cooling is more than that of cooling in air. Though above 600°C, the effect of cooling regime (either water or air) on the compressive strength is not significant (Mohamedbhai 1986). Xiao and Konig 2004 also reported similar conclusions from their study. The residual strength of concrete with cooling in the air though continues to decrease for a certain period and then some recovery would occur slowly (Lee et al. 2008). When cooling is carried out in the furnace, the strength loss of concrete is less as compared to concrete cooled in open air and in water (Xiao and Konig 2004, Lee et al. 2008).

1.2.1.2 Rate of heating and cooling on the compressive strength of concrete

Heating and cooling are the two phases during exposure to temperature cycles and it has been reported in the literature that higher the rate of heating and cooling, the greater would be the reduction in residual compressive strength of concrete (Malhotra 1956, Zoldners 1960, Khoury et al. 1985, Bazant and Kaplan 1996, Hertz 2005, Peng et al. 2006, 2008, Zaidi et al.2011). The residual strength is lesser for low temperature at

rapid heating rate because the matrix does not have much time to creep when the aggregate expands and the matrix shrinks (Hertz 2005). The matrix therefore seems to be more brittle giving more micro cracks, when the specimen is heated rapidly. On the other hand for higher temperatures, the rapidly heated concrete is stronger because it takes time for the calcium hydroxide to decompose and damage the concrete. High temperatures usually occurs on the surface of a structure. The literature mostly shows that the rates of heating and cooling have a significant effect on the residual strength of concrete heated to temperatures lower than 600°C. However, the rates of heating and cooling have relatively lesser effect on the residual strength of concrete heated to temperatures more than 600°C (Mohamedbhai 1986) because most of the micro cracking has been taken place and most of the moisture has been removed up to 600°C and beyond. If the heated concrete is allowed to cool down faster, the reformation of calcium hydroxide will take place at a slow rate in the days after cooling, and the concrete reaches its minimum strength several days after the fire. The speed of this regeneration process depends upon the moisture content of the ambient air and the size of the structure (Hertz 2005).

1.2.1.3 Effect of shape and size of specimens on the compressive strength of concrete

The shape and size of the specimens do affect the compressive strength of concrete subjected to high temperatures. It is reported that cubes have better residual strength than prisms (Komarovskii 1965). The temperature at the center of the larger dimension specimen will be lower than those of smaller dimension specimens at the same time due to the delay of the heat transfer. Accordingly, the loss of strength would be higher in the smaller dimension concrete specimen than in the larger dimension specimens when exposed to same fire duration (Komarovskii 1965, Davis 1967 and Li et al. 2004, Eskandari et al. 2010). However, the effect of specimen size on the retained compressive strength was not pronounced (Arioz 2009).

1.2.1.4 Effect of duration of exposure on the compressive strength of concrete

The longer the period of exposure to high temperatures, the more would be the deterioration in compressive strength due to crack generation and material deterioration. Most of the reduction in strength occurs within the first 30 days of long term exposure (Lankard et al. 1971, Nasser and Lothia 1971, Harada et al. 1972, Mohamedbhai 1986, Cho et al. 2005). The residual strengths after one hour of exposure at 200, 400, 600 and 800°C were about 80, 70, 60, and 30% respectively while the residual strengths after 2

hours or more exposure were found to be about 70, 60, 45, and 25% (Mohamedbhai 1986).

1.2.2 Residual Stress-Strain Relationship of Heated Concrete

For the assessment and retrofitting of fire-damaged concrete structures, it is important to study the residual stress-strain behaviour fire damaged concrete in order to predict the residual structural capacity. The residual stress-strain relationship of fire-damaged concrete is a complex function of the method of cooling and duration of exposure as well as the maximum temperature applied (Nassif 2006). Though the overall profile of the stress-strain curves of concrete does not change after heating, the peak value in the curve gets reduced due to induced degradation and occurs at a higher strain (Nassif et al 1996). The slope of the descending portion of stress-strain curves is reduced with increasing temperature.

Many researchers examined the stress-strain relationships of concrete during and after heating to high temperatures. Nassif (Nassif 2006) tested concrete cores to examine the stress-strain relationships of river gravel concrete and limestone concrete. The test results demonstrated that river gravel heated concrete after cooling with water exhibited a brittle failure mode below 320°C and exhibited gradual failure above 320°C due to increasing the internal plasticity, as shown in Fig. 1.4. On the other hand, in limestone concrete the brittle failure was observed only in un-heated cores while heated limestone concrete after cooling with water showed a gradual kind of failure as shown in Fig. 1.5. The effect of elevated temperatures on concrete strength and load-deformation behaviour of high strength concrete (HSC) and normal strength concrete (NSC) have also been investigated by many other researchers (Castillo and Durani 1990, Furumura et al. 1995, Freskakis 1979, Kodur et al. 1998, Kodur et al. 2008, Ali et al. 2010, Zaidi et al.2011, Ozawa et al. 2010, 2011). Harada et al. (Harada 1972) tested concrete cylinders heated in an electric furnace at a rate of 1.5°C/min and allowed to cool down gradually. The results confirmed that the gradient of the curves becomes gradual with rise in temperature. The curve is convex in the upward direction up to 400°C and becomes concave at 500°C, as shown in Fig. 1.6. The residual strain increases with increasing temperature. At 500°C, the residual strain is more than 50% of the total strain.
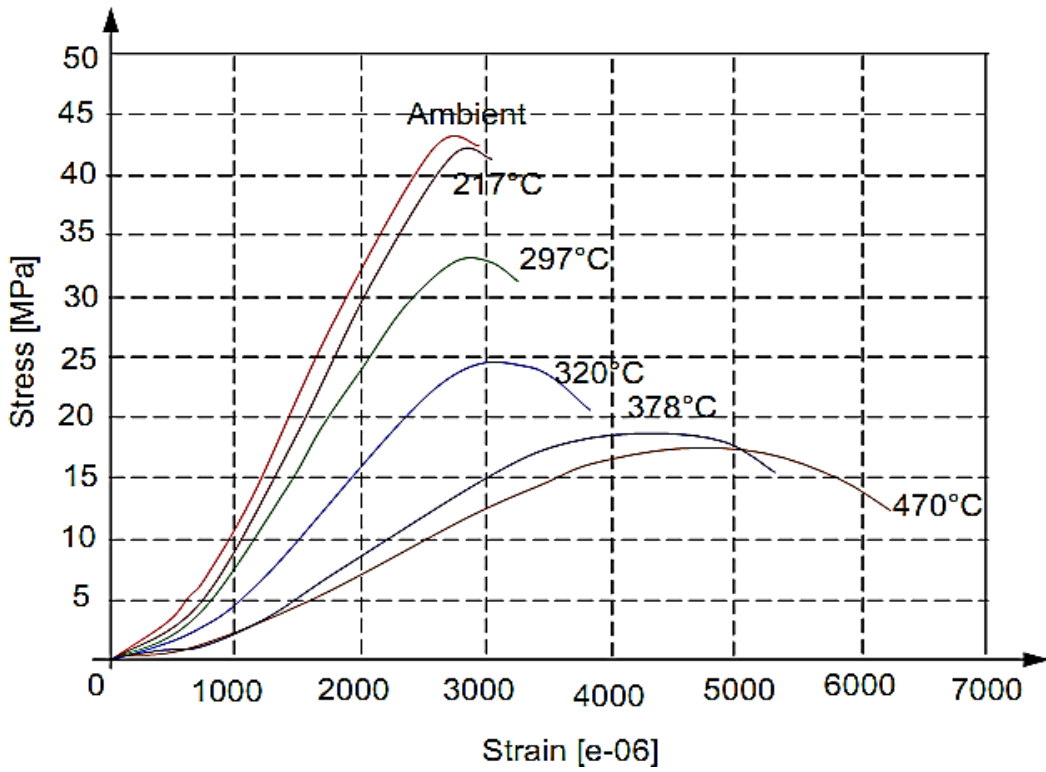
Fig.1. 4: stress-strain relationship of water quenched fire-damaged river gravel concrete (Nassif 2006).
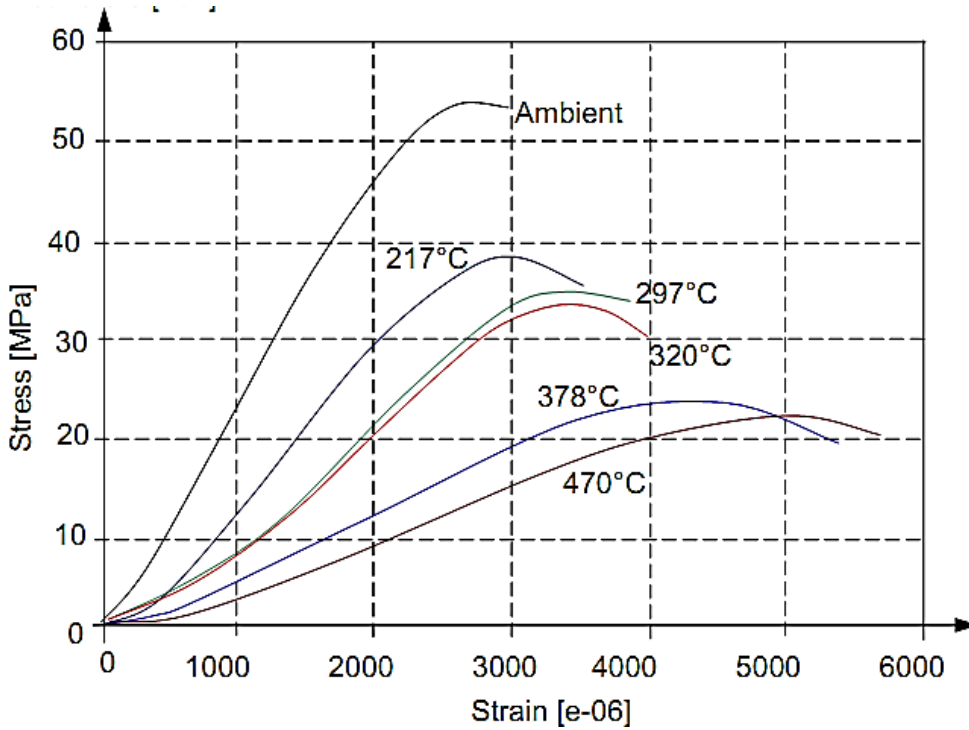
Fig.1. 5: stress-strain relationship of water quenched fire-damaged limestone concrete (Nassif 2006).

11
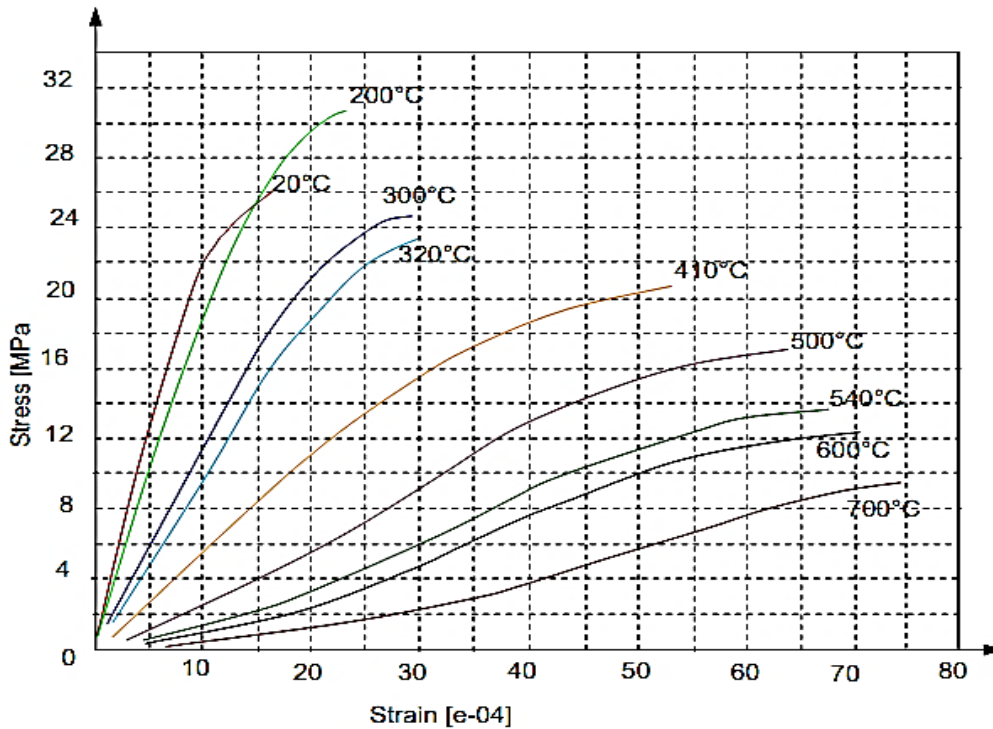
Fig.1. 6: Stress-strain curves of sand stone aggregate concrete (Harada et al. 1972)

Several models for prediction of residual stress-strain curves of concrete exposed to high temperatures were developed mainly for numerical analysis of the thermal response of concrete structures (Nielsen et al. 2004). Castillo et al (Castillo and Durrani 1990) examined the effects of transient high temperature on the load deformation behaviour of normal strength (27.6 Mpa) and high strength (62.1 Mpa) concrete. The rate of heating for all specimens was between 7 and 8°C/min. The results shown that for both the normal and high strength concretes, strain at peak load did not vary significantly within the temperature range of 100 to 200°C. Between 300 to 400°C, the strain corresponding to the peak load increased slightly. However, at temperatures ranging between 500 to 800°C, the strain at peak load increased significantly. At 800°C, the strain at peak load was three to four times the strain at room temperature, as shown in Figs. 1.7 and 1.8. Diederichs (Diederichs et al. 1988) performed unstressed tests on normal and high strength concrete made with Ordinary Portland Cement. The test results confirmed that high strength concrete failed in a more brittle manner than normal strength concrete. Furumura (Furumura et al. 1995) reported the results of stress-strain relationships of normal and high strength concretes. The results confirmed that modulus of elasticity, in general, decreased gradually with increase in temperature. Stress-strain curves of high strength concrete (FR60) showed a steeper slope than the normal strength

12

concretes (FR42, FR21) at 300°C, as shown in Fig. 1.9. The 42 MPa concrete shows flatter slope above 300°C, as shown in Fig. 1.10.
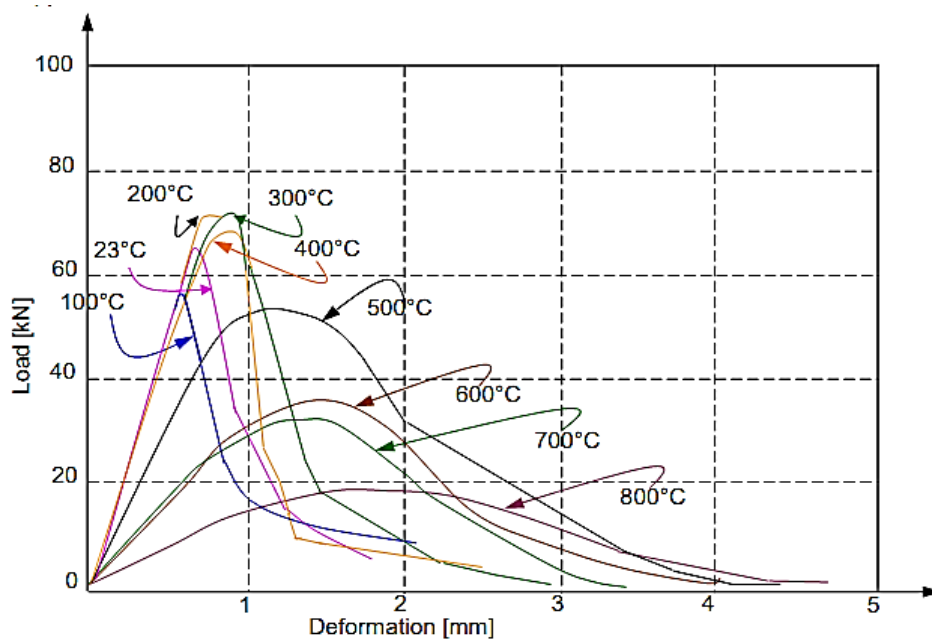
Fig.1. 7: Load deformation normal strength concrete at high temperatures (Castillo and Durrani 1990)
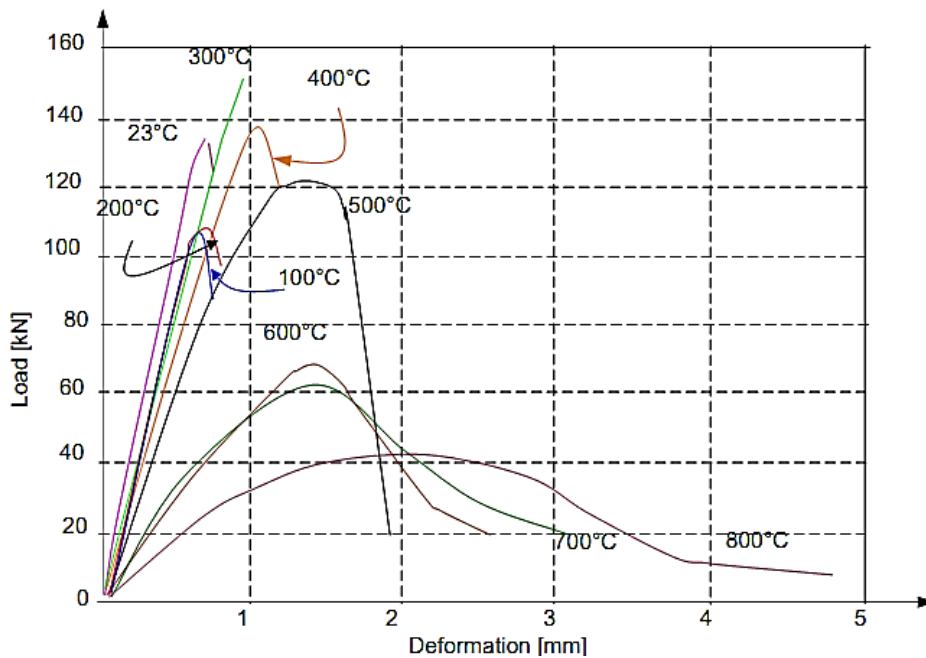
Fig.1. 8: Load deformation high strength concrete at high temperatures (Castillo and Durrani 1990)
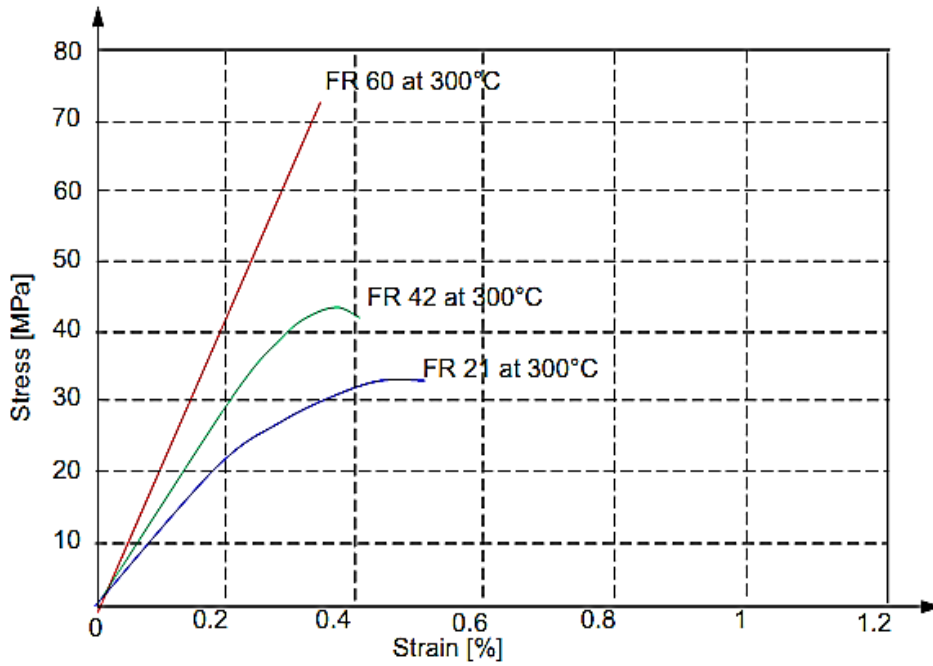
Fig.1. 9: Comparison of stress-strain relationships for concretes at 300°C
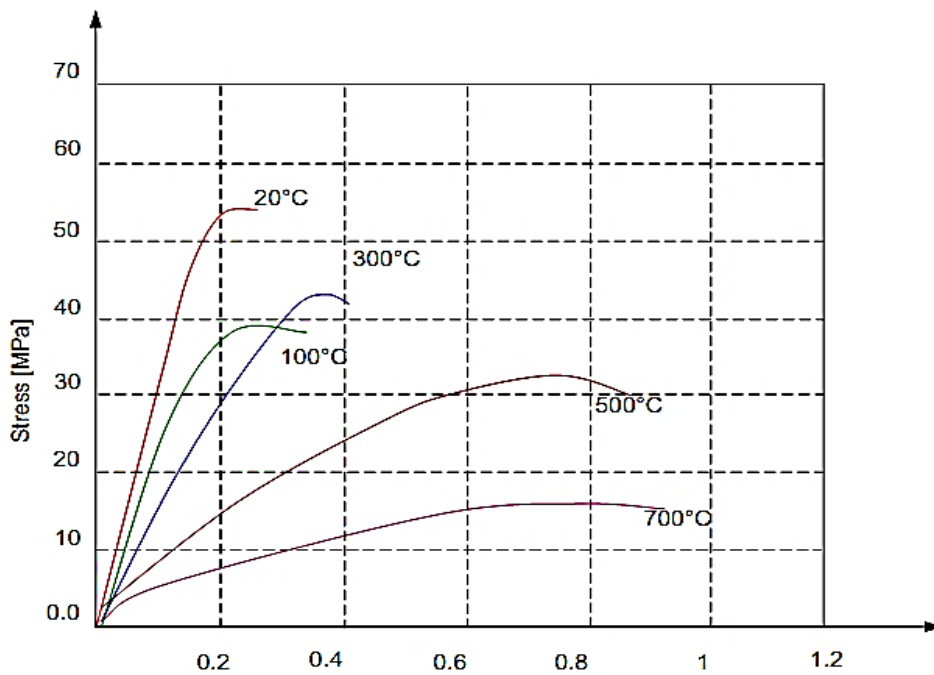
Fig.1. 10: Stress-strain relationships for NSC at different temperatures (Furumura et al. 1995)

1.3 ASSESSMENT OF FIRE DAMAGED CONCRETE STRUCTURES

Generally concrete structures are non-combustible and resist fires for a relatively longer period. However, long time exposure to fire results in deterioration of compressive strength and other properties of concrete and also degradation in properties

14

of reinforcing steel which may cause loss of serviceability or even load carrying capacity of structures. The concrete structures generally undergoes a number of changes when subjected to fire (Anderberg 2009) namely loss of prestress, residual deformations, cracking, loss of material by spalling, detailing and connection failure especially between steel and reinforced concrete members, changes in the visual appearance as dirty and colored surfaces etc. Three principal fears in estimating the effect of the fire on concrete structure before carrying out any repair work are (TR68):

➢ Seriousness of damage (spalling) or loss in strength of the concrete
➢ Loss in strength of steel reinforcement or embedded structural steel elements
➢ Damage or distress to the structure from movement, settlement or imposed loads.

The assessment of fire damages to structures follows a similar general process and procedures as in any other appraisal of existing structure. In making a decision about repairing a fire damaged building, considerations are given to aesthetic appearance, the reliability of repairs, the views of client, in addition to technical feasibility (Narendra et al. 2008, Anderberg 2009, Wang et al. 2010, Kodur et al. 2010, Yaqub 2010, and TR68)

1.3.1 Procedure for Estimating Fire Induced Damage

The procedure to assess the fire damaged concrete usually starts with preliminary inspection of the structure as shown in Fig. 1.11. Take instant steps to secure public safety and the safety of the structure; it may be necessary to prop members that are in a critical condition. Thereafter out on-site assessment of the structure to determine the extent of damage (by visual inspection, breakouts and/or non-destructive testing). Subsequently carry out laboratory testing of concrete and reinforcement samples to determine their residual strengths and confirm depth of fire-damage, supplemented by thermal modelling where appropriate. Determine structural capacity of members that are to be repaired, using reduced residual material properties, and hence determine additional concrete and reinforcement required to reinstate original capacity. Select appropriate repair methods and carry out work to restore the structure to its original capacity.

1.3.2 Assessment of Damage

To make assessment of fire damage there are two approaches, which can be used independently or combined together depending on the nature of the fire and type of the structure:

➢ Directly assess the properties of fire damaged concrete and reinforcement

> ➢ Calculate the residual strength of the fire damaged concrete and the reinforcement by ascertaining temperature profiles and fire severity

Direct in-situ assessment involves following three steps:

> ➢ Visual inspection and hammer soundings
>
> ➢ Non-destructive testing (e.g. rebound hammer, ultrasonic pulse velocity (UPV)
>
> ➢ Coring, sampling and subsequent laboratory testing (e.g. petrographic examination, Thermo-gravimetric analysis, strength testing of concrete and reinforcement samples).

The second methodology involves three steps, which should be confirmed by tests:

> ➢ Evaluation of fire severity
>
> ➢ Determination of temperature-profiles
>
> ➢ Assessment of residual strength of the reinforced concrete

1.3.2.1 Visual observation on site

Visual inspection may be aided by the use of magnifying hand lens (Ingham 2007). Inspection of cracking, spalling, deflections, surface crazing, colour changes, smoke damage and exposed steel reinforcement provide valuable information.

Cleaning: Smoke hides most of cracks, spalls and distortions in the structure. The structures may be cleaned by means of dry ice blasting, grit blasting, water blasting or chemical washing. Chemical washing and ice blasting tend to cause the minimum guaranteed damage to the structure. Grit blasting tends to create large amounts of blasting medium. Water blasting can cause damage to finished area below the fire.

Deformation: Deformation of structural member and related materials (coatings, pipes etc.) can provide valuable information to develop a heat intensity map. Excessive deflection, large extensive cracks, misalignment and distortion of members show that the load carrying capacities are reduced significantly and it is important to give more concentration to these zones of fire damaged structure. Deformations of fire affected members should be taken and compared with undamaged members of the similar structure to get additional strong ideas. Visual inspection of reinforced concrete structures is achieved to give each structural member a class of damage ranging from zero to four suggested by the Concrete Society (TR68), as shown in the Table 1.1

```
┌─────────────────────────────────────────────────────┐
│           Verify the Structure to Enter Safe          │
└─────────────────────────────────────────────────────┘
                          │
                          ▼
┌─────────────────────────────────────────────────────┐
│              Execute Preliminary site visit           │
│                                                       │
│   ➤  Identify Follow- up Area                         │
│   ➤  Note Temperature Indicator                       │
│   ➤  Determine Cleaning Method                        │
└─────────────────────────────────────────────────────┘
                          │
                          ▼
┌─────────────────────────────────────────────────────┐
│              Perform Detailed Evaluation              │
│                                                       │
│   ➤  Visual                                           │
│   ➤  Non-Destructive Testing                          │
│   ➤  Partially Destructive Testing                    │
└─────────────────────────────────────────────────────┘
                          │
                          ▼
┌─────────────────────────────────────────────────────┐
│                     Investigation                     │
│   ➤  Compare allowable and Applied Stresses           │
│   ➤  Identify Extent of Repair                        │
│                                                       │
└─────────────────────────────────────────────────────┘
                          │
                          ▼
┌─────────────────────────────────────────────────────┐
│                    Design Repairs                     │
│                                                       │
│   ➤  Select Materials                                 │
│   ➤  Develop Details                                  │
└─────────────────────────────────────────────────────┘
```

Fig.1. 11: Stages in the assessment and repair process (Narendra et al. 2008)

Colour: The colour of concrete changes during heating and it is irreversible. Therefore coloration of concrete at various depths allows an estimation of maximum temperature attained and the equivalent fire duration (Bessey 1950, TR15, Green 1971, Tucker 1981, CIB W14 Report 1990). The changes in concrete (color, surface appearance and condition) by temperature and can be used to estimate the effect of the fire as shown in Fig. 1.12. The normal grey colour of Ordinary Portland Cement Concrete changes to light pink at around 300°C and becomes darker attaining the

maximum intensity at about 600°C (Malhotra 1982). The temperature of 300°C is significant for three reasons. Firstly, a pink coloration occurs at this temperature (TR15, CIB W14). Secondly, below that temperature the effect of heat on concrete strength is likely to be structurally insignificant (Abrams 1977). Thirdly, above 300°C, a pink discoloration indicates the inception of significant loss of strength due to heating (TR68). The change of colour to pink tends to be more noticeable with siliceous aggregates. Calcareous and igneous crushed rock aggregates are less vulnerable to this effect (TR33). The change in colour is due to the transformation of ferric compounds present in aggregate or in the sand as impurities to ferric oxide (Malhotra 1982, Michael 1993). The intensity of colour depends upon the level of impurity and the colour changes have been noticed even with limestone aggregate concrete when river sand was used as fine aggregate (Malhotra 1982).
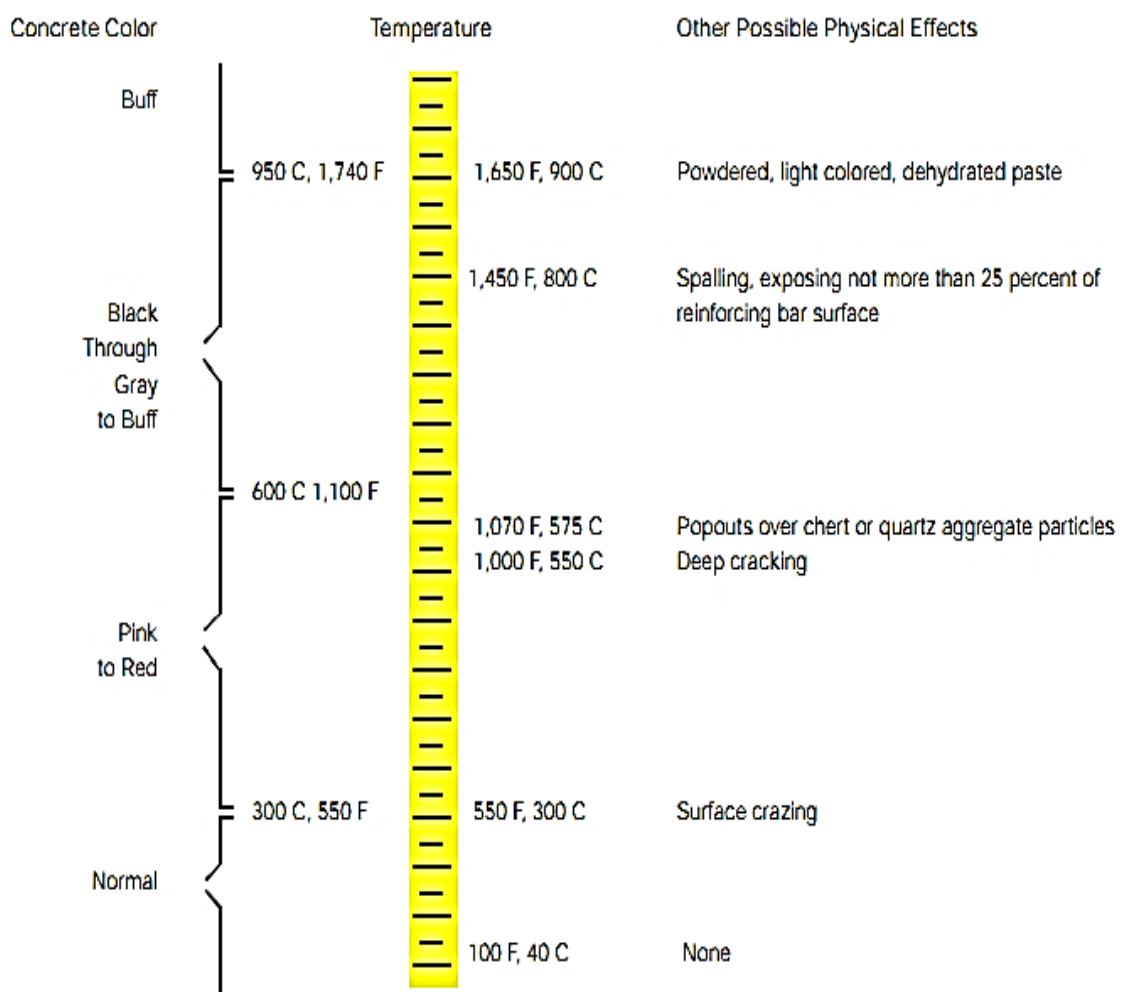
Fig.1. 12: Visual evidence of temperature (Green 1971)

Table 1. 1: Repair classification

Class of Damage	Repair classification	Repair requirement
0	Decoration	Redecoration if required
1	Superficial	Superficial repair of slight damage not needing fabric Reinforcement
2	General repair	Non-structural or minor structural repair restoring cover to reinforcement where this has been partly lost.
3	Principal repair	Strengthening repair reinforced in accordance with the load- carrying requirement of the member. Concrete and reinforcement strength may be significantly reduced requiring check by design procedure.
4	Major repair	Major strengthening repair with original concrete and reinforcement written down to zero strength, or demolition and recasting.

1.3.2.2 Non-destructive testing

Hammer sounding tests can be used as a screening test to locate areas where more detailed subsequent assessments are required. Concrete Society Technical Report No.15 (TR15) states that 'It may be sufficient to take soundings on the damaged concrete to determine the degree of deterioration. The "ring" of sound concrete and the "dull thud" of weak material are readily notable, and this test may be successfully done with hammer and chisel. Drilling resistance test can be used as an alternative of soundings with a hammer and chisel to determine the depth of weakened concrete (Michael 1993). A screwdriver is also useful to investigate surface areas for softened spots due to fire. The extent of delamination can be determined by means of chain dragging for large horizontal area such as slab and by means of hammer sounding for vertical and overhead surface (Narendra et al. 2008).

Schmidt hammer test: The Schmidt hammer test gives an idea of relative strength based on the impact hardness of the concrete. The rebound number of a standardized spring-loaded impact hammer is measured both on damaged and undamaged areas. The aim is to have a quick indication of the effect of a fire on the

impact hardness and thus indirectly on strength of a concrete. The previous authors have carried out numerous Schmidt hammer tests for the assessment of concrete quality of fire damaged concrete (Marosszeky and Michael 1987, Nasser 1987 and Schneider 1990). It is significant to understand when using a Schmidt hammer in the assessment of fire-damaged concrete that it can only indicate areas where the surface strengths are relatively lower compared with the undamaged areas. Moreover, only the qualitative evaluation of the degree of damage can be evaluated. As flat surface is needed to perform this test and large number of tests are advisable to reduce the effects of variability, therefore the rebound hammer is not in general suitable for use on spalled surfaces, which is commonly the case with fire-damaged concrete (TR68)

Ultrasonic pulse velocity test: The transmitting time through fire-damaged concrete is measured by the ultrasonic pulse velocity method and the degree of damage is investigated. As only the average transmitting time of concrete members is known, the distribution of the damage at various depths remains unknown (Nasser and Al-Manaseer 1987, Schneider 1990, Fu et al. 1992, Talukdar et al. 2005). The test consists of computing the time it takes for a pulse of vibration energy to travel through a concrete member. The vibration energy is introduced into the concrete by the transmitting transducer, which is attached to the surface with petroleum jelly. The distance between the transducers is divided by the transit time to obtain the pulse velocity through the concrete. The pulse velocity is proportional to the square root of the elastic modulus and inversely proportional to the mass density of the concrete. The elastic modulus of concrete has been found to vary in proportion to the square root of the compressive strength (BS EN12504-4).

1.3.2.3 Partially destructive Testing

Concrete core test: The most common direct method for ascertaining the damage in in-situ concrete is by testing cores extracted from fire damaged and undamaged concrete. If such a test indicates good strength, then one can be confident about the condition of the member from which the cores were taken. If the measured compressive strength is low, it shows the damage caused by heat. Such a result may also be due to local failure close to the exposed surface and the main body of the specimen may even be in a relatively better condition (Michael 1993). This is a well-established technique, facilitating visual inspection of the inner regions of a member together with strength examination. The other physical properties such as density, water absorption,

and indirect tensile strength can also be measured from the cores. Cores are also normally used for chemical analysis after going to strength testing. The penetration of heat can be studied on samples through the examination of colour changes of concrete in the sample, petro graphic analysis and thermo-gravimetric analysis.

1.4 REPAIR AND STRENGTHENING OF REINFORCED CONCRETE ELEMENTS AT AMBIENT CONDITIONS

There is an increasing demand for rehabilitation and strengthening of existing concrete (RC) structures due to deterioration, damage or need to higher structural capacity. This section presents a brief account of the previous literature on the various techniques used for repairing and strengthening of RC structures in normal room temperature conditions (other than the heat damage).

1.4.1 Externally Bonded Fibre Reinforced Polymer (FRP)

FRP materials were originally developed in early 1960's by aerospace and defense industries for specific applications such as in aircrafts, ships and military hardware's (ACI 440.2R-08). Therefore, significant amount of information is available on FRP properties at ambient conditions (Davies et al. 2004). In the last two decades, FRP composite materials are becoming progressively attractive for retrofitting and strengthening of civil engineering structures. This is because FRP's have strong, durable, light weight and ease of application characteristics and provides cost effective alternative solution for conventional repair materials. The early applications of FRP as repair and strengthening option started as a flexural strengthening material in RC bridge girders and as confinement strengthening of RC columns. Today, wide varieties of structural elements are being strengthened using FRP including beams, slabs, columns, shear walls, domes and trusses. These strengthening and retrofitting techniques widely utilize externally bonded FRP composites due to unique properties such as strength, light weight, corrosion and chemical resistance (Bakis et al. 2002).

In the recent years, considerable research work has been conducted on externally bonded FRP wraps for strengthening and on FRP reinforced concrete members. This includes overall structural response of FRP-strengthened members (Dortzbach 1999, Takeda et al. 1996, Mayo et al. 1999, Grace 2001, Shahrooz et al. 2002, Kodur et al. 2006, Williams et al. 2008), creep and fatigue effects (Scott et al. 1995; Yang and Nanni 2002), and factors contributing to durability enhancement (Toutanji and Gomez 1997,

Green et al. 2000, Neale 2001). Other notable research works include; increasing flexural strength of RC members (GangaRoa et al. 1998, Toutanji et al.1999, Dortzbach 1999, Grace et al. 1999, El-Hacha et al. 2001, Grace 2001, Sheikh 2002, Ashour et al. 2004, Toutanji 2006, Bousselham and Chaallal 2006, Barros et al. 2007, Monti and Liotta 2007, Balaguru et al. 2008, Tsonos 2008, Panda et al. 2011a), shear capacity enhancement (Chaallal et al. 1998, Khalifa et al. 1998, Kachlakev and McCurry 2000, Pellegrino and Modena 2002, Chen and Teng 2003, Teng et al. 2004, Zhang et al. 2004, Wang and Hsu 2009, Panda et al. 2011b), repair and rehabilitation of RC columns (Saadatmanesh et al. 1994, Mirmiran et al. 1998, Ehsani and Jin 1998, Lan et al. 1998, Triantafillou 1998, Ballinger et al. 2000, Darwish 2000, Sheikh 2002, Lam and Teng 2003, Harries and Carey 2003, Galal et al. 2005, Hosseini et al, 2005, Omar Chaallal 2006, Yousef 2007, Kumutha et al.2007, Ilki et al. 2008, Wang and Hsu 2008, Issa et al. 2009, Eid et al. 2009, Bambach et al. 2009, Turgay et al. 2010, Arghya et al. 2011, Al-salloum et al. 2011, Luca et al. 2011, Sezen and Miller 2011 Ramkrishna et al. 2012), retrofitting of columns in earthquake prone areas (Saatcioglu and Ozcebe 1989, Aycardi et al.1994, Ghobarah 2001, Elwood and Moehle 2003).

1.4.2 Ferro Cement as Repair Material

The credit of using Ferro-cement in the present day goes to Joseph Louis Lambot who in 1848 constructed several rowing boats, plant pots, seats & other items from a material he called "Ferciment" in a patent, which he took in 1852. Lambot's construction consisted of a mesh or grid reinforcement made of two layers of small diameter on bars at right angle & plastered with cement mortar with a thin cover to reinforcement. In the early 1940's a Italian Engineer - Architect, Pier Luigi Nervi, called this material as Ferro cement after about one hundred years. In 1972, the National Academy of Sciences of the United States of America set up an Adhoc Panel on the utilization of ferrocement in developing countries under the chairmanship of James P. Romualdi of Camegie-Mellon University, U.S.A. The report of the panel was first published in early 1973. As a result of the report people became aware of this material and started using it. In 1977 the American Concrete Institute (ACI) set up a Committee on ferrocement to review and formulate a code of practice for this material. ACI Committee 549 first codified the definition of Ferro cement in 1980, which was subsequently revised in 1988, 1993 and 1997. Ferro cement is a type of reinforced concrete having closely spaced multiple layers of reinforcing wire mesh completely embedded in mortar. The wire meshes are available

in hexagonal or square openings. Meshes with square openings are mostly preferred in Ferro cement construction due to higher efficiency. Meshes with square openings are available in welded or woven form. The ranges of mix proportions recommended for common Ferro cement construction are: sand-cement ratio by weight, 1.5 to 2.5, and water-cement ratio by weight, 0.35 to 0.5 (ACI Committee 549.1R-97). Normally, the aggregate consists of well graded sand that passes 2.36 mm sieve. The stiff mix is preferred, provided it does not prevent full penetration of the mesh. To improve the workability, the normal and high range superplasticizers are used nowadays. There are many methods for the construction of Ferro cement but the most common method is mortar placement. In this method the mortar is forced through mesh by hand plastering. Moist or wet curing is essential for Ferro cement construction.

Tremendous amount of research work is reported in the literature on Ferro cement as a construction material and a material for strengthening of RC and masonry structures (Mansur and Paramasivam 1985 and 1990, Kaushik et al. 1990, Nedwell et al. 1990, Walliuidin et el. 1994, Singh et al. 1997, Seshu et al.1998, Seshu 1998, Singh et al. 1998, Takiguchi et al. 2000, Seshu 2000, Takiguchi et al. 2001, Abdullah et al. 2001, Nassif and Najm 2004, Kazemi at el. 2005, Rathish and Rao 2006, Rathish et al. 2007, Kondraivendhan and Pradhan 2009, Xiong et al. 2011, Mourad et al. 2012, Amrul et al. 2013, Ivy et al. 2013). These studies have shown that the Ferro cement provides an effective confinement in concrete elements and has a great potential to be used as a strengthening material in developing countries. Ferro cement is reported to have many advantages over other types of repair and strengthening techniques like enhanced crack resistance combined with high toughness, its rapid construction with no heavy machinery involved, small additional weight it imposes, and its cost effectiveness for rehabilitation applications (Jeyasehar and Vidivelli, 2006). Since the skill required for the fabrication of Ferro cement is of low level and its constituents are locally available, Ferro cement can be an ideal repairing material.

1.4.3 High Performance/strength Fibre Reinforced Cementitious Composites for Repair and Strengthening

Though the research on fibre reinforced concrete (FRC) started long ago, the large scale structural applications of this material is still limited to a rather low percentage in most countries. Many studies have been reported on fibre reinforced concrete in the past (Destree 2000, Shannag 2002, Sorelli, et al. 2004, Beletti et al. 2004,

Skazlic 2005, Markovic 2006, Sivakumar & Santhanam 2007). Self-compacting fibre concrete with no reinforcement was successfully applied in long-span pre-stressed beam girders (Di Prisco & Plizzari 2003). The first high-strength fibre concrete composite (HSFRC) was developed about 15 years ago, and in contrast to conventional FRC, both the number of realized applications of HSFRC up to now and the number of innovative ideas are very promising. The most appreciated properties of HSFRC are the high compressive and tensile (flexural) strengths, good workability, high toughness and ductility and good durability compared to any conventional concrete. In the recent past, HSFRC has been successfully investigated and used as a repair material in the form of thin jackets for strengthening reinforced concrete structures (Alaee 2003, Alaee and Karihaloo 2003, Kaptijn, 2004, Meda 2005, Martinola et al. 2007, Bruhwiler 2008, Martinola et al. 2010, Farhat et al. 2007 and 2010, Bassam A. Tayeh et al. 2013). The advantages of this method over conventional RC jacketing are high compressive strength, high tensile strength, considerably improved toughness, there is no need to have reinforcement bars and stirrups and the thickness of the jacket can be as small as 15 – 40 mm.

1.4.4 Steel Plate (SP) Jacketing

The first familiar application of externally bonded steel plate for repairing or strengthening of reinforced concrete structure was found in 1964, when the basement beams of an apartment complex in South Africa were strengthened with epoxy bonded steel plate because of accidental omission of steel reinforcements during construction (Xanthakos 1996). Thereafter, this technique was used to strengthen a variety of structures in various countries (Bonaci and Maalej 2000). Steel plate can be bonded to concrete members as external reinforcement to increase their strength. The plates are glued to the member surface by epoxies. This requires a careful preparation of the member surface and application of epoxy layer. Steel plates can also be provided in the form of jackets all around the concrete members either by gluing to surface or by grouting. Through bolting is also suggested some times in addition to gluing for better function. Some major disadvantages that are associated with steel plate jacketing are its labour intensiveness, its weight, difficulty in handling, and its proneness towards corrosion. Thus this repair and rehabilitation technique is deficient in the sense that the material itself is subjected to the same sort of deterioration that affects the original structure (Karbhari et al. 1997).

The application of epoxy bonded steel plates has been used to strengthen bridges and buildings in several countries (Lerchental 1967, Lerchental and Rosenthal 1982, Bresson 1977, Raithby 1980, Swamy and jones 1980, Macdonald et al. 1982, Van Gemert and Van den Bosch 1983, Rennesund 1985, Klaiber 1987, Swamy et al. 1987, Iyer et al. 1989, Jones et al. 1988, Taljsten 1990, Elfgren and Taljsten 1992, Sarno et al. 2006). Strengthening using steel plates in bending has been investigated but efforts have also been made for strengthening in compression and shear (Jones et al. 1985). Ghobarah et al (1997) studied experimentally the failure modes of existing reinforced concrete beam-column connections and columns designed during the 1960s and 1970s. The effectiveness of using innovative corrugated steel jackets for enhancing the seismic shear strength and ductility of these types of connections was examined. The corrugated jacket was found to be efficient in rehabilitation of existing structures not meeting the current seismic code requirements. Wu et al (Wu et al. 2003) studied a new structural approach that uses composite partial interaction to improve the strength and ductility of rectangular reinforced concrete columns. By increasing the compressive resistance of concrete columns through composite partial interaction such as by bolting a steel plate to the compression face of a column, this new composite action approach is shown to be successful in delaying concrete crushing in the plastic hinge zone. Sarno et al (2006) assessed the feasibility of the application of Stainless Steel (SS) for seismic retrofitting of framed structures, either braced (CBF) or moment resisting (MRF) frames. The results of both inelastic static (pushovers) and dynamic (response history) analyses demonstrate that systems retrofitted with SS exhibit enhanced plastic deformations and excellent energy absorbing capacity. Adam et al (Adam et al. 2007) investigated the behavior of reinforced concrete columns jacketed by steel plate. Four different types of steel jacketing were incorporated and were tested concentrically until failure. Experimental results showed that the use of steel jacketing can increase the ultimate capacity by 50% to 100%.

1.5 REPAIR AND STRENGTHENING OF FIRE OR HEAT DAMAGED REINFORCED CONCRETE ELEMENTS

Various methods for repairing and strengthening of concrete structures, following a fire or heat, have been studied in the past (Marchant 1972, TR68). Externally bonded FRP wrapping, which is now the most promising repair option for strengthening under ambient conditions, has also been tried in strengthening fire or heat damaged reinforced

concrete structures (Saadatmanesh et al. 1994, Mirmiran et al. 1998, Ehsani and Jin 1998, Lan et al.1998, Triantafillou 1998, GangaRoa et al. 1998, Toutanji et al.1999, Ballinger et al. 2000, Darwish 2000, Sheikh 2002, Lam and Teng 2003, Harries and Carey 2003, Galal et al. 2005, Hosseini et al, 2005, Omar Chaallal 2006, Yousef 2007, Kumutha et al.2007, Ilki et al. 2008, Wang and Hsu 2008, Issa et al. 2009, Eid et al. 2009, Bambach et al. 2009, Turgay et al. 2010, Arghya et al. 2011, Al-salloum et al. 2011, Luca et al. 2011, Sezen and Miller 2011 Ramkrishna et al. 2012) However, due to the uncertainties regarding the behaviour of fibre reinforced polymer in any subsequent fire, limited research has been reported on the repairing of fire damaged concrete elements using FRP wrapping (Haddad et al. 2008, Udaya Kumar et al. 2009, Yaqub et al 2011a, 2011b, 2011c, 2012 & 2013, Bisby et al. 2011, Kai et al. 2011, Haddad et al. 2011, Hanan et al. 2013). Though there are some studies in the existing literature on fire performance of FRP strengthened reinforced concrete elements, only limited studies are reported in the field of FRP strengthening of fire or heat damaged reinforced concrete elements (Blontrock et al. 1999, 2000, Kodur et al. 2003, 2004, 2005, 2006, 2008, Bisby et al. 2005, Green et al. 2006, Williams et al. 2006, Barnes and Fidell 2006, Green et al. 2006, Chowdhury et al. 2007, 2008, Rafi et al. 2008, Tao et al. 2008, Williams et al. 2008, Tim et al. 2009).

Although Ferro cement is an old technology and has been used as a structural material for more than fifty years, its application in repairing fire damaged elements is a new one. Yaqub et al (Yaqub et al. 2013) carried out an experimental study to compare the efficiency of using Ferro cement and FRP jackets for the strengthening of heated and damaged circular and square columns. Experimental results showed that the use of Ferro cement jackets improved both the strength and stiffness of the strengthened columns. A combination of both ferrocement and FRP jackets was proposed to restore the strength, stiffness and ductility of fire-damaged columns. While several studies have previously been undertaken on the feasibility of using high strength fibre reinforced cementitious composites (HSFRC) for the rehabilitation and strengthening of structures under ambient conditions, but limited research has been reported on the repairing of fire damaged concrete elements using HSFRC (Haddad et al. 2007, Haddad et al. 2008, Haddad et al. 2011, Leonardi et al. 2011). Haddad et al. 2007 established that high-strength steel-FRC jackets may be considered as a promising material for the maintenance and rehabilitation of concrete structures. The results indicated that using HSFRC jackets enhanced the

ultimate load capacity with a corresponding increase in stiffness as well. Similarly, the steel plate (SP) jacketing is an old technology and has been used as a repair material for more than 50 years, yet its application in repairing fire damaged structures has not been investigated conclusively.

1.6 STUDIES ON BOND BETWEEN FRP AND CONCRETE

A good, strong and durable bond between the repair material and the substrate concrete is very important for the success of any repair job. Different repair materials have different bond characteristics with the parent concrete. Some previous researchers have attempted investigations on the bond properties of different repair materials with concrete, though under ambient temperature conditions only (Chajes et al. 1996, Bizindavyi and Neale 1999, Chen and Teng 2001, Nakaba et al. 2001, Yao et al. 2005, Guo et al. 2005, Mazzotti et al. 2008 and 2009). The performance of bond between different repair materials and substrate concrete damaged by heat or fire exposure has not been investigated. As externally bonded FRP wrapping is the most commonly used repair technique, it becomes important to investigate the bond characteristics between the FRP and the fire or heat damaged concrete. This is because the bond characteristics between the damaged concrete and the FRP are of primary importance for a FRP strengthening technique's ability to transfer loads from a fire damaged concrete member to the strengthening material.

To investigate the bond properties of the interface between externally bonded FRP and concrete, several test methods have been developed in the past under normal ambient temperature conditions as show in Fig. 1.13. The common aspect for these methods is that the bonding area is subjected to shear forces. In a study undertaken by Ueda and Dai (2005), a summary of bond test methods for externally bonded FRP are presented. The various authors have identified a number of parameters affecting the bond behavior for FRP strengthening under ambient temperature conditions namely bond length, bond width, stiffness of FRP, concrete strength, surface treatment of concrete, properties of bond layer, and interface defects (Van Gemert 1990, Chajes et al. 1996, Taljsten 1997, Maeda et al. 1997, Arduini and Nanni 1997, Bizindavyi and Neale 1999, Nakaba et al. 2001, Chen et al. 2001, Lorenzis et al. 2001, Yuan et al. 2004, Xiao et al. 2004, Yao et al. 2005, Guo et al. 2005, Mazzotti et al. 2008 and 2009). The previous works included both theoretical investigations based on fracture mechanics approach and development of empirical models based on regression of experimental data (Khalifa et al.

1999, Chen and Teng 2001, Yuan et al. 2004, Lu et al. 2006, Chen et al. 2006, Wu et al. 2010, Bilotta et al. 201, Chajes et al. 1996, De Lorenzis et al. 2002, Nakaba et al. 2001, Blontrock 2003, Wu et al.2005, Klamer 2006, 2008 and 2009, Leone et al. 2009, Gao et al. 2012, 2013). However, only very limited research has been carried out till date to determine the bond strength and other bond characteristics between the heat damaged concrete and FRP (Haddad et al. 2013). In view of this, the present study also attempts to investigate the behavior of bond between FRP and heat damaged concrete.
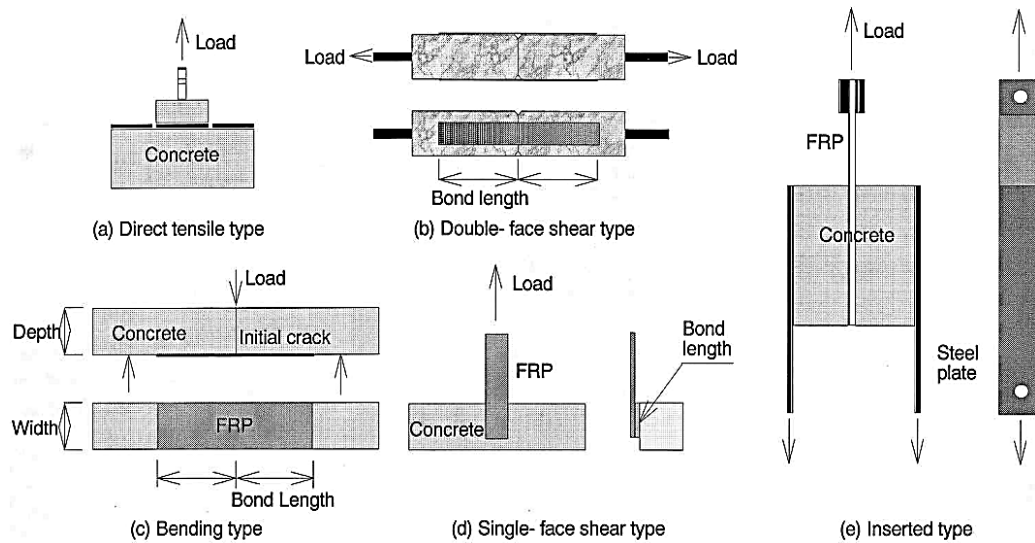
Fig.1. 13: Bond test techniques (Nakaba et al. 2001)

1.7 SUMMARY OF THE LITERATURE REVIEW

❖ Large number of research papers and reports are available on strengthening of reinforced concrete elements under normal ambient temperature conditions, while only limited studies have been carried out on strengthening and restoring of heat damaged concrete elements.

❖ Effectiveness of various commonly used techniques namely FRP wrapping, Ferro Cement (FC) jacketing, High strength fibre concrete (HSFRC) jacketing and Steel Plate (SP) jacketing in restoring and strengthening heat or fire damaged reinforced concrete elements needs to be investigated.

❖ Earlier investigations in this area, which are very few in number, have studied the strengthening of heat damaged RC elements which where cooled under normal cooling conditions only. The rate of cooling like water sprinkling or water quenching was not studied.

28

❖ Influence of cyclic temperature conditions becomes important in some situations like cooling tower, cooling container, nuclear container vessels. But strengthening of such cyclic heat damaged elements has not been studied in the past.

❖ In the previous limited number of studies on strengthening of heat damaged concrete elements, which used mainly FRP wrapping, the strength and stiffness enhancement of damaged concrete has been tried with only single layer of FRP jacketing. Thus strengthening of heat damaged reinforced concrete columns and beams with FRP wraps needs to be investigated conclusively in a more comprehensive way.

❖ In case of FRP strengthening technique, bond behavior between FRP and substrate concrete has been studied only under room temperature conditions. However, to the best of our knowledge no literature is available on bond behavior between FRP and heat damaged concrete.

❖ Design guidelines for repair and strengthening of reinforced concrete structures are available in ACI 440.2R-08 and CSA S806-02 and other similar codes under room temperature conditions only. However, no well formulated guidelines are available for strengthening of heat damaged concrete elements. Thus there is an urgent need of generating test data in this area, which can then become the essential input for the Codes and Standards.

1.8 RESEARCH OBJECTIVES

In view of the above, the main objectives of this research are:

1) To investigate the capabilities of fibre reinforced polymer (FRP) wraps, Ferro cement (FC) jacketing, high strength fiber reinforced concrete (HSFRC) jacketing and steel plate (SP) jacketing in repairing and restoring the structural performance of heat or fire damaged reinforced concrete elements.

2) To investigate the effectiveness of various strengthening techniques in restoring or strengthening of heat damaged reinforced concrete members with a special emphasis on parameters namely different elevated temperatures, rate of cooling and members damaged by cyclic heating.

3) As FRP wrapping is always considered a material of choice for the repair jobs under normal room temperature conditions, establishing its performance in restoring heat damaged reinforced concrete elements is the main focus of this

research. In this regard, investigating the bond characteristics between FRP and heat damaged concrete has been considered in detail.

4) The objective of this study is also to generate the required test data for formulating the necessary design guidelines for designing repair for the heat or fire damaged concrete structures, which would then become important for the practicing engineers who are involved in the field of repairing and strengthening of reinforced concrete structures.

1.9 SCOPE AND METHODOLOGY

In order to meet the above objectives, a detailed experimental program was undertaken. The test program was carried out in four different parts namely; 1) investigations on heat damaged reinforced concrete short circular section columns strengthened with FRP wraps, Ferro cement jacketing and HSFRC Jacketing 2) Investigations on heat damaged reinforced concrete short square section columns strengthened with FRP wraps, Ferro cement jacketing, Steel Plate jackets and HSFRC jackets, 3) Investigations on heat damaged reinforced concrete T-Beams strengthened with FRP wraps, Ferro cement jacketing and HSFRC jacketing and 4) Study on Bond behaviour between GFRP Laminates and Heat Damaged Concrete. A detailed scope and methodology adopted for the above mentioned four components has been explained below:

The whole experimental work primarily involved; casting the specimens (columns, beams and prisms), damaging the specimens by exposing them to different high temperatures, strengthening of the damaged specimens with different techniques and then testing of these strengthened and un-strengthened specimens under compression, flexure and single shear test. A total of 63 one-sixth-scale reinforced concrete short columns were cast and tested. All the specimens were of cylindrical shape (150 mm x 450 mm). The specimens were first exposed to temperatures ranging from room temperature to 900ºC. Experimental variables included temperature of exposure, type of strengthening, monotonic/ cyclic heating and type of cooling. The heat damaged specimens were strengthened with various techniques namely HSFRC, FC and GFRP jacketing. After strengthening the specimens were tested under uni-axial compression to obtain complete stress-strain response.

The second component of the experimental programme involved testing of 51 concrete short square specimens of size 150 × 450 mm. the variables included the temperature of exposure and type of strengthening scheme. After heat exposure, the heat damaged square columns which got cracked and spalled, were repaired before further strengthening. The spalled section was restored using micro-concrete. The specimens, which did not undergo any spalling, were directly strengthened by the appropriate technique. The corners of the heat damaged prisms were ground before strengthening to reduce the stress concentration at the corners of the prisms. Mechanical testing of the square columns was conducted after heating, cooling and strengthening. Monotonic concentric compression load was applied at a rate of 0.1 mm/min to capture the post peak behavior of the load deformation curve.

The third component of the experimental programme was designed to examine the efficiency of different strengthening techniques to restore the structural performance of heat damaged beams. A series of 27 reinforced concrete beams were constructed using normal strength concrete. All the beams were of same cross-section and length. Experimental variables included temperature of exposure and type of strengthening materials. Beam specimens were subjected to heat treatment using table mounted electrical furnace. The beams were exposed to two different target temperatures 600° C and 900°C after 150 days of curing. The T- beam were placed in the furnace upside down so that heat won't affect the flange directly, which indicate the real condition of the structure. The heating rate was set at 10°C /min, which has been shown to be reasonable for structures exposed to fire. Each target temperature was maintained for three hours to achieve a thermal steady state condition. The repaired heat damaged beams were strengthened at tension surface by various techniques and patterns namely HSFRC, FC and GFRP. After the strengthening process the simply supported T-beams were tested under four point loading to determine the load deflection curvatures. The performances of beams were assessed through the load deflection curves, and their individualities namely the ultimate load capacity, stiffness and ductility.

The fourth and the last component of the study was to investigate the bond behavior between FRP and heat damaged concrete. Under this part of the study, a total of 45 rectangular specimens of size150 mm x 150 mm x 300 mm were cast, heated, bonded and tested. After exposing to the desired elevated temperatures ranging from room temperature to 800°C, the concrete specimens were allowed to cool down naturally.

After heating and cooling, all the specimens were bonded with GFRP sheet. Experimental variables included temperature of exposure and bond length. Finally based on the experimental results analytical models have also been proposed for bond strength between FRP and heat damaged concrete.

1.10 ORGANIZATION OF THE THESIS

This thesis is organized in following six chapters:

Chapter 1 provides a brief introduction about the need of strengthening and gives an extensive literature review on behaviour of concrete subjected to elevated temperatures, evaluation of fire damaged concrete construction, techniques for strengthening of reinforced concrete structures, a reflection of the justification of research needs, scope and objectives of the current research, and organization of the thesis.

Chapter 2 reports the study on strengthening of heat damaged circular section short concrete columns. The properties of materials used in the experimental work, casting and heating procedures, instrumentation, testing procedure and analysis and discussion of the results are explained in detail.

Chapter 3 discusses the experimental investigations carried out on the strengthening of square section reinforced concrete short columns. All the test information including material properties, test methods and results are explained in detail.

Chapter 4 reports the methods and results of test program on strengthening of T shape reinforced concrete beam specimens.

Chapter 5 describes the test methods and results of experimental investigations on the bond characteristics between FRP and heat damaged concrete.

Chapter 6 presents the conclusions drawn from this research and scope for future research.

CHAPTER – 2

STRENGTHENING OF HEAT DAMAGED REINFORCED CONCRETE SHORT CIRCULAR COLUMNS

2.1 INTRODUCTION

Reinforced Concrete structures may require strengthening for various reasons. Heating or fire accidents in concrete structures demand repair and rehabilitation. The structures namely runways, launching pads, nuclear reactors, industrial structures, storage tanks of hot crude oils, cooling towers and skyscrapers exposed to fire temperatures, may require post heat repair and strengthening. Concrete structures generally perform well in fire and exhibit reasonably high resistance to temperature transients. However, extreme rapid heating and simultaneous cooling can cause large volume change due to thermal dilation, shrinkage due to moisture migration and eventual spalling due to high thermal stress and pore pressure build – up. Larger volume changes produce stresses resulting in micro cracking and large fractures. Majority of concrete structures are not destroyed due to fire or a thermal exposure, thereby providing the advantage of easy reparability and reusability. Many experimental studies have been undertaken in recent years to strengthen RCC columns using suitable retrofitting and strengthening techniques. Strengthening pattern involves the use of materials other than that in original structure. Conventional materials for strengthening include Fiber Reinforced Polymer, Ferro cement, High Strength Fiber Reinforced Concrete, Steel plate bonding etc. Significant research works have been undertaken on retrofitting the old concrete structures with FRP (Saadatmanesh et al. 1994, Ehsani and Jin 1998, Xiao and Wu 2000, Shamim A. Sheikh 2002, Lam and Teng 2003, Matthys et al. 2005, Shawn and Kent 2005, Omar Chaallal 2006, Sezen and Miller 2011, Kumutha et al.2007, Ilki et al. 2008, Wang and Hsu 2008, Issa et al. 2009, Eid et al. 2009, Okan 2010, Al-salloumet al. 2011, Luca et al. 2011).

A part from low maintenance cost and improvement in the service life of buildings, Fibre Reinforced polymer (FRP) wrapping has several benefits e.g. high strength, light weight, resistance to corrosion, low cost, and versatility. Also the interaction between concrete and fiber enhances concrete strength and ultimate strain. FRP jacketing is a very effective strengthening technique in columns with circular cross

section. Ferro cement (FC) is a special method, in which the wire mesh are uniformly dispersed in matrix to improve the properties such as tensile strength, flexural strength, toughness, crack control, fatigue resistance and impact resistance. Other advantages of FC include ease of availability of raw materials, which can be easily wrapped around concrete structures of various shapes and does not require skilled manpower. Increased strength and ductility was observed in FC encased short circular and square concrete columns with unreinforced and reinforced cores for both axial and eccentric loading conditions (Kaushik et al. 1990). Apparent stiffness and ultimate load carrying capacity has been increased by FC retrofit coatings in new structures and repair and rehabilitation of existing structures (Mansur and Paramasivam1985 and 1990, Kaushik et al. 1990, Nedwell et al. 1990, Seshu 2000, Abdullah and Katsuki 2003, Rathish et al. 2007, Kondraivendhan and Pradhan 2009, Xiong et al. 2011, Mourad et al. 2012, Ivy et al. 2013). HSFRC is a cementitious composite material, which offers outstanding combination of properties, such as high strength/weight ratio, high toughness, and excellent durability. HSFRC have also made striking advances and gained enormous momentum over the past few years. This is due in particular to several developments involving the matrix and the fiber-matrix interface. Several studies have previously been undertaken into the feasibility of using HSFRC for the rehabilitation and strengthening of structural members (Naaman, Shannag et al. 2002, Skazlic et al. 2009 Martinola et al. 2010, Haddad and Shannag 2007, 2008, Haddad et al. 2011).

2.2 RESEARCH SIGNIFICANCE

Till date very less research has been carried out on strengthening of heat damaged reinforced concrete columns with HSFRC, FC and FRP (Hanan Al-Nimry 2013, Yaqub et al. 2011, 2013, Bisby et al. 2011 and Leonardi et al. 2011). To the author's knowledge no such experimental studies have ever been performed on various heat damaged conditions on columns with these strengthening techniques. Thus the main aim of this research is to investigate the effectiveness of applying HSFRC, FC and GFRP jackets on various heat damaged reinforced concrete short columns.

2.3 EXPERIMENTAL PROGRAM

An experimental program was planned to investigate the effectiveness of various restoration techniques for fire damaged reinforced concrete circular section columns. A total of 63 one-sixth-scaled reinforced concrete columns were cast and tested. All the specimens were of cylindrical shape (150 mm x 450 mm). The details of the specimens

are illustrated in Table 2.1 and Fig. 2.1. Experimental variables included temperature of exposure, type of strengthening, monotonic/ cyclic heating and type of cooling. All the concrete specimens were cast in twenty three different series as shown in Table 2.1. The first two letters (CC) in the abbreviation denote circular column, the numeral (3, 6 and 9) indicates the temperature i.e. 300^0C, 600^0C & 900^0C, CY indicates cyclic heating, NA refers to Natural Cooling and WQ for Water quenching specimens. The geometry and other details of the reinforced concrete specimens are shown in Fig. 2.1. A clear concrete cover of 12.5 mm was provided between the confining tie and outer concrete surface of the specimens. A clear concrete cover of 15 mm was provided between the ends of the longitudinal reinforcement and the top and bottom surface of the specimens to prevent direct loading on the rebar during the compression testing. The hoop spacing was approximately one third to half of the core dimension of the specimen. Sufficient number of companion standard plain concrete cylinders (150 mm x 300 mm) and 150 mm cubes were also cast along with each series of main specimens. They were tested to get the average 28 days cylinder compressive strength of plain concrete (f'_c).
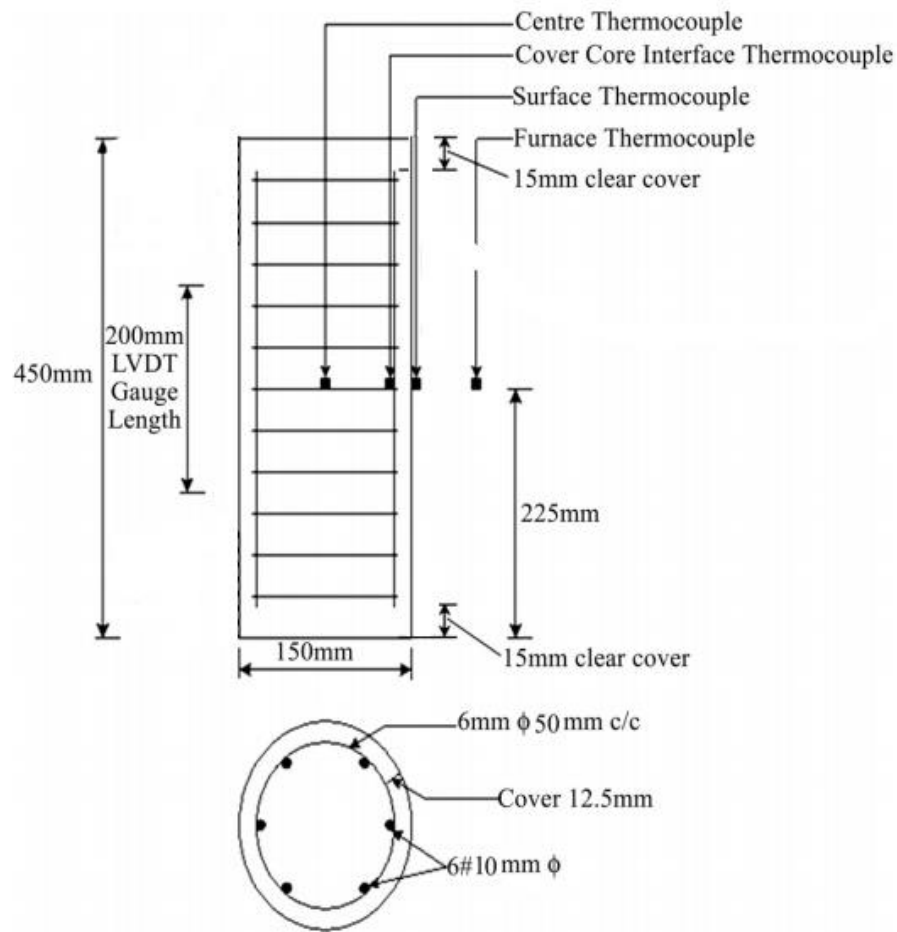
Fig. 2. 1: Size of specimens, reinforcement details and position of thermocouples

Table 2.1: Specimen details

Designation	Temperature of exposure (°C)	Wrapping Methods	Monotonic/ Cyclic Heating	Type of Cooling
CCA	Ambient	----	----	----
CC3	300	----	Monotonic	Normal
CC3 HSFRC		HSFRC		
CC3 FC		FC		
CC3 GFRP		FRP		
CC3 CY	300 CY	----	Cyclic	Normal
CC3CY HSFRC		HSFRC		
CC3 CY FC		FC		
CC3 CY GFRP		FRP		
CC6	600	----	Monotonic	Normal
CC6 HSFRC		HSFRC		
CC6 FC		FC		
CC6 GFRP		FRP		
CC9 NA	900 NA	----	Monotonic	Normal
CC9 NA HSFRC		HSFRC		
CC9 NA FC		FC		
CC9 NA GFRP		FRP		
CC9 WQ	900 WQ	----	Monotonic	Water Quenching
CC9 WQ HSFRC		HSFRC		
CC9 WQ FC		FC		
CC9 WQ GFRP		FRP		

2.3.1 Material Properties

A normal strength concrete mix was employed in the present study. The test specimens were cast using ordinary Portland cement of 43-grade, fine aggregate, coarse aggregate, tap water and steel reinforcing bars. The materials, in general, conformed to the requirements of the specifications laid down in the relevant Indian Standard Codes. The detailed characteristics of the materials are presented below:

2.3.1.1 Cement

OPC 43 grade cement conforming to IS 8112:1989 from single lot was used for preparing concrete mixes throughout the course of this investigation. To prevent the cement from the atmospheric effect, it was stored in an air tight silo available in the laboratory as soon as it was received. The collected cement samples were thoroughly tested in the laboratory to establish their feasibility according to the appropriate Indian standards (IS 4031:1988 and IS 4032:1985).The physical properties of the cement are

presented and compared with the requirements of IS: 8112 (1989) in Table-2.2. The chemical properties of cement are tabulated in Table 2.3.

Table 2. 2: Physical properties of cement

Characteristics	Result Obtained	Recommended values per IS 8112:1989 (BIS 1989)
Grade of cement	OPC 43	-
Specific gravity	3.14	-
Standard consistency of cement (%)	28	30
Setting time (i) Initial setting time (minimum) (ii) Final setting time (maximum)	 68 190	 30(minimum) 600(maximum)
Compressive strength (a) 3 days strength of cement (N/mm^2) (b) 7 days strength of cement (N/mm^2) (c) 28 days strength of cement (N/mm^2)	 23.80 35.50 44.10	 23 33 43
Soundness Le Chatelier method (mm)	1	10 (maximum)
Fineness of cement (m^2/Kg)	308	225(minimum)

Table 2. 3: Chemical composition of OPC 43 cement

Oxide	Test results (%)	Limiting % values specified as per is 8112: 1989
Silicon dioxide (SiO$_2$)	21.6	19-24
Sulfur trioxide (SO$_3$)	1.5	≤ 3
Ferric Oxide (Fe$_2$O$_3$)	3.9	1-4
Alumina(Al$_2$O$_3$)	5.2	3-6
Calcium Oxide(CaO)	61.7	59-64
Magnesia Oxide(MgO)	2.4	≤ 6
Sodium Oxide(Na$_2$O)	0.23	≤ 0.6
Potassium Oxide (k$_2$O)	0.18	-
LOI	1.1	≤ 5
IR	1.2	≤ 2

2.3.1.2 Steel reinforcing bars

Reinforcing bars of 10 mm diameter and of 469MPa yield strength were used as longitudinal reinforcement, while reinforcing steel of 548MPa yield strength with a diameter of 6 mm were used as lateral hoop reinforcement. The average stress-strain behavior of reinforcement bar, are shown in Fig. 2.2.
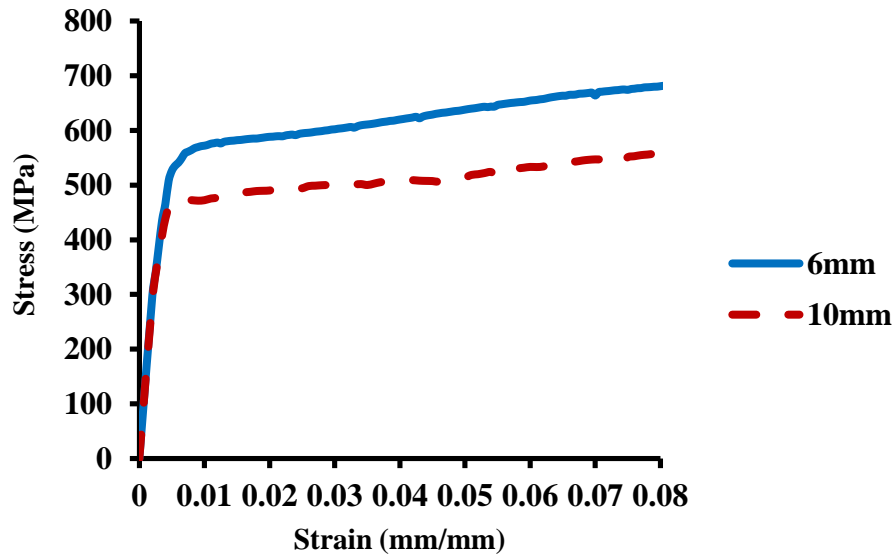
Fig. 2. 2: Stress-strain curve for reinforcing bars at ambient temperature

2.3.1.3 Fine aggregate

Locally available river sand was used as fine aggregate. The particle size distribution (sieve analysis) and other physical properties of the fine aggregate are given in Tables 2.4 and 2.5 respectively. On the basis of particle size distribution, the fine aggregate falls under zone II of IS 383 - (BIS 2002).

Table 2. 4: Sieve analysis of fine aggregate

IS Sieve designation	Weight retained (gm)	percentage weight retained	Cumulative % of weight retained	Cumulative % weight Passing	% Passing for grading zone- II IS 383:1970
10 mm	0	0	0	100	100
4.75 mm	15	1.5	1.5	98.5	90-100
2.36 mm	126	12.6	14.1	85.9	75-100
1.18 mm	173	17.3	31.4	68.6	55-90
600 μ	217	21.7	53.1	46.9	35-59
300 μ	326	32.6	85.7	14.3	8-30
150 μ	125	12.5	98.2	1.8	0-10
Residue	18	1.8	-	-	-
Total	1000	100	284		

Table 2. 5: Physical properties of fine aggregate

Characteristics	Requirements per IS 383: 1970	Obtained results
Grading	-	Conforming to grading Zone – II
Fineness modulus	2.0 to 3.5	2.84
Specific gravity	2.6 to 2.7	2.65
Water absorption (%)	-	1.41
Moisture content (%)	-	1.40

2.3.1.4 Coarse aggregate

Locally available crushed stone aggregate of maximum nominal size of 12.5 mm brought from a single source was used. Sieve analysis and other physical properties of the aggregate are given in Tables 2.6 and 2.7 respectively. Coarse aggregates were also first sieved through a 150 micron size sieve to remove dirt and other foreign material.

Table 2. 6: Sieve analysis of coarse aggregates

IS Sieve Designation	Weight retained (grams)	Percentage of weight retained (%)	Cumulative percentage of weight retained (%)	Percentage of weight passing (%)	Range specified for 12.5 mm downgraded coarse aggregate per IS 383:1970
20 mm	0	0	0	100	100
16 mm	0	0	0	100	-
12.5 mm	365	7.3	7.3	92.7	90-100
10 mm	725	14.5	21.8	78.2	40-85
4.75 mm	3870	77.4	99.2	0.8	0-10
2.36 mm	30	0.6	99.8	0.2	-
Residue	10	0.2	100	-	-
Total	5000	100.0	228.1	-	-

Table 2. 7: Physical properties of coarse aggregates

Characteristics	Requirements per IS 383: 1970	Obtained results
Fineness modulus	5.5 to 8	7.15
Specific gravity	2.6 to 2.7	2.70
Density (loose), kN/m^3	-	15.2
Water absorption (%)	-	0.87
Moisture content (%)	-	Nil

2.3.1.5 Water

The water for both mixing and curing of concrete should be free from deleterious materials. Thus potable water is usually used for this purpose. In the present investigation, potable tap water was used during the entire casting and curing period. The physical and chemical test results of the water are given in Table 2.8 and it can be observed that the water satisfied the requirements mentioned in IS 456 (BIS 2000).

Table 2. 8: Physical and chemical test results of water

Parameters/Tests	Units	Obtained results	IS limits per IS 456:2000 (Construction water)
pH	-	7.3	Not<6.00 (max)
Alkalinity	mg/L	235	250 mg/L (max)
Acidity	mg/L	18	50 mg/L (max)
TSS	mg/L	7	2000 mg/L (max)
Total organic solids	mg/L	10	200 mg/L (max)
Total inorganic solids	mg/L	40	3000 mg/L (max)
SO$_2$	mg/L	265	400 mg/L (max)
Chlorides	mg/L	457	2000 mg/L for concrete (max)

2.3.1.6 Silica fume

In the present investigation, silica fume of grade 920 U (including the silica content of more than 90 %) was used in slurry form. The physical and chemical properties of the chosen silica fume are presented in Table 2.9. It satisfied the requirements of relevant Indian standard IS 15388: 2003.

Table 2. 9: Physical and chemical test results of silica fume

Properties	Silica Fume (%)
Specific gravity	2.27
Silicon dioxide (SiO2)	92.4
Sulfur trioxide (SO3)	1.23
Ferric Oxide (Fe_2O_3)	1.2
Alumina(Al_2O_3)	3.8
Calcium Oxide(CaO)	31.6
Magnesia Oxide(MgO)	2.6
Sodium Oxide(Na_2O)	0.45
Potassium Oxide (k_2O)	0.32
LOI	3.07
IR	11.1

2.3.1.7 Super-plasticizer

A commercially available high range water-reducing admixture namely Glenium-51 based on modified poly-carboxylic ether (PCE) polymer confirming to IS 9103-1999, with specific gravity 1.10 and pale colour was used to prepare the slurry of required workability. The properties of super-plasticizer are presented in Table 2.10

Table 2. 10: Properties of super plasticizer

Properties	Values
PH	6.70
Relative density	1.10
Turbidity (NTO)	33.72
Ash Content	0.20
Solid Content	9.2

2.3.1.8 Fibre reinforced polymer (FRP)

The FRP composite used in the present study was of unidirectional E-Glass type fiber in resin. The properties of the dry fiber reinforced polymer as provided by the manufacturers are as shown in the Table 2.11

Table 2. 11: Properties of FRP composites

Type of Fiber	Fiber weight	Fiber density	Thickness	Tensile Strength	Elongation at Rupture
E – Glass 90/10	910 g/m²	2.75g/cm³	0.324mm	3400N/mm²	4.3%

2.3.1.9 Epoxy resin

The adhesives used for the wrapping of GFRP was of two types namely; primer and saturant. Each of the two solutions again comprised of two solutions; namely, resin and hardener which were mixed in equal ratio. Primer solution was used for the surface preparation of the concrete prior to the wrapping of GFRP and the saturant solution was applied after the application of the GFRP on the concrete surface. The properties of both the solutions are given in the Table 2.12 and Table 2.13.

Table 2. 12: Properties of primer

Sr.no	Property	Value
1	Mix Proportion	Part A : Part B = 1 : 1 By Weight
2	Form	Liquid
3	Mixed Density	1.09 Kg/ltr
4	Pot Life	60 Mins +/- 15 mins
5	Drying Time	7 – 9 Hours
6	Bond Strength	Failure in Concrete

Table 2. 13: Properties of saturant solution

Sr.no	Property	Value
1	Mix Proportion	Part A : Part B = 1 : 1 By Weight
2	Form	Liquid
3	Mixed Density	1.15 Kg/ltr
4	Pot Life	30 Mins +/- 15 mins
5	Bond Strength	> 2 N/mm2
6	Compressive Strength	70 N/mm2 at 7 days

2.3.1.10 Welded wire mesh

Welded wire meshe in the form of square grid mesh, which was locally available in the market, was used as the reinforcement in Ferro cement jacket. The properties of the welded wire mesh are given in Table 2.14
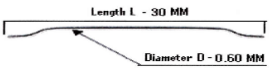
Table 2. 14: Properties of welded wire mesh

Type	Shape	Fabrication type	Wire Spacing in(mm)	Wire Diameter in (mm)	Yield Strength (MPa)
Steel Mesh	Square	Welded	13	0.96	385

2.3.1.11 Steel fiber

Hooked end type steel fibers were used throughout the investigation, wherever required. A volume fraction of 2% steel fiber was used in slurry mix for HSFRC jackets. The chemical composition of the fiber as supplied by the manufacturer was: Carbon = 0.039%, Manganese = 0.394%, Silica = 0.35 %, Sulphur = 0.010%. The physical properties of steel fiber are presented in Table 2.15.

Table 2. 15: Properties of steel fiber

Types of fiber	Geometrical configuration	Tensile Strength Fy(MPa)	Fiber diameter (mm)	Fiber length (mm)	Aspect ratio (L/D)	Tolerance
Hooked End	Length L - 30 MM Diameter D - 0.60 MM	1120	0.60	30	50	D/L ±10 %

2.3.1.12 Bonding agent

Bonding Agent is a two part solvent free bonding agent composed of liquid epoxy resin and hardener. It is used for bonding of structural concrete new to old concrete. This was used to restore the section of concrete lost by thermal spalling. The properties of epoxy resin are as given in the Table 2.16.

Table 2. 16: Properties of epoxy resin

Sr.no	Property	Value
1	Mix Proportion	Part A : Part B = 1 : 0.87 By Weight
2	Form	Liquid
3	Mixed Density	2-3m^2/ Kg
4	Pot Life	40Mins +/- 15 mins
5	Bond Strength	Failure of concrete
6	Compressive Strength	60 N/mm2 at 7 days

2.3.1.13 Micro concrete

Micro Concrete is supplied as a ready to use dry powder which requires only addition of clean water at site to produce a free flowing no shrink repair micro concrete. This is a cementitious material, with additives, which impart controlled expansion characteristics in the plastic state while minimizing water demand. The properties of micro concrete are as given in the Table 2.17. This material was used in restoring the section of spalled members.

Table 2. 17: Properties of micro concrete

Sr.no	Property	Value
1	Mix Proportion	3.75 - 4 liter water / 25kg
2	Form	Powder
3	% of water observation	0.45
4	Chloride content	Nil
5	Flexural Strength	>5 N/mm2
6	Compressive Strength	50 N/mm2 at 28 days

2.3.2 Concrete Mix

A normal strength concrete mix was designed and proportioned on the basis of guidelines laid down in IS: 10262 (BIS 2009). This concrete mix was used to fabricate the test specimens. The details of the designed mix proportions along with the 28-days and 90-days cylinder compressive strengths are given in Table 2.18.

Table 2. 18: Concrete mix proportions

Cement (Kg/m³)	Water (Kg/m³)	Sand (Kg//m³)	Coarse aggregate (Kg/m³)	Cylinder Compressive Strength, fc'(MPa)	
				28 days	150 days
450	202.5	658	1034	37.19	42.19

2.3.3 Mixing, Casting and Curing of Specimens

The quantities of various ingredients of the concrete viz. cement, sand, coarse aggregate and water were kept ready for the required proportions of each batch of casting. In the beginning, the fine aggregate and cement were mixed thoroughly to get a uniform mix in the dry state. The uniformity was indicated by the uniform colour of the dry mix and no concentration of any one material being visible. Then, the coarse aggregate were added to this dry mix and turned over many times in the dry condition

itself in a tilting type rotary drum mixer for about one minute. About 50% of the total water was then added slowly to get a uniform mix. After this, the remaining water was added and mixing was continued for about one minute. Before placing the green concrete in to the moulds the workability of concrete was measured in terms of both compaction factor and slump (Fig. 2.3). A desired level of workability was achieved for the mix of various batches. The average results of slump and compaction factor for the mixes of the two series are shown in Table 2.19. The moulds for casting the specimens were cleaned, brushed, oiled and placed on a vibrating table with a speed range of 12000 ± 400 revolutions per minute and an amplitude range of 0.055 mm. The green concrete was placed in the moulds in three layers and then the molds were vibrated properly to get a good compaction. The specimens were cast using steel moulds available in the laboratory.

Fig. 2. 3: Slump test of green concrete

Table 2. 19: Results of compaction factor and slump tests

Specimens of various series	Compaction factor	Slump (mm)
CCA	0.900	70
CC3	0.926	76
CC3 CY	0.908	72
CC6	0.916	80
CC9 NA	0.920	86
CC9 WQ	0.918	78

The day after the specimens were cast, they were de-molded, marked and immersed in water for curing. The curing period lasted for 28 days after which the specimens were kept in the lab atmosphere for another 120 days. Fig. 2.4 shows the various stages of test specimens during casting and curing.

Fig. 2. 4: Stages of casting, de-moulding, curing and laboratory condition of specimens

The surfaces of all the specimens were painted with white colour to enable monitoring of cracks during the testing. After 150 days of total ageing, the specimens were exposed to a single cycle of heating and cooling in a programmable electric furnace. Before the thermal exposure, three companion cubes were oven dried at 105 °C until constant mass is achieved in order to determine the moisture content. The moisture content of cubes was assumed to represent the moisture content of test specimens as the test specimens and the cubes were exposed to similar ageing conditions. The moisture

content ranged between 2.16 % to 2.28 % for the companion cubes of both the series as shown in Table 2.20.

Table 2. 20: Moisture content of companion cubes

Series of specimen	Moisture content % (by mass)
CCA	2.23
CC3	2.26
CC3 CY	2.16
CC6	2.21
CC9 NA	2.28
CC9 WQ	2.18

2.3.4 Heating of Specimens

The reinforced concrete column specimens were exposed to different chosen heating and cooling regimes in a high temperature muffle furnace. An electric furnace having outer dimensions 192 cm wide x 105 cm deep x 96 cm high, capable of attaining a maximum temperature of 1200°C (Fig. 2.5) was employed. The temperature inside the furnace was recorded with the help of thermocouples. The thermocouples were installed in the column during casting at three different locations i.e. at surface, cover-core interface and center of the specimen to monitor the temperature inside the column during heating regime (Fig. 2.1). The specimens were heated at different target temperatures ranging from 300°C to 900°C. Normally, maximum temperatures in the range of 1000°C to 1200°C are generally reached during fires. However, such high temperatures occur only at the surface of the structural elements and that too for a short duration. Therefore, a maximum target temperature of 900 ^{0}C was considered to be reasonable for the investigation. The lower limit of the maximum exposure temperature was taken as 300°C, because no significant effects were found on the residual properties of heated concrete below this temperature (Mohamedbhai 1986, Zhang et al. 2000, Zaidi et al. 2012). The heating rate was set at 10°C /min., which has been shown to be realistic for structures exposed to fire (Wu et al. 2002, Chen et al. 2009, Aydm and Baradan 2007, Peng et al. 2006). The target temperature was maintained and the thermal steady state

condition was achieved (Fig. 2.6a-c). After exposing specimens to the target temperatures for the desired time duration, the furnace was switched off and the samples were left in the furnace to allow natural cooling to room temperature. The rate of cooling was not controlled but the decrease of temperature in the furnace was measured through thermocouples during the whole cooling phase. The specimens, CC9WQ, were not cooled naturally, rather water quenching was employed, Fig. 2.7. The rate of cooling was not controlled but was measured constantly during complete testing. Data acquisition system was used for obtaining the thermocouple readings.

Fig. 2. 5: A view of furnace and Data logger
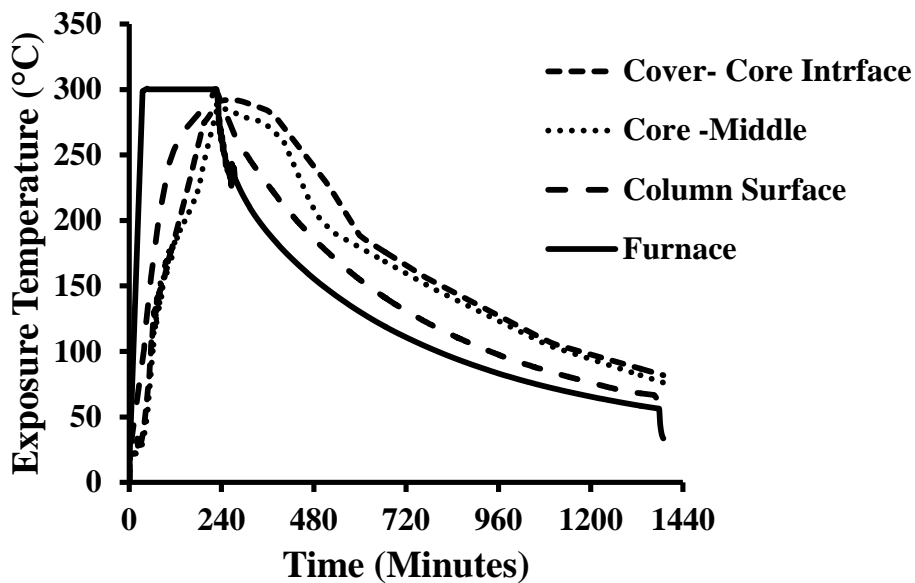
CC3 specimens exposed to 300°C

Fig. 2. 6: (a)-(c) - Typical time-temperature curves (contd.)
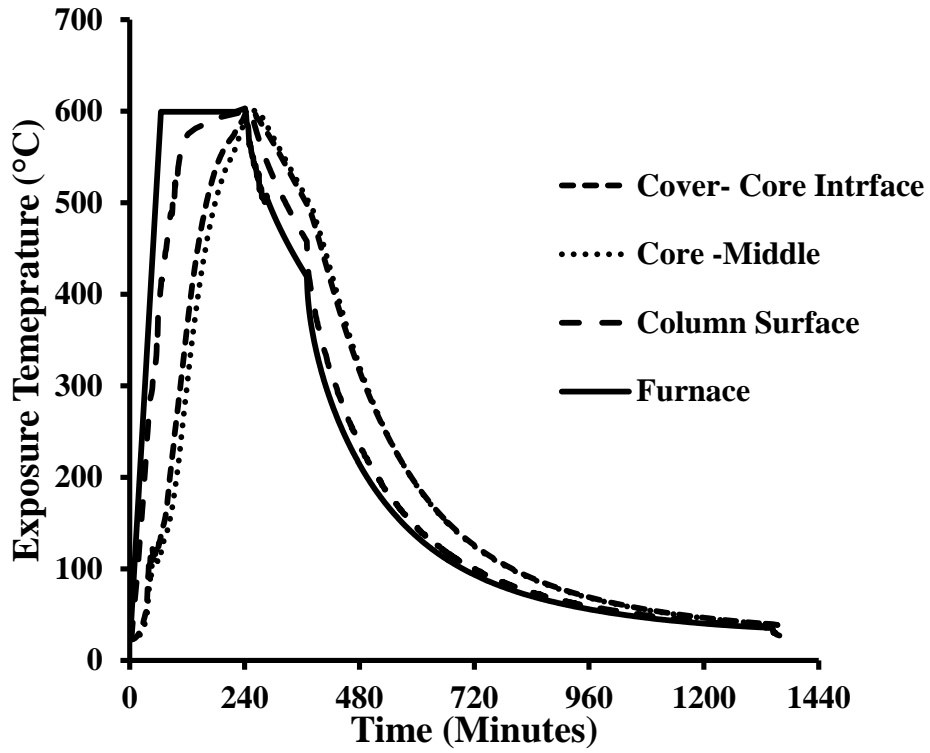
CC6 specimens exposed to 600 °C
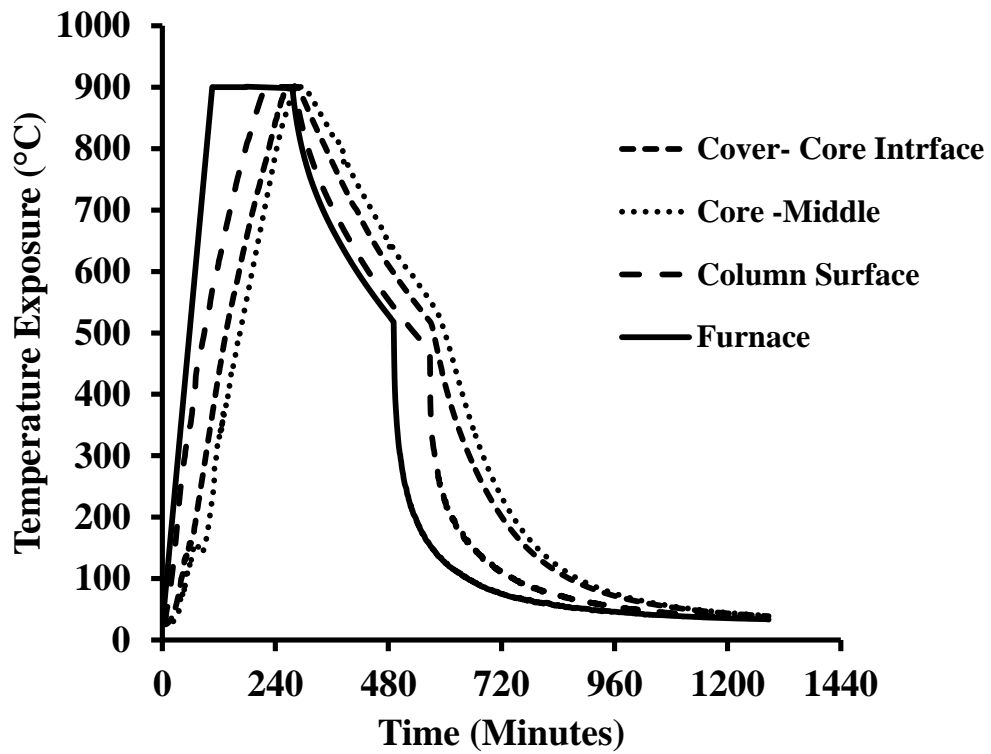
CC9 specimens exposed to 900 °C

Fig. 2.6: (a)-(c) - Typical time-temperature curves

Fig. 2. 7: Stages of Water Quenching

2.3.5 Observations after Heating

Heat induced damages in concrete specimens can be roughly detected by observing the concrete's surface. An assessment of fire damaged concrete usually starts with visual observation of colour change, cracking and spalling of concrete surface. In this study the colour of concrete changed to pink when the specimens were exposed to 300°C temperature and became light greyish at 600°C. However, the colour of specimens changed to ash white when exposed to 900°C. There was no visible cracking on the surface of the specimens heated up to 300°C. However some hairline cracks were observed at 600°C. The number of cracks became relatively pronounced at 900°C. The structure of the cement mortar after temperature exposure was observed to have become loose because of the pore expansion owing to the vaporization of the absorbed water. No spalling was noted in any of the heated and naturally cooled specimens. However in case of water quenched specimens spalling was observed (Fig. 2.8). During the cooling, the ionized CaO decomposed from Ca (OH)2 absorbed water and then became Ca (OH)2 again, which resulted in the expansion of the concrete volume (Zaidi et al. 2012 and Mehmet 2013).

50

Fig. 2. 8: Surface cracking and spalling observed in test specimens exposed to 900 °C and cooled naturally and water quenched

2.3.5.1 Ultrasonic pulse velocity testing

Ultrasonic pulse velocity (UPV) testing was conducted on each group of specimens before heating and seven days after heating. The transmitting and receiving transducers were placed on the opposite faces of the concrete columns and transducers were pressed firmly against the column surfaces until an unchanging reading was observed. The distance between the transducers was divided by the transit time to obtain the pulse velocity through the concrete. Three readings were taken in each column. Ultrasound values were then recorded by hand. The ultrasonic pulse velocity test results for all the specimens are shown in Fig. 2.9. This indicates that up to 400°C, the residual unstressed strength reduced rather gradually and above this temperature, it dropped sharply. This is due to the fact that above 500°C, the calcium silicates commence to decompose into quick lime and silica. This process is irreversible and there is a progressive loss of strength.

51
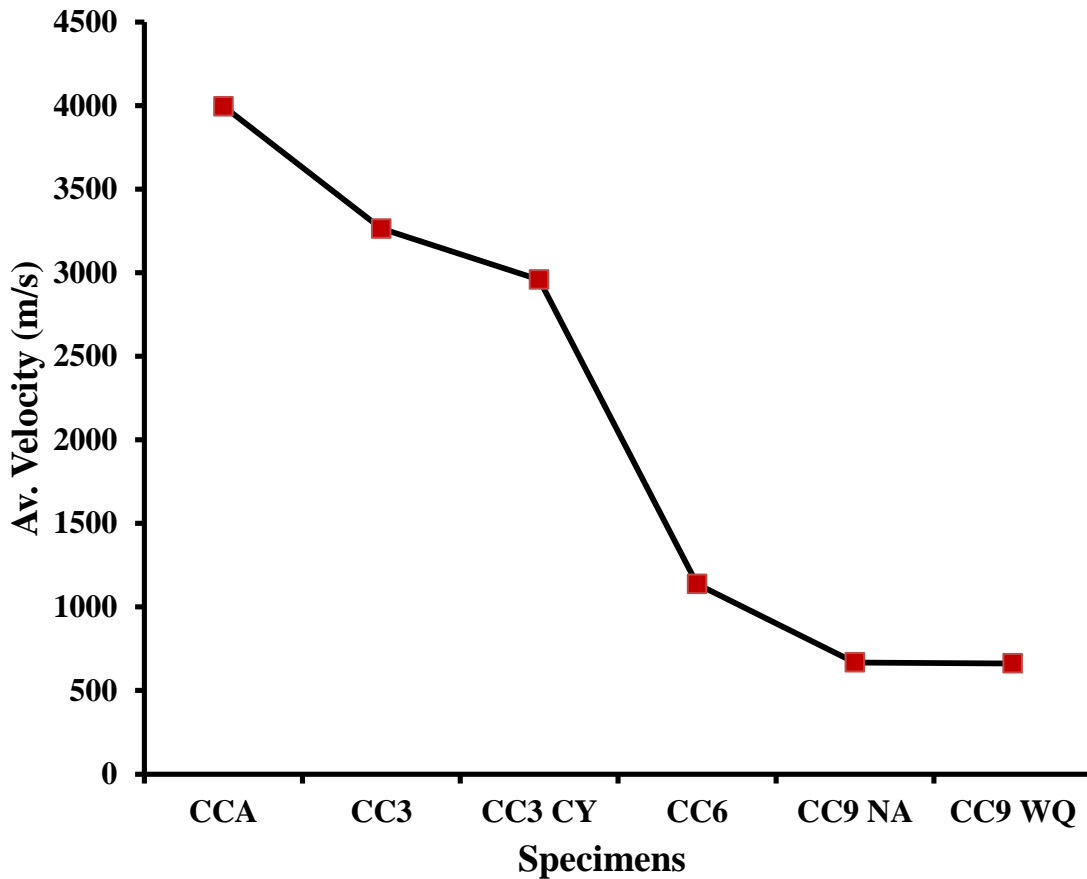
Fig. 2. 9: Ultrasonic pulse velocity v/s temperature

2.4 REPAIRING OF HEAT DAMAGED SPECIMENS

After heating and cooling the heat damaged specimens were inspected for damage and restoration. The specimens, which got spalled, were repaired with micro concrete before going ahead with the chosen strengthening schemes. These were the specimens heated to 900 °C temperature as other specimens heated at lower temperatures did not require section restoration. They were first repaired and their section was restored before wrapping. The porous concrete was removed using steel wire brush, chisels and hammer. The surfaces of specimen were cleaned thoroughly to ensure no dust. A bonding agent was applied on the surface of the specimen to achieve good bond between old concrete and new repair material i.e. micro concrete. The micro concrete was applied above the bonding agent with the help of a steel trowel, as shown in Fig. 2.10. The repaired reinforced concrete columns were cured for fourteen days in the laboratory atmosphere until strengthening.

Fig. 2. 10: Application of bonding agent and application of micro concrete

2.5 STRENGTHENING OF HEAT DAMAGED SPECIMENS

After repairing the heat damaged specimens, wherever required, all the specimens were strengthened with various techniques namely HSFRC, FC and GFRP jacketing. In all the specimens a primer epoxy bonding was applied after the surface was cleaned in order to provide good bonding between the substrata and the new strengthening material. A gap of 20 mm in un-strengthen concrete was left at the ends of concrete specimen to prevent jacket from direct loading while testing.

2.5.1 High Strength Fiber Reinforced (HSFRC) Strengthening

The heat damaged specimens meant for strengthening with HSFRC jacketing after surface preparation were placed vertically. Epoxy bonding agent was applied on the surface of the column to fill micro cracks and to provide a bond between the heat damaged concrete and HSFRC jacket. HSFRC slurry reinforced with hooked steel fiber at a volume fraction of 2% was poured into the moulds to form a 25 mm thick jacket around the specimens as shown in Fig. 2.11. Three companion cubes of 50 mm x 50mm were cast from the same slurry mix in order to monitor the strength of HSFRC jacket.

The column and cubes were then cured under moist condition using wet gunny bags for fourteen days. After fourteen days, the column and cubes were air cured at room temperature until testing.

Fig. 2.11: Stages of HSFRC jacketing

2.5.2 Ferro Cement (FC) Strengthening

After surface preparation, the heat damaged specimens were kept vertically, bonding agent was applied on the surface of the column to fill micro cracks and to provide a bond between the concrete and ferrocement laminate. The length and width of the wire mesh was cut with respect to the size of heat damaged column together with an additional 100 mm extra for overlapping. The column was wrapped with two layers of wire mesh, the first and the second layers of the wire mesh were tied together with steel wire at various locations. An overlap of 100 mm was provided in the lateral direction of the wire mesh. Wooden mallets were used to keep the wire mesh close to the surface of circular specimens. Slurry with high compressive strength of about 68.06 MPa was poured into the mould to form 25mm thick FC jacket. A clear cover of 20mm was

provided between the Ferro cement jacket and the ends of the column (Fig.2.12) to avoid direct axial loading on the jacket during testing.

Fig. 2.12: Stages of FC jacketing

All specimens were covered with damp gunny bags for fourteen days to maintain moisture condition. After fourteen days, the FC jacketed column and cubes were air cured at room temperature until testing.

2.5.3 Glass Fiber Reinforced Polymer (GFRP) Strengthening

Before GFRP jacketing the surface of the specimens was scraped lightly to remove surface contaminants. Firstly the surface of the concrete was coated with a layer of epoxy primer on the external surfaces of the concrete to fill air voids and to provide good bond strength. Thereafter, a thin layer of the two part saturant solution consisting of resin and hardener mixed as per the manufacturer's specifications was applied over the specimens. Then the first layer of GFRP sheets was wrapped around the specimen carefully. A roller was used to remove the entrapped air between the fiber and excess saturant so as to allow better impregnation of the saturant. Special attention was taken to

ensure that no air voids were left between the fiber and the concrete surface. After the application of the first wrap, a second layer of saturant solution was applied on the surface of the first layer with a lap of 100 mm in length. The roller was used again to remove any trapped air and to force the resin in the fibers (Fig. 2.13). All the specimens were stored at room temperature for at least 28days before testing.

Fig. 2.13: Stages of GFRP jacketing

2.6 INSTRUMENTATION AND TEST SETUP

The specimens were tested after complete cycle of heating, cooling and strengthening. Wooden ply piece of 3 mm were placed at the ends of the specimens before testing to ensure leveled surfaces and to distribute the load uniformly. The specimens were tested under monotonic concentric compression at a constant displacement rate of rate of 0.1mm/min to capture the complete post peak behavior using 2500 KN capacity UTM. The axial deformation of the specimens at the central region (gauge length 200 mm) was monitored with the help of two linear variable displacement transducers (LVDT). Two horizontal LVDTs were also fixed on opposite faces of the column (Fig. 2.14). Loads were recorded through in built load cell in the UTM. The

recorded data from the LVDTs and load cell were fed into a data acquisition system and stored on a computer.

Fig. 2.14: Test set up and arrangement of instruments on control specimens and on strengthen specimens

2.7 ANALYSIS AND DISCUSSION OF RESULTS

The results are given in the Tables 2.21 to 2.24 and the load strain curves are shown in (Figs. 2.20 to 2.25). Both axial and lateral displacements were measured. Tables provide the summary of results in terms of peak load, peak strain, secant stiffness and energy dissipation for the various specimens. Each result is the average of three tests. The main variables investigated in this part of the study was, the presence of heat damage, type of cooling, cyclic heating and type of repairing materials (GFRP, FC, HSFRC). The results are presented graphically in terms of load-deformation and stress-strain response based on the test data. The axial compressive behaviour of strengthened columns in terms of their stiffness, ductility, ultimate strain and the ultimate strength is evaluated and compared to those of the control specimens and heated damaged specimens. Load strain curves were plotted and strength, stiffness and deformability were computed.

2.7.1 Test Observations and Failure Modes

The reinforced concrete columns were tested under monotonic compression up to failure. The entire mechanical testing was carried out under room temperature. Crushing

failure was observed in all control and heat damaged columns (Fig. 2.15), at the ends due to the effect of stress concentration in these regions (Kumutha et al. 2007). The failure was particularly brittle, sudden and explosive, in nature in case of control specimens. But in case of heat damaged specimens the failure was gradual and exhibited ductile behavior with the increase in load (Yaqub 2011 and 2013). In case of specimens heated to 900°C, as the lateral ties got exposed to heat due to spalling of cover concrete, a crushing failure and opening of ties was noted.
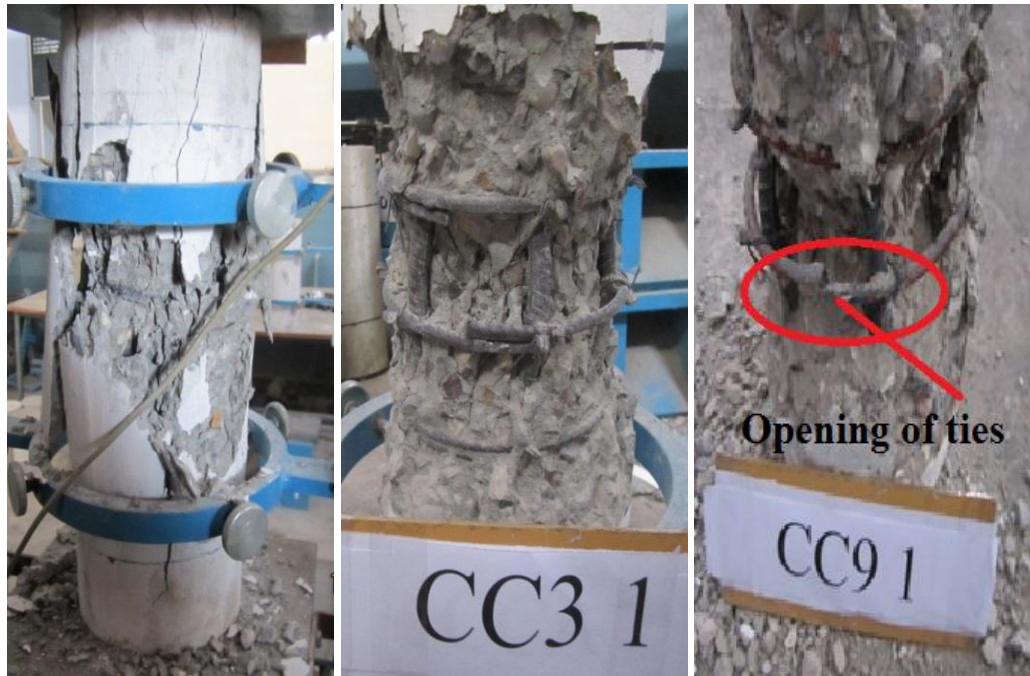
Fig. 2.15: Buckling of rebars, opening if ties and crushing failure of control and heat damaged specimens

In HSFRC jacketed columns, the failure initiated at top and bottom of the specimen due to stress concentration during loading (Kumutha et al. 2007). Diagonal and vertical cracks were observed in the specimen. Propagation and widening of vertical cracks was observed with the increase in loading after the specimen had reached its peak loading capacity. At this point; an increase in load created noise due to breaking of steel fiber, thereby indicating the stress transfer from the dilated concrete to the jacket. Bonding between the HSFRC jacket and core concrete remained enough and de-bonding was never observed throughout the test (Fig. 2.16). Generally in FC jacketed specimens also, the initial cracks formed at the ends of the specimen. With gradual increase in loading numerous vertical cracks were observed throughout the surface of the specimen. Beyond peak load the wire mesh started to bulge with breaking noise. This condition was observed in all the FC specimens. The steel wires of the welded mesh in the vertical

direction bulged, whereas those in horizontal direction got broken in full length of the specimens, resulting in crack propagation throughout the length of the specimen in vertical direction. In this case the failure and separation between the core and FC laminates was observed. The FC jacketed specimen's failure mode is shown in Fig. 2.17.

Fig. 2.16: Failure pattern of heat damaged reinforced concrete columns strengthened by HSFRC jacket

Fig. 2.17: Failure pattern of heat damaged reinforced concrete columns strengthened by FC jackets

59

The GFRP jacketed columns experienced a gradual failure in the initial stage, and ended with a sudden and explosive noise. It was observed that for the GFRP wrapped specimens, the jackets ruptured outside the overlap position at both the ends (Fig. 2.18). This is due to maximum stress concentration at these regions. In the specimen repaired with GFRP, prior to failure, a cracking noise was heard, indicating significant activation of the GFRP jackets. At the time of failure, loud noise was heard. The sudden and explosive failure indicates release of enormous amount of energy. The visual inspection of tested columns showed good bond between the jacket and the concrete representing no de-bonding at any stage of tests.

Fig. 2. 18: Failure pattern of heat damaged reinforced concrete columns strengthened by GFRP jacket

2.7.2 Influence of HSFRC, FC and GFRP Strengthening on Axial Strength

The heat damaged specimens were strengthened using different techniques including HSFRC, FC and GFRP. Fig. 2.19 shows the average axial compressive strength of the tested columns. It can be seen that a reduction in strength in the range of 4% to 81% was observed after heating the specimens. The Strength of heat damaged HSFRC jacketed specimens was higher than the heat damaged unstrengthen specimens, but still remained less than the control specimens in all cases as shown if Fig. 2.19. In case of FC jacketed specimens the axial compressive strength was higher than the

unstrengthen heat damaged specimens, but remained less than the control specimens except for 300°C heat damaged specimens, Fig. 2.19. The strength of GFRP jacketed specimen was considerably higher than both the heat damaged unstrengthen specimens and the control specimens. Since GFRP wrapping becomes active after core concrete fails due to the compressive forces, expansion of the concrete core in the radial direction makes the GFRP more and more active in resisting the axial compressive force. The average strength of heat damaged specimens strengthened with two layer of GFRP jackets was observed to have increased by 106%, 104%, 83%, 31% and 18% compared to that of control unheated specimens and 114%, 121%, 160%, 540% and 532% compared to that of the heat damaged specimens. It was observed that in control and heat damaged specimens the lateral ties opened at the overlap position (Fig. 2.15). The same behaviour was observed in specimen strengthened with GFRP; however the failure load was greater and was defined by failure of GFRP. This shows that the lateral steel tie confinement becomes insignificant when the columns are confined by both steel ties and FRP jackets.
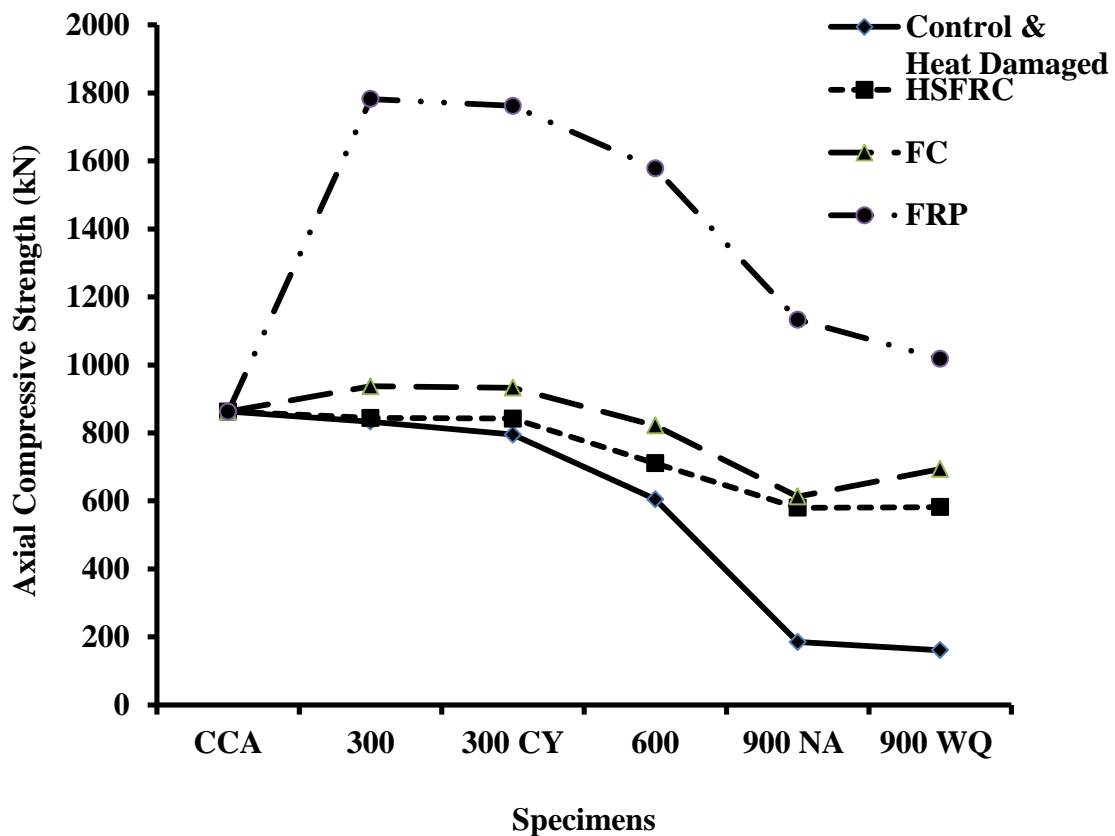
Fig. 2. 19: Axial compressive strength of Specimens

Table 2. 21: Test results

Specimen Designation	Peak Load Pu(kN)	Strain at Peak ε_{cc}	Strain at 0.8 Peak ε_{c80c}	Secant Stiffness (kN/mm)	Energy Dissipation (kN.mm)
CCA	863.14	0.00845	0.0107	513.690	1399
CC3	833.42	0.00850	0.0117	490.247	1519
CC3 HSFRC	844.97	0.00480	0.00805	880.177	1150
CC3 FC	937.81	0.00533	0.00755	884.726	1189
CC3 FRP	1782.3	0.01345	0.01425	662.565	4082
CC3CY	795.74	0.00794	0.01005	503.632	1190
CC3CY HSFRC	842.08	0.00659	0.0086	657.875	1194
CC3CY FC	933.73	0.00458	0.00645	1026.076	971
CC3CY FRP	1792.72	0.01360	0.0141	659.088	3436
CC6	605	0.01289	0.01915	236.328	1882
CC6 HSFRC	711.27	0.00659	0.00860	542.954	1074
CC6 FC	822.27	0.00713	0.00915	579.204	1254
CC6 FRP	1578.05	0.01737	0.0183	454.769	3680
CC9 NA	177.75	0.03420	0.0368	25.9868	945
CC9 NA HSFRC	580.126	0.00703	0.01305	414.375	1184
CC9 NA FC	613	0.00802	0.0127	383.125	1329
CC9 NA FRP	1133.12	0.04200	0.0429	134.895	6449
CC9 WQ	161.03	0.02421	0.0254	33.202	630
CC9 WQ HSFRC	582.29	0.00831	0.0117	350.777	990
CC9 WQ FC	694.87	0.00750	0.00925	460.178	959
CC9 WQ FRP	1018.33	0.02234	0.0247	227.814	3208
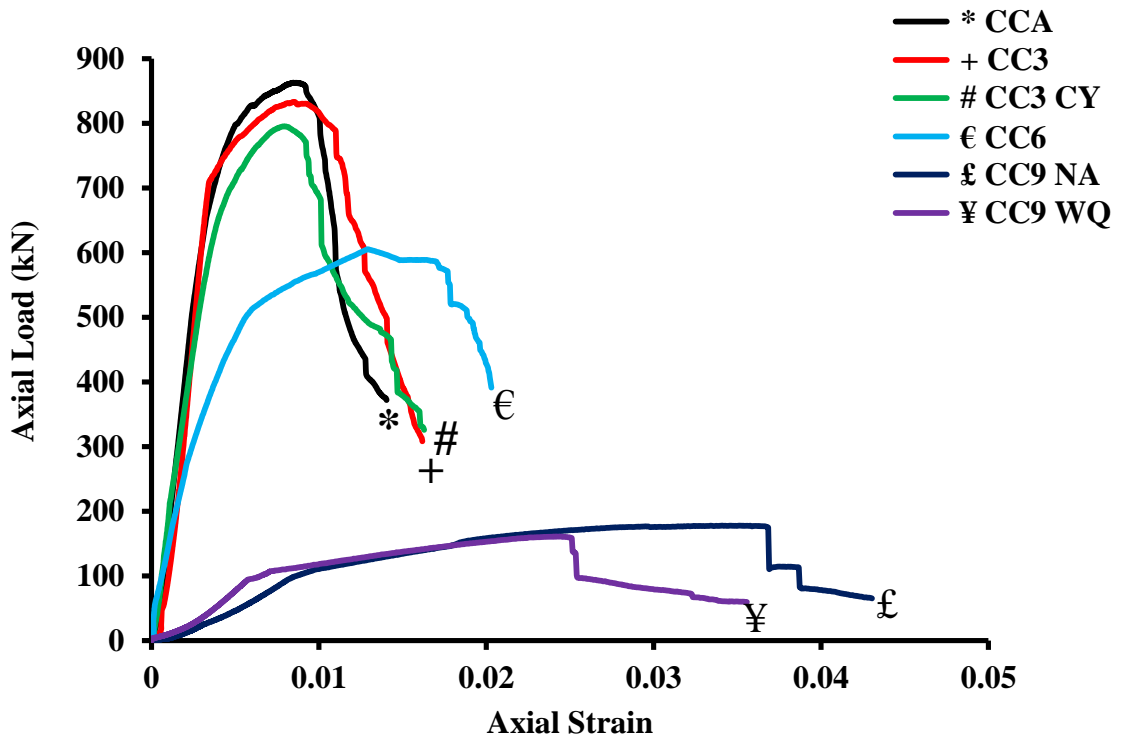
Fig. 2. 20: Load – axial strain comparison of control specimens and all heat damaged specimens
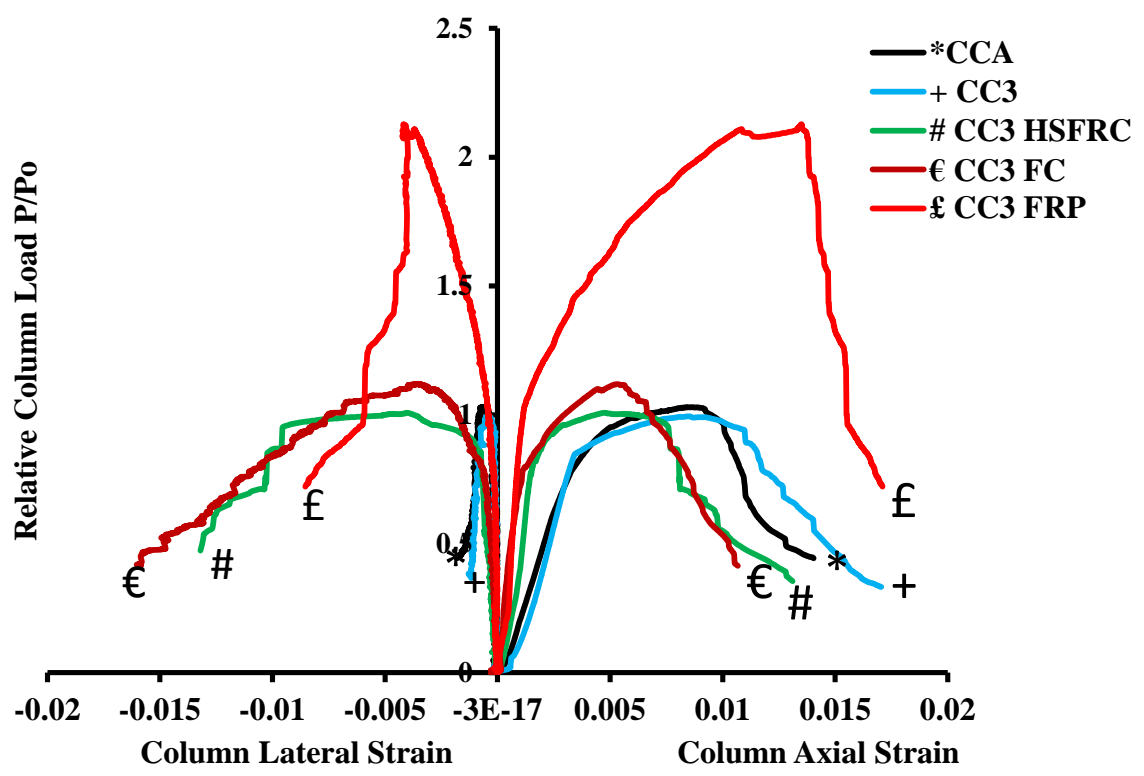
Fig. 2. 21: Load –axial & lateral strain comparison of strengthened specimens heated at 300^0 C
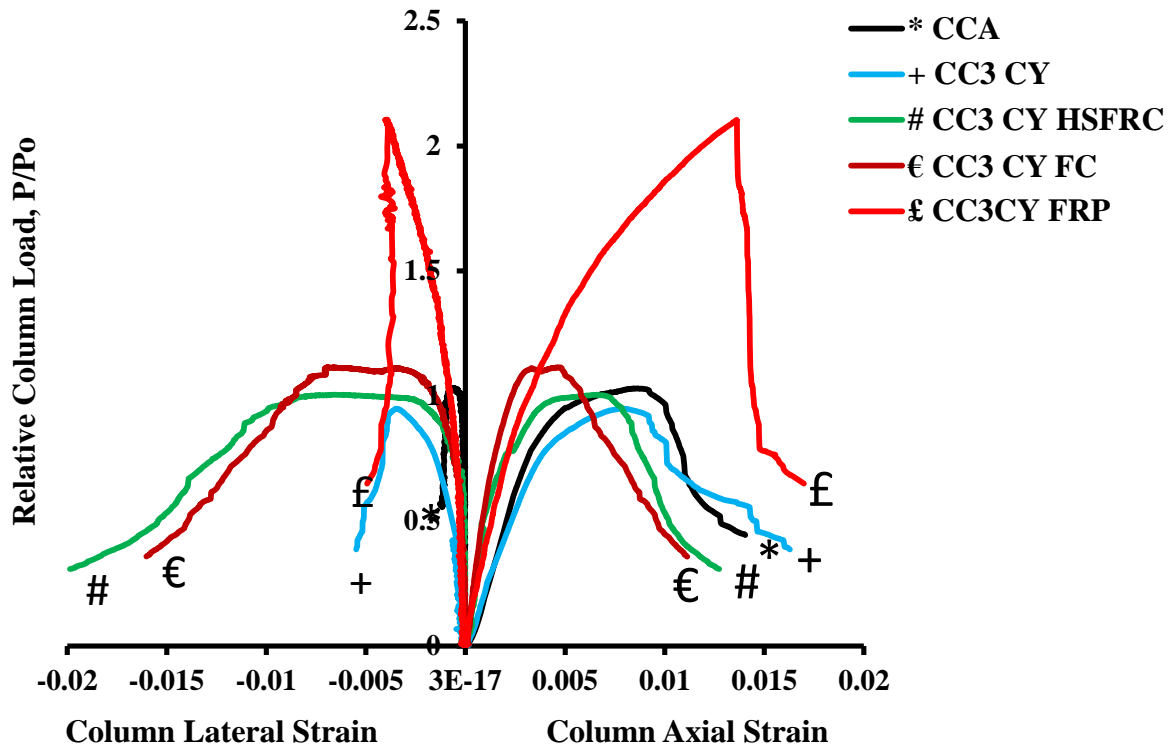
Fig. 2. 22: Load −axial & lateral strain comparison of strengthened specimens cyclically heated at 300^{0} C
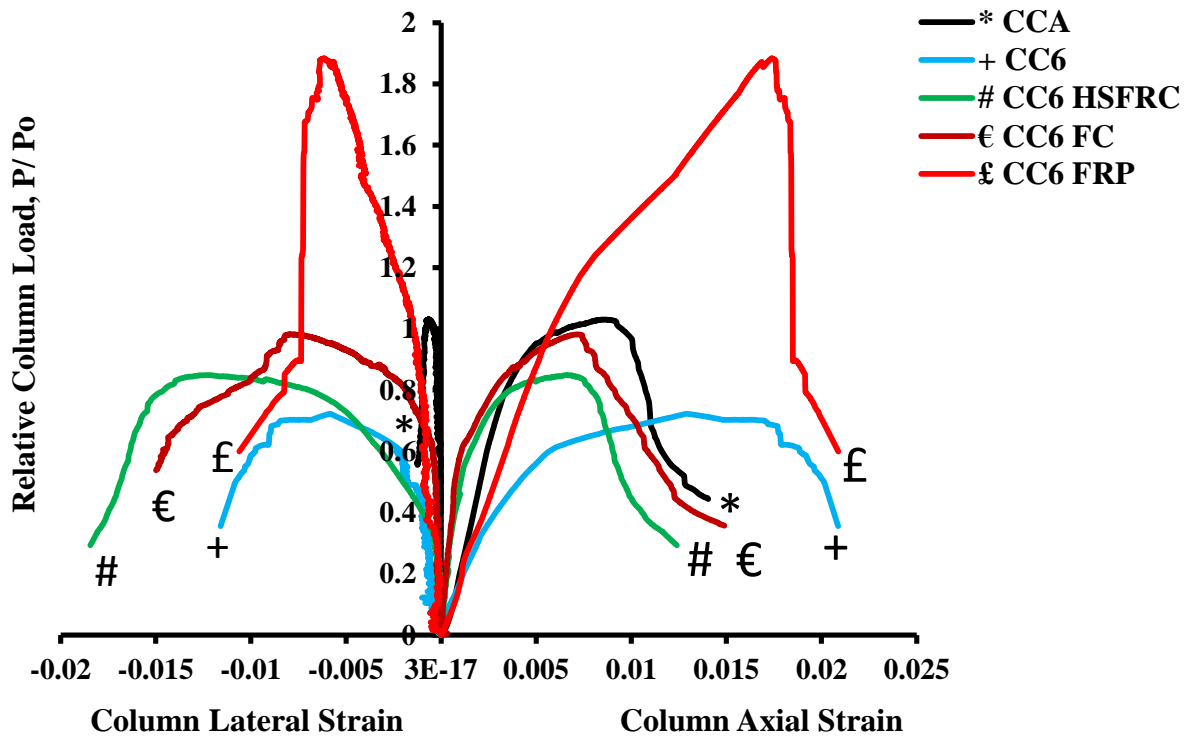
Fig. 2. 23: Load −axial & lateral strain comparison of strengthened specimens heated at 600^{0} C
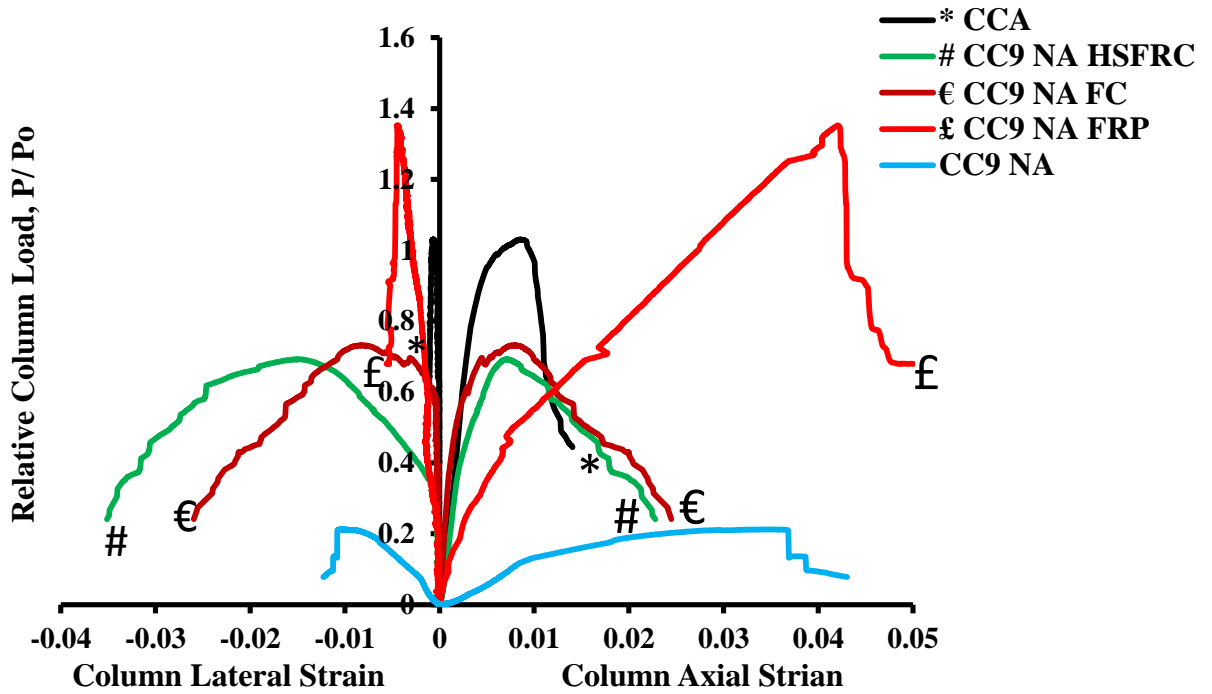
Fig. 2. 24: Load −axial & lateral strain comparison of strengthened specimens heated at 900^0 C (Normal Cooling)
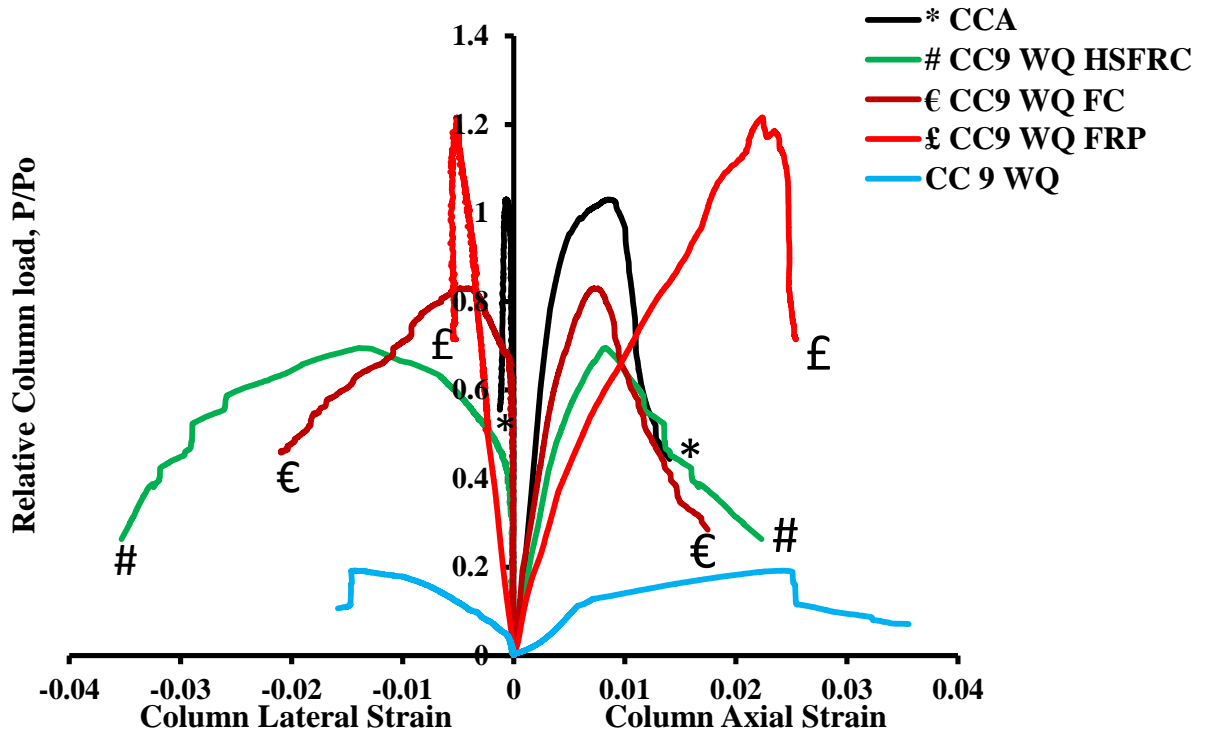
Fig. 2. 25: Load −axial & lateral strain comparison of strengthened specimens heated at 900^0 C (Cooling with Water Quenching)

Table 2. 22: Axial strength comparison of HSFRC, FC and GFRP strengthened columns

Method	Axial Compressive Strength (kN)										
	Ambient	300° C		300CY° C		600° C		900° C NA		900° C WQ	
		#	$	#	$	#	$	#	$	#	$
Control Specimens	(100 %)	-	-	-	-	-	-	-	-	-	-
Heat Damaged Specimens	-	(-4%)	(100 %)	(-8%)	(100 %)	(-30%)	(100 %)	(-79%)	(100 %)	(-81%)	(100 %)
Strengthened with HSFRC	-	(-2.4%)	(+1%)	(-2.4%)	(+6%)	(-17%)	(+15%)	(-32%)	(+227%)	(-32%)	(+261%)
Strengthened with FC	-	(+8.6%)	(+12%)	(+8.5%)	(+17%)	(-4.7%)	(+24%)	(-29%)	(+246%)	(-19%)	(+331%)
Strengthened with GFRP	-	(+106%)	(+114%)	(+104%)	(+121%)	(+83%)	(+160%)	(+31%)	(+540%)	(+18%)	(+532%)

With respect to control specimens; $ With respect to heat damaged unstrengthen specimens

2.7.3 Effect of Strengthening on Stiffness

In this study, strain of the specimens was measured as change in length normalized with original length and the secant stiffness of all the specimens was calculated from the measured ultimate axial load divided by the measured ultimate displacement at the mid-height of the specimens as shown in Fig. 2.26 (Kondraivendhan and Pradhan 2009, Yaqub et al. 2011). After heating to different temperatures, it was noted that the stiffness of the heat damaged columns reduced considerably when compared to control columns, Table 2.23. This is attributed to micro cracking and softening of the concrete due to the evaporation of water after heating. Fig. 2.27 shows the effect of variables on the stiffness of columns. The stiffness of HSFRC and FC jacketed specimens was higher than both the control and heat damaged specimens up to 600^0C. However in specimen heated to 900^0C, it was much greater compared to the heat damaged specimens but less than the of control specimens as shown in Fig. 2.27 and Table 2.23. This may be due to an increase of cross-sectional size, improvement of dimensional stability and integrity of the material. In case of GFRP, no significant improvement in restoration of stiffness of heat damaged specimens was noticed except in specimen heated to 300^0C, Fig. 2.27.

The restoration of stiffness of the heat damaged columns depends upon the confining action of HSFRC, FC and GFRP jackets. The confining effect is related to the load at which these systems begin to act. The confining effect of GFRP jacket takes place when the heated concrete specimen approaches its ultimate unconfined compressive strength. This means that before approaching the ultimate unconfined compressive strength, the GFRP jacket does not contribute in the structural response because it plays no part in the elastic range of the axially loaded heated specimen (Yaqub et al. 2011, 2013). Stiffness was observed to have increased in the case of HSFRC and FC jacketed columns, which may be due to the increase in cross sectional area offered by these techniques. On the contrary, the use of GFRP jacketing increases the compressive strength of heat damaged columns massively, but could not restore the stiffness property.
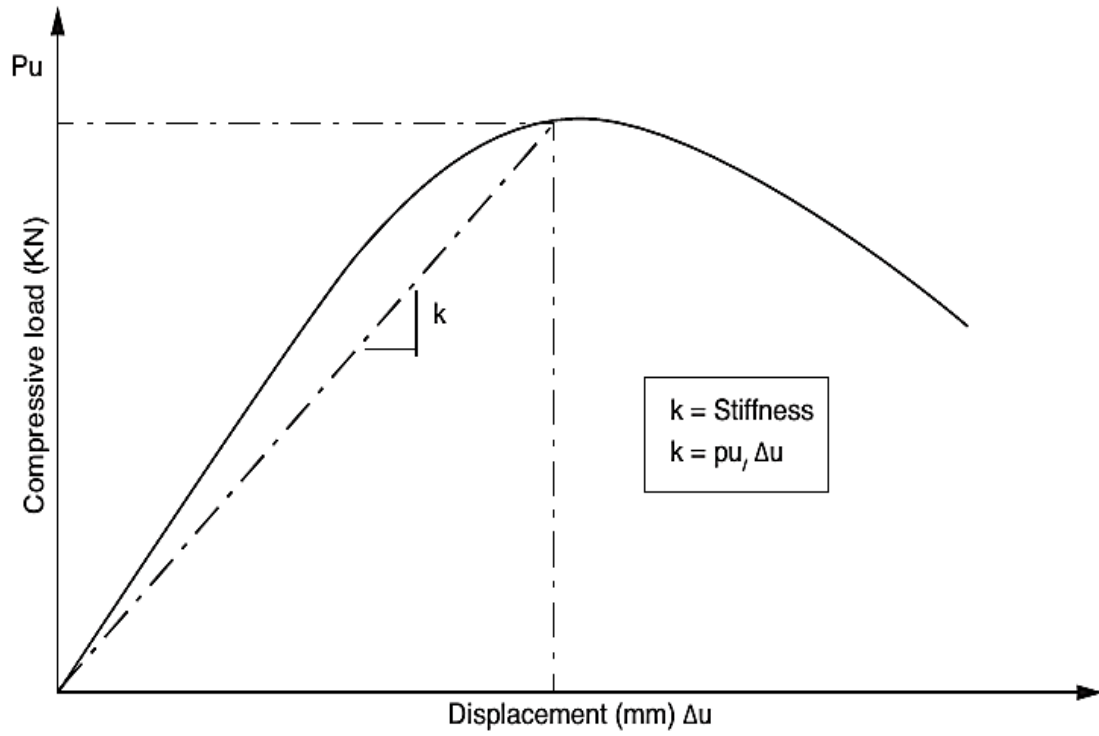
Fig. 2.26: Secant stiffness
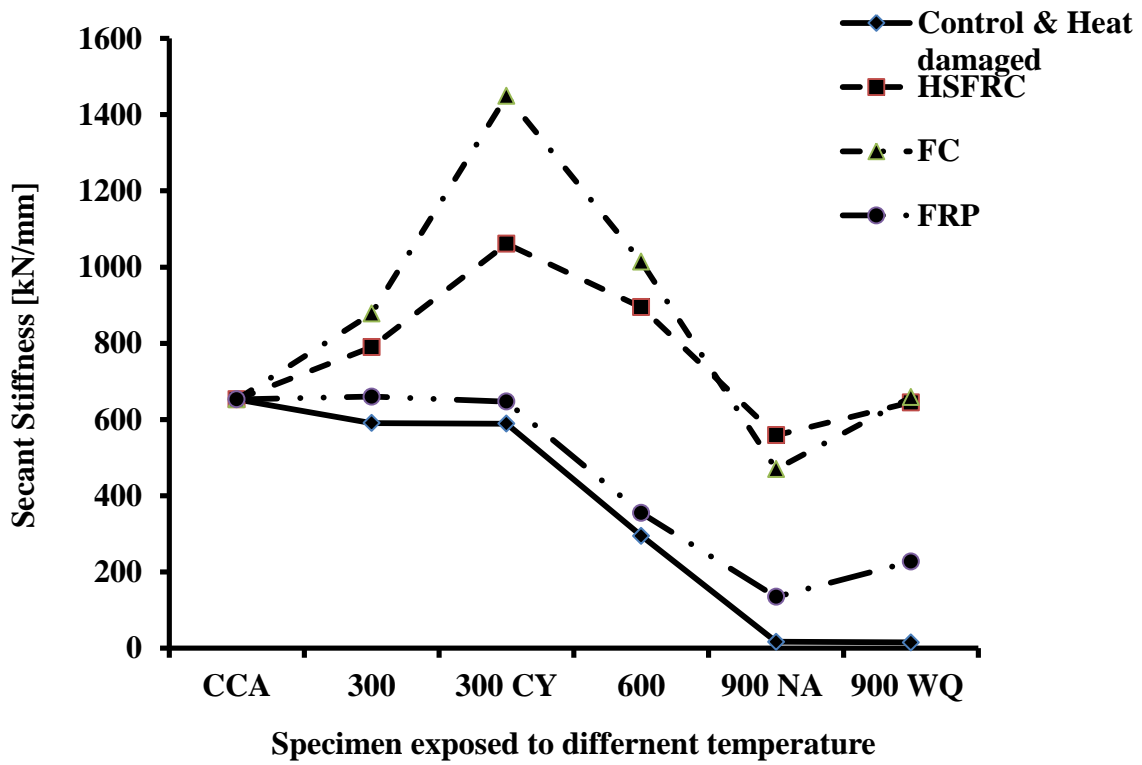
Fig. 2. 27: Comparison of secant stiffness

Table 2. 23: Secant stiffness comparison of HSFRC, FC and GFRP strengthened columns

Method	Secant Stiffness										
	Ambient	300° C		300CY° C		600° C		900° C NA		900° C WQ	
		#	$	#	$	#	$	#	$	#	$
Control Specimens	(100 %)	-	-	-	-	-	-	-	-	-	-
Heat Damaged Specimens	-	(-5%)	(100 %)	(-2%)	(100 %)	(-54%)	(100 %)	(-95%)	(100 %)	(-94 %)	(100 %)
Strengthened with HSFRC	-	(+71%)	(+79%)	(+28%)	(+34%)	(+6%)	(+129%)	(-19%)	(+1492%)	(-31%)	(+960%)
Strengthened with FC	-	(+72%)	(+80%)	(+100%)	(+109%)	(+13%)	(+145%)	(-25%)	(+1373%)	(-10%)	(+1293%)
Strengthened with GFRP	-	(+29%)	(+35%)	(+28%)	(+31%)	(-11%)	(+92%)	(-73%)	(+415%)	(-55%)	(+588%)

\# With respect to control specimens; $ With respect to heat damaged unstrengthen specimens

2.7.4 Effect of Strengthening Techniques on Deformability

Evaluation of the structural performance of strengthening techniques should also involve evaluating deformability and ductility of the repaired members. The results show that HSFRC and FC jacket techniques showed less deformation in comparison to heat damaged un-strengthen specimens. This might be due to increase in cross section area resulting from these techniques (Yaqub et al. 2013). However, the results indicate that the GFRP wrapping technique improves ductility also of the heated specimens. The deformability of heat damaged specimens wrapped with GFRP jacket was markedly more than the specimens strengthened with other jacketing methods. This could be due to the significant confinement provided by GFRP jacket to the heat damaged specimens.

The axial stress vs axial and lateral strains of the tested columns are shown in Figs. 2.21 to 2.25. The axial stress is given by the ratio of axial load to the cross sectional area of concrete, in which the contribution of GFRP was neglected. However, the contribution of a HSFRC and FC jacket in increasing the size of column was considered in the calculations. Fig. 2.20 shows the comparison between control column and heat damaged column, where it can be seen that the axial stress reduced significantly while the axial strains increased considerably after exposing the columns to different temperatures. Figs. 2.21 to 2.25 show the stress-strain relationship of heat damaged GFRP strengthened columns along with the control and heat damaged columns. The axial stress, strains and lateral strains increased tremendously in the GFRP wrapped column as compared to control and heat damaged columns. The GFRP wrapped columns attained a compressive strength higher than that of the unheated columns due to the fact that after heating concrete expands more under axial loading compared to unheated concrete. This lateral expansion causes higher tensile stress in the FRP jackets, which provides a greater restraining force.

Figs. 2.21 to 2.25 shows the stress-strain curves of unheated column, heat damaged column and heat damaged column strengthened with HSFRC and FC jackets. It is interesting to note that the axial strains were reduced in the heat damaged columns when strengthened with a both techniques compared to the heat damaged un-strengthened columns. This is due to the increase in cross-sectional size and the structural behavior of HSFRC and FC jackets. The Ultimate axial strain was found to be degrading even the lateral strain increased noticeably; this might be due to widening of cracks in HSFRC and FC jacket techniques.

2.7.5 Effect of Strengthening Technique on Energy Dissipation

      The energy dissipation is defined as the area under the concrete stress-strain curve. The energy absorption capacity values were calculated up to the 80% of Pu_{max} on the descending portion of the curve (Fig. 2.28). Table 2.24 shows the energy dissipation capacity values of all the specimens. It was observed that the specimens strengthened with GFRP dissipated more energy compared to HSFRC and FC jacketed specimens. This was due to the fact that GFRP jacketed specimens achieved higher strength and strains compared to other two strengthening techniques. GFRP strengthened specimens dissipated 129 to 360 % more energy compared to the control specimens, which was quite higher than the HSFRC and FC jacketed specimens. It was due to the fact that the HSFRC and FC strengthened specimens were stiffer and less ductile than the GFRP strengthened specimens. Further it can be noted from Figs. 2.24 and 2.25 that the specimens which were cooled naturally dissipated more energy compared to that in water quenched specimen.
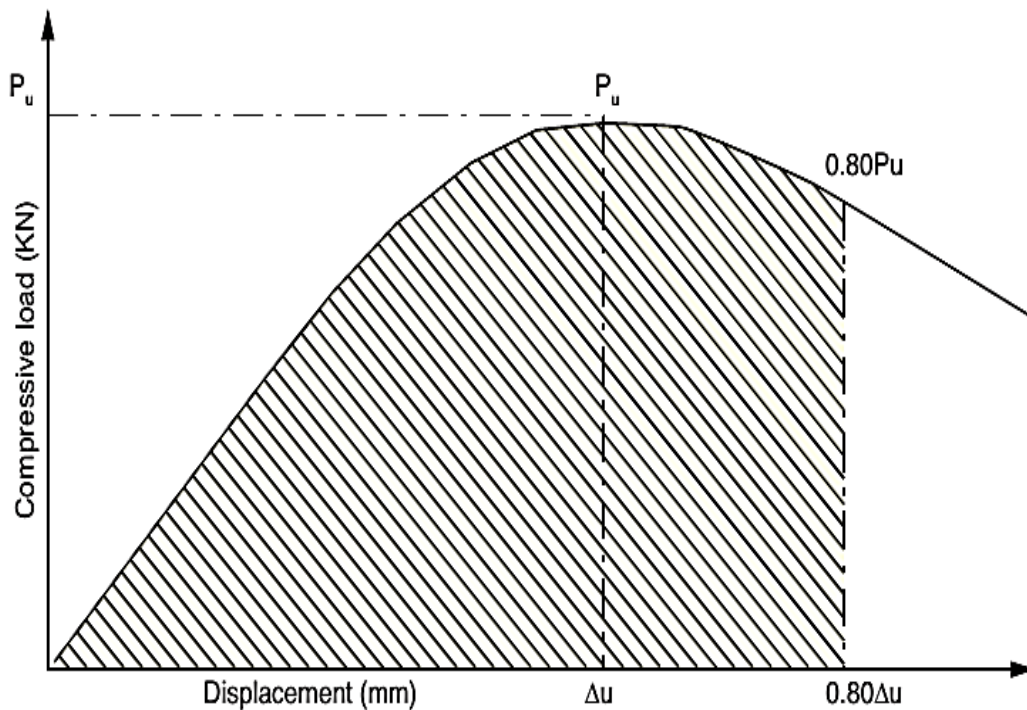
Fig. 2. 28: Energy dissipation calculation

Table 2. 24: Energy dissipation capability of HSFRC, FC and GFRP strengthened columns

Method	Ambient	Energy dissipation capability of columns									
		300° C		300CY° C		600° C		900° C NA		900° C WQ	
		#	$	#	$	#	$	#	$	#	$
Control Specimens	(100%)	-	-	-	-	-		-	-	-	-
Heat Damaged Specimens	-	(+8%)	(100%)	(-15%)	(100%)	(+34%)	(100%)	(-32%)	(100%)	(-55%)	(100%)
Strengthened with HSFRC	-	(-18%)	(-24%)	(-15%)	(+0.5%)	(-23%)	(-42%)	(-15%)	(+25%)	(-29%)	(+57%)
Strengthened with FC	-	(-15%)	(-21%)	(-30%)	(-18%)	(-10%)	(-33%)	(-5%)	(+40%)	(-31%)	(+52%)
Strengthened with GFRP	-	(+192%)	(+169%)	(+145%)	(+188%)	(+163%)	(+95%)	(+360%)	(+582%)	(+129%)	(+409%)

\# With respect to control specimens; $ With respect to heat damaged specimens

2.8   PREDICTED   CONFINEMENT   MODEL   STRENGTH   VERSUS EXPERIMENTAL CONFINED COMPRESSIVE STRENGTH

It is very important to compare the experimental results with the available design codes/guidelines to determine the accuracy of these codes to predict the ultimate axial strength of FRP confined concrete for design purposes. One of the major design codes/guidelines are selected for this study: the American Concrete Institute ACI Committee 440.2R, (2002). The code/guideline has its own design philosophy; however, the most common recommendation for the design of reinforced concrete (RC) columns is based on limit design principles which provide acceptable limits of safety against the ultimate and serviceability limits. The load combinations are amplified (amplifying factors greater than one) to account for the probability that the actual loads exceed the design loads. The design capacity is reduced (reduction factor less than one) to account for the probability that the calculated resistance is less than the actual resistance.

The strength reduction factors of the design code/guidelines are approached in two different ways. For the ACI Committee 440.2R (2002) guideline, the strength reduction factors (less than one) are multiplied to the overall nominal capacity. The factors are dependent on the nominal flexure, axial compression, and shear capacity. The performance reduction factors and the material resistance factors for axially loaded members used by the ACI Committee 440.2R (2002) are summarized in Table 2.25. The equations used by the ACI Committee 440.2R (2002) to calculate the maximum confinement pressure (fl) and the ultimate confined axial compressive strength ($f'cc$) of the FRP wrapped concrete specimens are presented in Table 2.26.

Table 2. 25: Strength performance reduction and material resistance factors

Codes/Guideline	Strength Performance Reduction Factors	FRP Additional Factors
ACI 440.2R (2002)	Φ= 0.75 (spiral) Φ= 0.65 (ties)	ψf= 0.95 CE=environmental reduction factor = 0.85

Table 2. 26: Summary of the design models for circular sections

Codes/Guideline	Confinement Pressure (fl)	Ultimate Compressive Strength (fcc')
ACI 440.2R (2002)	$$f1 = \frac{Ka\rho f\varepsilon feEf}{2}$$	$$fcc' = fc'\left[2.25\sqrt{1 + 7.9\frac{f1}{fc'}} - 2\frac{f1}{fc'} - 1.25\right]$$

Fig. 2.29 and Table 2.27 compare the predicted confined compressive strengths with the experimental tested confined compressive strengths of the heat damaged reinforced concrete circular columns wrapped with two layers of unidirectional glass fibre reinforced polymer jackets. The comparison study between the experimental and the confinement model reveals in need of discussion. The point is related to the high percentage difference in terms of the ultimate axial strength reported by the columns wrapped with the GFRP sheets. The ACI model is adopted from the confinement model proposed by Lam and Teng (2003). The confinement effectiveness coefficient kl suggested by Lam and Teng (2003) was 3.3. However, this parameter was derived based on experimental results performed on CFRP, GFRP and AFRP wrapped specimens. The ACI 440.2R-02 model includes an additional reduction factor ψf of 0.95. This shows the conservative approach of the ACI model, which also suggests that gaps concerning the behaviour of FRP confined concrete, still exists. The ACI 440.2R-02 model also includes an environmental reduction factor CE of 0.85.

From Fig. 2.29 and Table 2.27 it can be seen that the ACI Committee 440-2R-02 confinement model predictions are 27% to 67% lower than the experimental confined compressive strength of heat damaged circular columns wrapped with GFRP. This clearly shows that the ACI confinement models predicted lower confined compressive strengths for heated damaged reinforced concrete columns than the actual experimental tested confined compressive strengths. This could be due to the fact that the ACI confinement models are based on the undamaged concrete. The heat damaged concrete exhibited more lateral expansion compared to the control columns. Consequently; the fibre reinforced polymer is more activated in heat damaged concrete compared to undamaged concrete. Thus, in case of fire damaged concrete, the current existing

international design guidelines are more conservative for the prediction of confined compressive strength of heat damaged columns wrapped with FRP.
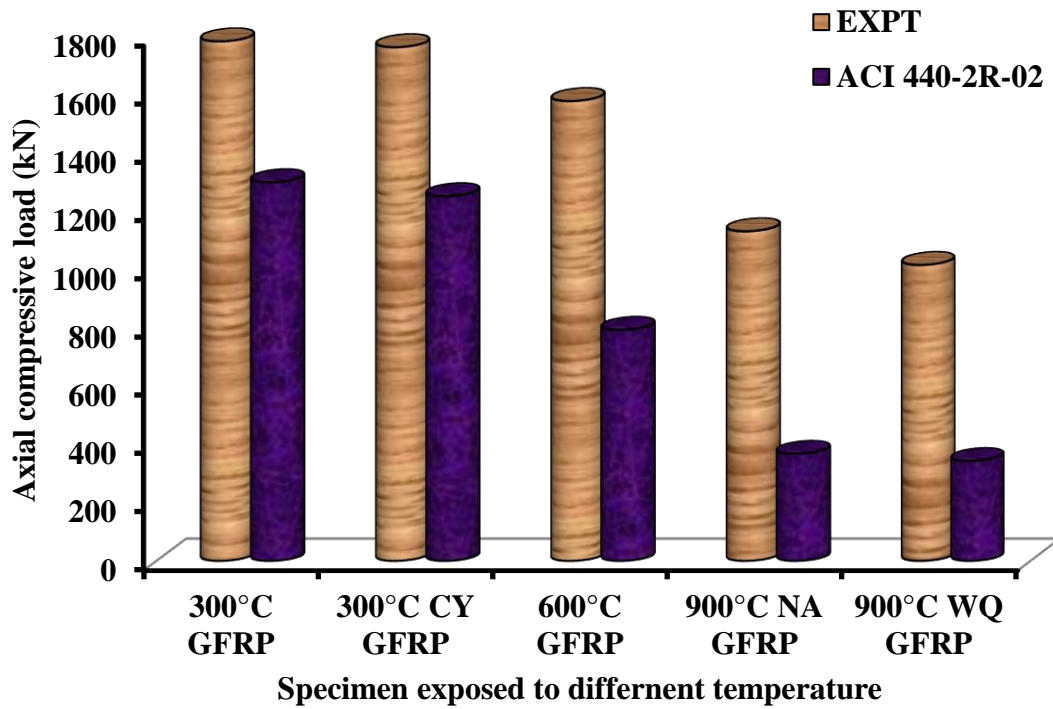
Fig. 2. 29: GFRP strengthened heat damaged columns

Table 2. 27: Theoretical confined compressive strength versus experimental confined compressive strength of heat damaged reinforced concrete columns

Specimen Designation	Temperature (° C)	ACI 440-2R-02 Theoretical Load[kN]	Experimental Peak Load [kN]
CCA	--	--	863
CC3	300° C	--	833
CC3 GFRP	300° C	1300	1782
CC3 CY	300° C CY	--	795
CC3 CY GFRP	300° C CY	1253	1762
CC6	600° C	--	605
CC6 GFRP	600° C	796	1578
CC9 NA	900° C	--	177
CC9 NA GFRP	900° C	372	1133
CC9 WQ	900° C	--	161
CC9 WQ GFRP	900° C	347	1018

2.9 CONCLUDING REMARKS

This study reports the test results of heat damaged reinforced concrete circular section short columns restored and strengthened with various commonly used techniques for strengthening of reinforced concrete members under normal temperature conditions. A total of 63 specimens were tested under this program. The test variables included temperature of exposure, type of strengthening, monotonic/ cyclic heating and type of cooling. The research program has contributed to the fundamental understanding of the complex mechanism of behaviour of concrete exposed to a complete cycle of heating and cooling. Important observations have been made on the effectiveness of various strengthening techniques in restoring the strength, stiffness and deformability of heat damaged concrete compression members.

CHAPTER – 3

STRENGTHENING OF HEAT DAMAGED REINFORCED CONCRETE SHORT SQUARE COLUMNS

3.1 INTRODUCTION

Since columns are the most important structural components of any building or structure, investigating damage caused in columns due to fire or heat and their subsequent restoration becomes important. As rectilinear or square shaped columns are the most commonly found columns in buildings, this chapter deals with the influence of elevated temperature and resulting restoration of short square columns. In the past, a lot of research has been reported on repairing and strengthening of square and rectangular RC columns with FRP confinement to address the distress caused by different causes except the damage caused by the fire and elevated temperatures (Mirmiran et al. 1998, Saadatmanesh et al. 1998, Chaallal et al. 2003, Harries and Carey 2003, Galal et al. 2005, Hosseini et al, 2005, Campione 2006, Yousef 2007, Sheikh and Li 2007, Kumutha et al. 2007, Ilki 2008, Wang and Hsu 2008, Wei et al. 2009, Bambach et al. 2009, Turgay et al. 2010, Abbasnia and Ziaadiny 2010, Silva 2011, Quiertant 2011). However, only limited research has been reported on the repairing of fire damaged concrete square columns (Yaqub et al. 2011and 2013). Previous studies have shown that Ferro cement jacketing (FC) can also provide an effective confinement strengthening in such concrete columns (Mansur and Paramasivam 1985 and 1990, Nedwell et al. 1990, Takiguchi and Abdullah 2000 and 2001, Abdullah and Takiguchi 2003, Rathish et al. 2006 and 2007, Kondraivendhan and Pradhan 2009, Xiong et al. 2011, Amrul et al. 2013). High strength fiber reinforced cement based composites (HSFRC) have also made striking advances and gained enormous momentum over the past few years. This is due in particular to several developments involving the matrix and the fiber-matrix interface. Several studies have previously been undertaken into the feasibility of using HSFRC for the rehabilitation and strengthening of RC columns (Bentur and Mindess 1990, Balaguru and Shah 1992, Shannag et al. 2005, Gustavo 2005, Meda et al. 2009, Skazlic 2009). The application of FC and HSFRC techniques in repairing and restoring fire damaged reinforced concrete rectangular or square columns however remains to be investigated.

Strengthening reinforced concrete columns by steel plate (SP) jackets is a common engineering practice for strengthening and repairs of columns because it is

inexpensive, does not require highly trained labor, unobtrusive, does not reduce space, easy to inspect and can be applied while the structure is still in use. But its application in repairing of fire damaged concrete columns has not yet been investigated. The present study explores the potential of use of these above mentioned strengthening schemes in restoring the compressive mechanical performance of RC short square columns (prisms) that have been damaged by heat by subjecting them to certain elevated temperatures. The effectiveness of HSFRC, FC, GFRP and SP jackets on heated damaged reinforced concrete prisms in terms of ductility, stiffness, strength gain, energy dissipation, failure mode were studied under this study.

3.2 EXPERIMENTAL PROGRAM

The main aim of this work is to study the effectiveness of different strengthening schemes in repairing heat damaged concrete short square columns, which shall also be addressed as prisms in the following sections. A total of 51 concrete short columns of size 150 mm x 150 mm x 450 mm were cast, heated, strengthened and tested. The key details of the test specimens i.e. concrete prisms are shown in Fig. 3.1 and Table 3.1. The main variables of the experimental study consist of temperature of exposure and type of strengthening scheme. All the concrete prisms were cast in seventeen different series as shown in Table 3.1. The first two letters (SC) in the abbreviations denote square column specimen, and the numeral (3, 6 and 9) indicates the temperature and MC denotes those specimens which were first repaired with micro concrete before being further strengthened.

Concrete was prepared with ordinary Portland cement, natural river sand, and crushed limestone aggregate of maximum size 12.5 mm. The concrete mix was designed using the specifications of IS: 10262-2009. The material properties, concrete mix proportions and 28 days cylinder compressive strength of the chosen concrete mix have already been reported in the previous chapter i.e. Chapter 2. The longitudinal reinforcement of 12 mm diameter with yield strength of 610 MPa and lateral ties of 6 mm diameter with 550 MPa yield strength were used. The stress-strain relationships of these reinforcement bars are illustrated in Fig. 3.2. All the prisms were of the same cross-section and length. The prisms were reinforced with four 12 mm diameter longitudinal bars and 6 mm diameter transverse bars spaced uniformly throughout the length of

prisms at 50 mm centers. The transverse bars were anchored with 135° hook at each end extending approximately by 60 mm into the concrete core.
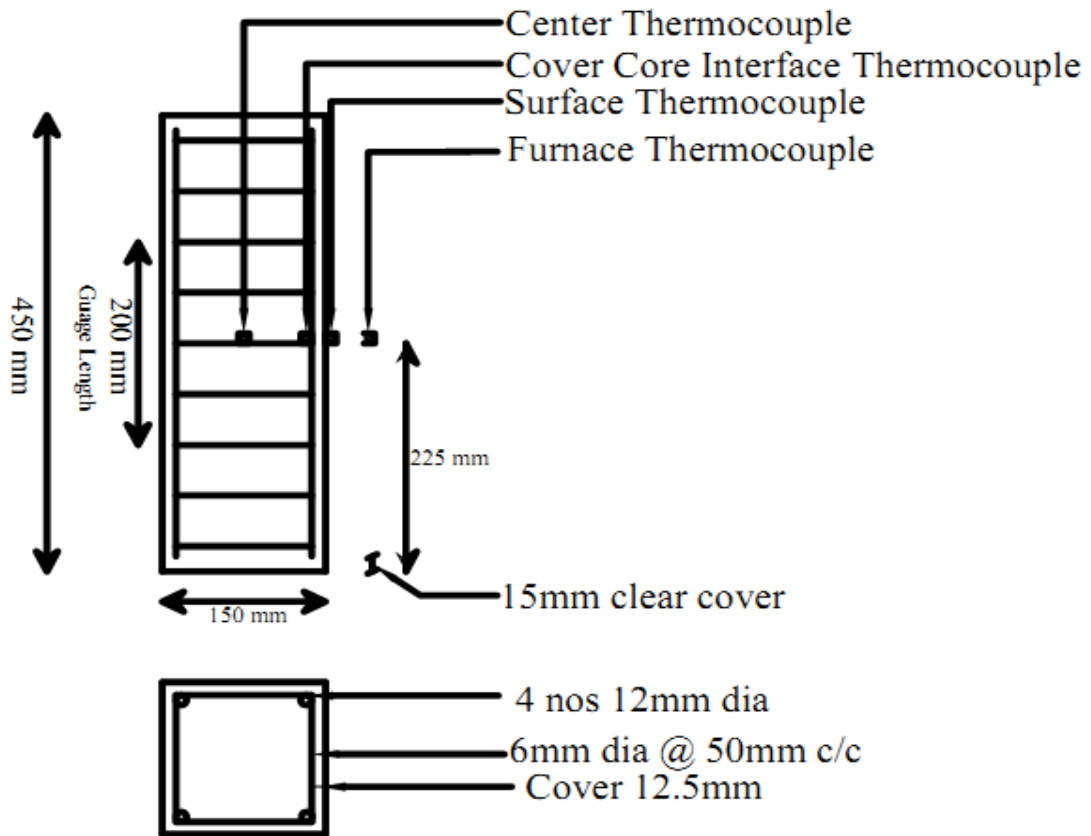
Fig. 3.1: Size of Prisms, reinforcement details and position of thermocouples
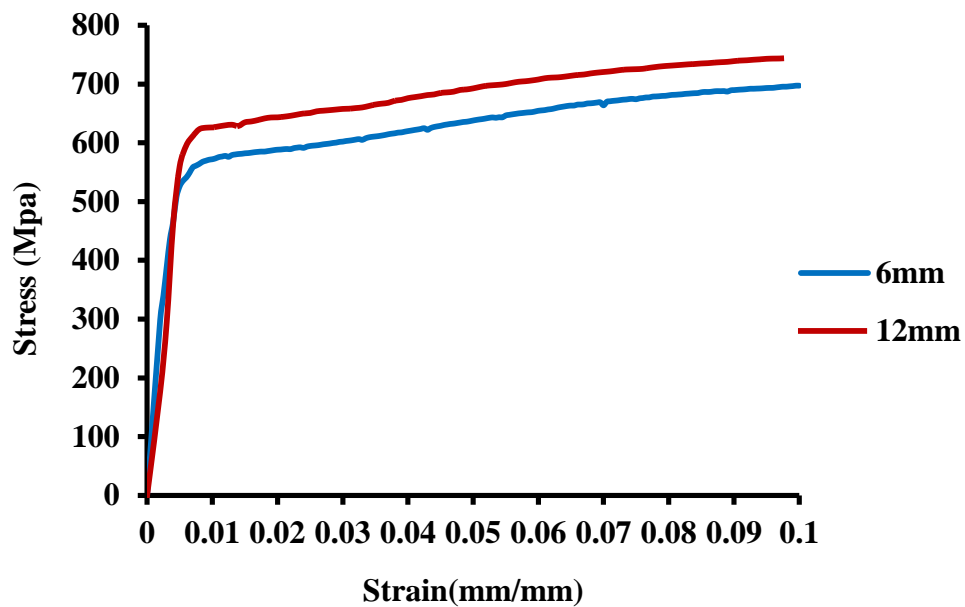
Fig. 3.2: Stress-strain curves for reinforcing bars

Table 3.1: Specimen details

Designation	Temperature exposure of (°C)	Strengthening Methods
SCA	Ambient	---
SC3	300	---
SC3 HSFRC	300	HSFRC
SC3 FC	300	FC
SC3 GFRP	300	FRP
SC3 SP	300	SP
SC6	600	---
SC6 HSFRC	600	HSFRC
SC6 FC	600	FC
SC6 GFRP	600	FRP
SC3 SP	600	SP
SC9	900	---
SC9 HSFRC	900	HSFRC
SC9 FC	900	FC
SC9 GFRP	900	FRP
SC9 SP	900	SP
SC9 MC	900	---

At the time of casting, all the ingredients were kept ready in required proportions for casting. A concrete cover of 12.5 mm was provided in all the specimens. A cover of 15 mm was also provided at the top and bottom surfaces to prevent direct loading of the bars. The specimens were cast using steel formwork in the laboratory. Similar procedure for mixing and casting as explained in Chapter 2 was employed here as well. Compaction was carried out using table vibrator. Two K type thermocouples were placed in each specimen during casting in order to monitor the temperature at the time of heating as shown in Fig. 3.3. One thermocouple was placed at the center of the prism at

mid-height, and the other was attached to one of the longitudinal bars at mid-height. After 24 hrs, the prisms were removed from the mould and submerged in water tank for curing. After a curing period of 28 days, the prisms were removed from the curing tank and kept in the laboratory for another 122 days. After 122 days of total ageing, the specimens were exposed to various heating regimes. Subsequent to a single heating and cooling cycle, the specimens were strengthened and tested under monotonic compression.

Fig. 3.3: Stages of thermocouple binding, reinforced gauges placed inside formwork and casting of square specimens

The slurry used in preparing HSFRC and FC jacket included ordinary Portland cement, natural sand, which was less than 600 micron, and silica fume. The mix proportions of slurry were 1:0.6:0.15:0.35:0.01 by weight of cement, sand, silica fume, water and super plasticizer respectively. The 28 days cube compressive strength and flow-ability of the slurry have already been explained in Chapter 2. The properties of GFRP used for the investigation was unidirectional with nonstructural weaves in the secondary direction to hold the fabrics together, thickness of FRP was about 0.324mm, average tensile strength of 3400 N/mm², and an ultimate elongation of 4.33%. The properties of epoxy resin used for bonding have already been explained in Chapter 2. The locally available Steel plate jacket was used in Steel plate jacketing technique. The steel plate was 410 mm long, 150 mm in width and 2.3 mm thick. The Steel plates were bonded to the sides of prisms using epoxy adhesive. The properties of epoxy adhesive are show in Table 3.2.

3.2.1 Moisture Content

The moisture exists in concrete in many forms namely free water, physically and chemically bound water and vapour. This moisture is extremely responsible for thermal softening, developing thermal expansion, drying shrinkage and build-up of pore pressures in concrete. As moisture content of heated concrete influences its mechanical and thermal properties, it is always important to report the moisture content of concrete.

Table 3.2: Properties of primer and saturant solution

Type of Material	Mix Proportion	Mixed Density	Pot Life	Bond Strength	Compressive Strength
Primer	1:1 by Weight of liquid	1.09Kg/l	73min ± 15min	Failure in Concrete	-
Saturant	1:1 by Weight of liquid	1.15Kg/l	30 min ± 15min	> 2N/mm²	65N/mm² @7 days

Sometimes it is required to eliminate the effect of moisture by keeping approximately similar moisture content in the test investigations unless moisture content itself is a test variable. Thus on the day of thermal testing of specimens, three numbers of companion cubes were dried completely until they achieved a constant mass in an oven at 105°C ± 2°C to measure moisture content for each series of specimens. The measured values of moisture content of the companion cubes were assumed as the moisture content of the corresponding main specimens. The measured average moisture contents of the concrete specimens are shown in the Table 3.3.

Table 3. 3: Moisture content of cube specimens

Series specimens	Moisture content % (by mass)
SCA	2.13
SC3	2.26
SC6	2.21
SC9	2.18

3.2.2 Heating of Specimens

A programmable electrical furnace as explained in Chapter 2 was used to heat the specimens. The specimens were exposed to three target temperatures, 300° C, 600° C and 900° C at an age of 150 days. The maximum temperature reached during real fires is generally of the order of 1000º C to 1200º C. The specimens were heated at a rate of 10^oC/min until the target thermal steady state temperature is achieved i.e, for about 3 hrs Fig. 3.4 (a-c). The heating rate of 10ºC/min means the rate of temperature rise inside the furnace, and not the temperature rise of inside the concrete prisms. The heating rate was set at 10° C /min., which has been shown to be realistic for structures exposed to fire (Wu et al. 2002, Chen. et al. 2009, Aydm and Baradan 2007, Peng et al. 2006). The temperature histories during the heating and cooling regimes in the specimens were recorded by means of a 0.6 mm thick (22 gauge) thermocouples. Both J-type (+ve Iron /-ve Constantan) and K-type (+ve Chromel /-ve Alumel) thermocouples were used. The maximum working range of J-type and K-type thermocouples were zero to 540ºC and zero to 1250ºC respectively. On completion of the exposure time, the samples were left in the furnace for natural cooling to room temperature. The thermocouples data was recorded in a computer through a data logger. It was possible to conduct only one such heating and cooling exposure test in a day.
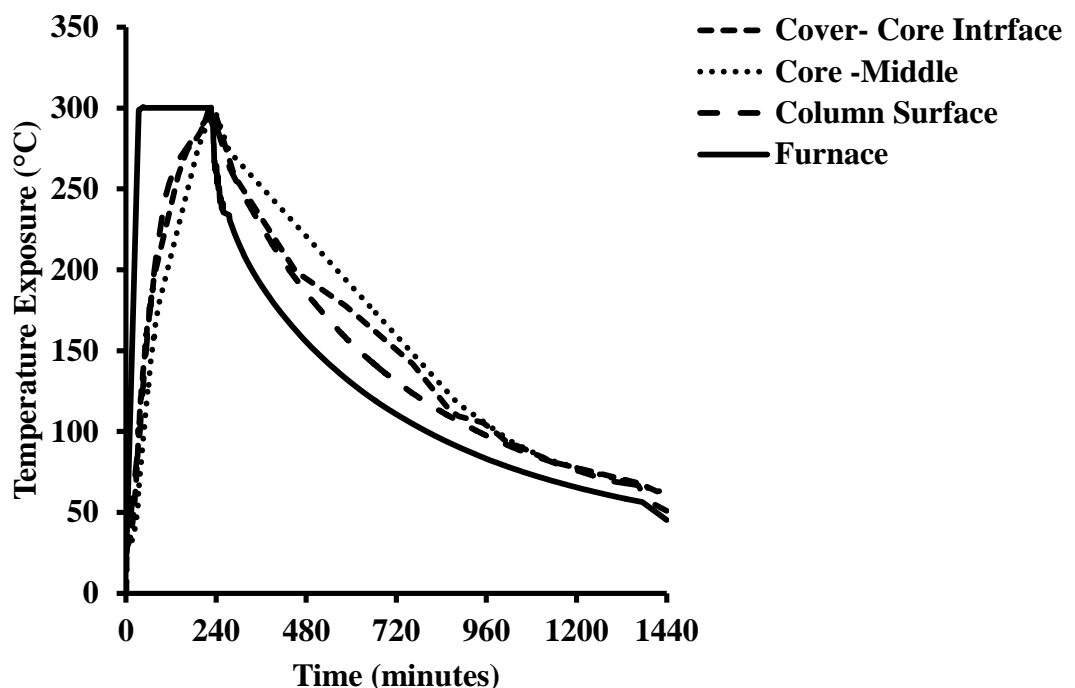
(a) SC3 specimens exposed to 300 ° C
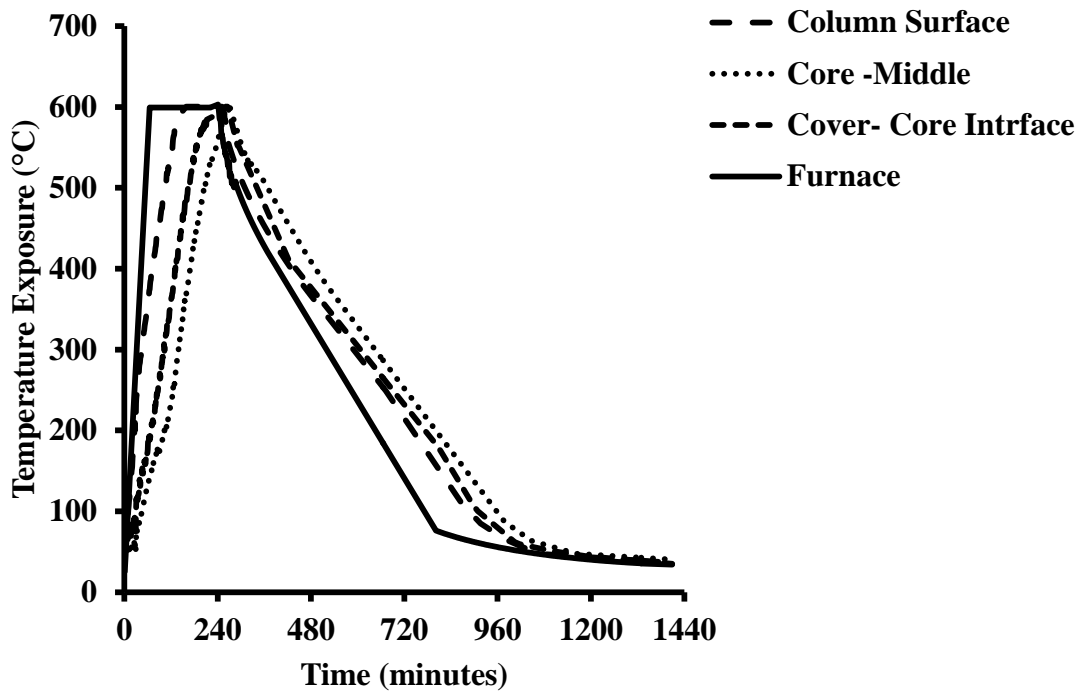
(b) SC3 specimens exposed to 600 ° C
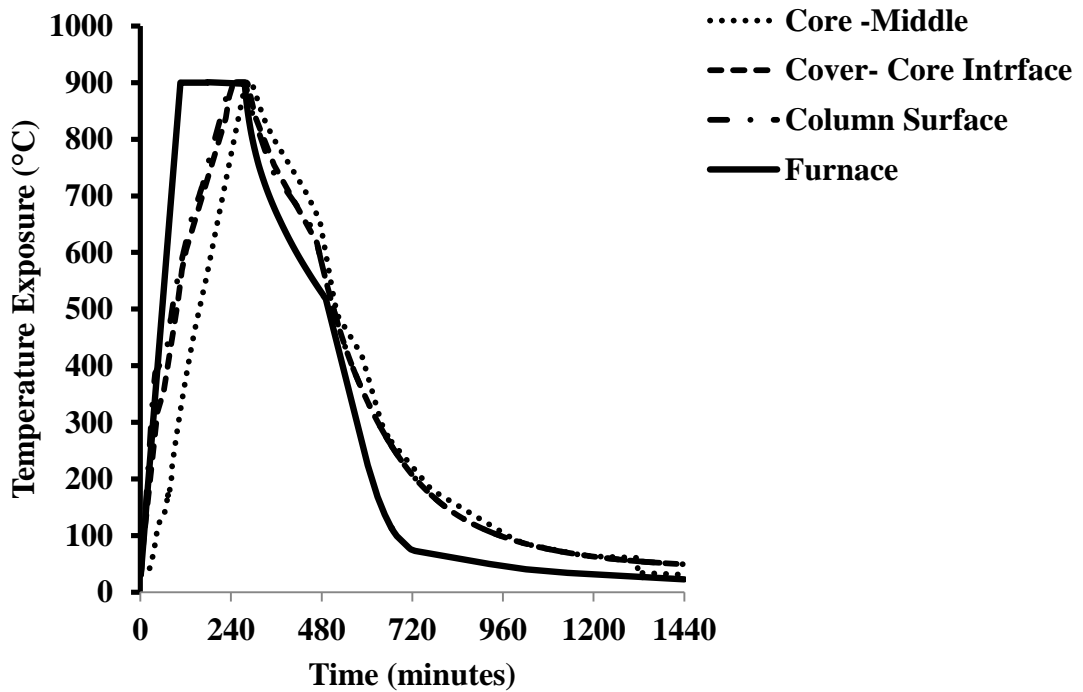
(c) SC9 specimens exposed to 900 ° C

Fig. 3.4: (a)-(c) - Typical time-temperature curves

3.2.3 Observations After Heating

Assessment of heat-damaged concrete generally starts with visual observation of colour change, cracking and spalling of concrete surface. In the present study, the observations during heating and cooling suggest that the colour of concrete in the specimens changed with the temperature of exposure. The change in the colour of concrete can be attributed to the change in the texture and composition of concrete and resultant crystal destruction during heating and cooling. The colour of concrete changed to pink when the specimens were exposed to 300° C. The colour of the specimens after heating up to 600° C temperature was recorded to be light grey. However, the ash white colour was visible in all the specimens exposed to 900° C.

There were no visible cracks on the surface of the specimens heated up to 300°C. However, some hairline cracks were observed at 600° C. The number of cracks became relatively pronounced at 900° C along with disintegration of concrete as shown in Fig. 3.5. However, no serious spalling was observed in concrete specimens at any exposure temperature. The damage accumulated during the cooling process further reduces the residual strength which leads to further expansion of crack day by day (Fig. 3.5).
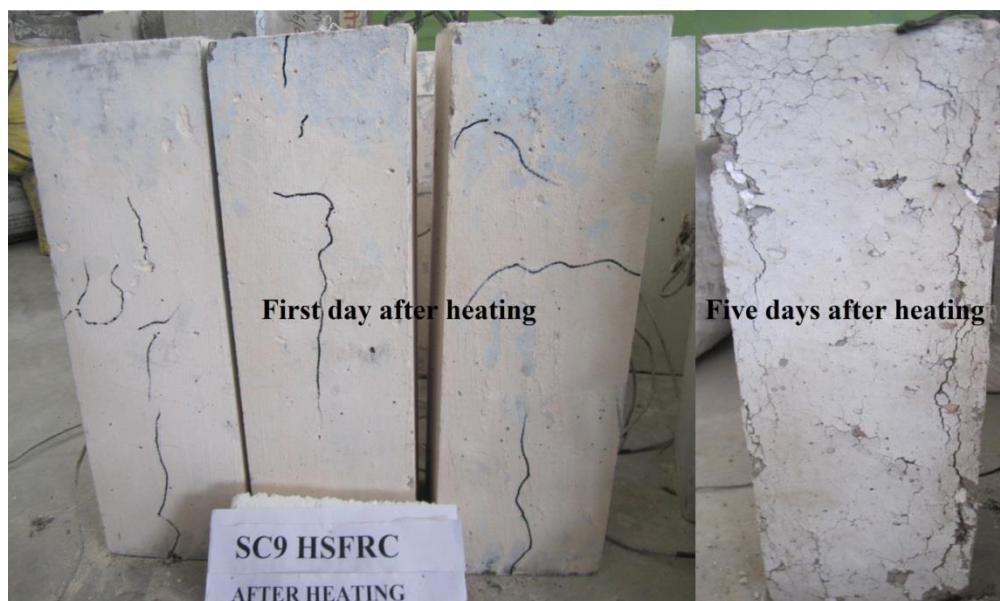
Fig. 3.5: Surface cracking observed in test specimens exposed to 900 °C

3.2.3.1 Ultrasonic pulse velocity testing

Ultrasonic pulse velocity (UPV) tests were conducted on all the specimens as per the procedure explained in Chapter 2. The pulse velocities reduced as the temperature of exposure increased. However, a significantly marked deterioration of concrete as indicated by the loss in pulse velocity was noted mainly for temperatures more than

400°C.This corroborates the findings of previous studies as well as of this study with respect to the results of heat damaged cylindrical specimens discussed in the previous Chapter.

3.3 REPAIRING AND RESTORATION OF SECTION OF HEAT DAMAGED SPECIMENS

After heat exposure, the heat damaged square columns, which got cracked and spalled, were repaired before further strengthening. The spalled sections were restored using micro-concrete. The loose concrete was removed using steel wire brush, chisel and hammer. The surface of specimen was cleaned thoroughly to ensure no dust. A bonding agent was applied on the spalled surfaces of the specimen to achieve good bonding between the old concrete and new repair material i.e. micro concrete as shown in Fig. 3.6. Once the bond coat became tacky, the micro concrete was applied to the specimens. The micro concrete repaired specimens were covered with damped gunny bags for 7 days and kept in laboratory conditions until strengthening. The specimens, which did not undergo any spalling, were directly strengthened by the appropriate technique. The corners of the heat damaged square columns were also ground before strengthening to reduce stress concentration at the corners.

Fig. 3.6: View of a typical specimen before repair and after application of micro concrete

3.4 STRENGTHENING OF HEAT DAMAGED SPECIMENS

After repairing, the heat damaged specimens were strengthened with various techniques namely HSFRC, FC, GFRP and SP jacketing. In all the specimens a primer epoxy bonding was applied after the surface was cleaned in order to provide good bonding between the substrata and the new strengthening material. A gap of 20 mm in unstrengthen concrete was left at the ends of concrete specimen to prevent strengthening jacket from direct loading while testing.

3.4.1 High Strength Fiber Reinforced Concrete (HSFRC) Strengthening

The heat damaged short columns, which were to be strengthened with HSFRC jacketing, were cleaned thoroughly to ensure no dust. A layer of Epoxy was applied on the surface of square columns to fill micro-cracks if any, and to provide good connection between the heat damaged concrete and the HSFRC jacketing. HSFRC slurry reinforced with hooked steel at a volume fraction of 2% with average compressive strength of 74.07 MPa was poured into the mould to form a 25 mm thick jacket as shown in Fig. 3.7. After 24 hrs, the strengthened specimens were demoulded and cured using damped gunny bags for another 14 days. After fourteen days, the test specimens and the companion cubes were air cured under laboratory environment conditions until testing.

Fig. 3.7: Strengthening process of HSFRC jacketing

3.4.2 Ferro Cement (FC) Strengthening

After surface preparation, the heat damaged specimens were held vertically, bonding agent was applied on the surface of the column to fill micro cracks and to provide bond between the heat damaged concrete and the Ferro cement laminate. The FC jacketing was carried out with two layers of welded wire mesh as shown in Fig. 3.8. An overlap of 100 mm was provided in the lateral direction of the wire mesh. Wooden mallets were used to keep the wire mesh close to the surface of specimen.

Slurry with high compressive strength of 68.06 MPa was poured into the mould to form 25mm thick FC jacket around the heated specimen. Spacing of about 20 mm was provided between the Ferro cement jacket and the ends of the column to prevent the jacket from direct axial loading during test. The strengthened square columns were covered with damped gunny bags for 14 days after demoulding. After fourteen days, the column and companion cubes were air cured in laboratory atmosphere until testing.

Fig. 3.8: Strengthening process of FC jacketing

3.4.3 Glass Fiber Reinforced Polymer (GFRP) Jacketing

Before application of GFRP, the surface of the specimens was scraped lightly to remove surface contaminants. Firstly the surface of the concrete was coated with a layer of epoxy primer on the external surfaces of the concrete to fill air voids and to provide good bond strength. Secondly, a thin layer of the two part saturant solution consisting of resin and hardener mixed as per the manufacturer's specifications was applied.

Later first layer of GFRP sheets was wrapped around the prisms carefully. A roller was used to remove the entrapped air between the fiber and excess saturant so as to allow better impregnation of the saturant. Special attention was taken to ensure that no air voids were left between the fiber and the concrete surface. After the application of the first wrap, a second layer of saturant solution was applied on the surface of the first layer with a lap of 100 mm in length. The roller was used again to remove any trapped air and to force the resin in the fibers. All the prisms were stored at room temperature for at least 28 days before testing (Fig. 3.9).

Fig. 3. 9: Strengthening process of GFRP jacketing

3.4.4 Steel Plate (SP) Jacketing

The steel plate jacket method consisted of four steel plates with each one covering four adjacent faces of the specimen and longitudinally bonded on the heat damaged surface. Before bonding the steel plates, the sides of the prisms were roughened with the help of a mechanical grinding machine. The bonding faces of the steel plates were cleaned with acetone. The steel plates were fixed on the sides of the specimen with the help of epoxy adhesives. Firstly the surface of the concrete was coated with a layer of

epoxy adhesive on the external surfaces of the concrete to fill air voids and to provide good bond strength. Secondly, a thin layer of the adhesive is applied on the steel plate. The gap were filled with adhesive, the plates were tightened with binding wire. The strengthened prisms were cured at laboratory environment for at least 28 days before testing (Fig. 3.10).

Fig. 3.10: Strengthening process of SP Jacketing

3.5 INSTRUMENTATION AND TEST SETUP

Mechanical testing of the test specimens was conducted after heating, cooling and strengthening. The specimens were tested with the help of 2500 kN capacity UTM (Fig. 3.11). Monotonic concentric compression load was applied at a rate of 0.1 mm/min. The axial contraction of the specimen at the middle portion (gauge length of 200 mm) was monitored using two linear variable displacement transducers (LVDT). Two LVDTs aligned horizontally were also fixed on opposite faces of the column to measure horizontal displacements. The mean lateral displacements were measured at the center of the prism and converted into an average lateral strain over the measured points of LVDT. Loads were recorded through an in built load cell in the UTM. The recorded data from the LVDTs and load cell were fed into a data acquisition system and stored on a computer.

90

Fig. 3. 11: Test set up and instrumentation

3.6 ANALYSIS AND DISCUSSION OF RESULTS

The test results of all the prisms tested under this program are given in Table 3.4. The response curves of square columns between applied axial load and the average axial and lateral strains measured by the LVDTs are given in Figs. 3.19 to 3.22. Table 3.4 provides the summary of peak load, peak strain, secant stiffness and energy dissipation as the average of three specimens. Figs. 3.19 to 3.22 illustrate the effect of different strengthening schemes on the load and deformability of heat damaged square columns. Both axial and lateral stress - strains curves were investigated. The heat damaged specimens exhibited relatively larger lateral displacements compared to the control specimens. Such large displacement owes to the pre-existing damage in the form of bond deterioration between reinforcing steel & concrete in the original specimen and cracks induced during heating.

3.6.1 Test Observations and Failure Modes

The specimens were tested under monotonic compression up to failure. Different failure modes were observed in the various control unheated and heat damaged specimens. The failure was particularly brittle, sudden and explosive in nature in case of control unheated specimens. But in case of heat damaged specimens the failure was gradual and exhibited ductile behavior with the increase in the axial load. The exposure of concrete to high temperatures results in softening of material due to deterioration in chemical and physical make up of concrete. It is believed that these changes along with the cracking of concrete at high temperatures make it ductile. In case of specimen heated to 900°C, it was noticed that the lateral ties were exposed due to spalling of cover concrete resulting in crushing failure as shown in Fig. 3.12. At 900°C, the heat induced disintegration and damage is very severe due to the loss in bond between aggregate surface and cement paste, which results in loss of integrity in aggregate-cement paste matrix. This is believed to be the reason of considerable damage noticed in the specimens exposed to 900°C tested under axial loads, especially in the cover concrete, which is unconfined and has maximum exposure to heat. This results in separation of unconfined cover concrete from the confined core concrete resulting into premature failure of cover concrete under loads. In the control and heat damaged specimens the vertical cracks started at the top followed by crushing of the concrete.

Fig. 3.12: Typical crushing failure of control and heat damaged square short columns

For strengthened HSFRC short square columns, the failure got initiated at top and bottom of the specimen due to stress concentration during loading. Diagonal and vertical cracks were observed in these specimens. Propagation and widening of vertical cracks was observed with increase in loading condition after the specimen had reached its ultimate loading capacity. At this point; increase in load created noise due to breaking of steel fibers there by indicating the stress transfer from the dilated concrete to the jacket. Bonding between the HSFRC jacket and concrete remained good enough as the de-bonding was never observed throughout the process (Fig. 3.13).

Fig. 3.13: Typical failure pattern of HSFRC strengthened square column specimens

However, for the FC jacketed scheme as the specimen approached the ultimate stages of loading a bursting sound was heard. The failure of the FC jackets was gentle without any sudden and explosive noise. The failure started at the bottom ends of specimens due to greater stress concentration. The welded mesh bulged out with a cracking sound just before the ultimate load point. Ductile failure was observed in FC jacketed columns. The failure in the corner indicated that the stress in the square jacket is likely to be concentrated at the corners; similar behavior was observed in a previous study (Yaqub et al. 2013). The failure mode of the heat damaged strengthened specimens repaired with FC jacket is shown in Fig. 3.14. The visual inspection of the strengthened

specimens showed that no de-bonding took place between the concrete and FC jackets. The failure pattern clearly shows that the wires of the weld mesh in the horizontal direction got broken, while wires in the vertical direction got buckled and broken at the corner (Fig. 3.14). Under axial compression, the stress in the square column tends to be concentrated in the lateral direction at the corners. The failure initiated with the development of vertical cracks followed by the yielding of the horizontal wires due to transverse tension at the corner of specimens.

Fig. 3.14: Typical failure pattern of FC strengthened square column

In the specimens strengthened with GFRP, a cracking noise was heard prior to failure. The failure of the specimens with GFRP jackets took long time but ended with a sudden and explosive noise. The sudden and explosive nature of the failure indicates the release of an immense amount of energy as a result of the uniform confining stress provided by the fibre jacket. It was observed that for the GFRP jacketed square specimens, the jackets ruptured externally at the overlap position at the top and bottom ends, as shown in Fig. 3.15. This is attributed to the stress concentration in these regions. It was observed visually that there was good contact between the jacket and the concrete indicating that no de-bonding took place during testing.
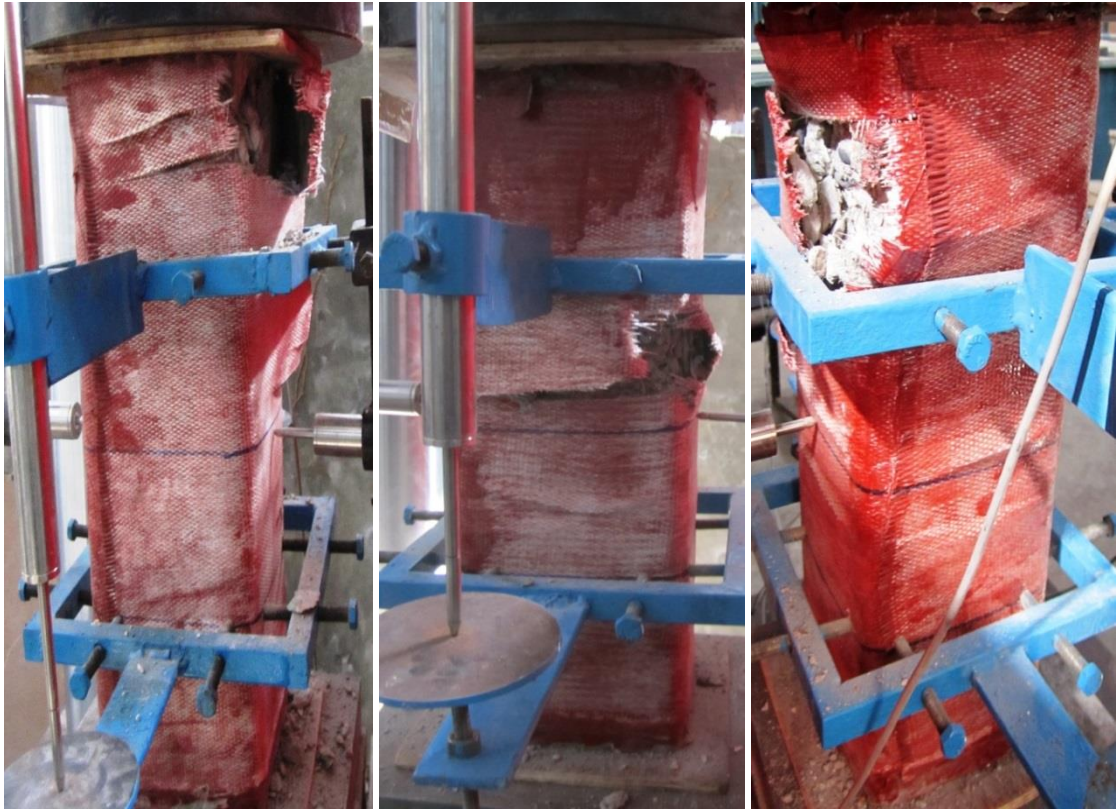
Fig. 3.15: Typical failure pattern of GFRP strengthened square column

The failure of the columns with steel plate jacketing was marked by the de-bonding during loading as shown in Fig. 3.16 i.e., failure occurred when the concrete part on either the top or bottom of the specimen got crushed under the applied load. The failure was gradual and exhibited a ductile behavior with increase in load. The visual inspection of the damaged columns showed good contact between the steel plate and the cover concrete.

The failure of the severely cracked square columns, which were micro concrete repaired only, were also tested and there failure was also relatively ductile. The visual inspection of the failure of the micro concrete repaired columns showed a good bond between the old concrete and epoxy resin adhered micro concrete. However, the failure was initiated due to the development of vertical cracks at the interface of micro concrete and the parent concrete (Fig. 3.17).

Fig. 3. 16: Typical failure pattern of SP strengthened square column

Fig. 3. 17: Typical failure pattern of micro concrete repaired specimens

Table 3. 4: Test results

Specimen Designation	Peak Load Pu(kN)	Strain at Peak ε_{cc}	Strain at 0.8 Peak ε_{c80c}	Secant Stiffness (kN/mm)	Energy Dissipation (kN.mm)
SCA	916	0.0060	0.0110	688.872	1932
SC3	883	0.0098	0.0140	450.683	1813
SC3 HSFRC	958	0.00400	0.00630	1066.815	976
SC3 FC	1055	0.00230	0.00330	2397.727	506
SC3 GFRP	1423	0.01004	0.0137	711.500	3214
SC3 SP	888	0.0090	0.0127	458.242	1516
SC6	648	0.00900	0.0179	344.680	1329
SC6 HSFRC	724	0.0064	0.0100	579.200	1284
SC6 FC	809	0.00420	0.00730	963.095	971
SC6 GFRP	1180	0.0183	0.02650	321.525	4431
SC6 SP	664	0.0103	0.0140	321.014	1491
SC9	193	0.0170	0.0249	55.619	725
SC9 HSFRC	483	0.0094	0.0154	256.914	1045
SC9 FC	565	0.0040	0.00922	614.130	862
SC9 GFRP	835	0.0337	0.0346	110.449	5674
SC9 SP	425	0.0127	0.0166	167.322	981
SC9 MC	347	0.0406	0.0560	70.242	1720

3.6.2 Effect of Type of Strengthening Technique on Axial Load Carrying Capacity of Specimens

It can be observed from the results that the compressive strength drastically reduced in heat damaged specimens (refer to Figs. 3.18 – 3.19, Table 3.5). It is observed from Tables 3.4 and 3.5 that the heat damaged specimens SC3, SC6 and SC9 have ultimate failure loads of 883 kN, 648 kN and 193 kN respectively compared to 916 kN for the corresponding unheated control specimen, SCA. This indicates that there was a decrease of 4%, 29% and 79% in ultimate load carrying capacity of specimens exposed to 300°C, 600°C and 900°C temperatures respectively. The degraded strength was restored when the heat damaged short columns were strengthened with different strengthening techniques (Figs. 3.20 – 3.22), which provided good confining effect to the specimens. The increase in strength was due to expansion of concrete laterally under axial compression, and this causes tensile stresses in the HSFRC, FC, GFRP and SP jackets. Owing to this tensile stress, the jackets confine the prisms and keep the prisms in stressed state. Consequently, due to this stressed state, the load carrying capacity of the square columns increased significantly.
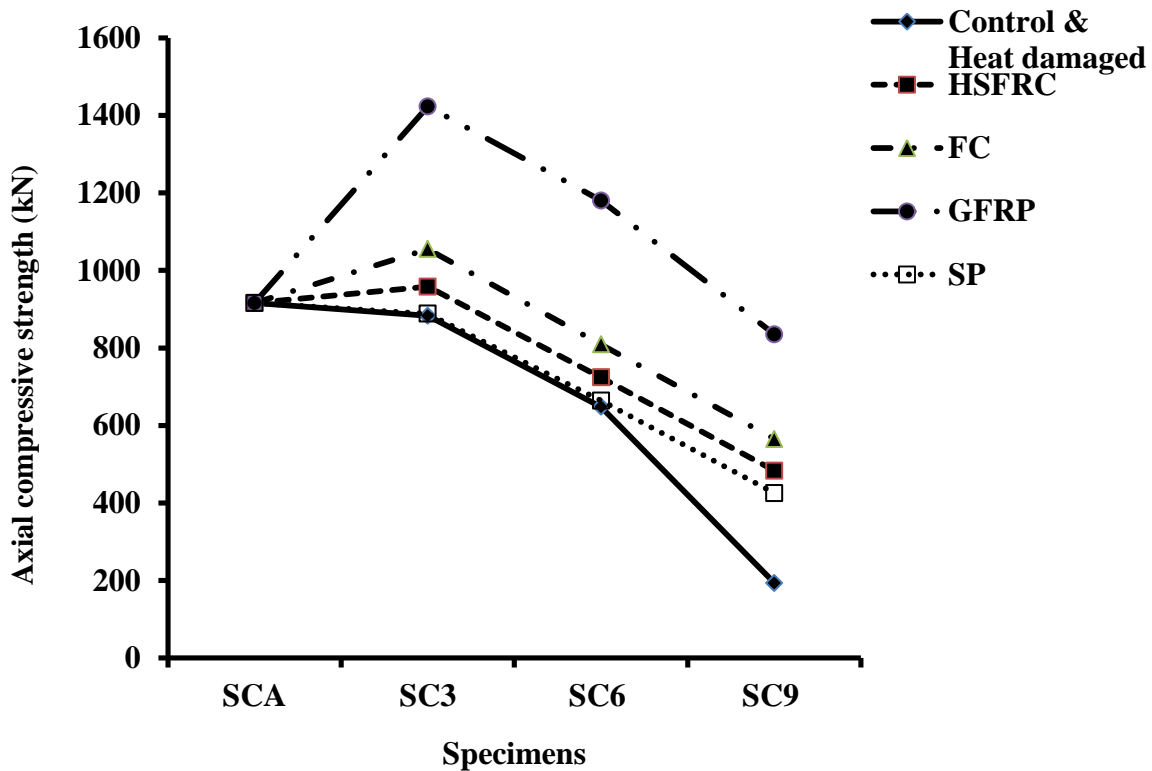
Fig. 3. 18: Axial compressive strength of square columns
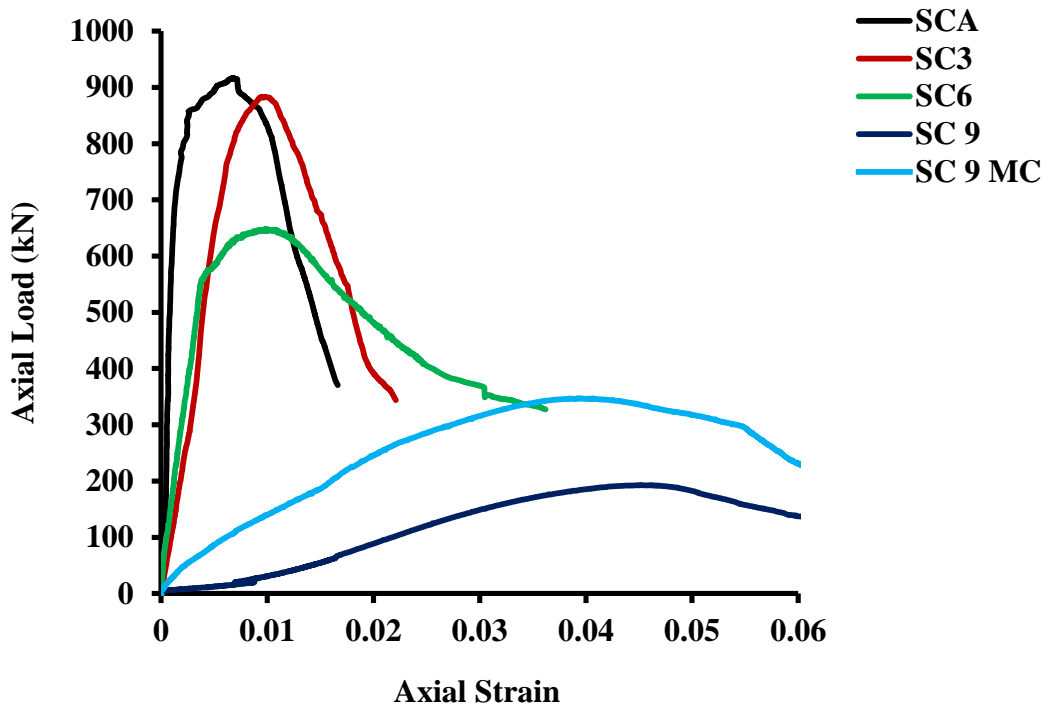
Fig. 3.19: Loads – axial strain Curves of control unheated columns and heat damaged columns
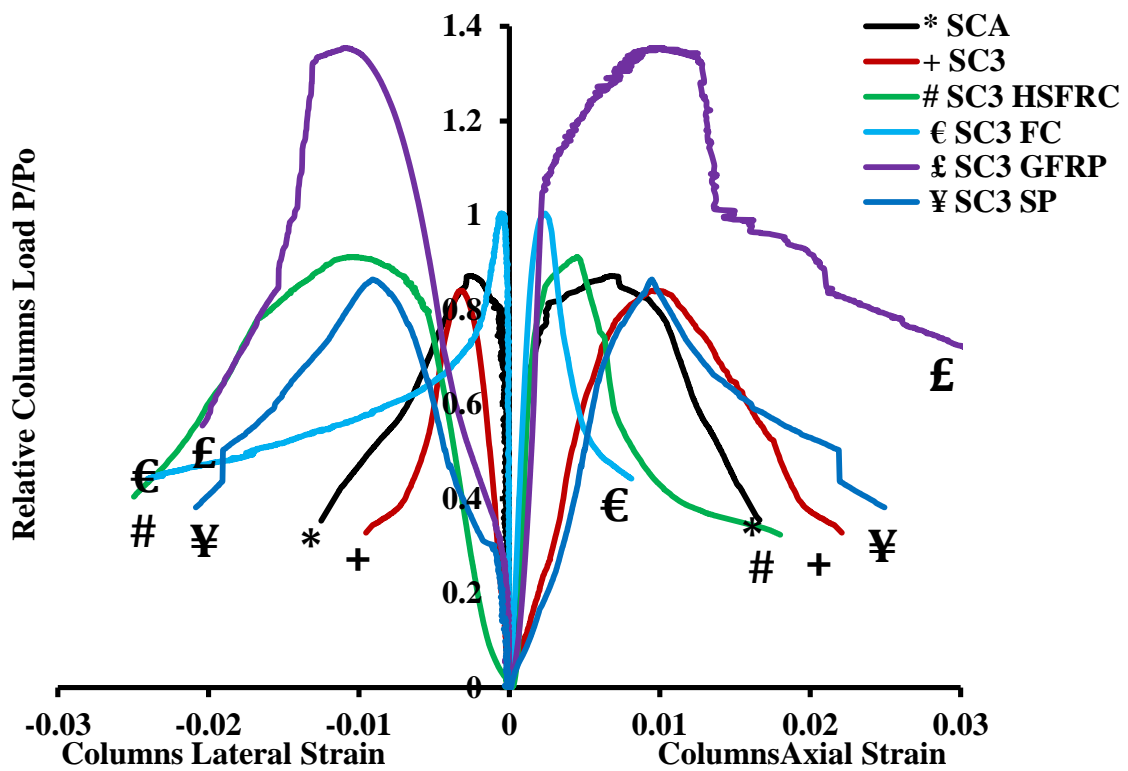
Fig. 3. 20: Load – axial & lateral strain curves of specimens heated at 300°C and strengthened with various techniques
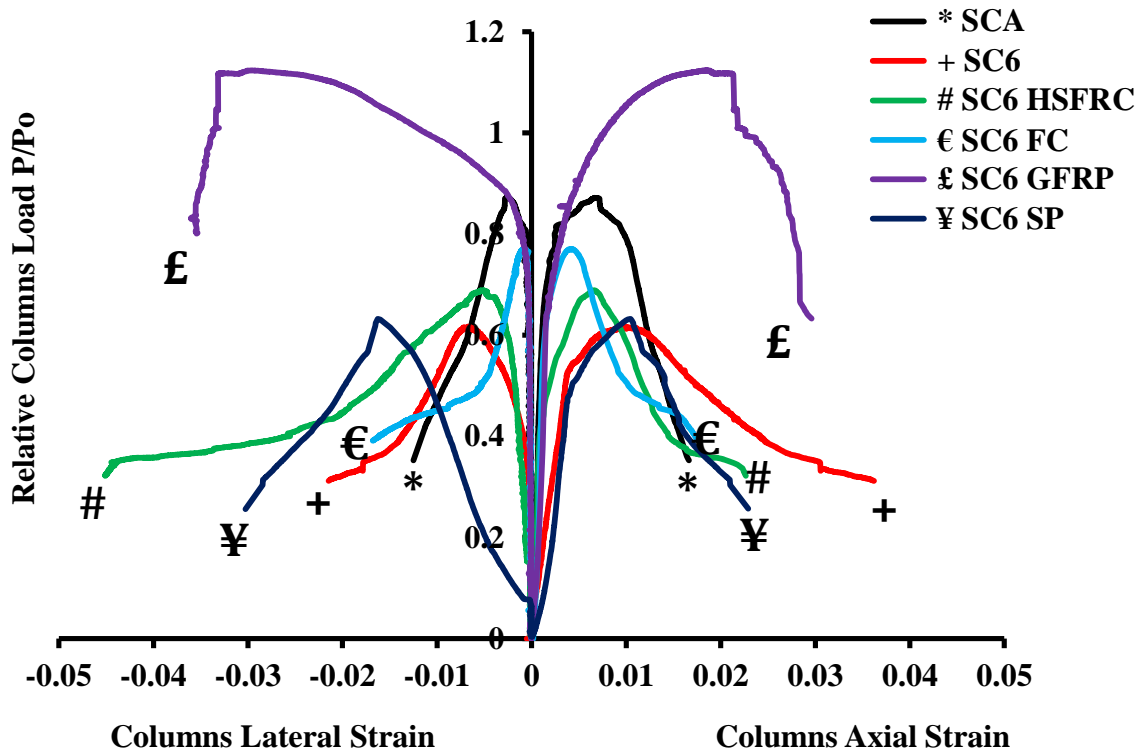
Fig. 3. 21: Load – axial & lateral strain curves of specimens heated at 600°C and strengthened with various techniques
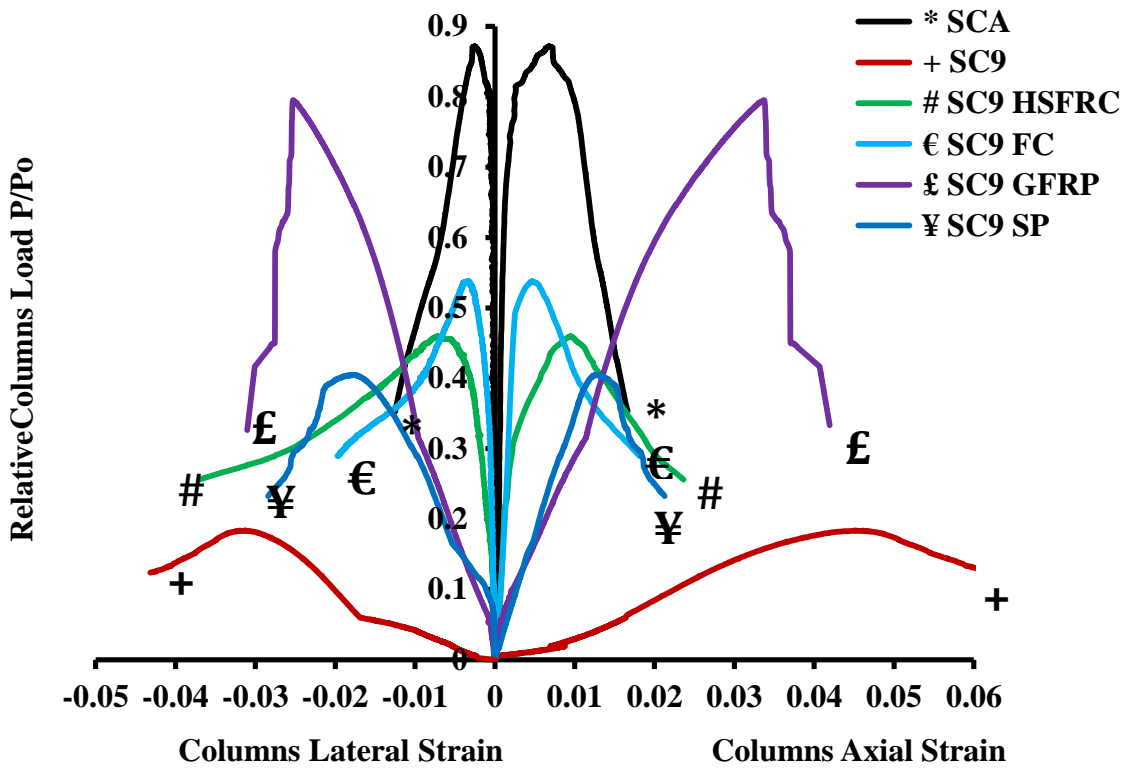
Fig. 3. 22: Load – axial & lateral strain curves of specimens heated at 900°C and strengthened with various techniques

100

As expected the strength of HSFRC jacketed specimens, which were exposed to different temperatures, was more than the corresponding un-strengthened heated specimens. The strength of HSFRC jacketed heated specimens was 8%, 12% and 150% more for specimens heated at 300°C, 600°C and 900°C temperatures respectively than the un-strengthened heated specimens Fig. 3.18 and Table 3.5. However, the HSFRC strengthening technique could not restore the strength of heat damaged specimens heated at 600°C and 900°C temperatures to their respective room temperature strength, though the strength of specimen heated at 300°C could be restored to the corresponding room temperature strength. Similarly in case of FC jacketed specimens, though the axial compressive strength was found to be higher than the heat damaged un-strengthened specimens by a margin of 19%, 25% and 192% respectively for the specimens heated to 300°C, 600°C and 900°C temperatures, but it remained less than that of the control unheated specimens. Only in the case of specimen heated to 300°C, it was possible to restore the strength of control unheated specimen by using FC technique Fig. 3.18. This increase in load carrying capacity is partly due to the greater cross-sectional area offered by the ferrocement jacket (40000 mm^2 in case of ferrocement repaired column, 22500 mm^2 in case of heat damaged column without strengthening).

However, the strength values of GFRP jacketed specimens were higher than the corresponding heat damaged un-strengthened specimens as well as the control unheated specimens at most of the considered temperatures. Only exception was the strengthened specimen heated at 900°C, where the GFRP could not restore the room temperature strength. In this strengthening scheme, the percentage strength gain of 61%, 34% and 330% were observed in the specimens heated at 300°C, 600°C and 900°C temperatures respectively with respect to the corresponding un-strengthened heated specimens. The strength of GFRP strengthened specimens heated 300°C, 600°C was found to be 55% and 29% more than the unheated control specimen. Since GFRP wrapping becomes active after core concrete fails due to the compressive forces, expansion of the concrete core in the radial direction makes the GFRP more and more active in resisting the axial compressive force. The strength of steel plate (SP) jacketed heated specimens was 1%, 2% and 120% more for specimens heated at 300°C, 600°C and 900°C temperatures respectively compared to the corresponding un-strengthened heated specimens. However, the steel plate strengthening technique could not restore the strength of heat damaged specimens to their respective room temperature strength.

3.6.3 Effect of Type of Strengthening Scheme on Stiffness Heated Specimens

The secant stiffness of square column specimens was calculated by dividing the ultimate measured compressive load by the ultimate axial deformation corresponding to peak as described earlier in Chapter 2, Section 2.7.3. The secant modulus provides a useful comparison of the effect of different strengthening schemes on the stiffness of strengthened heat damaged specimens (Figs. 3.20- 3.22). A significant loss in stiffness of concrete was noticed due to exposure to high temperatures (Fig. 3.23). The degradation of the heat damaged specimen's stiffness is mainly caused by the softening of concrete after heating to high temperatures. Voids and micro crack in the micro-structure of the concrete caused by heat have an important effect on its stiffness. On heating, the porosity of concrete is increased due to loss of moisture and due to the development of internal micro-cracking which ultimately results in stiffness loss. Fig. 3.23 shows the effect of HSFRC, FC, GFRP and SP jackets on the stiffness of heat damaged columns. The stiffness of both HSFRC and FC jacketed specimens was higher than both the control specimens for all the temperatures and heat damaged specimens heated up to 600°C temperatures.
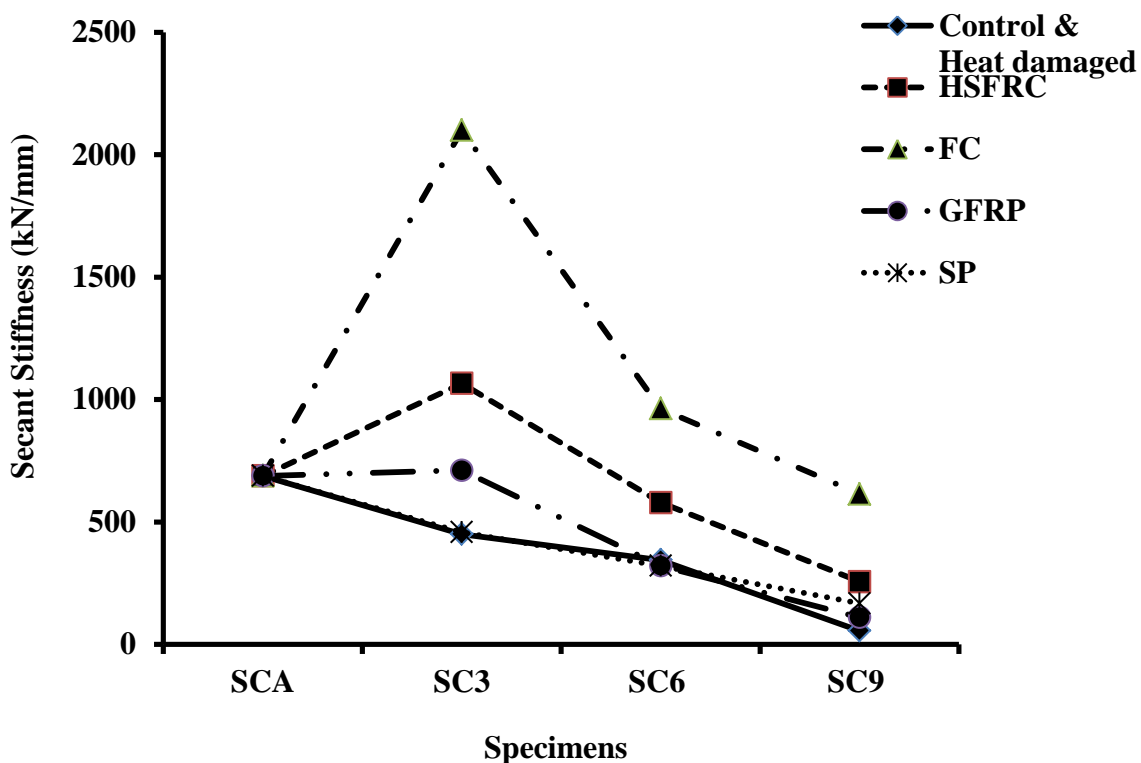
Fig. 3. 23: Comparison of secant stiffness of square columns

Table 3. 5: Comparison of axial strength

Method	Axial Compressive Strength (MPa)						
	Ambient	300° C		600° C		900° C	
		#	$	#	$	#	$
Control Specimens	(100%)	-	-	-	-	-	-
Heat Damaged Specimens	-	(-4%)	(100%)	(-29%)	(100%)	(-79%)	(100%)
Strengthened with HSFRC	-	(+4.5%)	(+8.5%)	(-21%)	(+12%)	(-47%)	(+150%)
Strengthened with FC	-	(+15%)	(+19.5%)	(-11%)	(+25%)	(-38%)	(+192%)
Strengthened with GFRP	-	(+55%)	(+61%)	(+29%)	(+34%)	(-9%)	(+332%)
Strengthened with SP	-	(-3%)	(+1%)	(-27%)	(+2%)	(-54%)	(+120%)

 # With respect to control specimens; $ With respect to heat damaged specimens

However, in specimens heated to 900^0C, though the stiffness was 360% and 1000% greater than the un-strengthened heat damaged specimens for HSFRC and FC strengthening respectively, the similar comparison with unheated control specimens showed strength values falling short by 63% and 10% compared to room temperature strength, Table 3.6. Fig. 3.23 compares the effect of GFRP jackets on the stiffness of heat damaged square columns. It is evident from this figure that the effect of GFRP on the stiffness improvement of heat damaged columns is negligible. This is due to the fact that the GFRP jackets had little confining effect on heat damaged square columns in the initial stages. The behaviour in terms of stiffness of GFRP wrapped heat damaged columns was similar to that of the heat damaged unwrapped columns, as shown in Figs. 3.20- 3.22.

In case of both GFRP and SP jacketed specimens, no significant improvement in restoration of stiffness in heat damaged specimens was observed (Table 3.6). The restoration of stiffness of the heat damaged specimen depends upon the confining action of HSFRC, FC, GFRP and SP jackets. The confining action of GFRP jackets takes effect when the heated concrete specimen approaches its ultimate unconfined compressive strength. Before approaching the ultimate unconfined compressive strength, the GFRP and SP do not contribute in the structural response because they are not active in the elastic range of the heated specimens when loaded axially as shown in Figs. 3.19 to 3.22. However, on the other hand, the HSFRC and FC jackets increased the stiffness of the heat damaged specimens due to the increase in the cross-sectional area of the specimens thus improving the dimensional stability of specimens. Comparing Figs. 3.18 and 3.23, it can be seen that the reduction in residual stiffness is higher than that of ultimate load. It is therefore more important when evaluating fire damaged concrete structures to consider deformation and stress redistribution.

3.6.4 Effect of Strengthening Technique on Deformability

The ductility of structural members is considered as one of the most critical parameters for evaluating its performance. Based on the stress-strain response of unheated, heat damaged specimens and heat damaged strengthened specimens as shown in Figs. 3.20 - 3.22, it is evident that the confinement with GFRP best improves the deformability of heated specimens. It can be observed that the post-peak portion of stress-strain curves of GFRP strengthened specimens is flatter and has lower slope than

Table 3. 6: Secant stiffness comparisons of strengthened specimens

Method	Secant Stiffness (kN/mm)						
	Ambient	300° C		600° C		900° C	
		#	$	#	$	#	$
Control Specimens	(100%)	-	-	-	-	-	-
Heat Damaged Specimens	-	(-34%)	(100%)	(-50%)	(100%)	(-92%)	(100%)
Strengthened with HSFRC	-	(+55%)	(+136%)	(-16%)	(+68%)	(-63%)	(+365%)
Strengthened with FC	-	(+248%)	(+432%)	(+40%)	(+179%)	(-10%)	(+1016%)
Strengthened with GFRP	-	(+3%)	(+58%)	(-53%)	(-7%)	(-84%)	(+100%)
Strengthened with SP	-	(-33%)	(+2%)	(-53%)	(-7%)	(-73%)	(+203%)

**# With respect to control specimens; $ With respect to heat damaged specimens*

the corresponding curves of specimens which were unheated and heated but were not strengthened. This trend was most prominent in GFRP strengthened specimens than in any other type of strengthening technique. This could be attributed to the fact that the failure of specimens was primarily due to tensile lateral strains. In control and heat damaged specimens without wrapping, the strain in the lateral direction reached the ultimate tensile strain of concrete at a relatively lower axial strain. However, in strengthened heat damaged specimens, the fibre endured this lateral tension and consequently increased the specimen capacity to carry a much higher value of axial and lateral strains. The deformability of heat damaged strengthened specimens wrapped with GFRP jackets was greater than the other strengthening schemes. Surprisingly HSFRC and FC strengthened specimen's exhibited lesser deformation ability than even the heat damaged un-strengthened specimens (Figs. 3.20-3.22). This might be due to the increase in cross section area due to strengthening techniques. It was also observed that the GFRP technique was more effective in increasing the deformability of heat damaged concrete than increase in load carrying capacity. This might be due to the confining action of GFRP strengthened specimens, which shows a ductile behavior.

3.6.5 Energy Dissipation of Specimens

The energy dissipation is usually defined as the area under the concrete stress-strain curve. The energy capacity values were calculated up to the 80% of Pu_{max} on the descending portion of the curve as described earlier in Chapter 2, Section 2.7.4. Table 3.7 provides the energy dissipation capacities of strengthened heat damaged specimens. It can be clearly marked that the specimens strengthened with GFRP dissipated maximum energy than any other strengthening techniques as evident from stress-strain curves shown in Figs.3.19-3.21. The GFRP strengthened specimens SC3 GFRP, SC6 GFRP and SC9 GFRP, which were earlier heated to $300^{°}$C, $600^{°}$C and $900^{°}$C temperatures respectively, showed 7%, 129% and 193% greater energy dissipation than the corresponding control unheated specimens (SCA) respectively.

The similar comparison with respect to heat damaged un-strengthened specimens showed the enhancements of 77%, 233% and 682% in energy dissipation for the specimens heated at $300^{°}$C, $600^{°}$C and $900^{°}$C temperatures. This could be due to the fact that GFRP jacketed specimens obtained higher strength and strain compared to other strengthening techniques. On the contrary the HSFRC, FC and SP strengthened specimen's showed lesser energy dissipation capacity than the un- heated control

specimens and heated un-strengthened specimens heated at $300°C$ and $600°C$ temperatures. It was due to the fact that the HSFRC, FC and SP strengthened specimens, with the amount of strengthening selected in the present study, could not provide a marked ductile and extended post-peak behavior resulting into relatively lower areas under the stress-strain curves. Nevertheless these strengthening techniques showed improvement in energy dissipation in case of specimens heated at $900°C$.

3.7 COMPARISON BETWEEN TEST RESULTS AND CODE PREDICTED VALUES

Attempt was made to compare the axial strength results of this study with the strength values predicted by the Code (ACI Committee 440.2R-02) specified equations. It may be mentioned here that the equations for predicting the strength of FRP confined and strengthened columns as per the Code are applicable to the strengthening of unheated concrete columns. The equations used by the ACI Committee 440.2R (2002) to calculate the maximum confinement pressure (fl)and the ultimate confined axial compressive strength ($f'cu$) of the FRP wrapped concrete specimens are presented in Table 3.8. Figs. 3.24 and Table 3.9 compare the predicted confined compressive strengths with the experimental compressive strengths of the heat damaged reinforced concrete square columns wrapped with two layers of unidirectional glass fibre reinforced polymer jackets. The comparison reveals a marked difference between the code predicted strengths and the test results. From the results shown in Fig. 3.24 and Table 3.9 it can be seen that the ACI Committee 440-2R-02 confinement model predictions are 5%, 23% and 36% lower than the experimental confined compressive strength of heat damaged square columns wrapped with GFRP. This could be due to the fact that the ACI confinement models are based on the concrete columns undamaged by heat. Thus, in case of fire damaged concrete, the current existing international design guidelines are more conservative for the prediction of confined compressive strength of heat damaged columns wrapped with FRP.

Table 3. 7: Energy dissipation capability of strengthened Specimens

Method	Ambient	300° C		600° C		900° C	
		#	$	#	$	#	$
Control Specimens	(100%)	-	-	-		-	-
Heat Damaged Specimens	-	(-6%)	(100%)	(-31%)	(100%)	(-62%)	(100%)
Strengthened with HSFRC	-	(-49%)	(-46%)	(-33%)	(-4%)	(-46%)	(+44%)
Strengthened with FC	-	(-74%)	(-72%)	(-48%)	(-27%)	(-55%)	(+19%)
Strengthened with GFRP	-	(+7%)	(+77%)	(+129%)	(+233%)	(+193%)	(+682%)
Strengthened with SP	-	(-21%)	(- 20%)	(+23%)	(+12%)	(-49%)	(+35%)

 # With respect to control specimens; $ With respect to heat damaged specimens

Table 3. 8: Summary of the design models for square sections

Codes/Guideline	Confinement Pressure (fl)	Ultimate Compressive Strength (fcc')
ACI 440.2R (2002)	$f1 = \dfrac{Ka\rho f\varepsilon feEf}{2}$	$fcc' = fc'\left[2.25\ \sqrt{1 + 7.9\dfrac{f1}{fc'}} - 2\dfrac{f1}{fc'} - 1.25\right]$
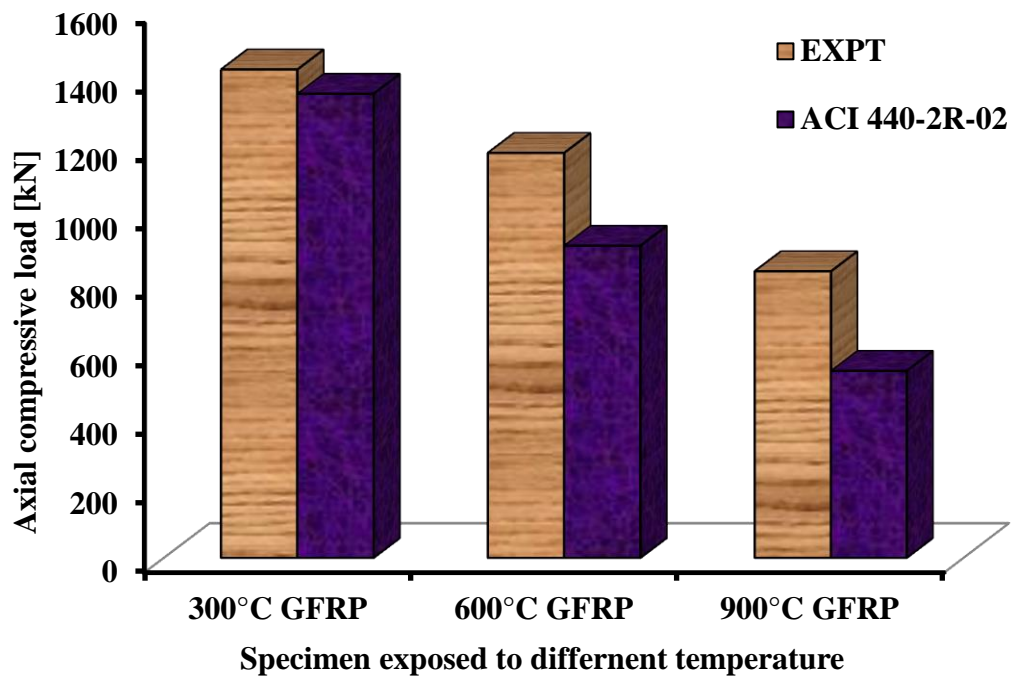
Fig. 3. 24: GFRP strengthen heat damaged square column specimens

Table 3. 9: Theoretical and Test Results

Specimen Designation	Temperature (° C)	ACI 440-2R-02 Theoretical Load [kN]	Experimental Peak Load [kN]
SCA	--	--	916
SC3	300° C	--	883
SC3 GFRP	300° C	1352	1423
SC6	600° C	--	648
SC6 GFRP	600° C	909	1180
SC9	900° C	--	193
SC9 GFRP	900° C	544	835

3.8 CONCLUDING REMARKS

This study reports the results of experimental investigation undertaken to gauge the effectiveness of various commonly used strengthening techniques in restoring and strengthening the lost mechanical properties of square concrete columns damaged by fire or any other heat source. A total of 51 short square column specimens were tested under this program. The test variables included degree of damage caused by different elevated temperatures and the type of strengthening scheme. The results have been analyzed and discussed in detail to fulfill the objectives of this investigation. Important observations have been made on the effect of various strengthening techniques on thermal and mechanical performance of heated concrete columns.

CHAPTER –4
A STUDY ON DIFFERENT TECHNIQUES OF
RESTORATION OF HEAT DAMAGED R.C. BEAMS

4.1 INTRODUCTION

The aim of the research presented in this Chapter is to examine the effectiveness of various restoration and strengthening techniques for reinforced concrete flexural members damaged by fire or any other heat source. Conventional restoration and strengthening techniques as explained in the previous Chapters namely Fiber Reinforced Polymer (FRP) Wraps, Ferro cement (FC) Jacketing, and High Strength Fiber Reinforced Concrete (HSFRC) Jacketing have been employed in this study also.

4.2 RESEARCH SIGNIFICANCE

Sufficient information exists in the literature on FRP strengthening of RC beams, which are distressed by factors other than the fire or elevated temperature (Saadatmanesh 1991, Chajes et al. 1994, Saadatmanesh and Malek1998, Khalifa et al. 1998, Almusallam and Al- Salloum 2001, Sheikh 2002, Teng et al. 2002 and 2004, Toutanji 2006, Bousselham and Chaallal 2006, Gao et al. 2006, Barros et al. 2007, Monti and Liotta 2007, Tsonos 2008, Ceroni 2010, Galal and Mofidi 2010, Panda et al. 2011a and 2011b). On the contrary only limited research has been reported on the restoration and strengthening of fire damaged concrete beams using FRP wraps (Reddy et al. 2006, Haddad et al. 2008, Udaya Kumar et al. 2009, Kaiet al. 2011, Haddad et al. 2011, Jiang-Tao et al. 2012). Similarly, though enough information exists in the literature on strengthening of RC beams with Ferro Cement (Kaushik and Dubey 1994, Paramasivam et al. 1994, Fahmyet al. 1997, Al-kubaisy and Zamin 2000, Seshu 2000, Nassif et al. 2003, Mourad and Shannag 2012, Khan et al. 2013), there is hardly any study on using this technique for restoring and strengthening fire damaged RC beams. Recently developed strengthening technique namely High strength fibre reinforced concrete has been investigated with reference to concrete beams for their capacity enhancement under normal ambient temperature conditions (Alaee 2003, Alaee and Karihaloo2003, Farhat et al. 2007, Martinolaet al. 2007 and 2010, Tayehet al. 2013), while this technique's capability in restoring the flexural capacity of fire damaged concrete beams has been investigated only to a limited extent (Haddad et al. 2008 and 2011, Leonardi et al. 2011).

4.3 EXPERIMENTAL PROGRAM

An experimental program was planned to examine the efficiency of various techniques for restoring and strengthening of heat damaged reinforced concrete beams. A series of 27 reinforced concrete beams were constructed using normal strength concrete mix. The normal strength concrete mix was the same as explained in the previous Chapters. Reinforced concrete beam specimens of T shape were constructed, as the beams in any framed concrete structure with reinforced concrete monolithic slabs behave as T beams. The details of the specimens are illustrated in Table 4.1 and Fig. 4.1. Experimental variables included temperature of exposure and type of strengthening technique. All the beams were cast in nine different series as shown in Table 4.1. The first two letters (TB) in the abbreviation denote T beam, the numeral (6 and 9) indicates the temperature of exposure i.e. 600^0C & 900^0C. The geometry and other details of the beam specimens are shown in Fig. 4.1.

Table 4. 1: Details of beam specimens

Beam designation	Beam condition	Strengthening methods
TBA	Control	none
TB6	Heat damaged 600^oC	none
TB9	Heat damaged 900^oC	none
TB6 HSFRC	Heat damaged 600^oC	High strength fiber reinforced concrete
TB6 FC		Ferrocement jacketing
TB6 GFRP		Glass fiber reinforced polymer
TB9 HSFRC	Heat damaged 900^oC	High strength fiber reinforced concrete
TB9 FC		Ferrocement jacketing
TB9 GFRP		Glass fiber reinforced polymer
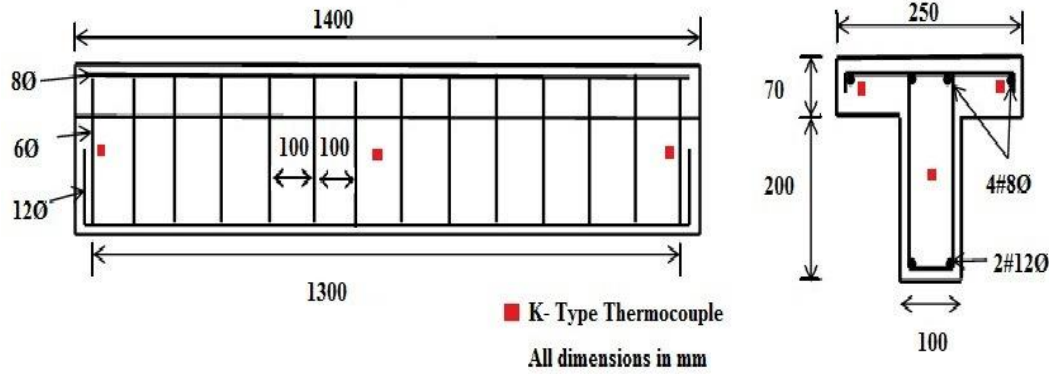
Fig. 4.1: Reinforcement Details of T- Beam

The concrete was prepared with crushed limestone aggregate of maximum size 12.5 mm, ordinary Portland cement, natural river sand (zone 2), and potable water. The companion standard plain concrete cylinders (100 × 200 mm) and cubes (150 mm × 150 mm) were also cast along with each series of beams to determine the nominal strength of concrete and moisture content respectively on the day of testing of beam specimens.The properties of various materials, casting procedure and detailed concrete mix proportions along with 28 days cylinder compressive strength of the concrete have already been explained in Chapter 2. The reinforcement design i.e. flexural and shear reinforcement were kept same in all the specimens. The tension reinforcement consisted of 2 numbers of 12 mm diameter bars having yield strength of 610MPa. Four bars of 8 mm diameter were also provided as hanger bars, which had yield strength of650MPa, while 550MPa yield strength bars of 6 mm diameter were used as shear reinforcement. The average stress-strain relationships established by performing at least three coupon tests for each type of reinforcement bar are illustrated in Fig. 4.2. The spacing of shear reinforcement was kept as 100mm as shown in Fig. 4.1.

All the T- beams were of same cross-section and length. A concrete cover of 15 mm was provided in all the beams. Five K type thermocouples were placed in each beam during casting in order to monitor the temperature at the time of heating. Three thermocouples were placed at the center of the web and two at the flange, as shown in Fig. 4.1.The specimens were cast using steel moulds in the laboratory as shown in Fig. 4.3. Needle vibrator was used during the casting of beams. After 24 hrs, the beams were removed from the moulds and covered with gunny bags for curing. The water curing period lasted for 28 days after which the beams were kept in the laboratory at ambient temperature and humidity conditions for another 120 days. After 150 days of total

ageing, the specimens were exposed to various heating regimes. Subsequent to a single cycle of heating and cooling, the specimens were strengthened and tested.
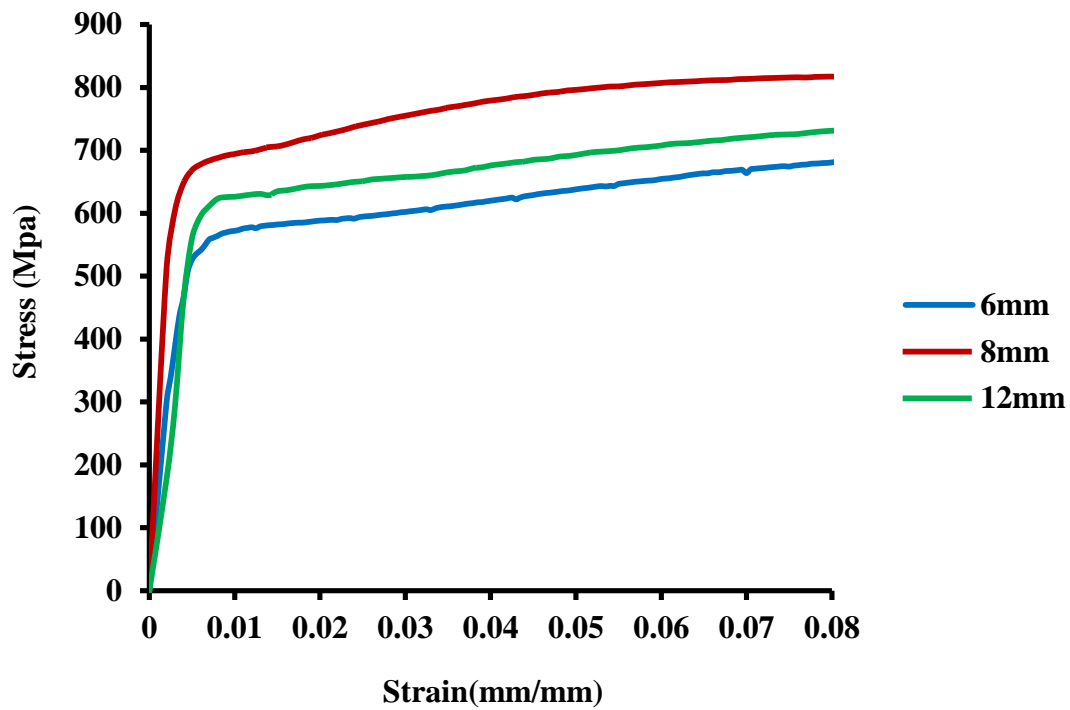
Fig. 4.2: Stress-strain curves of reinforcing bars

Fig. 4.3: Stages of casting T-beams

The properties of the constituents of the strengthening materials have already been explained in Chapter 2. The slurry used in preparing HSFRC and FC jackets included ordinary Portland cement, natural sand which was less than 600 micron and silica fume. The slurry mix proportions were 1:0.6:0.15:0.35:0.01 by weight of cement, sand, silica fume, water and super plasticizer respectively. The 28 days cube compressive strength and flow-ability of the slurry has already been explained in Chapter 2. Welded square wire mesh, which was locally available in the market, was used as the reinforcement in Ferrocement jacket. Acrylic polymer based bonding agents were used to bond old and new cementitious strengthening materials. The properties of acrylic polymer are show in Table 4.2. The properties of GFRP used for the investigation was uni-directional with nonstructural weaves in the secondary direction to hold the fabrics together, thickness of FRP was about 0.324mm, average tensile strength 3400 N/mm², and an ultimate elongation of 4.33%. The other properties of epoxy resin used for bonding FRP wraps have already been explained in Chapter 2.

Table 4. 2: Properties of acrylic polymer

Sr.no	Property	Value
1	Mix Proportion	Add cement to MPB in the ratio 1:1 by volume
2	Form	LiquidAcrylic Latex
3	Specific gravity	1.03 +/-0.02
4	Pot Life	40Mins +/- 15 mins
5	Bond Strength	Failure of concrete

4.3.1 Thermal Testing of Specimens

The Beam specimens were subjected to heat treatment using a specially fabricated table mounted electrical furnace. The programmable electrical furnace has a maximum heating capacity of heating up to a temperature of 1200°C, Fig. 4.4. It was possible to measure temperatures inside the furnace with K-type thermocouples. The beams were exposed to two different target temperatures of 600° C and 900°C after 150 days. The furnace was able to accommodate one beam at a time. The T- beam specimen

was placed in the furnace upside down so that the top face of the flange remains unexposed, which resembles the real condition of the roof beams in a building. The heating rate was set at 10^0C /min, which has been shown to be reasonable for structures exposed to fire. Each target temperature was maintained for three hours to achieve a thermal steady state condition as shown in Fig. 4.5. The heating rate of 10°C/minute means the rate of temperature rise inside the furnace, and not the rise of temperature inside the concrete specimens.

Fig. 4.4: A view of furnace and beam specimen
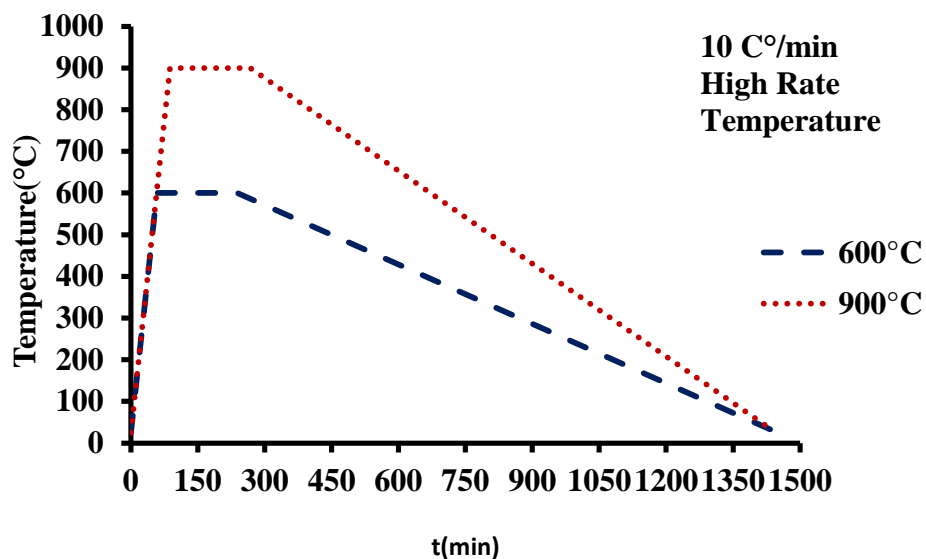
Fig. 4.5: Heating and cooling cycle

The temperature histories during the heating and cooling regimes in the specimens were recorded by means of thermocouples. On completion of the exposure time, the furnace was switched off and samples were left in the furnace for natural cooling to room temperature. The rate of cooling was not controlled but was measured

constantly during the complete testing. Data acquisition system was used for obtaining the thermocouple readings.

4.3.2 Observations after Heating

When evaluating the condition of damaged beams, visible damage and the results of visual inspection are used to identify damage and assess its magnitude at the first instance. Visible damage can be such as cracks, spalled areas, colour change etc. In this study the colour of concrete changed to light greyish at 600°C. However, the colour of specimens changed to ash white when exposed to 900°C. The colour change may be attributed to the changes in the chemical composition of cementing materials and aggregates. The observations of colour change due to the heating and cooling of concrete also gives an idea of the degree of temperatures reached. In the heated test specimens some hairline cracks were observed at 600°C. The number of cracks became relatively pronounced at 900°C.The cracks propagated laterally and longitudinally over the span with widths ranging from 0.1 mm to 1 mm. Due to high temperature especially at 900°C, the concrete suffered extensive cracking. The Fig. 4.6 illustrates the cracks observed on the surface of beam specimens exposed to 600°C and 900°C temperatures.
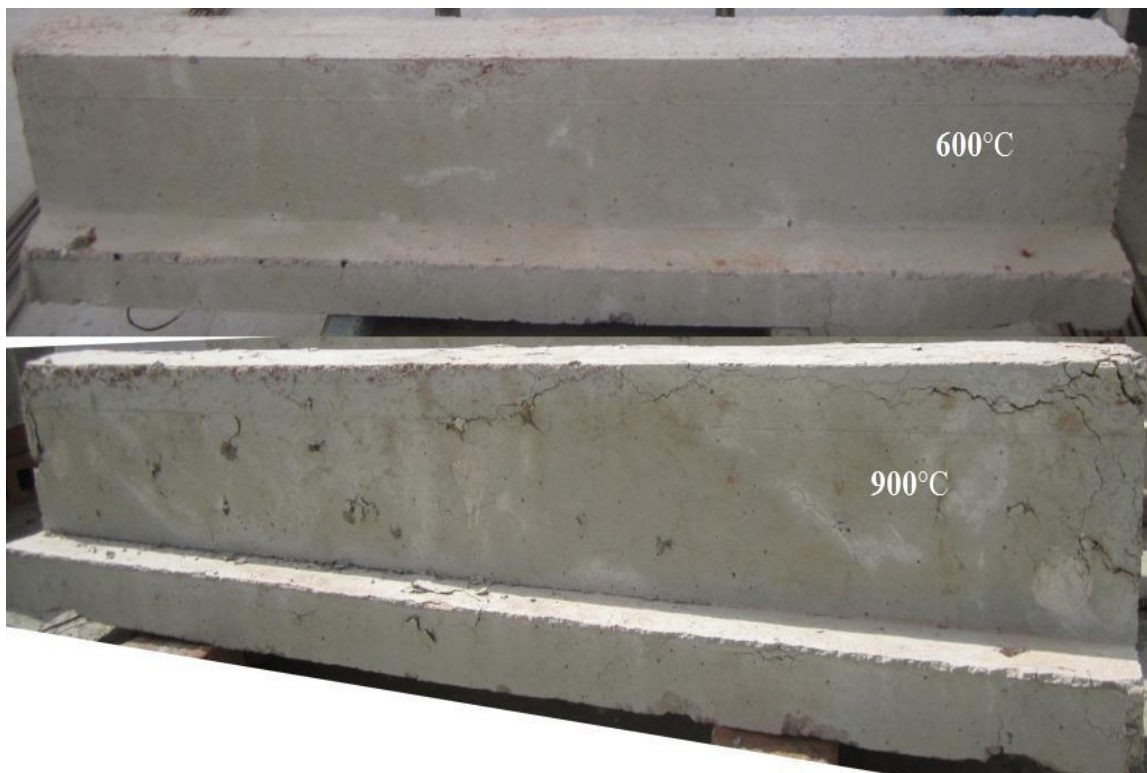
Fig. 4.6: Surface cracking observed in test specimens exposed to 600°C and 900 °C

4.3.2.1 Ultrasonic pulse velocity testing

Ultrasonic pulse velocity (UPV) testing was conducted on each group of beams before heating and seven days after heating. Testing procedures are already explained in Chapter 2. The average ultrasonic pulse velocity test results for all the specimens are shown in Fig. 4.7. The results corroborate the visual observations as the UPV values declined with heating confirming the occurrence of damage due to heat.
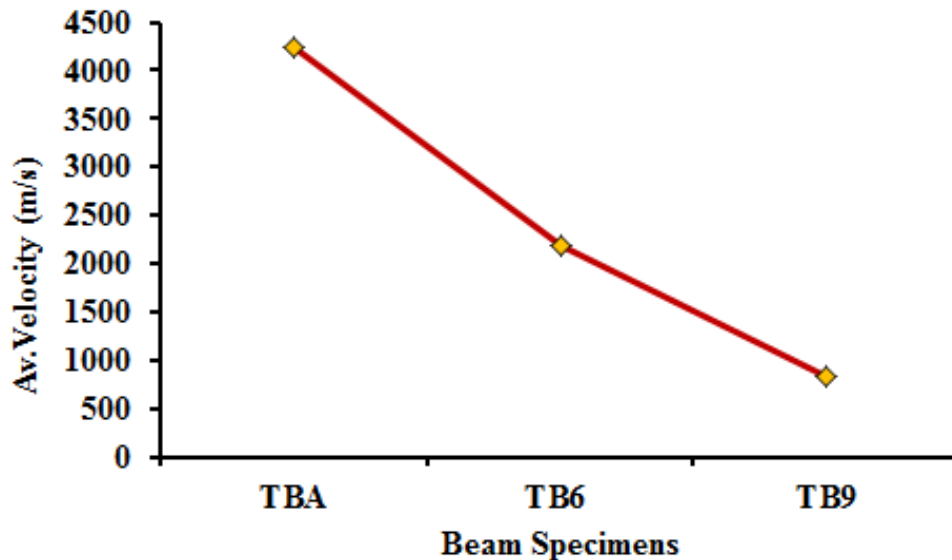
Fig. 4. 5: Average Ultrasonic pulse velocity in specimens before and after high temperature

4.4 RESTORATION OF SECTION OF HEAT DAMAGED BEAMS

After heat exposure, the heat damaged beams which got cracked and crumbled, were repaired before further strengthening. The cracked section was removed and restored using micro-concrete. The damaged cover concrete was removed using steel wire brush, chisel and hammer (Fig. 4.8). Then the surface of specimen was cleaned thoroughly by water and then by compressed air to ensure no dust. A primer coat of bonding agent was applied on the resulting surface of the specimen to achieve good bonding between the old concrete and new repair material i.e. micro concrete as shown in Fig. 4.8. The epoxy resins were prepared by mixing two components (resin and hardener components) strictly following the manufacturer's instructions. Once the bond coat became tacky, the micro concrete was applied to the specimens. The micro concrete repaired beams were covered with damp gunny bags for 7 days and kept in laboratory conditions until strengthening. The specimens, which did not undergo any damage, were

directly strengthened by the appropriate technique. The surface projection and corners of the beams were rounded off slightly to ensure that the strengthening materials were not damaged due to stress concentration at the corners of the beam specimens (Fig. 4.9).

Fig. 4.6: Restoration process of beam elements

Fig. 4.7: Grinding before strengthening of beams

4.5 STRUCTURAL STRENGTHENING OF BEAMS

The surface prepared and heat damaged beams were further strengthened by various techniques namely HSFRC, FC and GFRP (Fig. 4.10). In all the specimens a primer epoxy bonding was applied after the surface was cleaned in order to provide good bonding between the substrate and the new strengthening material. Steel moulds with the same shape as the beam specimens, but having larger dimensions were used to cast the

HSFRC and FC jacket on the faces of beams. These moulds allowed casting 20 mm cover at bottom, side of the web and bottom of flange. The beams were strengthened in such a way that they got strengthening both in flexure and shear. FRP was provided on the tension face of the web (i.e. bottom face) with fibres aligned parallel to the span in the entire length of the beam, while shear enhancement was made possible by putting FRP U wraps in the end shear dominating regions as shown in Fig. 4.10. However, due to the fabrication reasons the beams meant to be strengthened with FC and HSFRC, jacketing was provided on all the faces of web and flange except the top unexposed face of the flange.
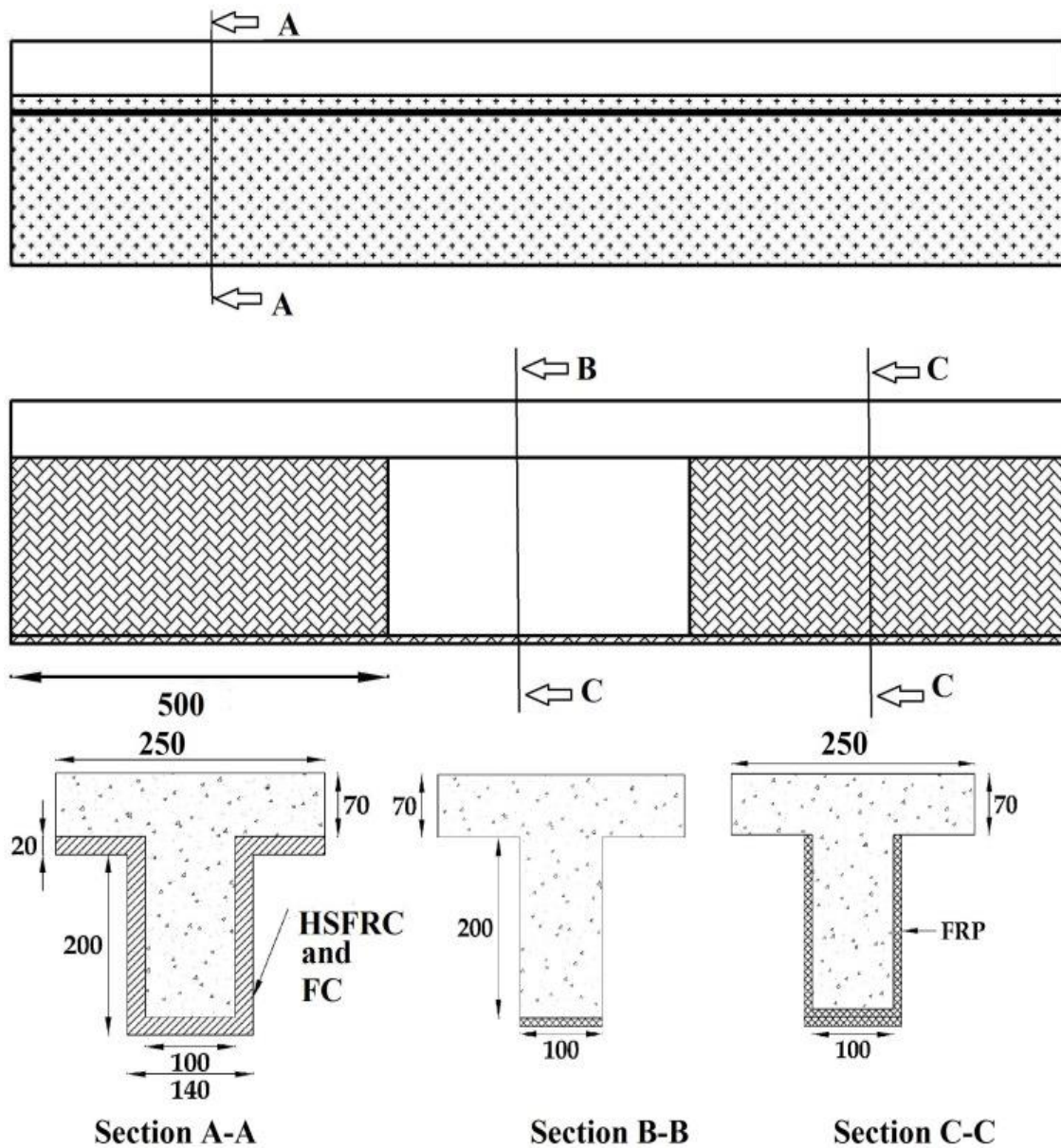
Fig. 4. 8: Strengthening schemes

4.5.1 HSFRC Jacketing

The heat damaged specimens meant for strengthening with HSFRC jacketing were placed inside the steel moulds as shown in Fig. 4.11. HSFRC slurry reinforced with hooked steel fiber at a volume fraction of 2% was poured into the steel mould to form a 20 mm thick jacket. After 24 hrs, the strengthened beams were demoulded and cured using wet gunny bags for another 28 days. Cubes and cylinder specimens were prepared from the fibrous slurry to obtain mechanical properties of the slurry. The standard cubes and cylinders were cured for 28days in wet gunny bags, then capped and tested under axial compression. The slurry with steel fiber had compressive strength of 72.65 MPa.

Fig. 4.9: HSFRC jacketing in progress

4.5.2 Ferro Cement Jacketing

The FC jacketing was constructed with two layers of welded wire mesh of 13mm x 13mm. At several places, the first and the second layers of the wire mesh were tied together with the same diameter of steel wire. Wooden mallets were used to keep the wire mesh close to the surface of T-Beams, while in web the mesh were anchored with small screws as shown in Fig. 4.12 to ensure required position. Slurry was poured into the moulds to form 20mm thick FC jacket (Fig. 4.12). With each specimen, three 50 mm slurry cubes were cast to determine the slurry compressive strength. The slurry mix had a

compressive strength of about 68.06 MPa. The strengthened specimens were covered with damp gunny bags for 14 days after demoulding.
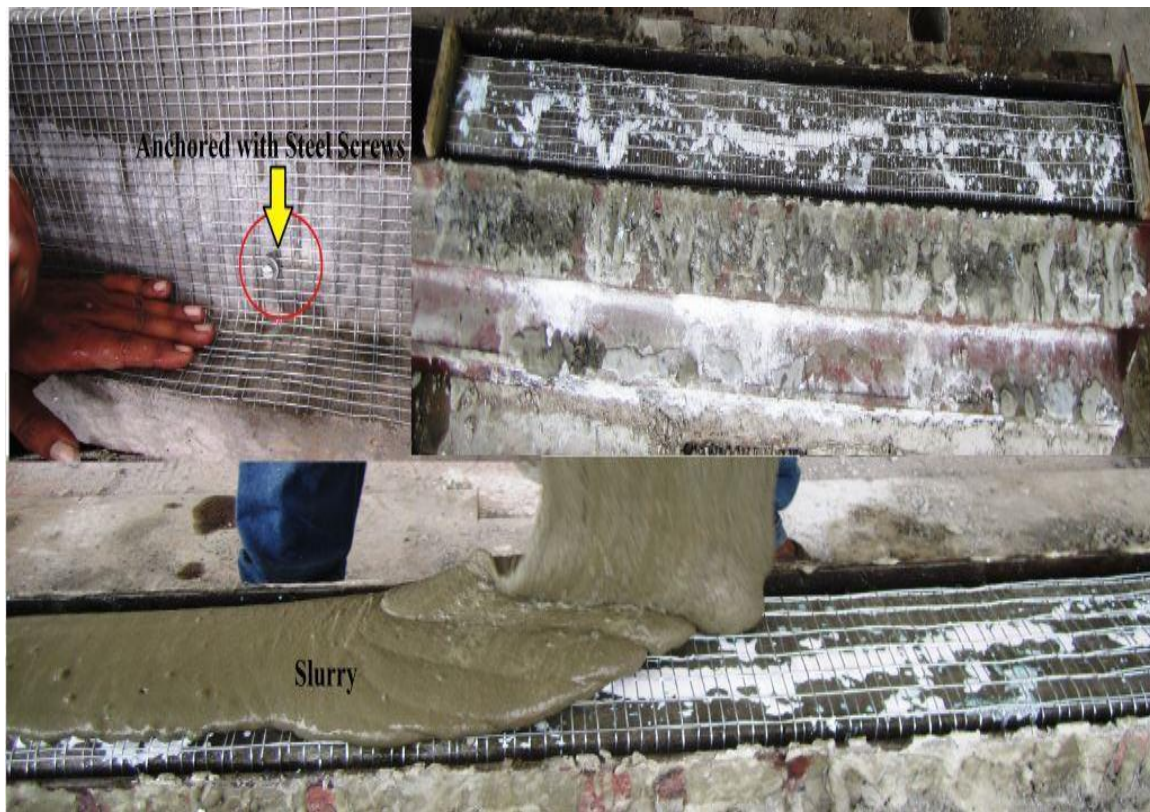
Fig. 4.10: FC jacketing in progress

4.5.3 GFRP Jacketing

Before GFRP jacketing the surface of heat damaged specimens were scraped lightly to remove surface contaminants. Then the surface of the concrete was coated with a layer of epoxy primer on the external surfaces of the concrete to fill air voids and to provide good bond strength. Thereafter, a thin layer of the two part saturant solution consisting of resin and hardener mixed as per the manufacturer's specifications was applied over the web at bottom and side of web on both sides of shear regions. Then the first layer of GFRP sheets was wrapped on the bottom of the web carefully. A roller was used to remove the entrapped air between the fiber and excess saturant so as to allow better impregnation of the saturant. Special attention was taken to ensure that no air voids were left between the fiber and the concrete surface. After the application of the first wrap, a second layer of saturant solution was applied on the surface of the first layer in length. The roller was used again to remove any trapped air and to force the resin in the fibers (Fig. 4.13). All the specimens were stored at room temperature for at least 28 days before testing.
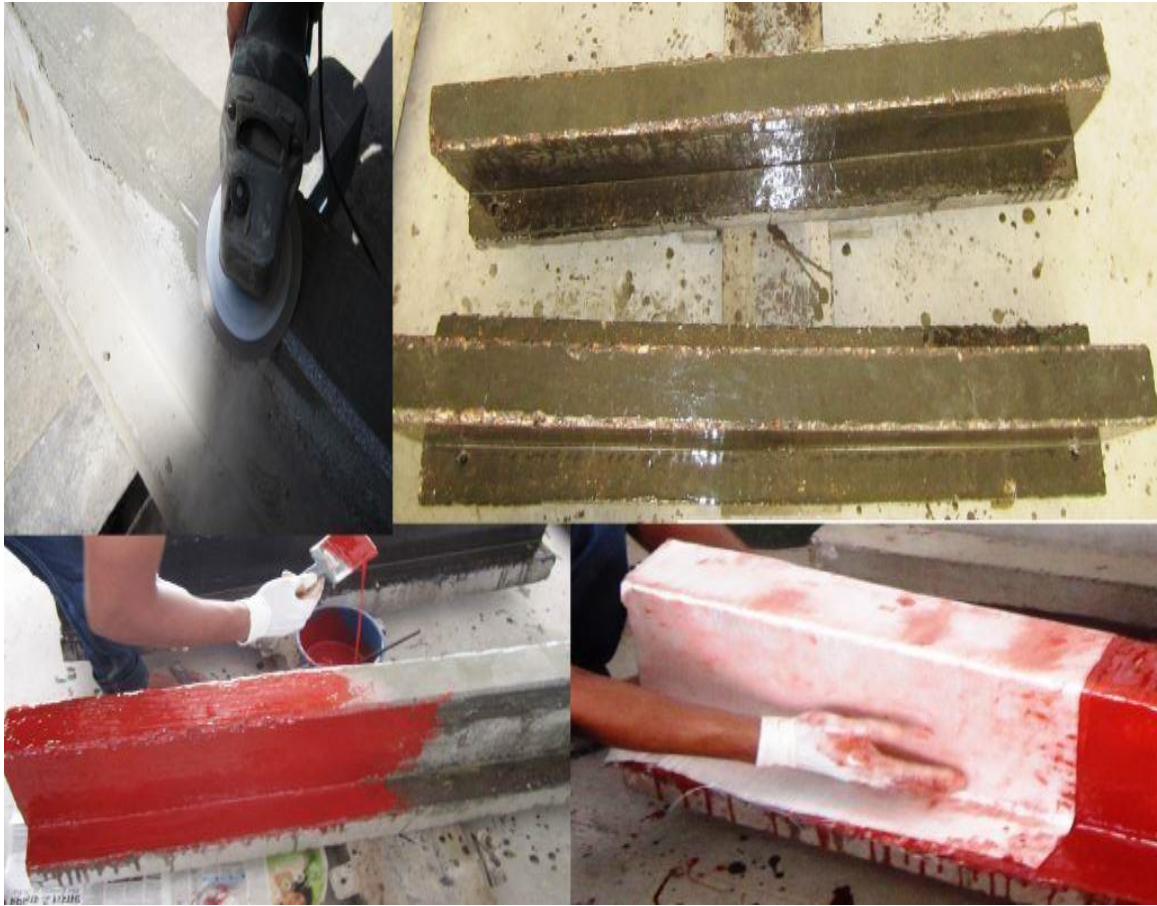
Fig. 4. 11: GFRP jacketing

4.6 INSTRUMENTATION AND FLEXURAL TEST SETUP

Mechanical testing of the specimens was carried out after a complete cycle of heating, cooling and strengthening. The T- beam specimens were tested in simply supported end conditions under four point loading. The load - deflection responses were captured using a 200 Ton capacity hydraulic hand operated jacks through load cells. The beams were tested under monotonic increasing load up to their collapse. The deflections of the beam were noted using linear variable differential transducers (LVDT), placed at five locations at the bottom of beams and were also connected to data logger as shown in Fig. 4.14. The strain gauges were also mounted on the bottom of web and side of web in GFRP jacketing to record strains in FRP. The recorded data from the LVDTs, strain gauges and load cell were fed into a data acquisition system and stored on a computer.
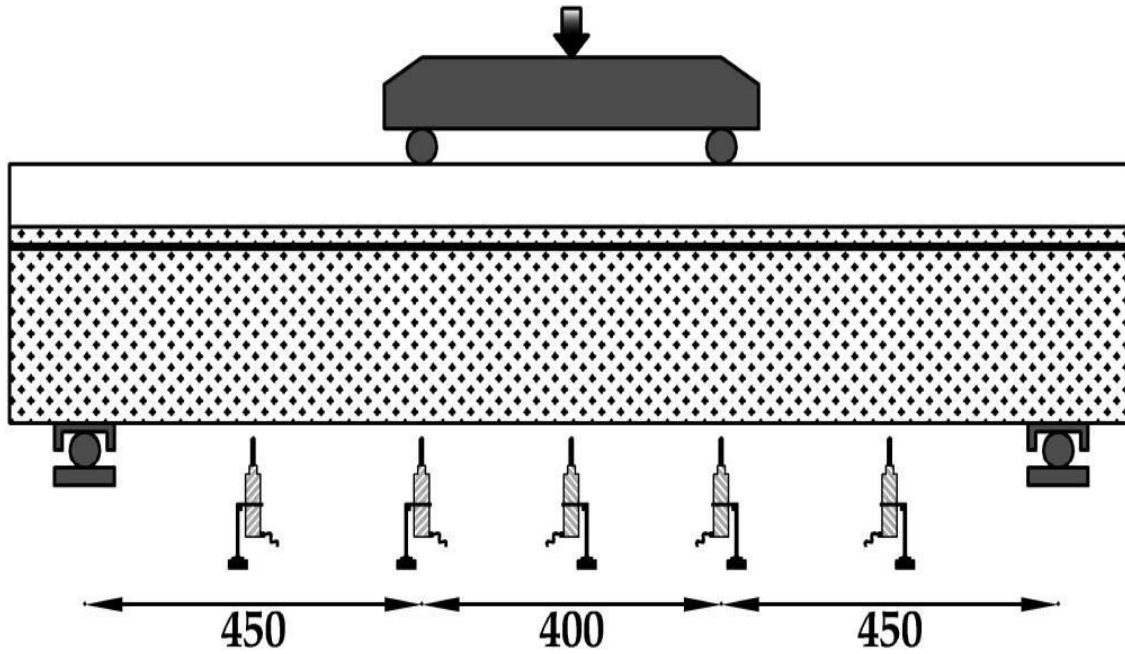
Fig. 4.12: Test setup

4.7 TEST RESULTS AND DISCUSSION

The performance of strengthened beams was assessed through the measured load deflection curves in terms of the ultimate load capacity, stiffness and ductility. The measured load deflection curves are shown in Figs. 4.15 – 4.19. Tables 4.3 to 4.6 furnish the various measured and computed key parameters of the specimens. The load corresponding to the yield point, P_y, and the load corresponding to the ultimate point, P_u are shown in the Table 4.3. The μ_Δ is the deflection ductility index, while Δ_y and Δ_u are the mid span deflections at yield load and ultimate load respectively. The μ_E is the energy absorption capacity and E_y and E_u are area under the load deflection diagram at yield load and ultimate load of beam respectively (Spadea et al. 1998).

4.7.1 Load-Deformation Relationships

The influence of temperature on the strength and deformability of the beams can be studied from Fig. 4.15. The average load-deformation curve of unheated beams is also shown for comparison. It can be noted that the strength and deformability of beams reduce as the temperature of exposure increases. A huge reduction in load and deformation can be noticed in the specimens exposed to a temperature of 900^oC, though it was not very significant in case of 600^oC heated specimens. The decrease in the strength and deformability can be attributed to the reduction in yield strength of steel and decrease in compressive strength of concrete with temperature.

124
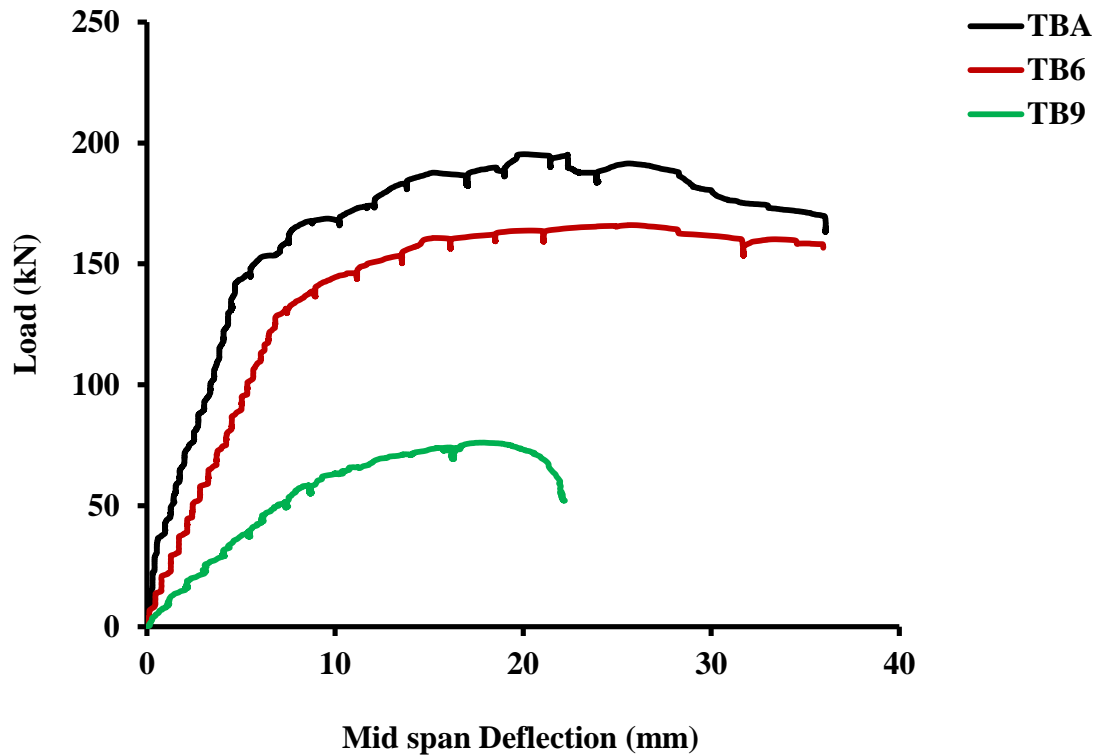
Fig. 4.13: Load–deflection relationships of control and heat-damaged specimens

The load – deflection curves for the heat damaged and strengthened beams using different techniques are shown in Figs. 4.16 – 4.19. It can be noticed that all the strengthening schemes improved the load carrying capacity and deformability of the heat damaged beams. However, the quantum of improvement in strength and deformability as indicated by the load-deformation relationships depended upon the initial heat damage (depending on the temperature of exposure) and the type of strengthening scheme. The increase in ultimate load capacity and deformability is due to the composites cross section and contribution of material used in strengthening. Fig. 4.16 shows that the strengthening techniques namely HSFRC and FC resulted in load capacity of strengthened beams even more than those of unheated beams in case of specimens heated at 600°C. The curves show that the deformation capacity of strengthened beams was also regained by these schemes when heated at 600°C.However, the strengthening schemes (HSFRC and FC jackets) although improved the load capacity of beams heated at 900°C with respect to heat damaged beams, they did not result in regaining the load capacity and deformability of control unheated beams, Fig. 4.17.
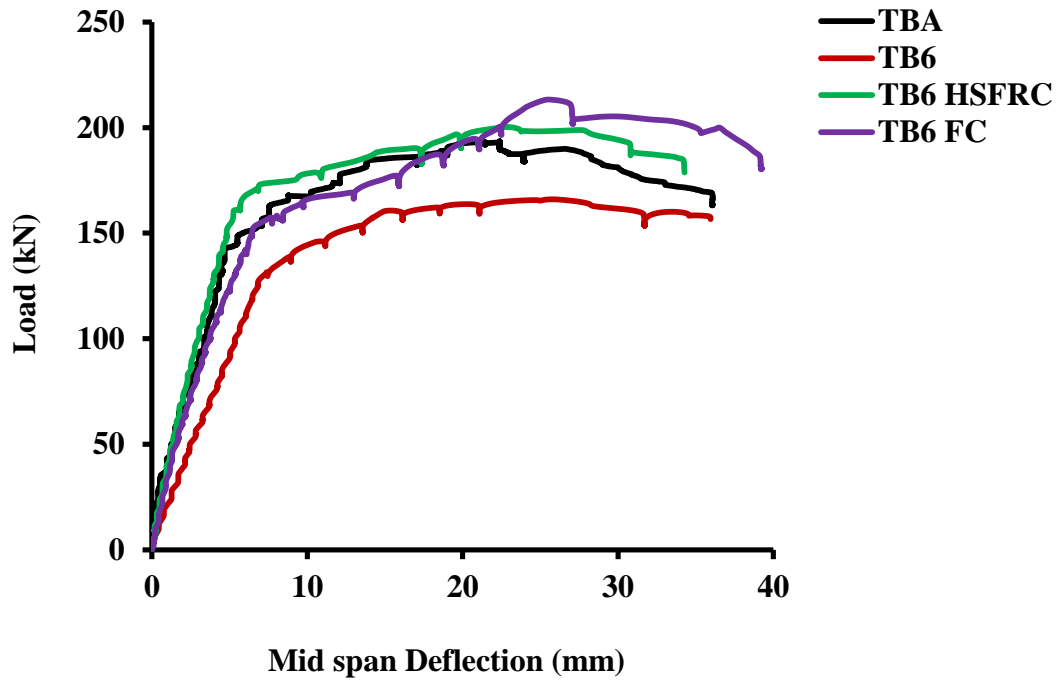
Fig. 4.14: Load–deflection relationships of un-strengthened and strengthened beams (FC and HSFRC) heated at 600° C temperature
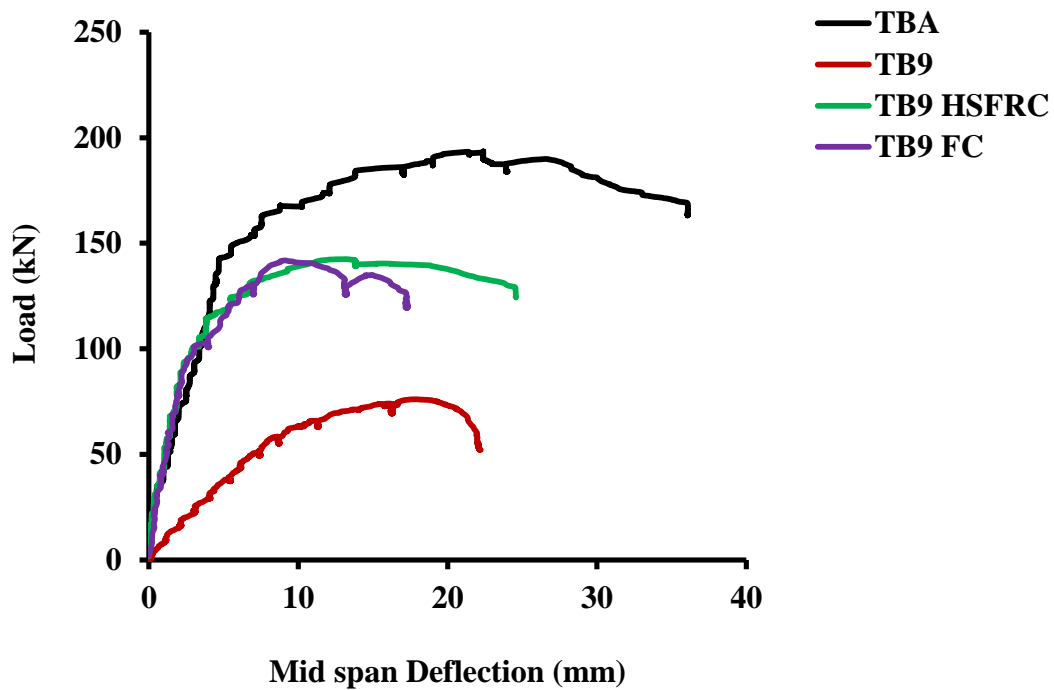
Fig. 4.15: Load–deflection relationships of un-strengthened and strengthened beams (FC and HSFRC) heated at 900° C temperature

Figs. 4.18 and 4.19 shows the load deflection behavior of beams heated at 600°C and 900°C and strengthened with GFRP jacketing. It is interesting to note that the GFRP strengthening technique was able to restore the room temperature flexural strength of the

beams for most of the beams heated both at 600°C and 900°C temperatures, while the post-peak deformability of the strengthened beams was brittle and no improvement in post-peak deformability was noticed in GFRP strengthening.
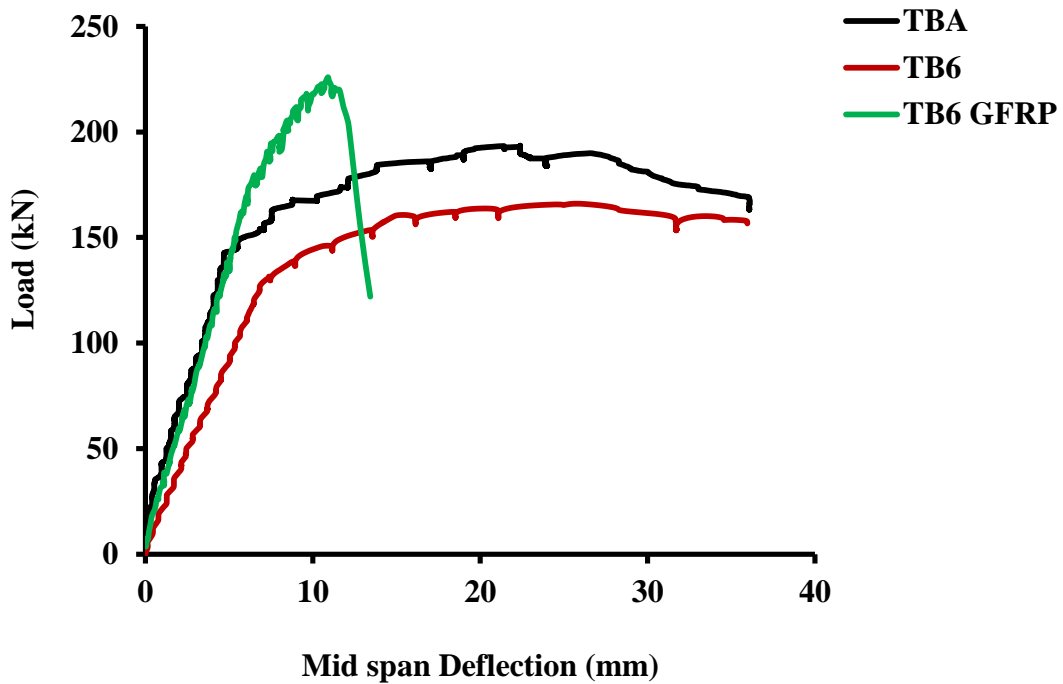
Fig. 4.16: Load–deflection relationships of un-strengthened and strengthened beams (FRP) heated at 600° C temperature
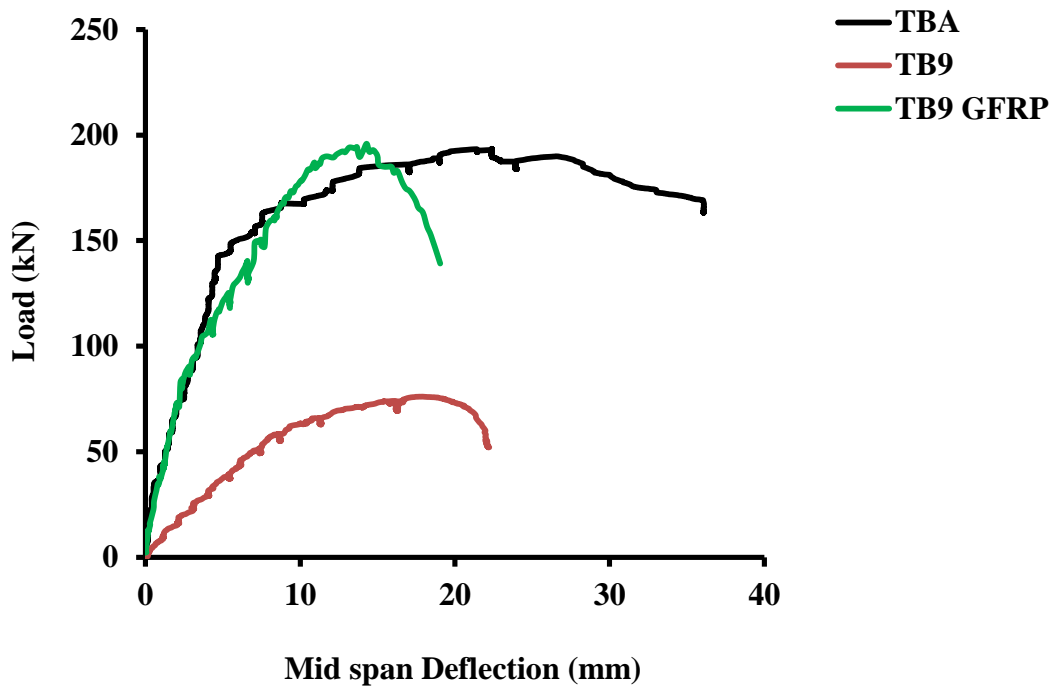
Fig. 4.17: Load–deflection relationships of un-strengthened and strengthened beams (FRP) heated at 900° C temperature

Table 4. 3: Strength and deformability parameters

T-Beam Designation	Load(kN)		Deflection		Deflection Ductility Factor	Energy		Energy Ductility Factor	Energy Dissipation	Failure Mode
	Yield Load P_y(kN)	Ultimate Load P_u(kN)	Δy(mm)	Δu(mm)	$\mu_\Delta = \Delta u/\Delta y$	E_y (kN.mm)	E_u (kN.mm)	$\mu_E = E_u/E_y$	(kN.mm)	
TBA	153	195.36	6.84	20.01	2.925	1457	4292	2.944	4292	Flexural
TB6	141	166.00	9.13	25.77	2.822	1031	3859	3.740	3859	Flexural
TB9	60	76.09	9.03	17.86	1.977	1096	2269	2.070	2269	Shear failure at support
TB6 HSFRC	142	197.63	7.82	28.81	3.684	720	4136	5.700	4136	Flexural
TB6 FC	153	201.30	7.71	23.7	3.073	832	3683	4.426	3683	Flexural
TB6 GFRP	194	225.90	7.48	10.89	1.455	1205	2121	1.760	2121	Flexural failure and debonding of shear fabric
TB9 HSFRC	98	138.88	3.68	12.14	3.298	456	1749	3.835	1749	Flexural
TB9 FC	106	141.43	3.68	15.65	4.252	360	1949	5.415	1949	Flexural
TB9 GFRP	140	195.91	6.99	14.29	2.044	1103	2428	2.201	2428	Debonding of fabric in shear region

128

The following sections present the influence of various parameters of the test program on the strength and deformability of the heat damaged beams.

4.7.2 Quantification of Strength, Stiffness and Deformability of Strengthened Beams

The results presented in Figs. 4.15 – 4.19 and Tables 4.3 – 4.6 indicate a clear decrease in the ultimate load capacity, stiffness, ductility and energy dissipation of beams due to exposure at elevated temperatures when heated to temperatures of 600°C and 900°C. The results indicate a loss of about 14% and 61% in the ultimate flexural capacity after heating to $600^{o}C$ and $900^{o}C$ temperatures respectively. It can be noted that only GFRP strengthening was capable of restoring the room temperature strength of beams damaged at $900^{o}C$ temperatures, while FC and HSFRC schemes could not restore the room temperature flexural strength of such heated beams. In case of beams heated at $600^{o}C$ temperature, all the strengthening schemes restored the room temperature strength though GFRP strengthening still showed more efficient performance. In case of specimens heated at $600^{°}C$, all the strengthening types showed reasonable enhancement in strength if compared with the strength of heat damaged unstrengthened beams, though the capability of various strengthening designs in restoring the room temperature strength was just sufficient at $600^{°}C$ temperature. The GFRP strengthening showed better enhancements in strength compared with FC and HSFRC strengthening. On the contrary, while all the three strengthening schemes showed tremendous increase in strength of $900^{0}C$ heat damaged un-strengthened beams, it was GFRP which was able to restore the room temperature strength of beams heated at $900^{0}C$ with other two techniques falling short in restoring the room temperature strength of heated beams at this temperature.

The secant stiffness of beams was calculated by dividing the maximum peak load by the deflection corresponding to peak as described earlier (Section 2.7.3, Chapter 2). The secant modulus provides a useful comparison of the effect of different strengthening schemes on the stiffness of strengthened heat damaged beams. A significant loss in stiffness of concrete was noticed due to exposure to high temperature (Fig. 4.20). The loss of 34% and 56% in stiffness of heat damaged beams was noted when heated at $600^{0}C$ and $900^{0}C$ temperatures respectively. The degradation of the heat damaged beam's stiffness is mainly caused by the softening of concrete after heating to high temperatures. Voids and micro cracks in the micro- structure of the concrete caused by heat have detrimental effect on its stiffness. On heating, the porosity of concrete gets

increased due to loss of moisture and due to the development of internal micro-cracking, which ultimately results in stiffness loss.

Fig. 4.20 and Table 4.5 show the effectiveness of HSFRC, FC and GFRP jackets in restoring the stiffness of heat damaged beams. In case of specimens heated at 600°C, all the strengthening types showed increase in stiffness if compared with the stiffness of heat damaged unstrengthened beams, it was GFRP which was able to show noticeable enhancement even in the room temperature stiffness of beams heated at 600°C with other two techniques falling short in restoring the room temperature stiffness of heated beams at this temperature. The GFRP strengthening showed considerably better enhancements in stiffness compared with FC and HSFRC strengthened heated beams. In case of beams heated at 900°C while all the strengthening schemes indicated considerable increase in the stiffness of heat damaged un-strengthened beams, only GFRP and HSFRC could restore the stiffness of control unheated and un-strengthened beams with FC strengthening just falling short. It can be seen that the reduction in residual stiffness was higher than that that of reduction in ultimate load. It therefore becomes more important when evaluating fire damaged concrete structures to consider deformation and stress redistribution.

Table 4. 4: Ultimate load carrying capacity of beams

Method	Ultimate Load(kN)				
	% increase (+) or decrease (-) with respect to control specimens			% increase (+) or decrease (-) with respect to reference heat damaged T-Beam	
	Room Temperature	600° C	900° C	600° C	900° C
TBA	100%	----	----	----	----
TB6	----	-14%	----	100%	----
TB9	----	----	-61%	----	100%
TB6 HSFRC	----	+1% *	----	+18%	----
TB6 FC	----	+3%	----	+21%	----
TB6 GFRP	----	+15%	----	+35%	----
TB9 HSFRC	----	----	-29%	----	+81%
TB9 FC	----	----	-27%	----	+85%
TB9 GFRP	----	----	+1%*	----	+156%

* Approximately the same

Table 4. 5: Stiffness of beams

Method	Secant Stiffness (kN/mm)				
	% increase (+) or decrease (-) with respect to control specimens			% increase (+) or decrease (-) with respect to reference heat damaged T-Beam	
	Room Temperature	600° C	900° C	600° C	900° C
TBA	100%	----	----	----	----
TB6	----	-34%	----	100%	
TB9	----	----	-56%	----	100%
TB6 HSFRC	----	-29%	----	+6%	----
TB6 FC	----	-13%	----	+31%	----
TB6 GFRP	----	+112%	----	+222%	----
TB9 HSFRC	----	----	+17%	----	+168%
TB9 FC	----	----	-7%	----	+112%
TB9 GFRP	----	----	+40	----	+221%
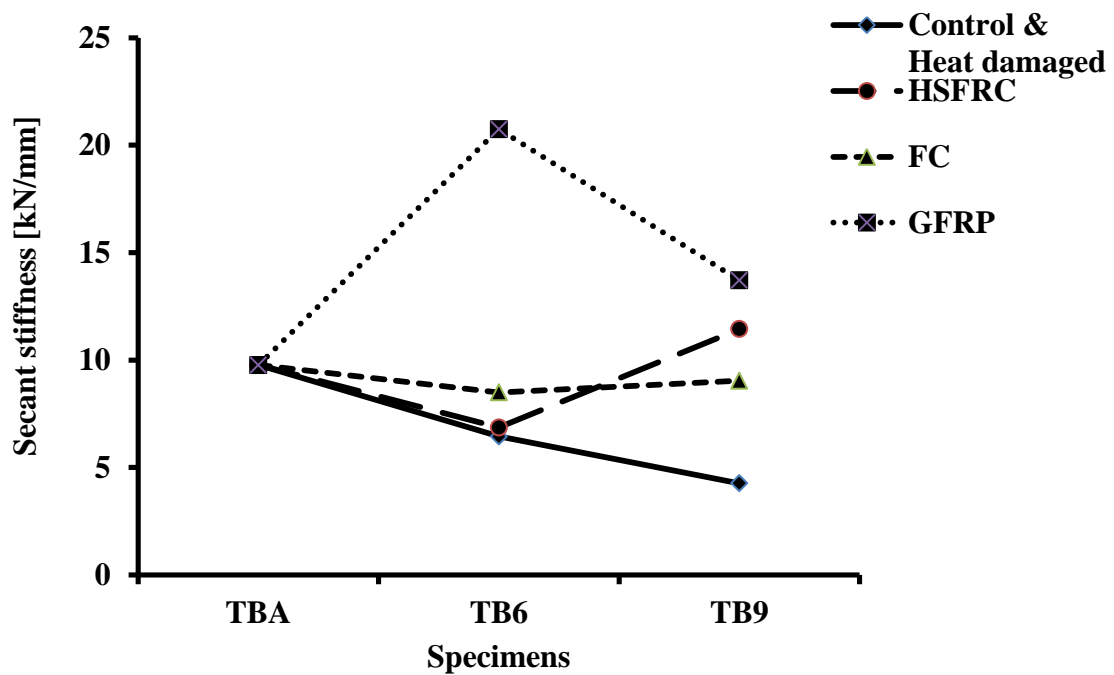
Fig. 4.18: Stiffness of beams

131

The deformability or ductility of structural members is considered as one of the most critical parameters for evaluating their performance. Ductility characterizes the deformation capacity of members (structures) after yielding, or their ability to dissipate energy. The effect of elevated temperatures on deformability of reinforced concrete beams and then capability of various employed strengthening techniques in restoring the deformability has been discussed in two ways. Deformation ductility, which is defined as the ratio of deflection at fracture to yield deflection has been worked out as shown earlier in Table 4.3. It has been defined as deflection ductility index. It can be noted from the results presented earlier in Table 4.3 that the deflection ductility index reduces as the temperature increases. The ductility indices of strengthened heat damaged beams show that FC and HSFRC strengthening designs showed increase in the ductility of heat damaged beams. However, GFRP strengthening showed lower deflection ductility due to its poor post-peak performance.

The deformation capacity was also evaluated in terms of energy dissipation capacity by computing the areas under the load-deflection curves. Higher energy absorption shows more plastic deformation before failure and hence a structure possessing higher energy dissipation capability would definitely be more ductile in nature. Table 4.3 also summarizes the results of deformability of test specimens in terms of energy absorption, while Table 4.6 shows the capability of various chosen strengthening techniques in improving the energy absorption capacity of heat damaged beams. The energy dissipation is calculated on the basis of area under the load–deformation curves obtained after the experimental tests. The energy capacity values were calculated up to the P_{umax} on the load deflection curves. The energy dissipation capacity of heat damaged beams reduced considerably when compared with undamaged beams. These reductions were 10% and 47 % when heated at 600^0C and 900^0C temperatures respectively as shown in Table 4.6. Beams strengthened with HSFRC jacketing though showed an increase in energy dissipation of 11% in case of 600^0C, it was lesser than that of control specimens by 59% in specimens heated at 900^0C. The energy dissipation for beams restored with Ferro cement jacket was found to be less than that of control beams at both the temperatures. The percentage reductions in energy were 14% and 54% for TB6 FC and TB9 FC respectively. Similarly, the GFRP scheme of strengthening also showed reduced energy absorption, which was 50% and 43% lesser than the control beams at 600^0C and 900^0C temperatures respectively. It can be

concluded that in spite of GFRP strengthening technique's capability of restoring the room temperature strength of beams, no improvement in energy absorption capacity is possible due to the brittle post peak failure of GFRP strengthened beams.

Table 4. 6: Energy dissipation of beams

Method	Energy dissipation capability of T- Beams (kN.mm)		
	% increase (+) or decrease (-) with respect to control specimens		
	Room Temperature	600° C	900° C
TBA	100%	----	----
TB6	----	-10%	----
TB9	----	----	-47%
TB6 HSFRC	----	+11%	----
TB6 FC	----	-14%	----
TB6 GFRP	----	-50%	----
TB9 HSFRC	----	----	-59%
TB9 FC	----	----	-54%
TB9 GFRP	----	----	-43%

4.7.3 Crack Pattern and Failure Modes

As mentioned earlier, all the beam specimens were tested under four point loading. The load was increased monotonically till failure. The behavior of all the beams was tracked carefully during the entire testing duration. The occurrence of first crack, subsequent propagation of cracks, nature of cracking and ultimate failure was monitored. The failure modes are shown earlier in Table 4.3. Comparisons were drawn between different specimens with respect to their first crack load and the same are shown graphically in Figs. 4.21(a-c). It can be noted that the undamaged beams developed flexural tensile crack in the hinge region at an average load of 43kN as shown in Fig. 4.22. The flexural tensile cracks gradually propagated at the bottom of the beam within the middle third of the span. As the load was increased, shear cracks also began to develop between the support and loading points. Around 153kN, the beam started to yield and the beam finally failed in flexure at a load of 195kN. In specimens heated to 600$^{\text{o}}$C, the first crack load was noted to be 26kN and flexural cracks developed pre-

maturely in the mid- span region and then subsequent shear cracks were noted in shear span region but the beams finally failed in flexure at an average load of 166kN. The Fig. 4.23 shows a typical failure mode for 600° C heat damaged beams. As the temperature of exposure increased the failure load further decreased and in specimens subjected to a temperature of 900°C the first crack load got reduced to 21kN. The behavior and failure pattern of the beams heated at 900°C was also different as evident from Fig. 4.24. Though the failure started with flexural cracking in middle flexural region, the shear cracks started relatively earlier and the number of shear cracks was considerable more than the flexural cracks. Interestingly, the 900°C heat damaged beams exhibited a sudden failure in shear region possibly due to significant decrease in shear strength of concrete due to heating.

The heat damaged beams strengthened with HSFRC failed in flexure. The vertical flexural cracks formed in the mid span region though with increasing load these cracks traveled towards the compression area and resulted in crushing of concrete in the compression zone. The first crack formed in HSFRC strengthened beams was at an average load of 35kN that is about 18% more when compared with corresponding un-strengthened heat damaged beams. During testing the strengthened beams had lesser number of cracks compared to corresponding unheated and heat damaged beams as shown in Figs. 4.22 - 4.24. In HSFRC strengthened beams, the width of vertical flexural cracks was smaller at a given stage of loading compared to un-strengthened undamaged and damaged beams. However, at the final stages of loading before failure, the cracks got widened in strengthened beams and the width was higher than that in undamaged beams. The failure of 900°C heat damaged beams and strengthened with HSFRC was in flexure in contrast to the corresponding un-strengthened beams, which failed in shear, Fig. 4.25.

The failure of heat damaged beams strengthened with Ferro Cement jacketing was also largely similar to the failure of HSFRC strengthened specimens. The first crack (in flexural region) formed in FC strengthened beams at average load of 48kN and 46kN in 600° C and 900° C heat damaged beams respectively, which is more by 12% and 7 % when compared with undamaged control beams. The cracks were mainly concentrated in the concrete at areas of high bending moment on either side of the repair. Ultimate failure was found to be due to the breakdown of the welded steel mesh in tension zone. Larger number of hair line cracks were observed in 600°C heat damaged FC beams,

while relatively fewer hair line cracks were observed in 900°C heat damaged FC beams. The failure of heat damaged beams was characterized by the widening of some cracks in the middle region as shown in Fig. 4.26.

Failure modes of the heat damaged beams strengthened with GFRP are shown in Fig. 4.27. The development and propagation of cracks was relatively slower in GFRP strengthened beams compared to that in undamaged control beams, heated un-strengthened beams and HSFRC & FC strengthened beams. The GFRP strengthened beams underwent relatively lesser deflection during the test and the cracks were mainly confined in the flange of beams. The deflections were mainly concentrated in the middle region between the load points. This is corroborated by the strains in GFRP sheets as shown in Fig. 4.28. These strains were measured in GFRP by fixing strain gauges on the sheets at midpoint of beams and at the locations of the application of two point loads. The load carrying capacity of the beams kept on increasing till the appearance of cracks and there after the beams failed suddenly in brittle fashion. The first crack load in GFRP strengthened beams was significantly more than those in HSFRC and FC strengthened beams. The ultimate failure of GFRP strengthened beams, which were heated at 600°C temperature, was flexural failure and debonding of fabric in shear region. In 900°C heat damaged and GFRP strengthened beams, debonding of GFRP fabric was observed in the shear region as the beam failed indicating a shear failure.
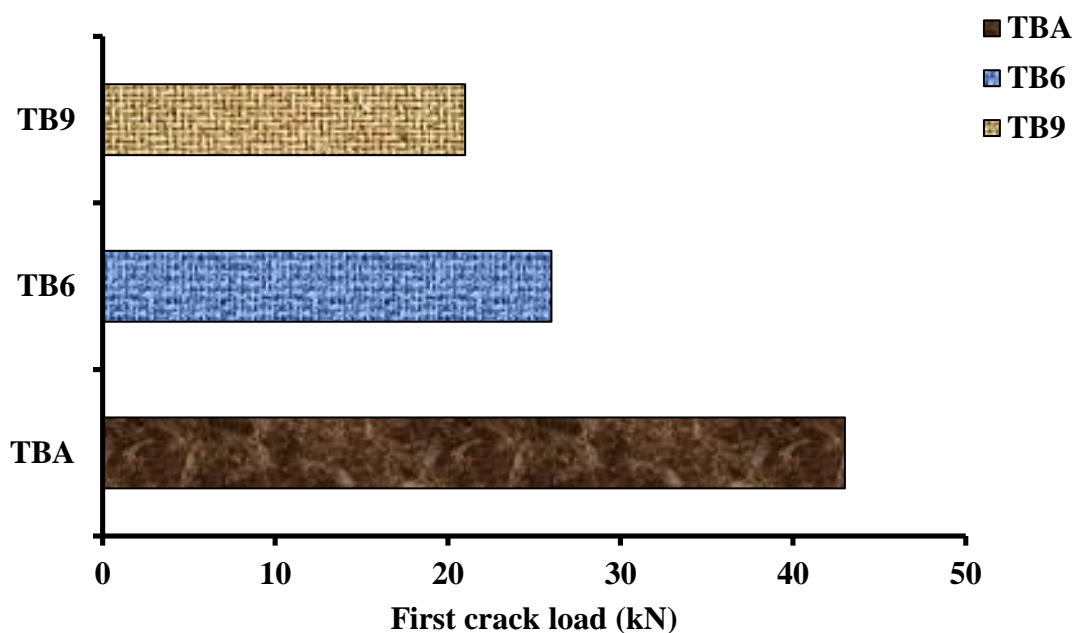
(a) Beams exposed to different temperatures
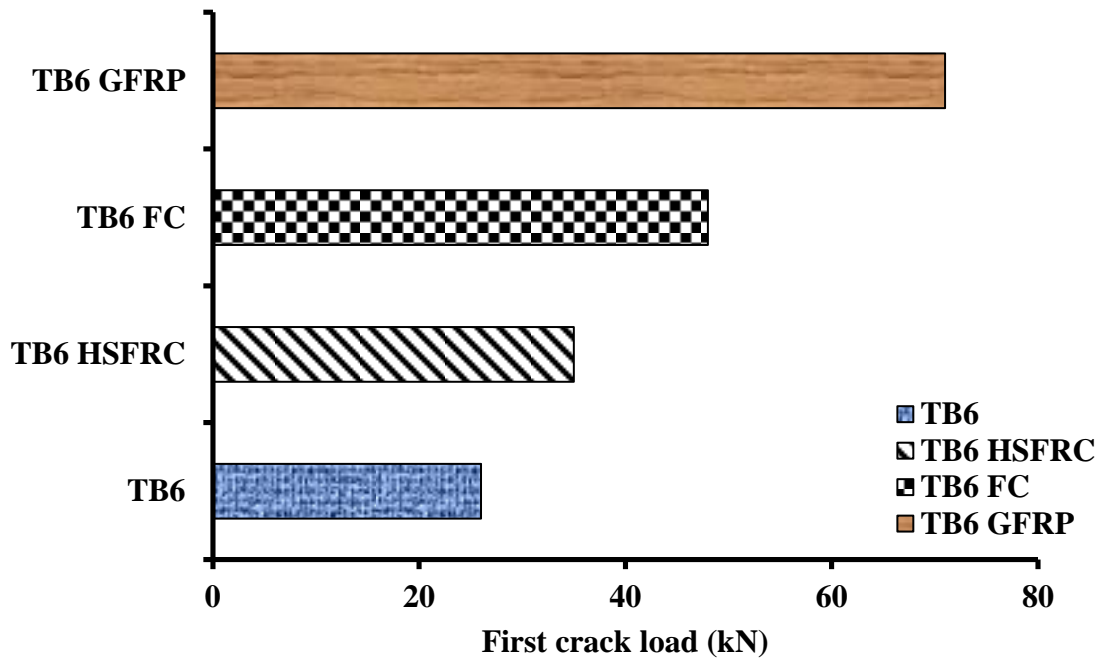
(b) Beams exposed to 600° C and then strengthened
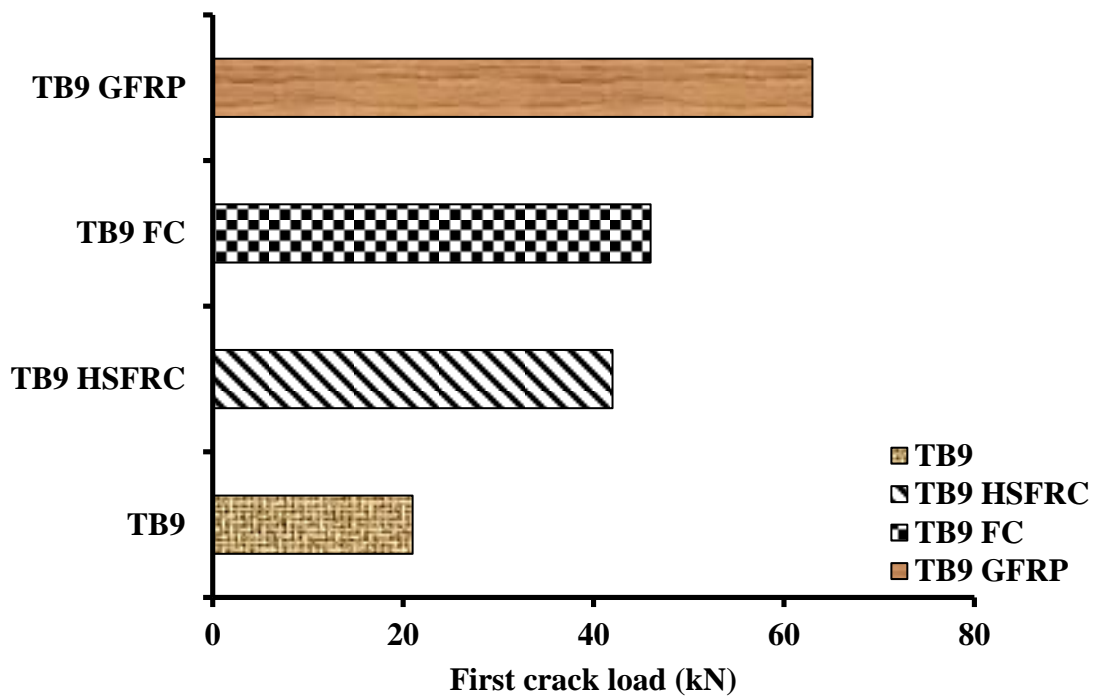
(c) Beams exposed to 900° C and then strengthened

Fig. 4.19: (a)-(c) - Comparison of first crack load

Fig. 4.20: Failure pattern of undamaged beams

Fig. 4.21: Failure pattern of 600° C heat damaged beams
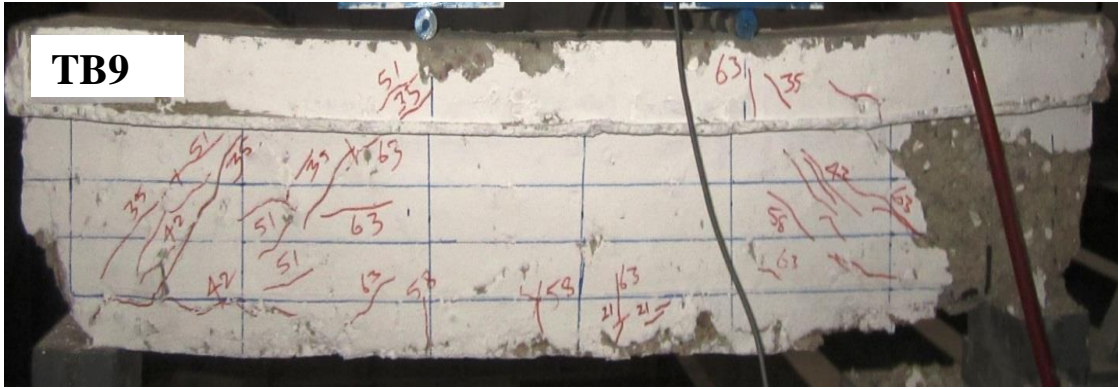
Fig. 4.22: Failure pattern of 900° C heat damaged beams

Fig. 4. 23: Failure pattern of 600° C and 900° C heat damaged beams strengthened with HSFRC

Fig. 4. 24: Failure pattern of 600° C and 900° C heat damaged beams strengthened with
FC
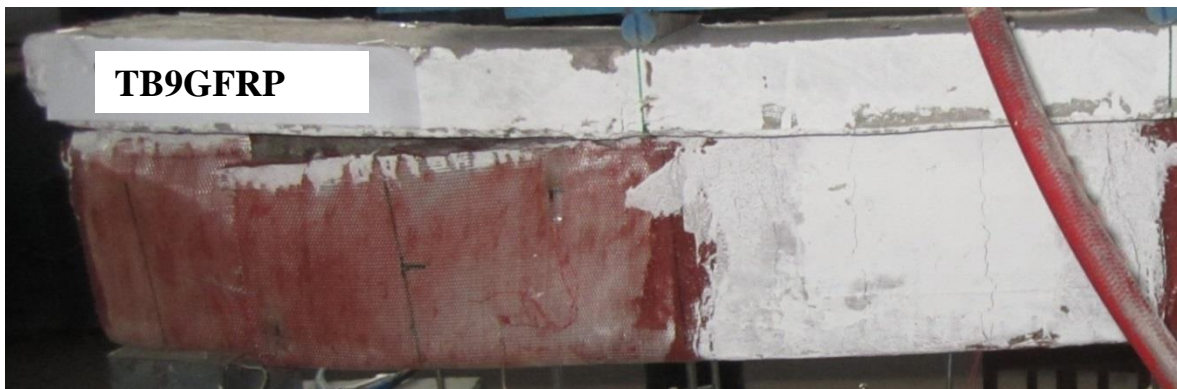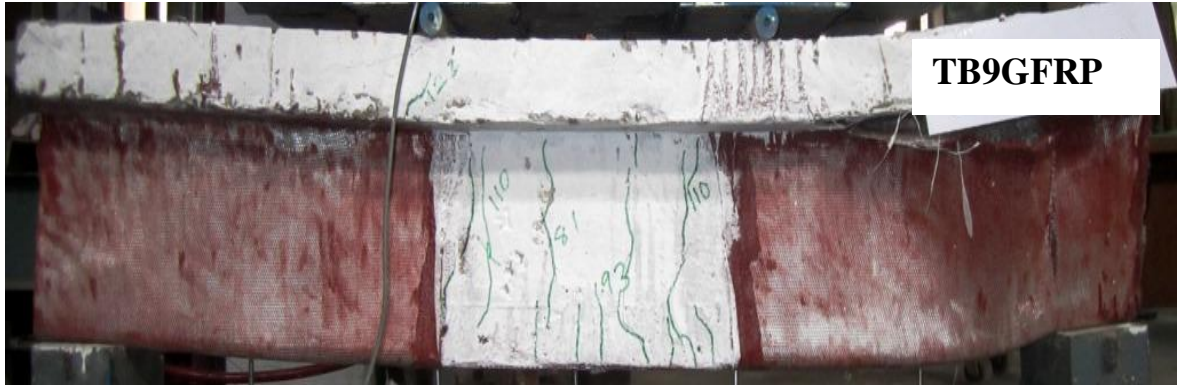
Fig. 4. 25: Failure pattern of 600° C and 900° C heat damaged beams strengthened with GFRP
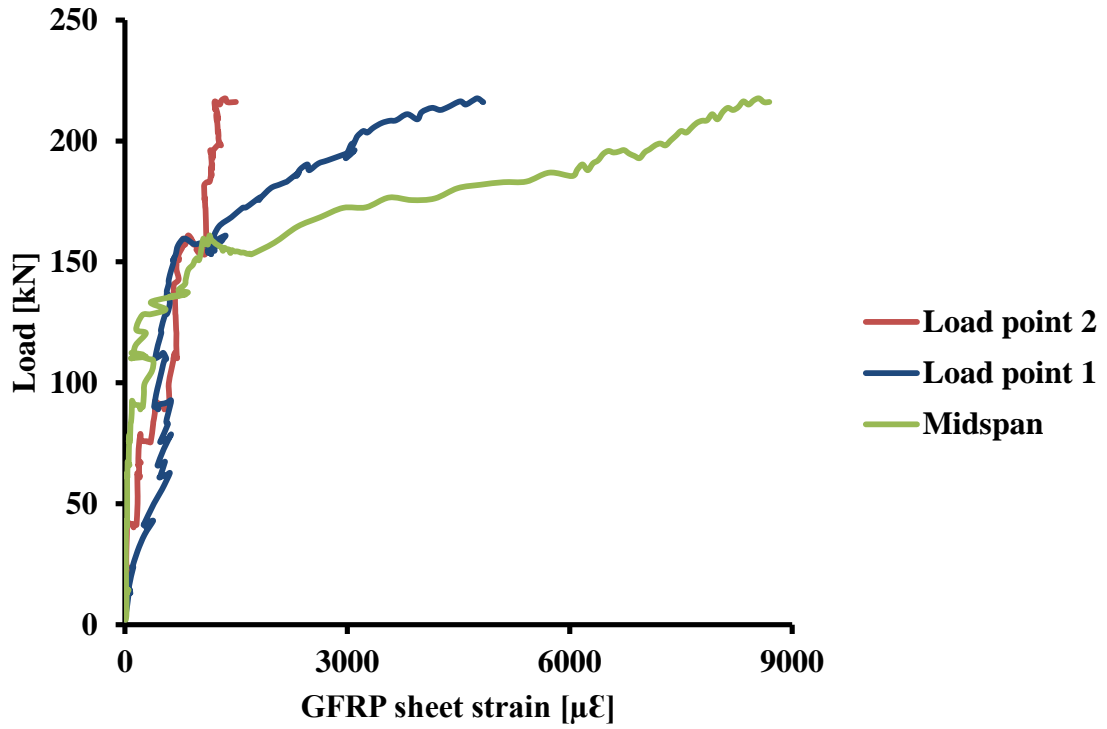
(a) Beams exposed to 600° C and strengthened with GFRP
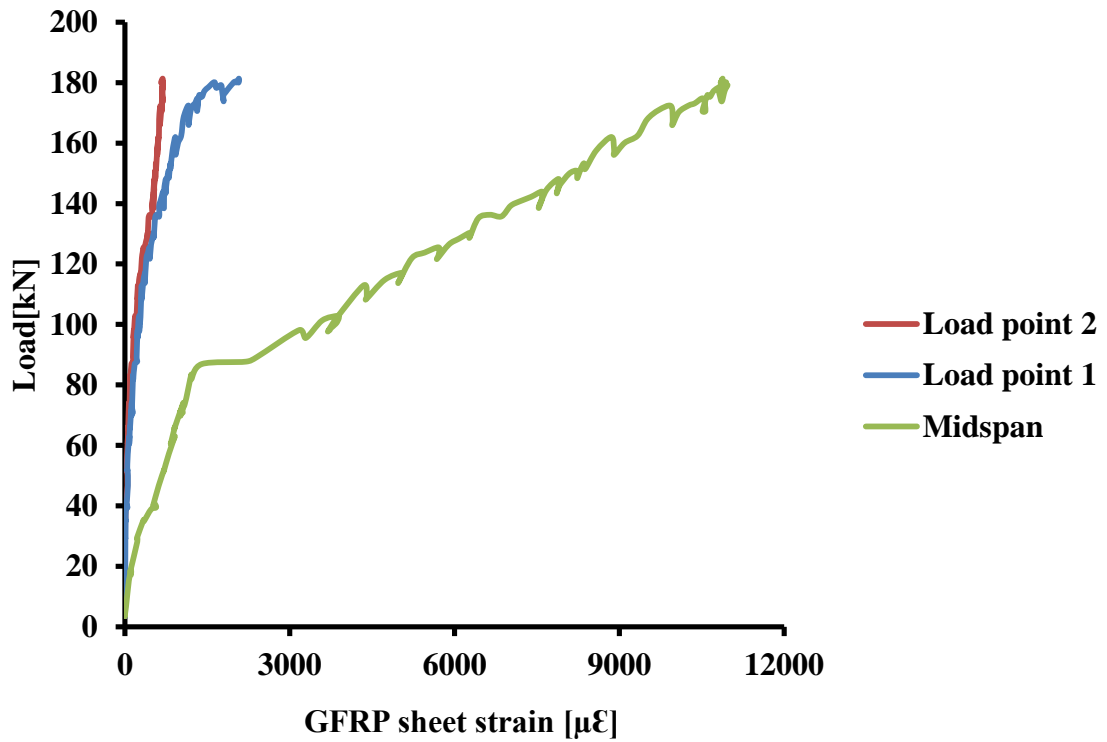
(b) Beams exposed to 900° C and strengthened with GFRP

Fig. 4. 26: (a)-(b) – Strain in GFRP

4.8 CONCLUDING REMARKS

This study focused on investigating the structural performance of strengthened heat damaged reinforced concrete T beams. Three different types of strengthening schemes namely Ferro cement, High strength Fibre concrete and Glass Fibre Polymer were employed. The aim of the study was to evaluate the capability of these strengthening techniques in restoring the flexural capacity of beams damaged by exposure at elevated temperatures. A total of 27 beams were tested under this program. The test variables included degree of heat damage i.e. temperature of exposure and type of strengthening. The results have been analyzed and discussed in detail to fulfill the objectives of this investigation.

CHAPTER – 5

BOND PROPERTIES OF GFRP LAMINATE WITH HEAT DAMAGED CONCRETE

5.1 INTRODUCTION

Till late 1980s, the rehabilitation of civil infrastructure generally meant placing more reinforced concrete, bonding steel plates, or applying some sort of post-tensioning to the structure. Since early nineties, the strengthening and retrofitting techniques have increasingly used externally bonded FRP composites, which have proved to offer unique properties in terms of strength, light weight, chemical resistance and ease of application. Nowadays many strengthening options can be accomplished using FRPs (Täljsten 2002). For flexural strengthening of beams, slabs or girders, FRP plates or sheets can be epoxy bonded to the tensile face of concrete with fibers parallel to the principal stress direction. Shear and torsion strengthening can be provided by placing two face or U-jacket FRP sheets on the sides of beams. Columns are typically strengthened by wrapping FRP around the column in the hoop direction, thus increasing confinement of the concrete core. An important issue in the strengthening of concrete structures using FRP composites is to design against various debonding failure modes, especially for flexural elements such as beams and slabs. The possible debonding failures of FRP strengthened reinforced concrete elements are reported to be (i) plate end interfacial debonding; (ii) intermediate flexural crack induced interfacial debonding; (iii) delamination of FRP along with cover concrete and (iv) intermediate flexural-shear crack induced interfacial debonding (Buyukozturk and Hearing 1998, Chen and Teng 2001, Teng et al 2002).

Research on the behavior of bond between the FRP and the concrete is reported in the literature on the basis of tension tests with direct shear type specimens (Udea and Dai 2005, Van Gemert 1990, Chajes et al. 1996, Taljsten1996, Maeda et al. 1997, Bizindavyi and Neale 1999, Nakaba et al. 2001, Chenet al. 2001, Lorenzis et al. 2001, Yuan et al. 2004, Xiao et al. 2004, Yao et al. 2005, Guo et al. 2005, Mazzotti et al. 2008 and 2009). Another group of researchers studied the effect of bond between FRP sheets and concrete theoretically, wherein the work included both fracture mechanics approach and development

of empirical models based on regression of experimental data (Khalifa et al. 1998, Chen and Teng2001, Yuan et al. 2004, Lu et al. 2005, Wu et al. 2010, Bilotta et al. 2011). A critical review of the literature indicates that most of the previous studies were undertaken on bond behavior of FRP with concrete, which was not damaged by heat or exposure to fire. As an exposure at elevated temperature is expected to influence the bond properties of FRP with heated concrete, only limited research has been taken up on this topic in the past (Blontrock 2003, Wu et al.2005, Klamer 2006, 2008 and 2009, Cai 2008, Leone et al. 2009, Gao et al. 2012). Further, these previous studies targeted temperatures only up to 100°C, while temperatures during fire may go in the range of 1000°C. Only one study is reported in the literature, where the authors investigated bond behavior of FRP with heat damaged concrete interface using double shear specimens with concrete heated at temperatures up to 600°C (Haddad et al. 2013). The heated specimens were bonded with carbon FRP (CFRP) sheets using a special epoxy at three widths and one bond length and subsequently tested under double shear test. In view of the above, there is an urgent need of investigating the behavior of bond between the FRP sheets and the heat damaged substrate concrete in order to enable designing FRP strengthening for Fire or heat damaged reinforced concrete structures.

5.2 RESEARCH SIGNIFICANCE

To establish restoration techniques for heat damaged concrete structures involving externally applied composite sheets and thereby to design the FRP, a good under-standing of the debonding strain and other bond properties is required. Existing design provisions talk only of debonding failure assuming bond properties of FRP with concrete at ambient temperature (ACI 440.2R-08 and CSA S806-02). Thus in this study an attempt has been made to investigate the bond behavior of FRP with concrete, which was heated to elevated temperatures of up to 800^{0}C. The tests conducted focus on both the bond strength and force transfer on different bond lengths. Tests were performed using a single-lap shear test specimen, using a constant bond width but different heat exposure conditions. The experimental results are presented and discussed in terms of strains within the composites during the load test, bond strength–slip, transfer length, bond strength and mode of failure. The experimental results have been used to derive a mathematical model to find the debonding strain of FRP strengthened heat damaged flexural member by modifying the model proposed by Chen and Teng (2001).

5.3 EXPERIMENTAL PROGRAM

The single shear pull-off test is a commonly used method for investigating the bond behaviour of FRP systems with concrete (Yao et al. 2005). This method has been adopted in this experimental study to investigate the bond behavior of FRP with heated concrete. Experimental program primarily aimed at determining the effect of elevated temperatures on the bond performance of FRP with concrete. A total of forty five concrete blocks were cast, heated, bonded and tested. The relevant details of the test specimens are illustrated in Table 5.1 and Fig. 5.1. Experimental variables included temperature of exposure and bond length. The normal strength concrete mix as explained in Chapter 2 was used here also to cast the bond test specimens. The concrete was made with ordinary Portland cement, natural river sand, crushed limestone aggregate of maximum size 12.5 mm and tap water. The concrete mix was designed using the specifications of IS: 10262-2009. The detailed concrete mix proportions along with 28 days cylinder compressive strength of the concrete are summarized in Chapter 2. In this study, E – Glass 90/10 unidirectional fiber sheets were used. GFRP composed of an epoxy based matrix and E – Glass 90/10 fibers. A two component room temperature cure epoxy resin adhesive namely saturant was used as the component of the GFRP. Mechanical properties of E – Glass 90/10 glass fiber sheets and the epoxy used in this experimental program are already given in Chapter 2.

The single shear test specimens were cast and tested in triplicate in order to get the average of three results thus making 15 independent cases. The companion standard plain concrete cylinders (100 x 200 mm) and cubes (150 mm x 150 mm) were also cast along with each series to determine the nominal strength of concrete and moisture content respectively on the day of testing of bond specimens. The specimens (Blocks) were of size 150 mm x 150 mm x 300 mm. The test specimens were cast in a horizontal position in the laboratory using steel moulds. All the specimens were cast in different series as shown in Table 5.1. The first three letters (SST) in the abbreviation denote single shear test, and the numeral (2, 4, 6 and 8) indicates the temperature of exposure and the numeral (L_f1, 1.5 and 2) denotes bond length. The details of mixing and casting procedure have already been explained in Chapter 2. After 24 hours, the specimens were removed from the moulds and submerged in a water tank for curing. The water curing period lasted for 28 days after which the specimens were kept in the laboratory at ambient temperature and humidity conditions for

another 30 days until they reached equilibrium moisture content. After 60 days of total ageing, the specimens were exposed to various heating regimes. Subsequent to a single heating and cooling cycle, the specimens were tested under single shear test.

Table 5. 1: Test plan

Designation	Temperature of exposure (°C)	Bond length L_f
SSTA L_f1	Ambient	100mm
SST2 L_f1	200	
SST4 L_f1	400	
SST6 L_f1	600	
SST8 L_f1	800	
SSTA L_f2	Ambient	150mm
SST2 L_f2	200	
SST4 L_f2	400	
SST6 L_f2	600	
SST8 L_f2	800	
SSTA L_f3	Ambient	200mm
SST2 L_f3	200	
SST4 L_f3	400	
SST6 L_f3	600	
SST8 L_f3	800	
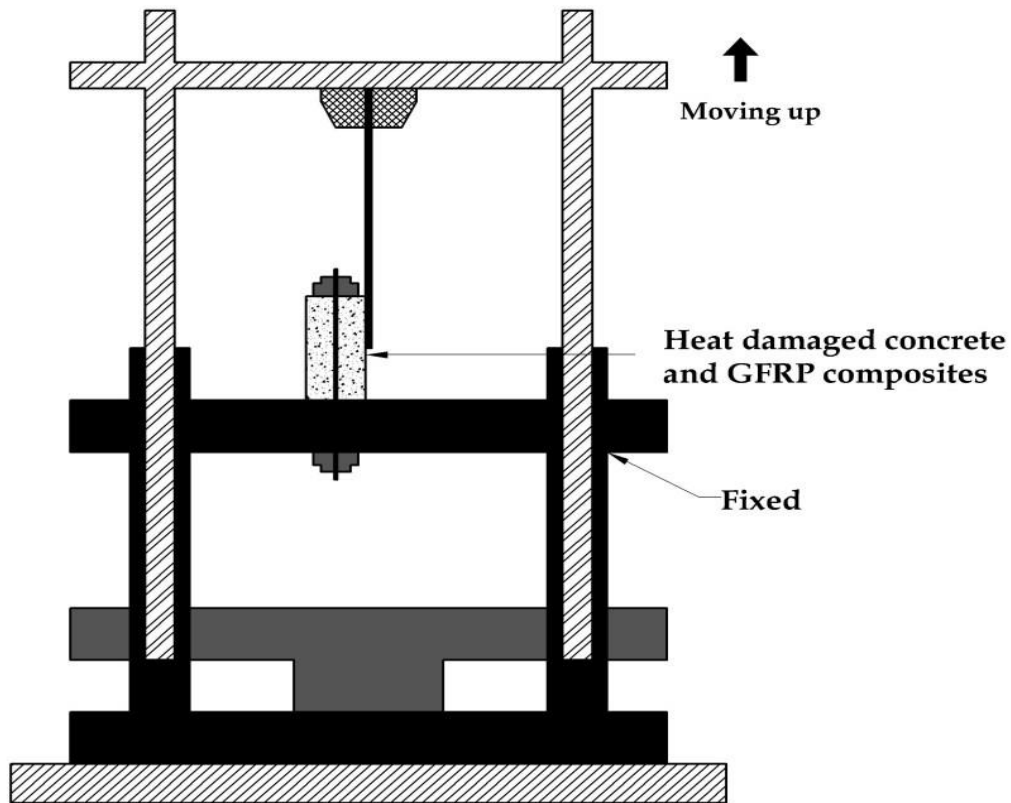
Fig. 5.1: Single shear test setup

Before thermal testing, three companion cubes were dried at 105ºC until constant mass in order to determine the moisture content. The moisture content of cubes was assumed to represent the moisture content of bond test specimens as the test specimens and the cubes were exposed to similar ageing conditions. The moisture content of concrete by mass ranged between 2.23% to 2.44% for the companion cubes of all the three series as shown in Table 5.2.

Table 5. 2: Moisture content

Specimens	Moisture Content % (by mass)
SSTLf1	2.44
SSTLf1.5	2.23
SSTLf2	2.26

5.3.1 Heating of Specimens

A programmable electrical furnace as explained in Chapter 2 was used to heat the single shear specimens. The temperature inside the furnace was measured and recorded by using thermocouples. At an age of 60 days, the specimens were heated in the furnace to different target temperatures ranging from room temperature to 800ºC. The heating rate was set at 10ºC /min and each target temperature was maintained for 3 hrs to achieve a thermal steady state as shown in Fig. 5.2. The heating rate was chosen on the basis of the fact that normally, for fire protection, a heating rate of 10º C/min is adopted (Phan et al. 2002, Zhang et al. 2000). After exposing the specimens to target temperatures for the desired time duration, the furnace was switched off and the samples were left in the furnace for 24 hours to allow cooling within the furnace. Thereafter, the door of the furnace was opened and the samples were left in the furnace to allow natural cooling to room temperature. The rate of cooling was not controlled but was measured during complete test. The data from the thermocouples was recorded in a computer through a data logger.
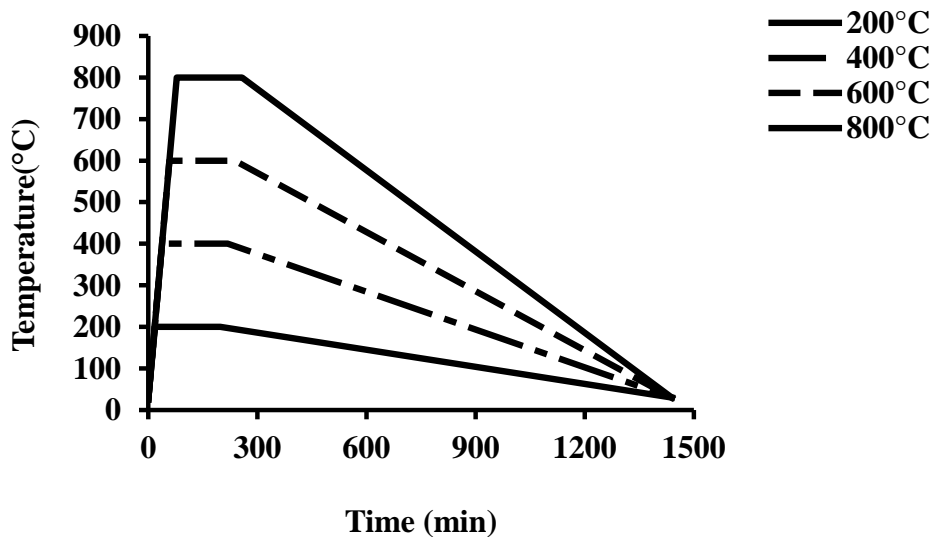
Fig. 5.2: Heating cycles (200, 400, 600 & 800°C)

5.3.2 Observations after Heating

There was no visible cracking on the surface of the specimens heated up to 400ºC. The concrete started to crack when the temperature increased to 600ºC, however, the cracks were not significant at this temperature level and only few hairline cracks were observed.

The number of cracks became relatively pronounced at 800ºC and map like hairline cracks could be clearly noticed on the surface of the specimens exposed to 800ºC. Fig. 5.3 illustrates some typical concrete specimens after treatment at different temperature. For the determination of the amount of mass loss of concrete due to thermal treatment, the masses of the all the specimens were recorded before and after the heat exposure. Fig. 5.4 show the average mass loss values of concretes specimens at varying temperatures. The mass loss of the specimens tested at room temperature is considered to be zero for the sake of comparison. The results show that the mass loss of concrete increases with an increase in the temperature of exposure. However, the relationship between the mass loss of concrete and exposure temperature is non linear. At temperatures above 200ºC, the concrete showed higher mass losses when compared to the normal strength concrete. Based upon the test results, the variation of the overall mass loss through evaporation process of concrete specimens can be divided into three stages. Firstly, when concrete was exposed to temperatures ranging from ambient to 400ºC, the moisture loss increased very rapidly because of the evaporation of free water, capillary water and chemically bound water. During the exposure temperatures between 400 to 600ºC, the rate of mass loss decreased relatively and at this stage it is believed that only the small amount of the remaining gel water evaporated from the gel pores. With the increase of temperature above 600ºC, the rate of mass loss again became rapid. During this third stage, several changes are expected to occur in the concrete micro-structure and this could also be the consequence of decomposition of hardened cement paste and aggregates, release of CO_2 and the sloughing off of the surface of concrete.

Fig. 5.3: Crack pattern in heated specimens

A series of ultrasonic pulse velocity tests were also carried out on concrete before and after exposure to high temperatures. The ultrasonic pulse velocity test results for all the specimens are shown in Fig. 5.5. As noted in the previous Chapters, in connection with reinforced concrete columns and beams, the pulse velocity decreased with the increase of temperature of exposure.
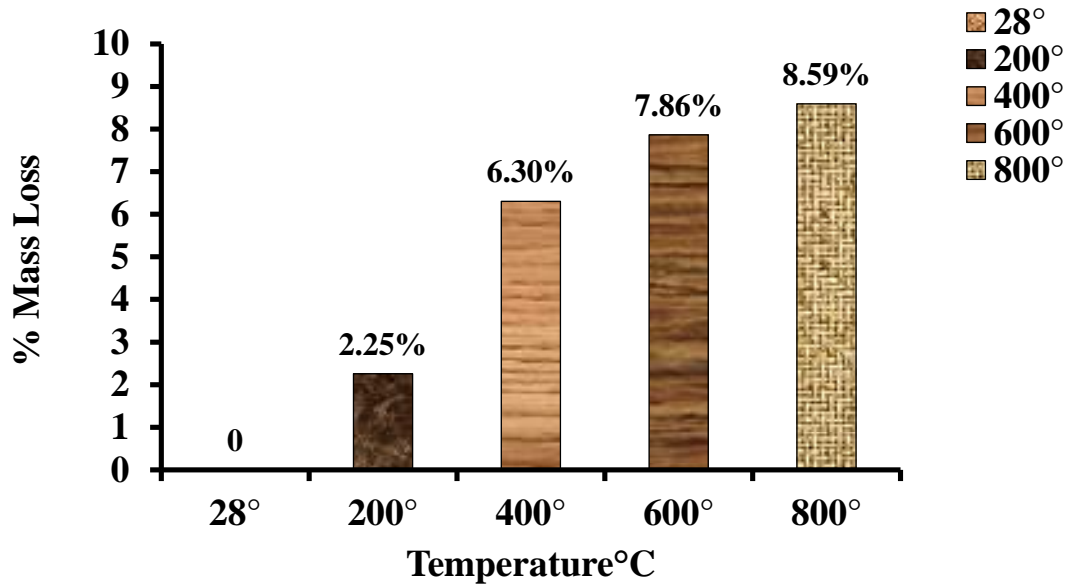
Fig. 5.3: Mass loss after high temperature exposure
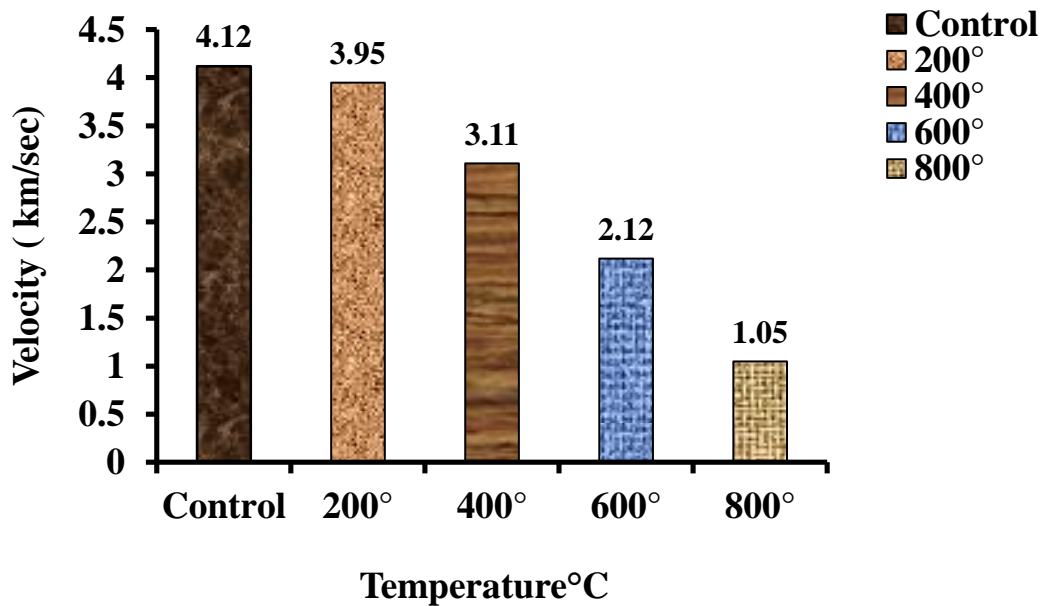
Fig. 5.4: Ultrasonic pulse velocities in specimens after high temperature exposure

152

5.3.3 Bonding GFRP to Concrete Specimens

After heating and cooling, the control and heat damaged specimens were bonded with GFRP sheets using bonding agent with various bond lengths (100mm, 150mm and 200mm). Before bonding the GFRP sheet the surface of the specimens was scraped lightly to remove surface contaminants (Fig. 5.6a). Then, the surface of the specimens was treated by hand grinding blade to remove the mortar till the aggregate became clear. The GFRP sheets were cut using a special scissor to the chosen lengths and width. Consequently the surface of the concrete was coated with a layer of epoxy primer on the surface of the concrete to fill air voids and to provide good bond strength (Fig. 5.6b). Thereafter, a thin layer of the two part saturant solution consisting of resin and hardener mixed as per the manufacturer's specifications was applied over the specimens (Fig. 5.6c). Then the layer of GFRP sheet was bonded on the specimen carefully. A roller was used to remove the entrapped air between the fiber and excess saturant so as to allow better impregnation of the saturant (Fig. 5.6d). Special attention was taken to ensure that no air voids were left between the fiber and the concrete surface. All the specimens were stored at room temperature for at least 28 days before testing (Fig. 5.7). After the GFRP sheets were allowed to cure for three days, strain gauges were applied. Fig. 5.8 shows the location of strain gauges for each length of GFRP sheet. For the 4-inch (100-mm) and the 6-inch (150-mm) bonded lengths, there were two strain gauges placed along the centerline of the GFRP sheet in the bonded region. For the 8-inch (200-mm) bonded length, there were three strain gauges in the bonded region.

5.3.4 Instrumentation and Loading Test Setup

The single shear tests were carried out by making a special arrangement in a laboratory universal testing machine using a specially fabricated mild steel plate firmly connected to the testing machine. Fig. 5.9 shows the test set up used in the investigations. The concrete block was firmly mounted to the bottom crosshead with 35 mm thick steel plates as shown. The single shear test was performed by dragging the GFRP sheet upward from the specimen and the applied load was measured with the help of a pressure sensor. The load was applied in a monotonically increasing manner. Thee load- bond slip were monitored by two linear variable displacement transducers (LVDT), which were attached on the sides of GFRP sheet with the help of steel clamps as shown in Fig. 5.9. The strain gauges

were fixed on the GFRP strips to monitor the GFRP strains. The readings from the LVDT's, strain gauge and the pressure sensor were recorded with the help of the data acquisition system. After the test, the modes of failure were also noted carefully.

Fig. 5. 5(a-d): Process of bonding GFRP sheet to SST Specimens

Fig. 5. 6: Specimens after GFRP bonding
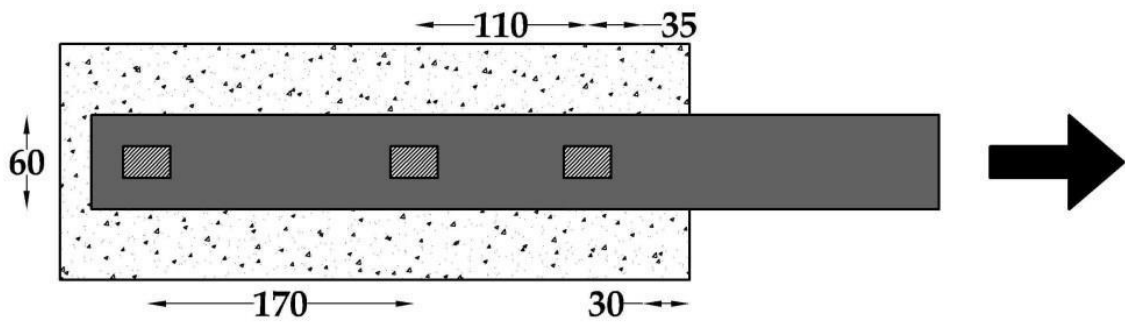
Fig. 5. 7: Position of strain gauges (200mm bonded length)

Fig. 5. 8: Test set up showing Instrumentation and loading

5.4. RESULTS OF SINGLE SHEAR BOND STRENGTH TESTS

The GFRP sheets were loaded in tension and the load was increased monotonically to failure. The data was recorded with the help of the data acquisition system. Both displacement and strain were measured in all these tests. The experiments were performed in three separate series with each series consisting of fifteen specimens. Each series had different bond length, temperatures but had constant number of plies of GFRP.

5.4.1. Failure Modes

Thirty test specimens failed due to debonding of concrete adjacent to the adhesive-concrete interface in which 4mm to 25mm thick layer of concrete got detached with the GFRP composite after failure (Fig. 5.10). Though the failure occurred in concrete (delamination of cover concrete), the word debonding is being used here to define failure

156

because it has been generally used by many researchers in the past in similar cases (Teng et al. 2002). Eleven specimens failed in terms of debonding at the adhesive concrete interface where the concrete quantity attached to the FRP composite was very less after failure (Fig. 5.10). Table 5.3 indicates the failure modes noted in each series of specimens. For those specimens who failed by debonding (delamination) in concrete, the failure started with the occurrence of crack adjacent to the loaded end of the concrete specimen. Later the cracks, inclined to the longitudinal axis of the GFRP composites, were noticed on the adjacent sides of GFRP composites. With increase in the load, the cracks in the concrete surface initiated debonding of GFRP from the concrete from the loading end. The moment final failure reached, the GFRP strip got completely separated from the test specimen along with a layer of concrete (including fractured aggregates) with it. The thickness of the concrete layer on the debonded GFRP composite was found to be lesser for the specimens heated to lower temperatures i.e. up to 400°C. The thickness of delaminated concrete with debonded GFRP increased with the increase in temperature beyond 400°C. The time taken to debonding failure depended on the bond length of the GFRP composites. It was very short for a small bond length and vice versa. The debonding area of the concrete specimens was rough with the aggregates being evidently visible (Fig. 5.10).

The specimens, which had failure by means of debonding at the adhesive concrete interface, had almost similar failure mode as described above, but the concrete attached to the GFRP composite was very little and that too was noted near the loaded ends (Fig. 5.11). A sound was heard during the early to middle stages of loading, which signified the starting point of GFRP slippage out of concrete. When ultimate load was reached, a loud noise was heard due to sudden energy release as a result of debonding of GFRP strips from the concrete. Failure sounded like a gunshot as the GFRP debonded followed even by dislodging of LVDTs in some specimens. Fig. 5.10 and Table 5.3 show the modes of failure of specimens with different bond length.

Table 5. 3: Test results

Specimen	Temperature (°C)	FRP Bond Length (mm)	Ultimate Bond strength (kN)	Failure Mode[*]
$SSTAL_{f1}$	0	100	16.10	DBACI
$SST2L_{f1}$	200		16.65	DBACI
$SST4L_{f1}$	400		16.37	DBACI
$SST6L_{f1}$	600		12.84	DBC
$SST8L_{f1}$	800		10.31	DBC
$SSTAL_{f1.5}$	0	150	16.96	DBACI
$SST2L_{f1.5}$	200		16.22	DBC
$SST4L_{f1.5}$	400		15.65	DBC
$SST6L_{f1.5}$	600		15.13	DBC
$SST8L_{f1.5}$	800		12.77	DBC
$SSTAL_{f2}$	0	200	18.46	DBACI
$SST2L_{f2}$	200		17.27	DBC
$SST4L_{f2}$	400		16.72	DBC
$SST6L_{f2}$	600		15.38	DBC
$SST8L_{f2}$	800		12.75	DBC

*DBACI: debonding at adhesive concrete interface; DBC: debonding in concrete
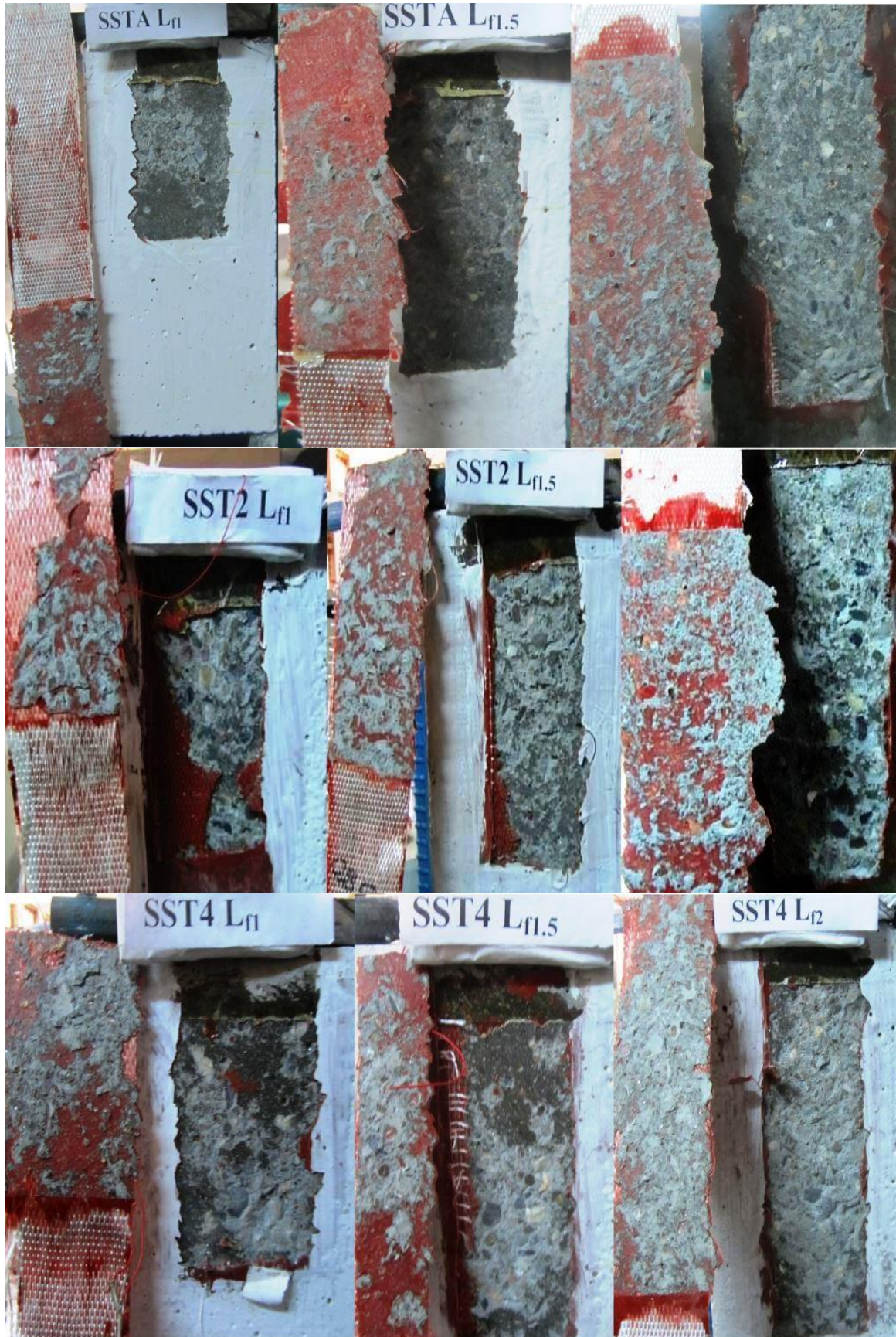
Fig. 5.10: Typical mode of failure of specimens with different bonded area/length (Cont)
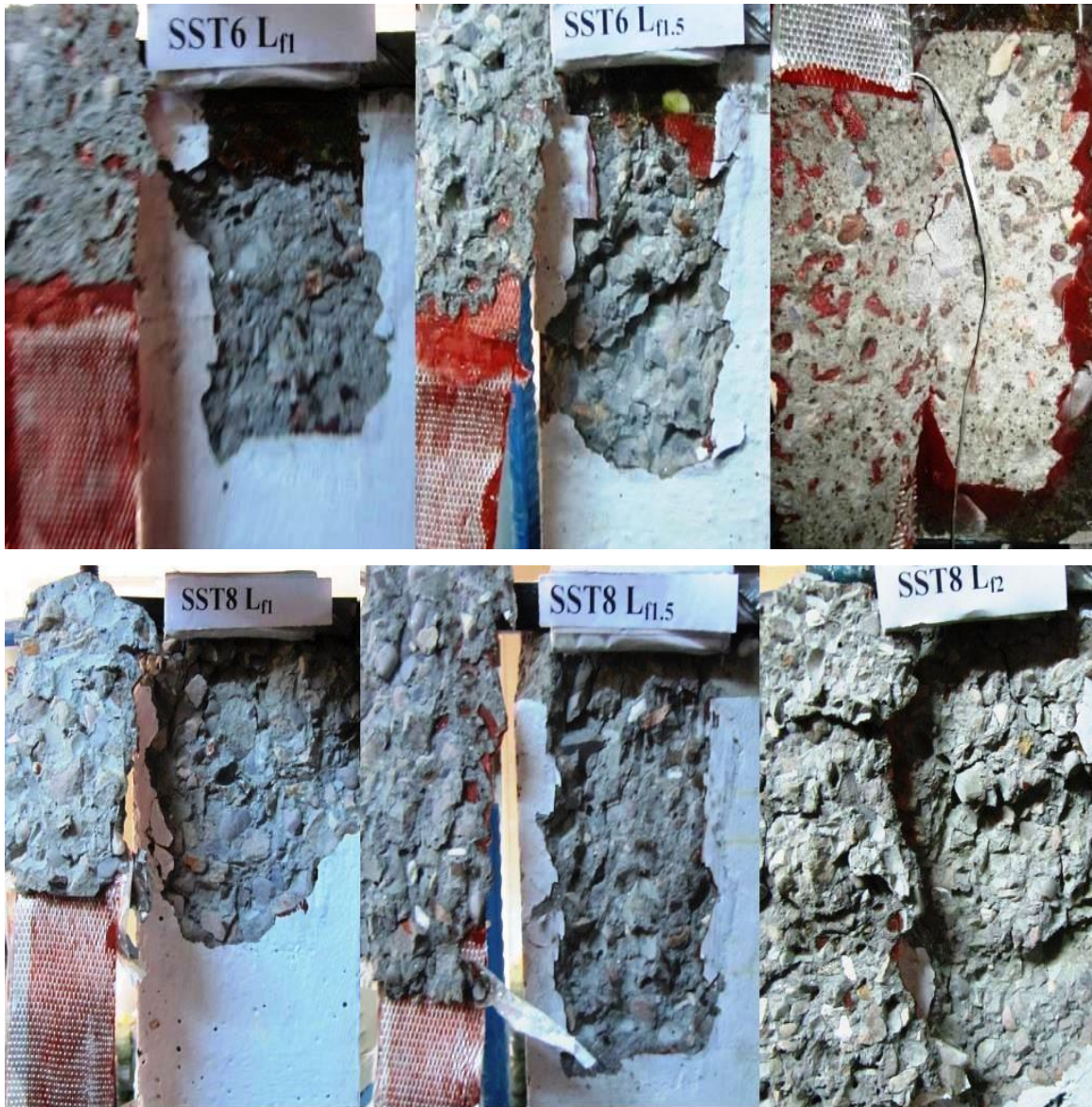
Fig. 5. 9: Typical mode of failure of specimens with different bonded area/ length

5.4.2 Load Slip Behavior

The load-slip relationships and curves were drawn using the experimental data obtained. Fig. 5.11 (a-c) shows the load–slip curves of the three series of test specimens. It can be noted that initially the slip increased almost linearly with the load. However, in specimens heated to temperatures more than 400°C, the increase in displacement was not found to be linear with the load even in the initial stages of loading. In general, the heat damaged specimens showed faster increase in slip owing to softening of concrete due to exposure to high temperature. In specimens, except those exposed to 800°C, the curves rose almost similarly in the initial stages of loading, though they deviated in the later part of loading. The specimens heated at higher temperatures, especially at 600°C and 800°C, the final portions of the load slip curves became flatter, which was more evident at

800°C. Before the initiation of debonding failure corresponding to the ultimate load, the debonding propagated towards the unloaded end with the occurrence of relatively faster displacement. It can be observed from the load-slip curves that the behavior remained almost similar up to 400°C temperature, but the peak load decreased as the temperature increased and a significantly flatter curve with reduced load was noted in specimens heated at 800^{0}C.
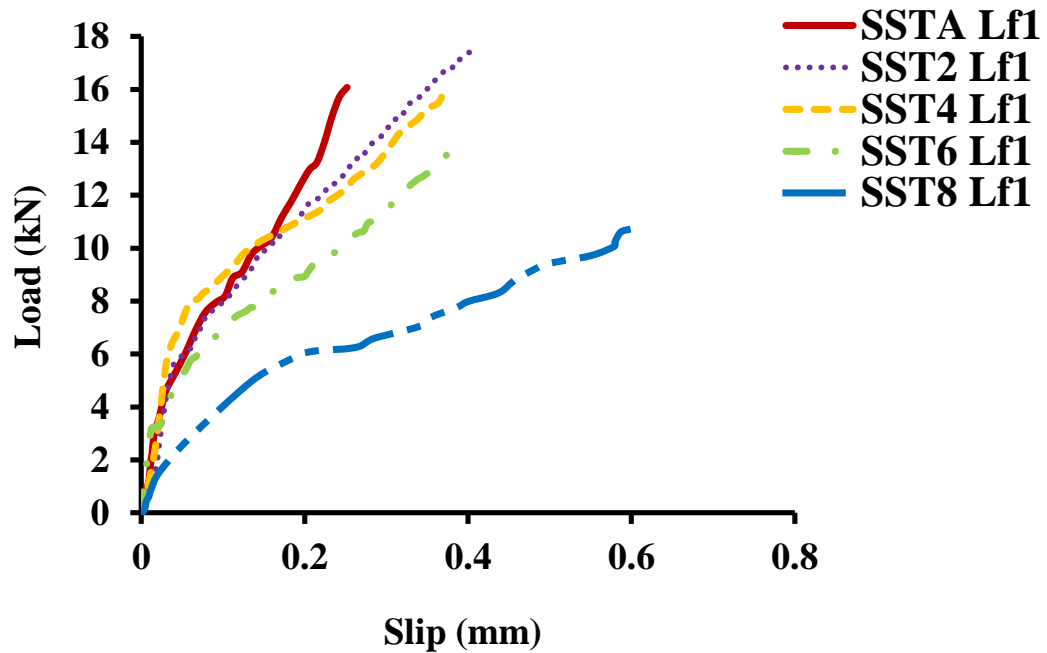
(a) Specimens exposed to different temperatures with L_f 100mm
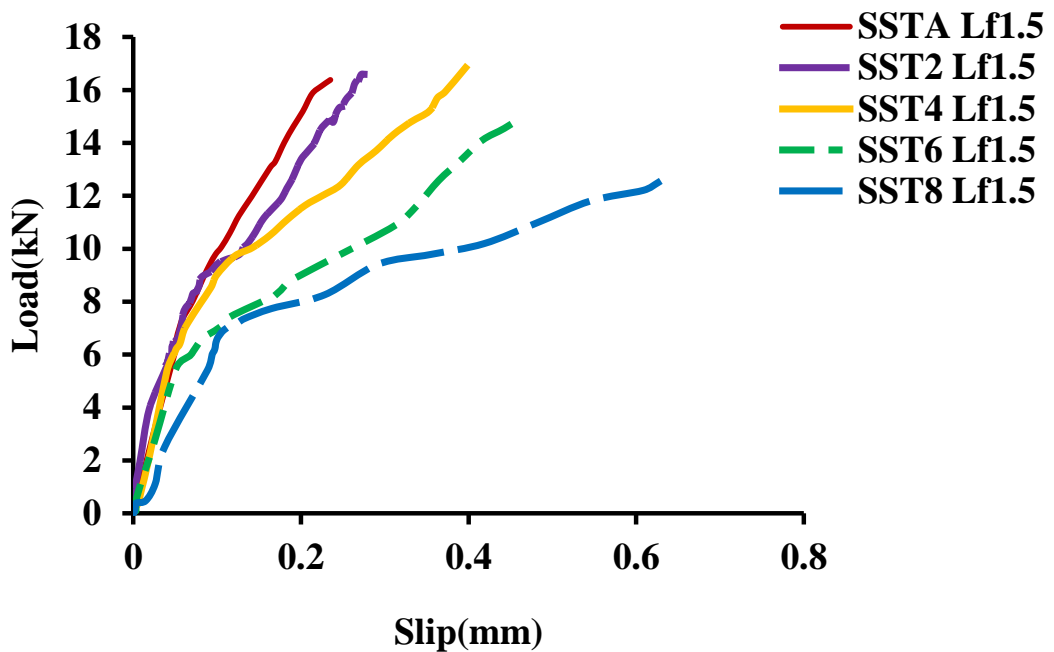
(b) Specimens exposed to different temperatures with L_f 150mm
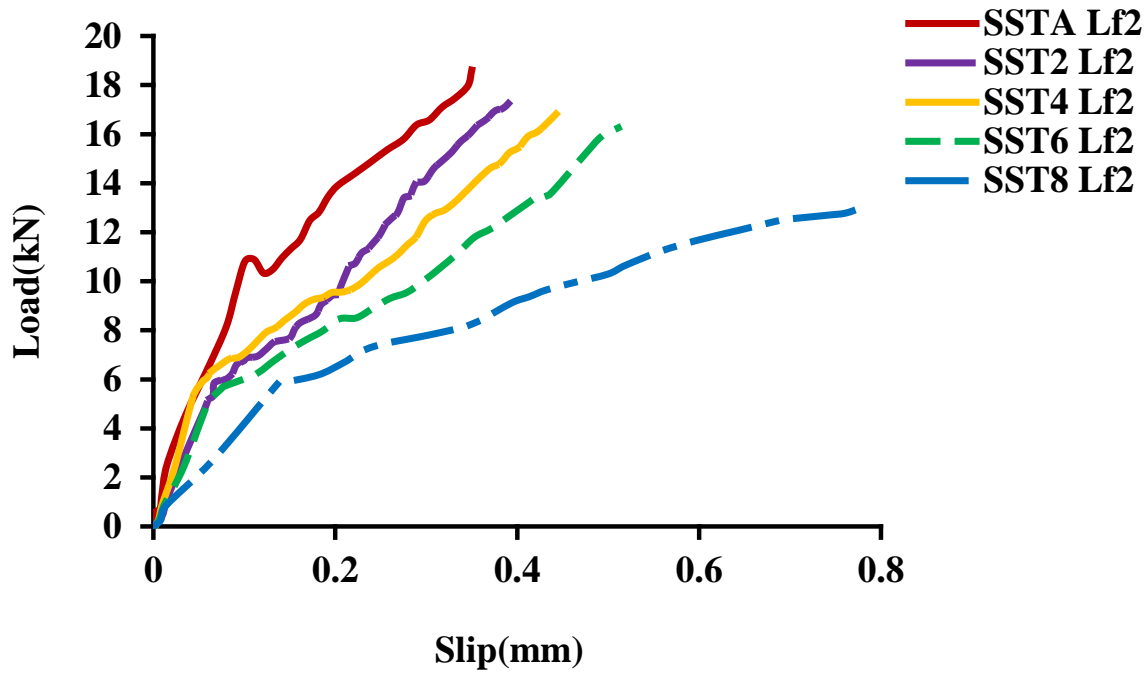
(c) Specimens exposed to different temperatures with L_f200mm

Fig. 5. 10: (a)-(c) Bond–slips curves

5.4.3 Strain Distributions and Bond Strength

The strain gauges readings were used to develop the strain distribution plots along the bonded length. Strains were captured at three different locations in GFRP as mentioned earlier. The first strain corresponding to the distance 0 mm was calculated directly based on basic mechanics (involving F, A, σ, E) as the readings from the strain gauge here were found to be influenced by the local bending of the GFRP strip. Two strain gauges, one each at 35mm and 70 mm from the location corresponding to x=0 were mounted to capture the strains in 100 and 150 mm bond length specimens. Three strain gauges, each at 35, 110 and 170 mm from x=0 location were mounted to captured the strains for 200mm bond length specimens. The strain distributions along the bond length are presented in Figs. 5.12 – 5.14. For better understanding of strain distributions, strains associated with 30, 50, 70, 90 and 100 percent of failure load in each case, are plotted with the distance from the loaded end. In the specimens having bond length of 100 and 150 mm, the increase of GFRP strain was found to be gradual until 90 percent of ultimate failure load. But in larger bond lengths (200mm) the increase of GFRP strain was observed to be relatively gradual only until 70 percent of failure load. This propagation of debonding is clearly reflected by the strain distributions shown in Fig. 5.12 - 5.14.

162

The strain distributions show a decrease in strains towards the end of the GFRP strip. This was also manifested by the failure pattern and the debonding patterns. The debonding of GFRP strip always started at the loading end. The strain distribution along the bonded length explains the amount at which the applied tensile load is transferred from the composite sheet to the concrete. The strains in the composite sheets became smaller, particularly for the longer bond lengths. It has been noticed that the strain values at the ultimate load were considerably lower in the 600°C and 800°C heated specimens compared to the control unheated specimens and other lesser heat damaged specimens. This could be due to the occurrence of micro-cracking of concrete after heating. Table 5.4 shows the average bond strength (maximum bond stress) of heat damaged specimens at failure load, maximum measured slip and the corresponding maximum strain. The results show that the average bond stress (calculated using the total bond area) decreases as the bond length increases. This is due to the fact that for longer bond lengths, the complete bond is not exploited. However, longer bond lengths would be better in terms of having ductile failure.
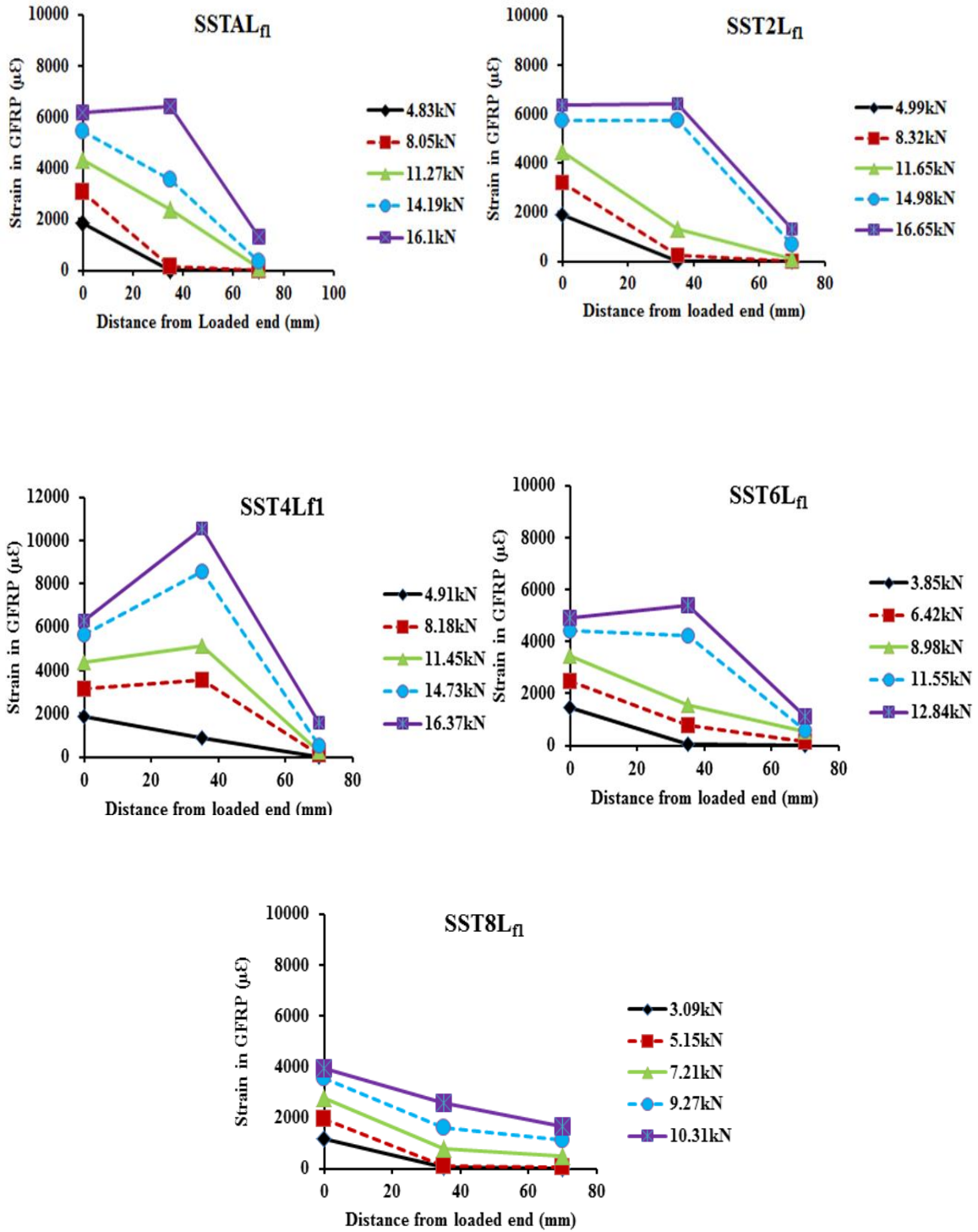
Fig. 5. 11: Strain distribution in L_f1
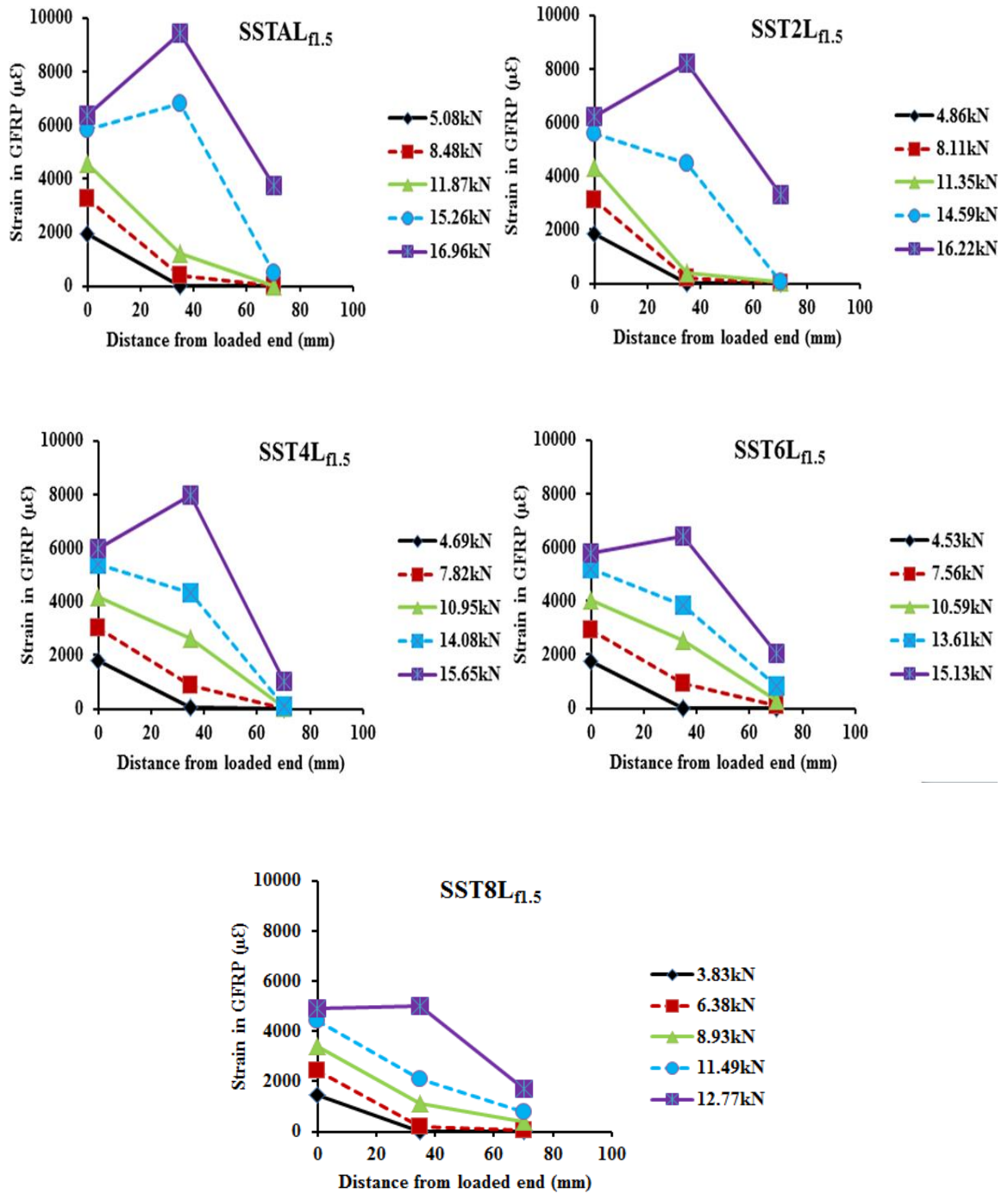
Fig. 5. 12: Strain distribution in L_f 1.5
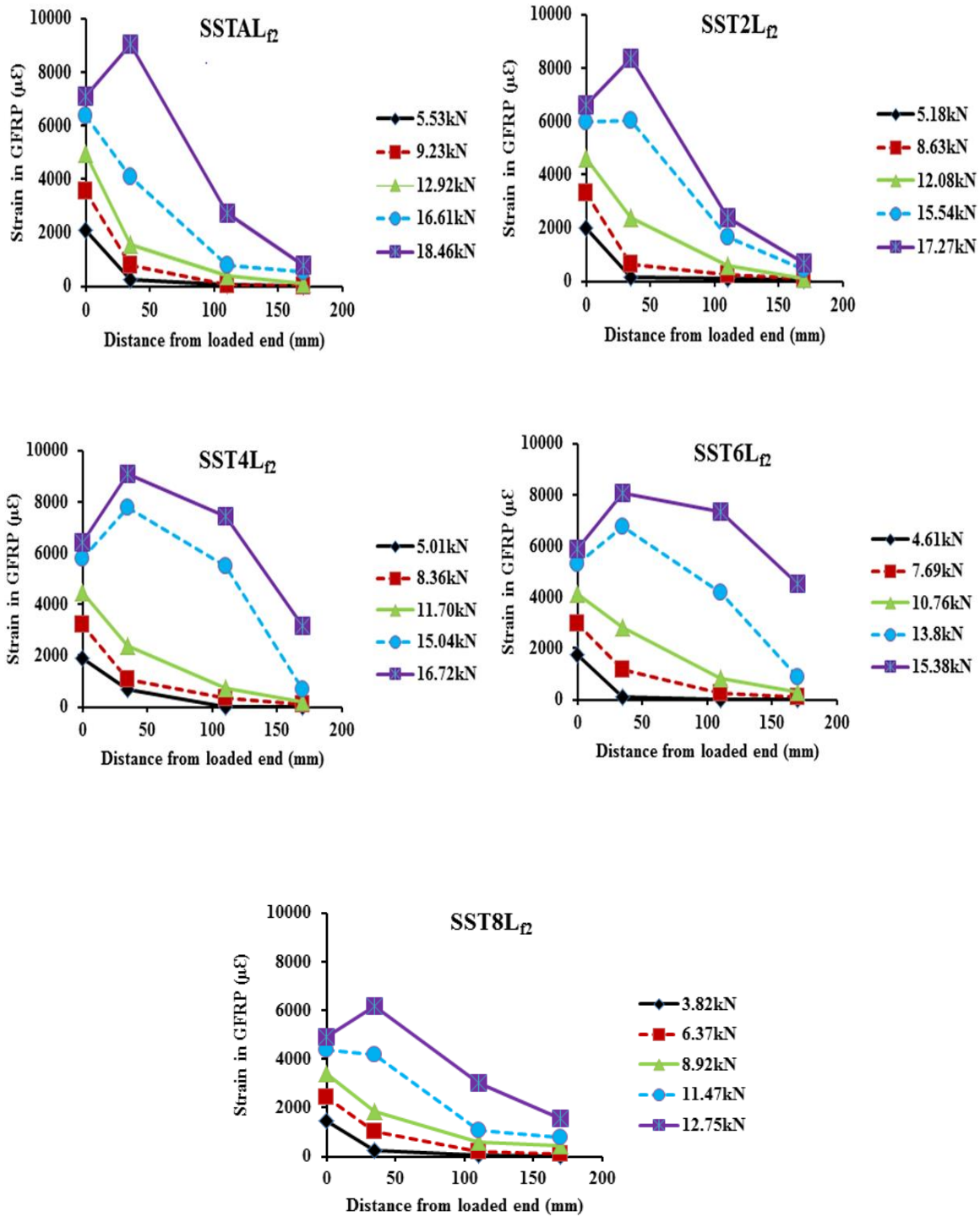
Fig. 5. 13: Strain distribution in Lf2

Table 5. 4: Bond Stress, Maximum slip and Ultimate bond strain results

Specimen	Maximum Bond stress (MPa)	Measured Slip(mm)	Maximum Strain ($\mu\mathcal{E}$)
SSTAL$_{f1}$	2.68	0.25	6425
SST2L$_{f1}$	2.7	0.4	6425
SST4L$_{f1}$	2.72	0.37	10532
SST6L$_{f1}$	2.14	0.38	5404
SST8L$_{f1}$	1.80	0.59	2590
SSTAL$_{f1.5}$	1.88	0.23	9431
SST2L$_{f1.5}$	1.80	0.27	8226
SST4L$_{f1.5}$	1.73	0.39	7949
SST6L$_{f1.5}$	1.68	0.46	6420
SST8L$_{f1.5}$	1.41	0.62	5007
SSTAL$_{f2}$	1.53	0.35	9038
SST2L$_{f2}$	1.43	0.39	8354
SST4L$_{f2}$	1.39	0.44	9084
SST6L$_{f2}$	1.28	0.51	8042
SST8L$_{f2}$	1.06	0.77	6151

5.4.4 Effect of Bond Length

Fig. 5.15 shows the significance of bond length on the bond properties of GFRP with heat damaged concrete. The relationships between the ultimate failure bond load with the length of bond are shown in the Fig. 5.15. In general ultimate bond strength increases with increase in bond length from 100 mm to 200 mm irrespective of the temperature of exposure. The failure load increased in the range of 5% to 38% when the

bond length increased from 100 to 200 mm for the various specimens. In some isolated cases, a marginal decrease in bond strength of approximately 4% was also noted. This reduction in these cases suggests that the bond length might have exceeded the effective bond length (Woo et al. 2010). Thus it is believed that the extra bond length only increases the time to failure. It can be said that an increase in bond length beyond the length needed to transfer stresses between the GFRP and the concrete (effective bond length) can provide some warning time prior to the GFRP-concrete system failure, while the extra length will not significantly impact the failure load. Table 5.4 and Fig. 5.15 show that the GFRP contact length has an impact on the ultimate bond strength as well as on corresponding slip. The ultimate bond stress was found to be 2.68, 1.88 and 1.53 MPa for control specimens with bond length 100, 150 and 200 mm. This reflects that the ultimate bond stress decreased with the increase of bond length. In addition, the slip at ultimate bond stress 100, 150, 200mm bond length is 0.25, 0.23 and 0.35 respectively. As the results, the bond slip at ultimate bond stress flow opposite behaviour of ultimate bond stress. The ultimate bond stress was found to be 2.7, 1.8 and 1.43 MPa respectively for the specimens exposed to 200°C with bond lengths 100, 150 and 200 mm, with the specimens exposed to 400°C the stress values are 2.72, 1.73 and 1.39 MPa respectively and with the specimens exposed to 600°C the bond stress values for the three bond lengths vary as 2.14, 1.68 and 1.28 MPa respectively. It can be noticed that a decrease in the bond stress takes place as the exposure temperature increases however till 600°C the decrease is very less. With the specimens exposed to 800°C the bond stress values were found to be 1.8, 1.41, and 1.06 MPa respectively for the specimens with the bond lengths 100, 150 and 200 mm. At 800 °C the decrease in the bond stress is very much pronounced which can be attributed to the deterioration of the concrete as is evident from the failure mode of the specimens which is the debonding of concrete for the 800 °C exposed specimens. The slip shows an increasing trend with the increase in exposure temperature as shown in the table 5.4. The slip was measured to be 0.4, 0.27 and 0.39 mm respectively in the specimens with bond lengths 100, 150 and 200 mm exposed to 200°C. For the specimens exposed to 400°C the respective slips were measured to be as 0.37, 0.39 and 0.44 mm, with the specimens exposed to 600°C the bond slips were measured to be 0.38, 0.46 and 0.51 mm respectively and when the exposure temperature was increased to 800°C the bond slips increase drastically to 0.59, 0.62 and 0.77 respectively in the specimens with bond lengths 100, 150 and 200 mm.
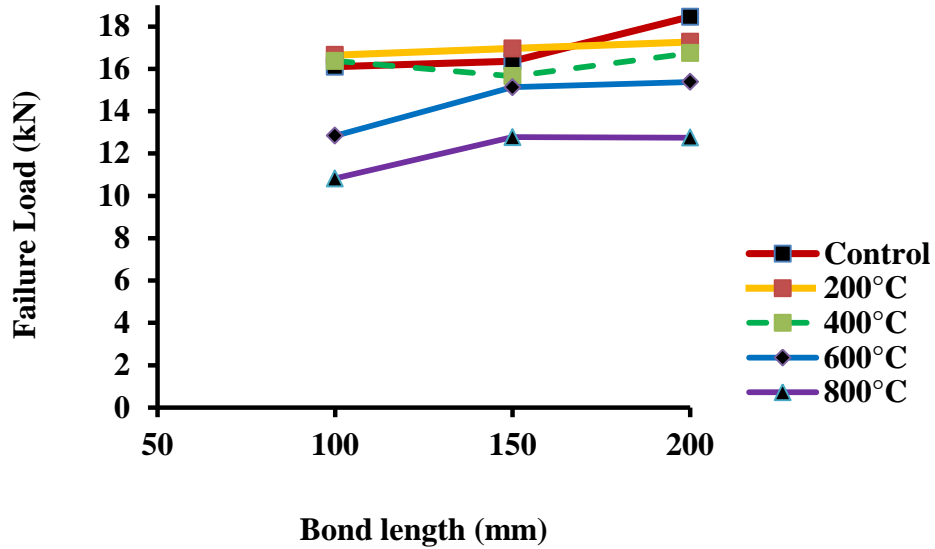
Fig. 5. 14: Effect of bond length

5.5 BOND STRENGTH MODEL

Many models have been proposed in the literature to predict the bond behavior between concrete and FRP sheets under normal room temperature conditions (Khalifa et al. 1998, Chen and Teng 2001, Wu et al. 2001, Xiao et al. 2004, Lu et al. 2005, Yao et al. 2005, Mazzotti et al. 2008, Wu et al. 2009). While some empirical models are based on the regression of test data, others have been proposed theoretically based on fracture mechanics approach. Most of the proposed empirical models were developed based on pull off type tests and use parameters namely FRP to concrete width ratio, bond length, and axial stiffness of FRP sheets. Temperature of heat damaged concrete was not considered in the earlier models. However, Haddad et al. (Haddad et al. 2103) proposed an empirical model for the bond strength of FRP with heat damaged concrete based on their experimental data. But this model considered a maximum temperature of exposure of 600°C only. An attempt has been made in this study to develop a bond model for heat damaged concrete which was exposed to temperatures up to 800°C. The model proposed by Chen and Teng (Chen and Teng, 2001) for room temperature conditions is being modified here to make it applicable for heat damaged concrete.

The bond strength (ultimate failure load) of FRP-concrete interface as proposed by Chen and Teng (Chen and Teng, 2001) under room temperature conditions is:

$$\mathrm{Pu} = 0.427 \times \beta p \times \beta L \times bp \times Le \times \sqrt{fc'} \qquad (5.1)$$

Where,

$$Le = \sqrt{\frac{Ep \times tp}{\sqrt{fc\prime}}}; = \left(\frac{2-\left(\frac{bp}{bc}\right)}{1+\left(\frac{bp}{bc}\right)}\right)^{\frac{1}{2}}; \beta L = \left\{\sin\left(\frac{\pi L}{2Le}\right)\right\} \text{ if } L<Le \text{ ; } \beta L = 1 \text{ if } L>Le \qquad (5.2)$$

Where Ep, tp, bp are modulus of elasticity, thickness and width of FRP sheets, respectively; *fc'*, bc are the concrete compressive strength and width of concrete block, respectively; Le, L are the effective bond length and bond length, respectively. Experimental results have shown that when concrete is exposed to high temperatures, the compressive strength, tensile strength and stiffness properties are highly affected. It is expected that a decrease in compressive strength of heat damaged concrete would influence the bond strength and bond length including effective bond length. Thus the effective bond length would increase with the decrease in compressive strength of concrete due to heat damage. In order to enable the application of above mentioned Chen and Teng model (Chen and Teng 2001) for predicting the bond strength of FRP with heated concrete, the parameters of the model should be modified. Therefore, a temperature dependent compressive strength (*fc'*) as proposed in a previous study (Chang et.al 2006) is introduced here in above mentioned bond strength model of Chen and Teng (Chen and Teng 2001). The modified model to predict the bond strength of heated concrete with FRP can then be presented as:

$$Pu = \alpha \times \beta p \times \beta L \times bp \times (fcT\prime)^{0.25} \times (Ep \times tp)^{0.5} \qquad (5.3)$$

Where,

$$Le = \sqrt{\frac{Ep \times tp}{\sqrt{fcT\prime}}}; \beta p = \left(\frac{2-\left(\frac{bp}{bc}\right)}{1+\left(\frac{bp}{bc}\right)}\right)^{\frac{1}{2}}; \beta L = \left\{\sin\left(\frac{\pi L}{2Le}\right)\right\} \text{ if } L<Le \text{ ; } \beta L = 1 \text{ if } L>Le \quad (5.4)$$

$$fcT\prime = fc\prime\left(1.008 + \frac{T}{450\times\ln\left(\frac{T}{5800}\right)}\right) \geq 0.0 \quad 20°C \leq T \leq 800°C \text{ (Chang et.al 2006) (5.5)}$$

α is a regression coefficient, $\beta p, \beta L$, $fcT\prime$ are bond width factor, bond length factor and compressive strength of the concrete at elevated temperatures respectively. A non-linear regression analysis was carried out on the present test data to find a suitable value for "α". The proposed model then becomes:

$$Pu = 0.4016 \times \beta p \times \beta L \times bp \times (fcT\prime)^{0.25} \times (Ep \times tp)^{0.5} \qquad (5.6)$$

The proposed model was validated with the test results of this study. The statistical parameters and the comparison between the predicted and test values are shown in Table 5.5 and Fig. 5.16. This shows that the proposed model is in good agreement with the test results.

Table 5. 5: Statistical parameters for validation

Data Source	Average	SD	COV	COD	r	P/T
Present model	0.97096	0.11378	0.11718	0.886	0.94158	0.593

Note: SD=standard deviation; COV=coefficient of variance; COD = coefficient of determination; r = correlation coefficient and P/T: predicted to test ratio.
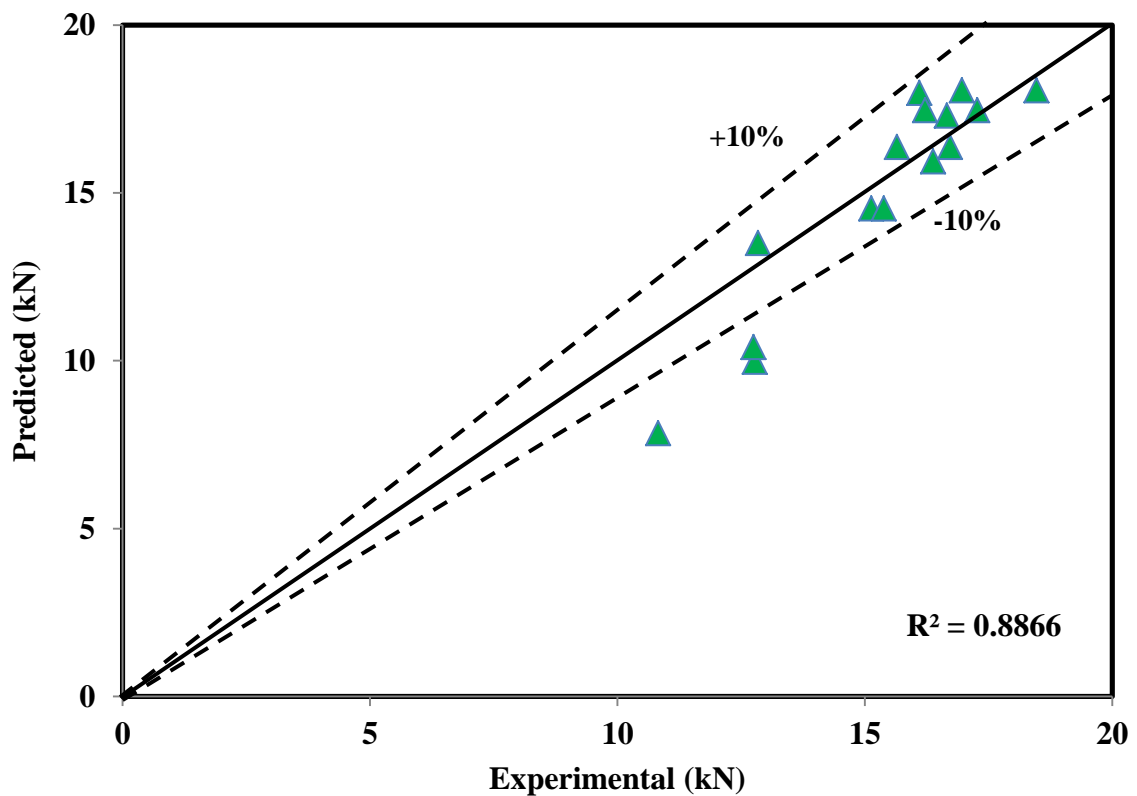
Fig. 5. 15: Bond strengths: test results versus predictions from proposed bond strength model

5.6 DESIGN IMPLICATIONS

In practical design, generally a designer needs to know the ultimate debonding strain of FRP. For designing FRP strengthening for fire or heat damaged flexural members, the knowledge of debonding strain for FRP with heat damaged substrate concrete is required. Thus, an attempt has been made here to develop an equation for determining the ultimate debonding strain of FRP with heat damaged concrete as given below:

The bond stress, σp, can be determined by dividing the ultimate load, from Eq. (5.6), by the resisting area as σp = Pu / bp tp which can be written as

$$\sigma p = 0.4016 \beta p \beta_L \sqrt{\frac{Ep \sqrt{fcT'}}{tp}} \tag{5.7}$$

From Eq.(5.7) we can conclude that fiber with high young's modulus but lower thickness has withstand higher stress, since we can hardly improve the strength of concrete using strengthening process (Chen and Teng 2001).

The ultimate debonding strain in GFRP in heat damaged specimens can be determined by dividing the stress in GFRP (σp) at failure by tensile strength of GFRP (*fp*) and thus can be given by

$$\frac{\sigma p}{fp} = \frac{0.4016 \beta p \beta L}{Ep \varepsilon p} \sqrt{\frac{Ep\sqrt{fcT'}}{tp}} = \frac{0.4016 \beta p \beta L}{\varepsilon p} \sqrt{\frac{\sqrt{fcT'}}{Eptp}} \tag{5.8}$$

Eq. (5.8) which is the ultimate debonding strain in GFRP in heat damaged specimens can be rewritten as

$$\varepsilon p = 0.4016 \sqrt{\frac{\sqrt{fcT'}}{Eptp}} \tag{5.9}$$

Where, Ɛp ultimate strain in GFRP. This equation can be used to calculate the ultimate debonding strain in GFRP in heat damaged concrete specimens.

5.7 CONCLUDING REMARKS

This study focused on investigating the bond behavior of GFRP with heat damaged concrete. The parameters of investigation were temperature of exposure and bond length. The specimens were cast and tested under single shear mode. The results have been analyzed and discussed in detail to fulfill the objectives of this investigation. The study addresses an important gap in the literature i.e. understanding the bond performance of GFRP with concrete damaged by exposure to elevated temperatures. A model has been proposed to predict the bond strength and ultimate debonding strain for GFRP with heated concrete. This information shall become a significant input data for designing FRP strengthening for fire damaged or heat damaged concrete structures.

CHAPTER-6
CONCLUSIONS

6.1 GENERAL

This research focused on investigating the effectiveness of various strengthening techniques in upgrading and restoring the structural performance of compression and flexural reinforced concrete members damaged by fire or by any other accident involving exposure to elevated temperatures. To this end, the capabilities of Ferro Cement (FC) jacketing, High Strength Fibre Reinforced Concrete (HSFRC) strengthening technique, Glass Fibre Reinforced Polymer (GFRP) wrapping and Steel Plate (SP) jacketing have been investigated experimentally. The study involved testing of 63 short columns of circular section, 51 short columns of square section and 27 T shape beams. Various parameters related to the strengthening techniques and heating were investigated within the constraints of the available resources and an attempt has been made to draw meaningful conclusions from the investigations. The research program has contributed to the fundamental understanding of designing post fire retrofit solutions for reinforced concrete structures.

6.2 CONCLUSIONS

Within the scope of the present investigation, the following main conclusions may be drawn:

1. In line with the previous studies, this study also proves that the strength of reinforced concrete compression and flexural elements degrade when exposed to elevated temperatures. The axial compressive strength of square and circular section columns was found to have reduced by 4%, 29%, 79% and 4%, 30%, 81% respectively after exposing to temperatures of 300°C, 600°C and 900°C respectively. The reinforced concrete T-beams experienced a reduction of 14% and 61% in their ultimate flexural strength after an exposure at 600°C and 900°C temperatures respectively. Thus the results of this study show that the detrimental effects of elevated temperature on strength become significant only when temperature reach 600°C and more.

2. The decrease in residual stiffness of heat damaged members was greater than the reduction in their compressive strength. The residual stiffness of heat damaged

square and circular section columns was found to be 34%, 50% & 92% and 5%, 54% & 95% respectively of their room temperature value after exposing to temperatures of 300°C, 600°C and 900°C respectively. The reinforced concrete T-beams experienced a reduction of 34% and 56% in their residual stiffness after an exposure at 600°C and 900°C temperatures respectively.

3. The results show that the deformability of both reinforced concrete compression members and beams deteriorates as the temperature of exposure increases. A reduction in deformability measured in terms of energy dissipation (area under the load deformation curves) in circular section columns was 32% and was 62% in square columns as the temperature of exposure increased from room temperature to 900°C. The energy dissipation in reinforced concrete beams reduced by 47% as the heating temperature rose to 900°C.

4. The axial compressive strength of heat damaged reinforced concrete columns increased significantly in case of GFRP strengthened specimens. HSFRC, SP and FC jacketing techniques were found to be relatively less effective in increasing the compressive strength of heat damaged columns compared to GFRP jacketing. While GFRP confinement strengthening was quite capable even in restoring the room temperature axial strength of heat damaged columns, the HSFRC, FC and SP techniques though showed increase in strength compared to un-strengthened heat damaged columns they were not entirely capable of restoring the room temperature strength of columns. However, the amount of restoration depends upon the initial degree of heating i.e. temperature of exposure.

5. With respect to the deformability and ductility of columns, again GFRP confinement strengthening has been found to be quite effective. On the contrary, the HSFRC, FC and SP techniques of strengthening performed inadequately in restoring the deformability of fire damaged concrete columns. The specimens repaired with HSFRC, SP and FC jacketing techniques actually exhibited lesser deformability compared to the corresponding control unheated columns and even heat damaged un-strengthened columns in some instances. The GFRP confinement strengthening successfully restored the deformability of both circular and square section heat damaged columns. The deformability of columns, which was gauged in terms energy dissipation as well, also indicated that GFRP confinement strengthening scheme faired considerably better than the

176

other techniques of strengthening employed in this study. In fact GFRP wrapped columns heated at 900°C temperature showed 363% & 193% more energy dissipation capacity than that for un-strengthened circular and square section columns respectively under room temperature conditions.

6. On the contrary the secant stiffness property of heat damaged concrete columns could not be restored by GFRP confining jacketing technique. Interestingly, the HSFRC and FC strengthening techniques were capable of improving the stiffness and in fact restoring the stiffness of heat damaged columns.

7. All the strengthening techniques employed in this study showed reasonable enhancement in strength compared to the strength of heat damaged un-strengthened beams in case of beams heated at 600°C, though the capability of various strengthening designs in restoring the room temperature strength was just sufficient at 600°C temperature. The GFRP strengthening showed better enhancements in strength of heat damaged beams compared with FC and HSFRC strengthening. While all the three strengthening schemes showed significant increase in strength of 900^{0}C heat damaged un-strengthened beams, it was GFRP which was able to restore the room temperature strength of beams heated at 900^{0}C with other two techniques falling short in restoring the room temperature strength of heated beams at this temperature.

8. The GFRP strengthening showed considerably better enhancements in stiffness of heat damaged reinforced concrete beams compared to FC and HSFRC strengthening schemes. In case of beams heated at 600°C, all the strengthening types showed increase in stiffness if compared with the stiffness of heat damaged un-strengthened beams. Similarly all the strengthening schemes indicated considerable increase in the stiffness of heat damaged un-strengthened beams heated at 900^{0}C temperature also. However, only GFRP could restore the room temperature stiffness of beams heated at 600°C and both GFRP and HSFRC could restore the stiffness of control unheated and un-strengthened beams at 900^{0}C temperature.

9. The results show that the GFRP strengthened heat damaged beams showed lower energy absorption capacity. However, FC and HSFRC strengthening designs provided better results and showed an increase in the energy dissipation of heat damaged beams at all the temperatures. None of the strengthening schemes could

restore the energy dissipation of heated beams to their room temperature value. It can be concluded that in spite of GFRP strengthening technique's capability of restoring the room temperature strength of beams, no improvement in energy absorption capacity is possible due to the brittle post peak failure of GFRP strengthened beams.

10. The load corresponding to the first crack in heat damaged beams increases considerably when the damaged beams are strengthened with different strengthening techniques. It was found to be more in case of both GFRP and FC strengthened beams than in HSFRC strengthened heated beams.

11. The results of this study show that the exposure at elevated temperatures changes the failure mode of reinforced concrete beams. Though the ultimate failure of control unheated beams and beams heated at 600°C were essentially a flexural failure, the beams heated at 900^{0}C temperature failed in shear. The strengthening of beams with the techniques under reference, however, ensured flexural failure with only exception being the GFRP strengthened beam heated at 900^{0}C.

12. This study has also attempted to investigate an important issue concerning design of GFRP strengthening for fire damaged concrete structures, which is bond between GFRP and heat damaged concrete. It was found that the elevated temperature has an effect on effective bond length and the bond strength of GFRP heat damaged concrete strengthening system. The ultimate bond strength increases with the increase in bond length irrespective of temperature when the specimen is exposed to more than 400^{0}C temperatures. The bond strength reduces significantly when the temperature increases. Further, it was found that the average bond stress at failure decreases as the bond length increases.

13. It was found that the debonding failure of GFRP from heat damaged concrete surface changes when the temperature of exposure changes. It was found that a typical debonding failure involving debonding of composite from concrete surface changes to a typical delamination failure involving separation of concrete with GFRP as the temperature of exposure increases. The thickness of the delaminated concrete layer with GFRP composite was less for specimens subjected to temperatures less than 400°C. However thickness was more in 600°C and 800°C heat damaged specimens.

178

14. A model has been proposed in this study to estimate the bond strength of GFRP with heat damaged concrete based on the test results. Good agreement was obtained between the proposed model and the test results. As more and more data is made available in the future, the present model can be further refined and improved. The proposed model is also capable of computing the debonding strain of GFRP strengthened fire damaged flexural concrete members.

BIBLIOGRAPHY

1.   ACI Committee 549, Guide for the design, construction, and repair of ferrocement. (1988), ACI Structural Journal, 85,325–51.

2.   Abbasnia, R. and Ziaadiny, H. (2010). "Behavior of concrete prisms confined with FRP composites under axial cyclic compression" Engineering Structures 32, pp. 648–655.

3.   Abdul Rahim, Sharma, U.K., Murugesan, K., Sharma, A. and Arora, P. (2013), "Multi-response optimization of post-fire residual compressive strength of high performance concrete", Construction and Building Materials, 38(2), 265-273.

4.   Abdullah, A; and Takiguchi, K; (2000) "Experimental Investigation on Ferrocement as an Alternative Material to Strengthen Reinforced Concrete Column," Journal of Ferrocement, V. 30, No. 2, pp. 177-190.

5.   Abrams. M. S, (1977), "Performance of concrete structures exposed to Fire", PCA, Research and Development Bulletin.

6.   Abrams, M. S. (1971), "Compressive strength of concrete at temperatures to 1600 F", Temperature and concrete, Detroit (MI): American Concrete Institute, SP-25, pp.33–59.

7.   Adam J. M, Ivorra S, Giménez E, Moragues J. J, Miguel P, Miragall C, Calderón P. A. (2007). "Behaviour of axially loaded RC columns strengthened by steel angles and strips. Steel Composite Structures; 7(5):405–19.

8.   Ahmad, S. H. and Shah, S.P. (1982), "Stress-strain curves of concrete confined by spiral reinforcement", ACI Journal, 79 (6), pp. 484-490.

9.   Ahmed, A. E., Al-Shaikh, A. H., Arafat, T. I. (1992) "Residual compressive and bond strengths of limestone aggregate concrete subjected to elevated temperatures", Magazine of Concrete Research, 44, No. 159, June, 1 17-125.

10.   Aiello, M. A., Focacci, F. and Nann, A., (2001), "Effects of Thermal Loads on Concrete Cover of Fiber- Reinforced Polymer Reinforced Elements: Theoretical and Experimental Analysis", ACI Materials Journal, V. 98, No. 4, pp. 332-339.

11.   Ali, F., Nadjai, A., Silcock, G. & Abu-Tair, A. (2004), "Outcomes of a major research on fire resistance of concrete columns", Fire Safety J., 39(6), pp. 433-445.

12. Alaee F. J. (2003). "Fracture model for flexural failure of beams retrofitted with CARDIFRC. Journal of Engineering Mechanics, 129, pp.1028.

13. Alaee, F. J and Karihaloo, B. L. (2003). "Retrofitting of RC beams with CARDIFRC, ASCE Journal of composites for Construction, 7, 174-186.

14. Almusallam, T. H and Al-salloum, Y. A. (2001). "Ultimate strength prediction for RC beams externally strengthened by composite materials". Composites: Part B, 32. 609-619.

15. Al-Kubaisy, M. A, and Jumaat, M. Z. (2000). "Flexural behaviour of reinforced concrete slabs with ferrocement tension zone cover", Construction and Building Materials 14, 245 -252

16. Al-salloum, Y. A., Elsanadedy, H. M., and Abadel, A. A., (2011),"Behavior of FRP-confined concrete after high temperature exposure". Construction and Building Materials, 25(2), 838-850.

17. Amrul Kaish A. B. M, Alam. M. R, Jamil. M and Wahed. M. A. (2013), "Ferrocement Jacketing for Restrengthening of Square Reinforced Concrete Column under Concentric Compressive Load", Procedia Engineering 54, 720 – 728.

18. Anderberg, Y., (2009), "Assessment of fire-damaged concrete structures and the corresponding repair measures". Concrete Repair, Rehabilitation and Retrofitting II, pp 631-636.

19. Arduini M., Tommaso A.D., and Nanni A. (1997). "Brittle Failure in FRP Plate and Sheet Bonded Beams", ACI Structural Journal, Vol. 94, No. 4, 363-370.

20. Arghya Deb and Bhattacharyya. S. K. (2011) "Failure modes for FRP wrapped cylindrical concrete columns" Journal of Reinforced Plastics and Composites, Vol.30 (7), 561-579.

21. Arioz.O, (2009), "Retained properties of concrete exposed to high temperatures: Size effect", Fire and Materials, 33(5): p. 211-222.

22. Ashour, A. F., El-Refaie, S. A., and Garrity, S. W. (2004). "Flexural strengthening of RC continuous beams using CFRP laminates." Cement and concrete composites, 26(7), 765-775.

23. Aslani F. and Bastami, M. (2011) "Constitutive Relationships for Normal- and High-Strength Concrete at Elevated Temperatures", ACI Materials Journal, V. 108, No. 4, pp. 355-364.

24. Assessment of fire-damaged concrete structures and repair by gunite. Concrete Society Technical Report No.15

25. Assessment and repair of fire-damaged concrete structures. Concrete Society Technical Report No.33.

26. Assessment, design and repair of fire-damaged concrete structures. Technical Report-68, Concrete Society, Camberley, UK

27. Aycardi, L. E., Mander, J. B., and Reinhorn, A. M. (1994). "Seismic resistance of R.C. frame structures designed only for gravity loads: Experimental performance of subassemblages." ACI Structural Journal, 91(5), 552-563.

28. Bakis C. E, Bank L. C, Brown V. L, Cosenza E, Davalos J. F, Lesko J. J, Machida A, Rixkalla S. H, and Triantafillou T. C. (2002). "Fiber reinforced polymer composites for construction-state-of-the-art review". Journal of Composite for Construction, 2: 73-87.

29. Balaguru, P., and Shah, S.P., "Fiber Reinforced Cement Composites," McGraw Hill, New York, 1992.

30. Ballinger, C., Maeda, T., and Hoshijima, T. "Strengthening of reinforced concrete chimneys, columns and beams with carbon fiber reinforced plastics." Fiber Reinforced-Plastic (FRP) Reinforcement for Concrete Structures: Properties and Applications, 233–247.

31. Bambach. M. R, Jama. H. H and Elchalakani. H. H. M, (2009) "Axial capacity and design of thin-walled steel SHS strengthened with CFRP. Thin Walled Structures 47(10): pp. 1112-1121.

32. Baruah, P. and Talukdar, S. (2007), "A Comparative Study of Compressive, Flexural, Tensile and Shear Strength of Concrete with fibres of different origins", Indian Concrete Journal, 81 (7), pp. 17-24.

33. Barros, J. A. O., Dias, S. J. E. and Lima, J. L. T. (2007). "Efficacy of CFRP-based techniques for the flexural and shear strengthening of concrete beams". Cement & Concrete Composites 29, 203–217.

34. Barnes, R., and Fidell, J. (2006). "Performance in fire of small-scale CFRP strengthened concrete beams." Journal of Composites for Construction, 10, 503-508.

35. Bassam A. Tayeha, Abu Bakarb. B. H, Megat Joharib. M. A and Yen Lei Voo. (2013). "Evaluation of Bond Strength between Normal Concrete Substrate and Ultra High Performance Fiber Concrete as a Repair Material" Procedia Engineering 54, 554 – 563.

36. Bazant, Z. P. and Kaplan, M. F. (1996), "Concrete at High Temperature", Material Properties and Mathematical Models. Longman Group Limited, London, pp. 196.

37. Bessey. G. E, (1950) "The visible changes in concrete mortar exposed to high temperatures". Technical paper.No.4: part-II.National Building Studies, HMSO, London.

38. Behnooda, A and Ghandehari, M. (2009) "Comparison of compressive and splitting tensile strength of high-strength concrete with and without polypropylene fibers heated to high temperatures", Fire Safety Journal 44, 1015–1022.

39. Beletti, B., Cerioni, R., Plizzari, G. (2004): "Fracture of SFRC slabs on grade", in 6th Rilem Symposium on Fibre Reinforced Concrete (BEFIB 2004), pp. 723-733.

40. Benmrce, A. and Guenfoud, M. (2005), "Experimental behaviour of high strength concrete column in fire", Magazine of Concrete Research, 57(5), pp. 283-287.

41. Bentur, A., and Mindess, S., (1990). "Fiber Reinforced Cementitious Composites," Elsevier Applied Science, London, UK, 1990

42. Bisby, L A. , Chen, J. F., Li, S. Q., Stratford, T. J. , Cueva, N. and Crossling, K. (2011), "Strengthening fire damaged circular concrete columns with FRP", Journal of Advanced Composites in Construction, Warwick : Net Composites Ltd., pp. 130-141.

43. Bisby, L. A., Green, M. F. and Kodur, V. K. R., (2005), "Modeling the Behavior of Fiber Reinforced Polymer-Confined Concrete Columns Exposed to Fire", ASCE, Journal of Composites for Construction, Vol. 9, No. 1, pp. 15-24.

44. Bisby, L.A., Chen, J.F., Li, S.Q., Stratford, T.J., Cueva, N., Crossling, K., (2011) "Strengthening Fire-Damaged Concrete by Confinement with Fibre-Reinforced Polymer Wraps". Engineering Structures, 33, 3381–3391.

45. Bilotta, A., Ceroni, F., Nigro, E., and Pecce, M. (2011a). "Bond Efficiency of EBR and NSM FRP Systems for Strengthening Concrete Members. Journal of Composites For Construction 757-772.

46. Bilotta, A., Ludovico M. D., Manfredi. G. and Nigro, E. (2011b). "FRP-to-concrete interface debonding: Experimental calibration of a capacity model". Composites: Part B 42 1539–1553.

47. Bizindavyi, L. and Neale, K. W. (1999). "Transfer Length and Bond Strength for Composites Bonded to Concrete, Journal of Composites for Construction, 3(4), 153-160.

48. Blontrock, H., Taerwe, L., and Matthys, S. (1999). "Properties of fiber reinforced plastics at elevated temperatures with regard to fire resistance of reinforced concrete members." 188, 43-54.

49. Blontrock, H., Taerwe, L., and Vandevelde, P. (2000). "Fire tests on concrete beams strengthened with fibre composite laminates." Third PhD Symposium, Vienna, Austria

50. Bonaci, J.F, and Maalej, M., (2000), "Externally bonded FRP for service life extension of reinforced concrete infrastructures", Journal of Infrastructure Systems, ASCE, 6(1), pp 41-51.

51. Bousselham, A., and Chaallal, O. 2004. "Shear strengthening reinforced concrete beams with fiber-reinforced polymer: Assessment of influencing parameters and required research." ACI Structural Journal, 1012, 219–227.

52. BS8110: Part 2: 1985: Structural use of concrete. Part 2: Code of practice for special circumstances, British Standards Institution, London.

53. Buchanan, A. H. (2002) "Structural design for fire safety", John Wiley & Sons, 421pp.

54. Buyukozturk. O and Hearing. B. (1998). "Failure behavior of precracked concrete beams retrofitted with FRP. Journal of Composites for Construction, 2(3): 138-144.

55. Bureau of Indian Standards (2000), "Indian Standard Plain and Reinforced Concrete, Code of Practice, IS 456:2000, (Fourth Revision)", BIS New Delhi, 100pp.

56. Bureau of Indian Standards (2002), "Indian Standard Specification for coarse and fine aggregate from natural sources for concrete, Code of Practice, IS 383:1970, (Reaffirmed 2002)", BIS New Delhi, 21pp.

57. Bureau of Indian Standards (2005), "Indian Standard 43 Grade Ordinary Portland Cement Specification, Code of Practice, IS 8112:1989, First revision, (Reaffirmed 2005)", New Delhi, 8 pp.

58. Bureau of Indian Standards (2008), " Ductile detailing of reinforced concrete structures subjected to seismic forces-Code of practice, IS 13920:1993, (Reaffirmed 2008)", BIS New Delhi, 16pp.

59. Bureau of Indian Standards (2008), "High strength deformed steel bars and wires for concrete reinforcement-specification, IS 1786: 2008, (Fourth revision)", BIS New Delhi, 12 pp.

60. Bureau of Indian Standards (2008), "Non-destructive testing of concrete: Part 1 Ultrasonic pulse velocity, IS 13311(part 1):1992, (Reaffirmed 2008)", BIS New Delhi, 7pp.

61. Bureau of Indian Standards (2008), "Methods of non-destructive testing of concrete: Part 2 Rebound hammer, IS 13311(Part 2):1992, (Reaffirmed 2008)", BIS New Delhi, 5pp.

62. Bureau of Indian Standards (2008), "Methods of physical tests for hydraulic cement: Part 1 Determination of fineness by dry sieving, IS 4031(Part 1):1996, (Reaffirmed 2005)", BIS New Delhi, 4 pp.

63. Bureau of Indian Standards (2008), "Methods of physical tests for hydraulic cement: Part 2 Determination of finesses by specific surface by Blaine air permeability method, IS 4031(Part 2):1999, (Reaffirmed 2008)", BIS New Delhi, 7 pp.

64. Bureau of Indian Standards (2005), "Methods of physical tests for hydraulic cement: Part 3 Determination of soundness, IS 4031(Part 3):1988, (Reaffirmed 2005)", BIS New Delhi, 4pp.

65. Bureau of Indian Standards (2005), "Methods of physical tests for hydraulic cement: Part 4 Determination of consistency of standard cement paste, IS 4031(Part 4):1988, (Reaffirmed 2005)", BIS New Delhi, 2pp.

66. Bureau of Indian Standards (2005), "Methods of physical tests for hydraulic cement: Part 5 Determination of initial and final setting times, IS 4031(Part 5):1988, (Reaffirmed 2005)", BIS New Delhi, 2pp.

67. Bureau of Indian Standards (2005), "Methods of physical tests for hydraulic cement: Part 6 Determination of compressive strength of hydraulic cement (other than masonry cement), IS 4031(Part 6):1988, First revision (Reaffirmed 2005)", BIS New Delhi, 3pp.

68. Bureau of Indian Standards (2005), "Methods of chemical analysis of hydraulic cement, IS 4032:1985, First Revision, (Reaffirmed 2005)", BIS New Delhi, 42pp.

69. Bureau of Indian Standards (2009), "Recommended guidelines for concrete mix design, IS 10262:1982, (Reaffirmed 2009)", New Delhi, 21pp.

70. Bresson. J., (1977). "Application of Steel Plates". pp 42-47.

71. Brühwiler. E. and Denarie, E. (2008). "Rehabilitation of concrete structures using Ultra-High Performance Fibre Reinforced Concrete. The Second International Symposium on Ultra High Performance Concrete, Germany.

72. Campione, G. (2006). "Influence of FRP wrapping techniques on the compressive behavior of concrete prisms". Cement & Concrete Composites 28, pp. 497–505.

73. Castillo, C., and Durani, A.J. (1990). "Effect of transient high temperature on high-strength concrete", ACI Material Journal, 87(1), 47-53.

74. Ceroni, F. (2010). "Experimental performances of RC beams strengthened with FRP materials". Construction and Building Materials 24, 1547–1559.

75. Chakrabarti, S. C. and Jain, A. K. (1999), "Strength properties of concrete at elevated temperature, A review", The Indian Concrete Journal, pp. 495-500.

76. Chaallal, O., Nollet, M. J., and Perraton, D. (1998). "Strengthening of reinforced concrete beams with externally bonded fiber-reinforced-plastic plates: design guidelines for shear and flexure." Canadian Journal of Civil Engineering, 25(4), 692-704.

77. Chaallal. O, Shahawy. M and Hassan. M, (2003). "Performance of axially loaded short rectangular columns strengthened with carbon fibre reinforced polymer wrapping. Journal of Composites for Construction, 7(3): pp. 200-208

78. Chan, S.Y.N., Luo, X. and Sun, W. (2000), "Effect of high temperature and cooling regimes on the compressive strength and pore properties of high performance concrete", Construction and Building Materials Journal, V. 14 pp. 261-266.

79. Chang, Y. F., Chen, Y. H. Shen, M. S. and Yao, G. C. (2006), "Residual stress strain relationship for concrete after exposure to high temperature", Cement and Concrete Research, 36, pp. 1999-2005.

80. Chajes, M. J., Finch, William. W., Januszka, T. F. and Thomson, T. A. (1996). "Bond and Force Transfer of Composite Material Plates Bonded to concrete, ACI Structural Journal, 93(2), 208-217.

81. Chajes, M. J., Thomson, T. A, Januszka, T. F. and William W. F. (1994). "Flexural strengthening of concrete beams using externally bonded composite materials". Construction and Building Materials, 8 (3), pp. 191-201.

82. Chen J. F. and Teng J.G. (2001). "Anchorage Strength Models for FRP and Steel Plates Bonded to Concrete", Journal of Structural Engineering, 127, (7), 784-791.

83. Chen J. F, Pan W. K. (2006). "Three dimensional stress distribution in FRP-to-concrete bond test specimens. Construction and Building Materials. 20(1-2): 46-58

84. Chen, J. F., and Teng, J. G. (2003). "Shear capacity of FRP-strengthened RC beams: FRP debonding." Construction and Building Materials, 17(1), 27-41.

85. Cheng, F. P., Kodur, V. K. R. and Wang, T. C. (2004), "Stress Strain curves for high strength concrete at elevated temperatures", Journal of Materials in Civil Engineering ASCE, 16(1), pp. 84-90.

86. Cho. T. L, Chih. C. H, Chun. Y.C and Chun. C. M, (2005) "Tracking concrete strength under variable high temperature", ACI Material Journal 102(5), pp. 322-329.

87. Chowdhury, E. U., Bisby, L. A., Green, M. F., and Kodur, V. K. R. (2008). "Residual behaviour of fire-exposed reinforced concrete beams prestrengthened in flexural with fiber-reinforced polymer sheets". Journal of Composites for Construction, 12(1): 61-68

88. Chowdhury, E. U. Bisby L. A. Green, M. F., and Kodur, V. K. R. (2007b). Investigation of insulated FRP-wrapped reinforced concrete columns in fire. Fire Safety Journal, 42(6-7): 452-460

89. Cioni, P., Croce, P. and Salvatore, W., (2001), "Assessing fire damage to r.c. elements", Fire Safety Journal, V. 36, pp. 181-199.

90. Cusson, D. and Paultre, P. (1994), "High strength concrete columns confined by rectangular ties", Journal of Structural Engineering ASCE, 120(3), pp. 783-804.

91. Cusson, D. and Paultre, P. (1995), "Stress-strain model for confined high strength concrete", Journal of Structural Engineering ASCE, 121(3), pp. 468-477.

92. Darwish, M. N. (2000). "Upgrading Reinforced Concrete Columns by Jacketing with Carbon Fiber-Reinforced Plastic (CFRP) Sheets." Special Publication, 193, 488- 502.

93.   Davis.H.S. (1967), "Effect of high-temperature exposure on concrete", Materials Research and Standards, 7(10): pp. 452-459.

94.   Davies, J. M., Wang, Y. C., and Wong, F. M. H. (2004). "Polymer composites in fire". Proceedings of Advanced Composites for Structural Applications in Construction, Guildford, Surrey, UK, 3-17.

95.   De Lorenzis L, Nanni A. (2002). "Bond between near-surface mounted fiber-reinforced polymer rods and concrete in structural strengthening", ACI Structure Journal, 99(2):123-131.

96.   Destrée, X. (2000): "Structural application of steel fibre as princpal reinforcing: conditions - design - examples", proceeding. 6th Int. RILEM-Symposium on Fibre Reinforced Concrete - BEFIB 2000, pp. 328-337.

97.   Demirel, B. and Kelestemur, O. (2010), "Effect of elevated temperature on the mechanical properties of concrete produced with finely ground pumice and silica fume", Fire Safety Journal, V. 45, pp. 385–391.

98.   Denarie. E and Bruhwiler. E. (2006). "Structural Rehabilitations with ultra-High Performance FiberReinforced Concretes. International Journal for Restauration of Building and Monuments, pp.453-467.

99.   Desai, S.B., (1998), "Design of reinforced concrete beams under fire exposure", Magazine of Concrete Research, V. 50, No. 1, pp. 75-83.

100.   Diederichs, U. and Schneider, U. (1981), "Bond strength at high temperatures", Magazine of Concrete Research: 33, 1 15: pp. 75-84.

101.   Diederichs, U., Jumppanes, U. M. and Penttala, V. (1988), "Materials properties of high strength concrete at elevated temperature", Transaction 13th IABSE Congress, Helsinki Finland, pp. 489-494.

102.   DiMaio, A., Giaccio, G. and Zerbino, R. (2002), "Non-destructive tests in the evolution of concrete exposed to high temperature", ASTM Journal Cement, Concrete and Aggregate 24(2), pp58-67.

103.   Di Prisco, M., Plizzari, G., Meda, A., Sorelli, L. (2003): "Application of FRC for long-span prestressed roof girders", in International RILEM Workshop "Test and Design Methods for SFRC: Background and Experiences", pp. 98-107.

104. Dortzbach, J. (1999). "Carbon Fiber Reinforcing Polymers as Negative Moment Reinforcing in Repair of Composite Steel Parking Deck." SP 188, American Concrete Institute.

105. Saadatmanesh, H, Ehsani, M. R., & Jin, L., (1998)."Repair of Earthquake-Damaged RC Columns with FRP Wraps", ACI Structural Journal, 94(2), 206-214.

106. Ehm, C., Schneider, U. and Kordina, K. (1986), "Effect of Bi-axial loading on the high temperature behaviour of concrete", Fire Safety Science, Proceedings of the First international Symposium. pp.281-290.

107. Eid, R., Roy, N., Paultre, P., &Asce, M., (2009), "Normal- and High-Strength Concrete Circular Elements Wrapped with FRP Composites". Journal of Composites for Construction, 13(2), 113-124.

108. El-Hacha, R., Wight, R. G., and Green, M. F. (2001). "Prestressed fibre-reinforced polymer laminates for strengthening structures." Progress in Structural Engineering and Materials, 3(2), 111-121.

109. Elghazouli, A.Y., Cashell, K.A. and Izzuddin, B.A. (2009), "Experimental evaluation of the mechanical properties of steel reinforcement at elevated temperature", Fire Safety Journal, V. 44, pp. 909-919.

110. Elfgren L., and Taljsten. B., (1992). "Externally Bonded reinforced, Bond in Concrete from research to practice. International Conference Organized by CEB, PP 1130 -1134.

111. Eskandari H., Muralidhara S., Raghuprasad B. K., and Venkatarama Reddy B.V., (2010)." Size effect in self consolidating concrete beams with and without notches" Indian Academy of Sciences, Vol. 35, Part 3, pp. 303–317.

112. Eurocode 2, (2004), "Design of concrete structures: Part 1-2: general rules- structural fire design", European Committee for Standardisation, Brussels, BS EN 1992-1-2, 2004.

113. Fahmy, Ezzat H., Shaheen, Youysry B. I. and Korany Y. S. (1997). " Repairing Reinforced Concrete Beams by ferrocement" Journal of Ferrocement: 27,(1), pp 19-32,

114. Faris Ali, Ali Nadjai, Choi S., (2010)."Numerical and experimental investigation of the behavior of high strength concrete columns in fire" Engineering Structures, 32, 1236-1243.

190

115. Farhat, F. A., Nicolaides, D., Kanellopoulos. A. and Karihaloo. B.L. (2007). "High performance fibre-reinforced cementitious composite (CARDIFRC) – Performance and application to retrofitting" Engineering Fracture Mechanics 74, 151–167.

116. Farhat F. A, Nicolaides D, Kanellopoulos A, and Karihaloo B. L (2010). Behaviour of RC Beams Retrofitted with CARDIFRC after Thermal Cycling. Journal of Materials in Civil Engineering, 22.

117. Felicetti, R. (2008), "Recent advances and research needs in the assessment of fire damaged concrete structures", fib workshop on Fire design of concrete structures. Coimbra: in press.

118. Felicetti, R. and Gambarova, P.G. (1998), "Effects of high temperature on the residual compressive strength of high strength siliceous concretes", ACI Materials Journal, V. 95, No. 4, July-August 1998, pp. 395-406.

119. FEMA (2000), "Pre-standard and commentary for the Seismic rehabilitation of buildings / FEMA 356, 2000, Chapter 1: Rehabilitation Requirements", Table C1-3, pp. 14.

120. FEMA 356 (2000), "Prestandard and commentary for the seismic rehabilitation of buildings," 518pp.

121. Fitiany, S.F.E and Youssef, M.A., (2009), "Assessing the flexural and axial behaviour of reinforced concrete members at elevated temperatures using sectional analysis", Fire Safety Journal, V. 44, pp. 691–703.

122. Fletcher, I. A., Welch, S., Terero, J. L., Carvel, R. O. and Usmani, A. (2007), "The Behaviour of concrete Structures in Fire", Journal of Thermal Science, V. 11 (2), pp.33-57.

123. Foster, S. J. (1999), "Design and detailing of high strength concrete columns", Research report No. R-375, March, University of New South Wales, Sydney, Australia.

124. Foster, S. J., Liu, J. and Sheikh, S. A. (1998), "Cover spalling in HSC columns loaded in concentric compression", Journal of Structural Engineering ASCE, 124(12), pp 1431-1437.

125. Franssen, J.-M. (2005), "Structures in Fire, Yesterday, Today and Tomorrow", Proceedings, 8th Int. Symp. Fire Safety Science, Beijing, China, pp. 21-35.

126. Freskakis, G.N. (1980), "Behaviour of reinforced concrete at elevated temperatures", Paper 3-4, Second ASCE conf. on Civ. Eng. And nuclear power, Vol. 1, Paper 3-5, pp. 3-5-1 to 3-5-21, Knoxville, Tennessee.

127. Freskakis, G.N. et al., (1979), "Structural Properties of Concrete of Concrete at Elevated Temperature", Civil Engineering Nuclear Power, Vol. 1, ASCE Natl. Convention, Boston April 1979.

128. Fu, Y. F., Wong, Y. L. Poon, C. S. and Tang, C. A. (2005), "Stress–strain behaviour of high-strength concrete at elevated temperatures", Magazine of Concrete Research, 57(9), pp. 535–544.

129. Fu, S., Ide, M. and Sato, H., (1992). "A Study on Measurement of Degree of Fire-Damage in Concrete by Ultrasonic Method" (in Japanese), Meeting for Reading Research Papers of JAFSE, pp.54-57.

130. Galal. K, Arafa. A and Ghobarah. A, (2005), "Retrofit of RC square short columns". Engineering Structures, 27(5): pp. 801-817.

131. Galal, K. and Mofidi, A. (2010). "Shear Strengthening of RC T-Beams Using Mechanically Anchored Unbonded Dry Carbon Fiber Sheets". Journal of Performance Of Constructed Facilities. 24(1), 31–39

132. Georgali, B. and Tsakiridis, P.E. (2005), "Microstructure of fire-damaged concrete" Cement and Concrete Composite, 27 pp, 255-9.

133. Ghan, Y. N., Peng, G. F., Anson, M. (1999), "Residual strength and pore structure of high-strength concrete and normal strength concrete after exposure to high temperatures, Cement and Concrete Composites, 21, pp. 23-27.

134. Ghandehari, M. Behnood, A. and Khanzadi, M., (2010) "Residual Mechanical Properties of High-Strength Concretes after Exposure to Elevated Temperatures", Journal of Materials in Civil Engineering, Vol. 22, No. 1, pp. 59-64.

135. Ghobarah. A, Galal. K. E, (2004). "Seismic rehabilitation of short rectangular RC columns. Journal of Earthquake Engineering (JEE). 8(1):45-68.

136. Giroldo F. and Bailey, C. G. (2008), "Experimental bond behaviour of welded mesh reinforcement at elevated temperatures", Magazine of Concrete Research, 60, No. 1, February, 23–31.

137. Guo. Z. G.,Cao. S. Y., Sun. W. M. and Lin X. Y. (2005).” Experimental Study on Bond Stress-Slip Behaviour Betweenfrp Sheets and Concrete”. Proceedings of the International Symposium on Bond Behaviour of FRP in Structures. pp 77-85.

138. Gao, W. Y., Teng, J. G., and Dai, J. G. (2012). “Effect of temperature variation on the full-range behavior of FRP-to-concrete bonded joints”, Journal Composite Construction. 16(6), 671 –683.

139. Gao, W. Y., Teng, J. G., and Dai, J. G. (2013). “Bond - Slip Model for FRP Laminates Externally Bonded to Concrete at Elevated Temperature” Journal of Composites for Construction. 17(2). 217-228.

140. Gao, B., Kim, J. K., and Leung, C. K. Y. (2006). “Strengthening efficiency of taper ended FRP strips bonded to RC beams”. Composites Science and Technology 66, 2257–2264.

141. Shahrooz, B. M., and Boy, S. (2004). "Retrofit of a Three-Span Slab Bridge with Fiber Reinforced Polymer Systems—Testing and Rating." Journal of Composites for Construction, 8, 241-247.

142. Green, M. F., Bisby, L. A., Beaudoin, Y., and Labossière, P. (2000). "Effect of freeze thaw cycles on the bond durability between fibre reinforced polymer plate reinforcement and concrete." Canadian Journal of Civil Engineering, 27(5), 949- 959.

143. Green, M. F., Kodur, V. K. R., and Bisby, L. A., (2006). "FRP retrofitted concrete under fire conditions." Concrete International, 28(12), 37-44

144. Grace, N. F. (2001). "Strengthening of negative moment region of reinforced concrete beams using carbon fiber-reinforced polymer strips." ACI Structural Journal, 98(3), 347-358.

145. Grace, N. F., Sayed, G. A., Soliman, A. K., and Saleh, K. R. (1999). "Strengthening reinforced concrete beams using fiber reinforced polymer (FRP) laminates." ACI structural Journal, 96(5), 865-874.

146. Green, J. K., (1971). “Reinstatement of Concrete Structures After Fire, (Part 1),”The Architects’ Journal, 14, pp. 93-99.

147. Gustavo J. Parra-Montesinos. (2005). “High-Performance Fiber-Reinforced Cement Composites: An Alternative for Seismic Design of Structures”. ACI Structural Journal, 102, 5, pp 667-675.

148. Haddad, R H, Al-Rousan. R. and Almasry. A., (2013). "Bond-slip behavior between carbon fiber reinforced polymer sheets and heat-damaged concrete." Composites: Part B 45, 1049–1060.

149. Haddad, R H, Shannag, M. J., and Hamad, R. J., (2011), "Repair of heat-damaged reinforced concrete T-beams using FRC jackets". Magazine of Concrete Research, 59 (3), 223-231.

150. Haddad, R H, Al-mekhlafy, N., and Ashteyat, A. M., (2011), "Repair of heat-damaged reinforced concrete slabs using fibrous composite materials". Construction and Building Materials, 2011, 25(3), 1213-1221.

151. Haddad, Rami H, and Shannag, M. J., (2008), "Repair of heat-damaged RC shallow beams using advanced composites". Materials and Structures, 2008, 287-299.

152. Haddad, R. H., Al-Saleh, R. J. and Al-Akhras, N. M. (2008), "Effect of elevated temperature on bond between steel reinforcement and fibre reinforced concrete", Fire Safety Journal, 43, pp. 334–343.

153. Hamid Eskandari, Muralidhara S, Raghu Prasad B.K., Venkatarama Reddy B.V. (2012) "Fracture properties of Self Compacting Concrete for Notched and Un-notched Beams" . Global Journal of researches in engineering Civil and Structural engineering. 12 (1).

154. Hanan Al-Nimry, Rami Haddad. Saad Afram., Mohammed Abdel-Halim. (2013). "Effectiveness of advanced composites in repairing heat-damaged RC columns". Materials and Structures.

155. Handoo, S.K, Agarwal, S. and Agarwal, S.K. (2002), "Physicochemical, mineralogical, and morphological characteristics of concrete exposed to elevated temperatures", Cement Concrete Research, 32 pp.1008-18.

156. Harmathy.T.Z and Berndt.J.E, (1966), "Hydrated Portland Cement and lightweight concrete at elevated temperatures". ACI, Structural Journal, 63(1), 93-112.

157. Harada. T, Takeda. J, Yamane. S and Furumura. F, (1972) "Strength, elasticity, and thermal properties of concrete subjected to elevated temperatures", ACI Structural Journal 34(SP34-21), pp. 377-406.

158. Harries. K .A and Carey. S. A, (2003), "Shape and gap effects on the behaviour of variably confined concrete. Cement and Concrete Research, 33(6): p. 881-890.

194

159. Hertz, K. D. (2003), "Limits of spalling of fire exposed concrete", Fire Safety Journal, 38, pp. 103-116.

160. Hertz, K. D. (2004), "Reinforcement data for fire safety design", Magazine of Concrete Research, 56(8), pp. 455-459.

161. Hertz, K. D. (2005), "Concrete strength for fire safety design", Magazine of Concrete Research, 57(8), pp. 445-453.

162. Hong, K. N., Han, S. H. and Tac-Yi, S. (2006), "High strength concrete column confined by low volumetric ratio lateral ties", Engineering Structure, 28, pp. 1346-1353.

163. Hota GangaRao, V.S. and Vijay, P.V. (1998). "Bending Behavior of Concrete Beams Wrapped with Carbon Fabric", Journal of Structural Engineering, ASCE, 124(1), 3-9.

164. Hosseini. A, Ali. R. K and Fadaee. S, (2005), "Seismic performance of high strength concrete square columns confined with carbon fibre reinforced polymers. Canadian Journal of Civil Engineering, 32(3): 569-578.

165. Huang, Z. (2010), "The behaviour of reinforced concrete slabs in fire", Fire Safety Journal V. 45, pp. 271–282.

166. Iyer S. L., Sivaramakrishnan C. and Amaram., (1989)." Testing of reinforced concrete bridges for external reinforcement. Structural Materials and Structures Conference pp 116-122.

167. Ilki, A., Peker, O., Karamuk, E., Demir, C., and Kumbasar, N., (2008). "FRP Retrofit of Low and Medium Strength Circular and Rectangular Reinforced concrete columns". Journal of Material Civil Engineering. 20(2), 169–188.

168. Ivy Fung-yuen Ho, Eddie Siu-shu Lam; Bo Wu; and Ya-yong Wang. (2013)." Monotonic Behavior of Reinforced Concrete Columns Confined with High-Performance Ferrocement" Journal of Structural Engineering, 139 (4) 574–583.

169. Jeyasehar, C. A. and Vidivelli, B. (2006). "Behaviour of RC Beams Rehabilitated with Ferrocement Laminates". Proceedings of the Eighth International Symposium and Workshop on Ferrocement and Thin Reinforced Cement Composites.

170. Jeongwon, Ko Researcher, Dongwoo Ryu and Takafumi Noguchi, (2011), "The spalling mechanism of high- strength concrete under fire", Magazine of Concrete Research, 2011, 63(5), 357–370.

171. Jiang-Tao Yu, Yuan Liu, Zhou-Dao Lu and Kai Xiang. (2012). "Flexural performance of fire damaged and rehabilitated two span reinforced concrete slabs and beams", Structural Engineering and Mechanics, 42(5), pp 1-15.

172. Jones, P., Swamy, R.N., and Charif, A., (1988), "Plate Separation and anchorage of reinforced concrete beams strengthened by epoxy-bonded-steel plates", The Structural Engineer, 66 (5), 85-94.

173. Kabhari, V. M., Engineer, M.M., and Eckel, D.A., (1997), "On durability of composites rehabilitation schemes for concrete: Use of peel test" Journal of Material and Science, 32(1), pp 147-156.

174. Kachlakev, D., and McCurry, D. D. (2000). "Behavior of full-scale reinforced concrete beams retrofitted for shear and flexural with FRP laminates." Composites Part B: Engineering, 31(6-7), 445-452.

175. Kai Xiang, Guohui Wang, Weiping Han, and Jiangtao Yu. (2011). "Moment Redistribution of Two-span Fire-damaged Reinforced Concrete T-Beams Strengthened with CFRP Sheets". Advanced Materials Research 255-260, pp 399-409.

176. Khan, S.U., Rafeeqi, S. F. A. and Ayub, T. (2013). "Strengthening of RC Beams In Flexure Using Ferrocement" IJST, Transactions of Civil Engineering, 37, pp 353-365

177. Kaptijn, N. (2004): "A new bridge deck for the Kaag bridges: the first CRC application in cibil infrastructure", 1st Int. Symp. on Ultra High Performance Concrete, pp. 49-59.

178. Kaushik S, Prakash A, Singh A., (1990)," Inelastic Buckling of Ferrocement Encased Columns. In: Proceedings of the Fifth International Symposium on Ferrocement", 327–41.

179. Kaushik, S. K. and Dubey, A. K. (1994). "Performance Evaluation of RC Ferrocement Composite Beams" Proceedings of Fifth International Symposium, UMIST, pp 240- 256.

180. Kazemi, M. T, Morshed, R (2005), "Seismic Shear Strengthening of R/C Columns with Ferrocement Jacket", Cement & Concrete Composites, 27: 834–842.

181. Klamer, E. L., D. A. Hordijk and C. S. Kleinman (2006) "Debonding of CFRP laminates externally bonded to concrete specimens at low and high temperatures' in Mirmiran, A. and Nanni, A. (Eds.) Third International Conference on FRP Composites in Civil Engineering (CICE 2006), pp. 35-38.

182. Klamer, E. L., Hordijk, D. A., and Hermes, M. C. J. (2008). "The influence of temperature on RC beams strengthened with externally bonded CFRP reinforcement." Heron, 53(3), 157 –185.

183. Klamer, E. (2009). "Influence of temperature on concrete beams strengthened in flexure with CFRP." Ph.D. thesis, Eindhoven Universityof Technology, Eindhoven, Netherlands.

184. Kent, D. C. and Park, R. (1971), "Flexural members with confined concrete", Journal of Structural Division. ASCE, 97, pp.1969-1990.

185. Khalifa, A., Gold, W. J., Nanni, A., and Aziz, A. (1998). "Contribution of externally bonded FRP to shear capacity of flexural members." ASCE Journal of Composites for Construction, 2(4), 195-203.

186. Khalifa, A.; Alkhradaji, T.; Nanni, A.; and Lansburg, S. (1999). "Anchorage of Surface Mounted FRP Reinforcement," Concrete International, ACI.

187. Khoury, G. A. (1992), "Compressive strength of concrete at high temperature", A Reassessment Magazine of Concrete Research, 44(161), pp. 291-309.

188. Khoury, G. A., Majorona C. E., Pesavento, F. and Schrefler B. A. (2002), "Modeling of heated concrete", Magazine of Concrete Research, 54(2), pp. 77-101.

189. Khoury, G. A. (2000), "Effect of Fire on Concrete and Concrete Structures", Progress in Structural Engineering and Materials, 2(4) pp. 429-447.

190. Khoury, G. A. and Anderberg, Y. (2000), "Concrete spalling review", A report on Fire Safety Design, Swedish National Road Administration

191. Khoury, G. A., Grainger, B. N. & Sullivan, P. J. E., (1985), "Transient thermal strain of concrete: literature review, conditions within specimen and behaviour of individual constituents", Magazine Concrete Research, 37 (132), pp. 131-144.

192. Khoury, G.A., Majorana, C.E., Pesavento, F., and Schrefler, B.A. (2002). "Modelling of heated concrete", Magazine of Concrete Research, 54(2), pp. 77-101.

193. Klaiber F.W., Dunker. K. F., Wipf T. J. And Sanders W. W., (1987). "Method of strengthening existing highway bridges. Transportation Research Board, Washington, 16.

194. Kim, G. Y., Kim, Y. S. and Lee, T. G. (2009), "Mechanical properties of high strength concrete subjected to high temperature by stressed method", Transactions Nonferrous Metals Society of China, 19, pp. 128-133.

195. Kishor S Kulkarni, Subhash C. Yaragal and K S Babu Narayan., (2011) "Effect of elevated temperatures on mechanical properties of micro -cement based high performance concrete" International Journal of Applied Engineering and Technology, 1 (1) pp. 24-31.

196. Kodur V.K.R. and Dwaikat, M.B., (2008), "Effect of Fire Induced Spalling on the Response of Reinforced Concrete Beams", International Journal of Concrete Structures and Materials Vol.2, No.2, pp. 71-81.

197. Kodur, V. K. R. and Sultan, M. A. (1998), "Structural behaviour of high strength concrete columns exposed to fire NRCC-41736", National Research Council Canada.

198. Kodur, V. K. R., Cheng, F. P., Wang, T. C. and Sultan, M. A. (2003), "Effect of strength and fibre reinforcement on fire resistance of high strength concrete columns", Journal of Structural Engineering, 129(2), pp. 253-259.

199. Kodur, V. K. R., Dwaikat, M. B. and Fike, R. S., (2010), "An approach for evaluating the residual strength of fire-exposed RC beams", Magazine of Concrete Research, V. 62, No. 7, pp. 479–488.

200. Kodur, V.K.R., Bisby, L. A. and Green, M. F., (2006), "Experimental evaluation of the fire behaviour of insulated fibre-reinforced-polymer-strengthened reinforced concrete columns", Fire Safety Journal, V. 41, pp. 547–557.

201. Kodur, V. K. R., Bisby, L. A., and Green, M. F. (2006). "FRP retrofitted concrete under fire conditions." Concrete International, 28(12), 37-44.

202. Komarovskii.A.N, (1965), "Design of Nuclear Plants", 2nd edition.

203. Kondraivendhan, B., & Pradhan, B., (2009), "Effect of ferrocement confinement on behavior of concrete. Construction and Building Materials, 23(3), 1218-1222.

204. Kumar, R. and Bhattacharjee, B. (1995), "Systematic assessment of extent of damage and residual strength of Fire affected building structures", Proceedings of the National Conference on Civil Engineering. Material and Structures, Jan 19-21, Osmania University Hyderabad, India, pp. 476-487.

205. Kumutha, R., Vaidyanathan, R., Palanichamy, M.S., (2007), "Behaviour of Reinforced Concrete Rectangular Columns Strengthened using GFRP". Cement & Concrete Composites, 29, 609–615.

206. Lamont, S., Usmani, A.S. and Gillie, M., (2004), "Behaviour of a small composite steel frame structure in a long-cool and a short-hot fire", Fire Safety Journal, V. 39(5), pp. 327–357.

207. Lam,L., and Teng, J. G.(2003). "Design –Oriented Stress-Strain Model for FRP Confined Concrete". Construction and Building Materials, 17, 471-489.

208. Lan, Y. M., SoteIino, E. D., and Chen, W. F. (1998). "State-of-the-art Review of Highway Bridge Columns Retrofitted with FRP Jackets." Structural Engineering Rep. No. CE-STR-98-5.

209. Lankard, D. R, Birkimer, D. L, Fondriest. F and Snyder, M. J. (1971), "Effects of moisture content on the structural properties of Portland Cement Concrete exposed to temperatures up to 500F". American Concrete Institute, Detroit, 25(SP25-03), 59-102.

210. Laskar A. I, Talukdar S (2008), " A new mix design method of high performance concrete", Asian Journal of Civil Engineering, 9, 1, pp 31- 39.

211. Lee, J.S., Xi, Y., and Willam, K. (2008) "Properties of Concrete after High Temperature Heating and Cooling", J. of Materials, ACI, July-Aug. 105(4), 334-341.

212. Legeron, F. and Paultre, P. (2003), "Uniaxial confinement model for normal and high strength concrete columns", Journal of Structural Engineering ASCE, 29(2), pp. 241-252.

213. Leonardi, A., Meda, A., & Rinaldi, Z., (2011), "Fire-damaged R / C Members Repair With High-Performance Fibre-Reinforced Jacket. Stress": The International Journal on the Biology of Stress, 47, 28-35.

214. Leone, M., Matthys, S., and Aiello, M. A. (2009). "Effect of elevated service temperature on bond between FRP EBR systems and concrete." Composite. Part B: Engineering., 40(1), 85 –93.

215. Lerchental H., (1967). "Bonded sheet metal reinforcement for concrete slab." Bullentin in Rilem No. 37, pp 263-269.

216. Lerchental H., and Rosenthal I., (1982). "Flexural behavior of concrete slab reinforced with steel sheet." Materiaux et Construction , 15(88), pp 279-282.

217. Li L. and Purkiss, J. A. (2005), "Stress–strain constitutive equations of concrete material at elevated temperatures", Fire Safety Journal, 40, pp. 669-86.

218. Li, M., Qian, C. and Sun, W. (2004), "Mechanical properties of high-strength concrete after fire", Cement and Concrete Research, 34, pp. 1001-1005.

219. Lie, T. T. (1992). "Structural fire protection", New York American Society of Civil Engineers.

220. Lorenzis, L. De., Miller, B., and Nanni, A. (2001). "Bond of Fiber-Reinforced Polymer Laminates to Concrete", ACI Material Journal, 98(3), 256-264.

221. Luca, A. D., Asce, M., Nardone, F., Matta, F., Asce, A. M., Nanni, A., Asce, F., et al.,(2011), "Structural Evaluation of Full-Scale FRP-Confined Reinforced Concrete Columns". Journal of Composites for Construction, 15(1), 112-123.

222. Lu X .Z. Jiang. J.J., Teng J. G. and Ye. L. P. (2006). "Finite element simulation of debonding in FRP-to-concrete bonded joints" Construction and Building Materials 20, 412–424.

223. Maeda, T., Asano, Y., Sato, Y., Ueda, T., and Kakuta, T., (1997). "A Study on Bond Mechanism of Carbon Fiber Sheet", Non-Metallic (FRP) Reinforcement for Concrete Structures, 3 rd International Symposium, 1, pp. 279-286.

224. Macdonald M. D. and Calder A. J. J., (1982). "Bonded steel plating for strengthening concrete structures, International journal of Adhesion and Adhesives, 2(2), pp 119-127.

225. Manuel A.G. Silva. (2011). "Behavior of square and circular columns strengthened with aramidic or carbon fibers" Construction and Building Materials

226. Martinola, G., Meda, A., Plizzari, G. A., & Rinaldi, Z., (2010),"Strengthening and Repair of RC Beams with Fiber Reinforced Concrete". Cement and Concrete Composites, 2010, 32(9), 731-739.

227. Martinola G, Meda A, Plizzari GA, Rinaldi Z. (2007). "Strengthening of R/C beams with high performance fiber reinforced cementitious composites. HPFRCC 5 – high performance fiber reinforced cement composites. pp. 389–98.

228. Malhotra, H. L. (1956), "The effect of on the compressive strength of concrete", Magazine of Concrete Research (London) 8, pp. 85-94.

229. Malhotra, H. L. (1982), "Design of fire-resisting structures", London, Surrey University Press.

230. Mander, J. B., Priestly, M. J. N. and Park, R. (1988), "Theoretical stress-strain model for confined concrete", Journal of Structural Engineering ASCE, 114(8), pp. 1804-1826.

231. Mander, J.B., Priestly, M.J.N. and Park, R. (1988), "Observed stress-strain behaviour of confined concrete", Journal of Structural Engineering ASCE, 114(8), pp. 1827-1849.

232. Mansur, M.A., and Paramasivam, P., (1985). "Ferrocement Under Combined Bending and Axial Loads," International Journal of Cement Composites and Lightweight Concrete, 7(3), pp. 151-158.

233. Mansur, M.A., and Paramasivam, P., (1990), "Ferrocement Short Columns under Axial and Eccentric Compression", ACI Structural Journal, 87(5): 523-529.

234. Mayo, R., Nanni, A., Gold, W., Barker, M., and Rolla, M. O. (1999). "Strengthening of Bridge G270 with externally-bonded CFRP reinforcement." SP-188, American Concrete Institute, Proc., 4th International Symposium on FRP for Reinforcement of Concrete Structures (FRPRCS4).

235. Markovic, I. (2006). "High-Performance Hybrid-Fibre Concrete", PhD thesis, New Delft University

236. Mazzotti C, Savoia M, Ferracuti B. (2008). "An experimental study on delamination of FRP plates bonded to concrete. Construction and Building Materials, 22(7): 1409-1421.

237. Mazzotti C, Savoia M, Ferracuti B. (2009). "A new single-shear set-up for stable debonding of FRP–concrete joints". Construction and Building Materials 23, 1529–1537

238. Meda. A, Plizzari. G. A, Rinaldi. Z. and Martinola G, Strengthening of R/C existing columns with high performance fiber reinforced concrete jacket". Concrete Repair, Rehabilitation and Retrofitting II. pp 1263-1269.

239. Mehmet BurhanKarakoc., (2013) "Effect of cooling regimes on compressive strength of concrete with lightweight aggregate exposed to high temperature. Construction and Building Materials, 41, 21–25.

240. Michael, Y. L. Chew. (1993). "The Assessment of Fire Damaged Concrete" Building and Environment, 28(1), pp. 97-102.

241. Mirmiran. A, Shahawy. M, Samaan. M, Echary. H. E, Mastrapa. J. C and Pico. O, (1998). "Effect of column parameters on FRP confined concrete. Journal of Composites for Construction, 2(4):175-185.

242. Mohamedbhai, G. T. G. (1986), "Effect of exposure time and rate of heating and cooling on residual strength of heated concrete", Magazine of Concrete Research, 38(136), pp. 151-158

243. Mohamedbhai, G. T. G., (1982), "Residual strength of reinforced concrete members subjected to elevated temperatures", Proc.Instn Civ. Engrs., Part 2, V. 73, pp. 407-420.

244. Monti. G, Liotta. M. A, (2007). "Tests and design equations for FRP-strengthening in shear". Construction and Building Materials, 21 (4), pp. 799-809.

245. Morley, P. D. and Royles, R., (1979/80), "The Influence of High Temperature on the Bond in Reinforced Concrete", Fire Safety Journal, 2 pp. 243 – 255.

246. Monal S Rao, Subhash C. Yaragal, Kiran Sara Chacko, Nivedita G and Babu Narayan K.S. (2012) "Studies on elevated temperatures and quenching effects on blended concretes" International Journal of Applied Engineering and Technology, 1 (1), pp. 48-60.

247. Mourad, S. M., & Shannag, M. J., (2012), "Repair and strengthening of reinforced concrete square columns using ferrocement jackets". Cement and Concrete Composites, 34(2), 288-294.

248. Muhammad Masood Rafi, Ali Nadjai, Faris Ali, Didier Talamona.(2008) "Aspects of behaviour of CFRP reinforced concrete beams in bending" Construction and Building Materials 22, 277–285.

249. Mutairi, N. M. A. and M. S. A., Shaleh, (1997), "Assessment of Fire-Damaged Kuwaiti Structures", ASCE, Jourrnal of Materials in Civil Engineering, 9, I, pp. 7-14.

250. Nasser, K. and Al - Manaseer, A., (1987). "Comparison of Nondestructive Testers of Hardened Concrete", ACI Material Journal, pp.374-380.

251. Nasser. K. W and Lothia. R. P., (1971), "Mass concrete properties at high temperatures", ACI Structural, 68(3): pp. 180-188.

252. Naaman, A. E. High Performance Fiber Reinforced Cement Composites : Classification and Applications CBM-CI International Workshop, Karachi, Pakistan, 389-401.

253. Nakaba, K., Kanakubo, T., Furuta, T., and Yoshizawa, H. (2001). "Bond Behavior between Fiber-Reinforced Polymer Laminates and Concrete, ACI Structural Journal, 98(3), 359-167.

254. Narendra. K. Gosain., Ray. F. Drexler and Dilip Chodhuri, (2008). "Evaluation and Repair of Fire-Damaged Buildings", Structure Magazine pp 18-22.

255. Nassif. M. K, Bandyopadhyay. K. K and Reich. M, (1996), "Thermal degradation of concrete in the temperature range from ambient to 315°C", United States Department of Emergency report, Washington D.C October, 1996.

256. Nassif.A, (2006), "Post fire full stress-strain response of fire-damaged concrete" Fire and Materials, 30, 323-332.

257. Nassif, H. H, and Najm H, (2003), "Experimental and analytical investigations of ferrocement composite beams", Cement & Concrete Composites article pp. 182-187

258. Nedwell P, Ramesht M, Rafei-Tanhanaki S., (1990), "Investigation into the Repair of Short Square Columns Using Ferrocement". In: Proceedings of the Fifth International Symposium on Ferrocement, 1990, 277–85.

259. Neale, K. (2001). "Strengthening Reinforced Concrete Structures with Externally Bonded Fibre Reinforced Polymers. Design Manual No. 4." ISIS Canada.

260. Omar. C, Munzer, H and Michel , (2006). "Circular Columns Confined with FRP: Experimental versus Predictions of Models and Guidelines". Journal of Composites for Construction, 10(1), pp4-12.

261. Ozawa. M, Uchida S., Kamada T., Morimoto H. (2012) "Study of mechanisms of explosive spalling in high-strength concrete at high temperatures using acoustic emission". Journal of Construction & Building Materials, 37, 621-628.

262. Ozawa M., Lustoza D.R., Morimoto H., Fumoto F., (2011). "Permeability of High Strength Concrete with different Fibers at High Temperature" 2nd International RILEM Workshop on Concrete Spalling due to Fire Exposure. pp 281-288.

263. Ozawa M , H. Morimoto. (2010) "High-Strength Concrete Reinforced Jute Fiber and Water-Soluble PVA Fiber under High Temperature, Proceeding of Sixth International Conference on Structures in Fire, 864-871, Michigan (USA).

264. Panda, K. C., Bhattacharyya, S. K., and Barai, S. V. (2011a), "Optimization study of RC T-beams strengthened in shear with side bonded GFRP sheet" International Journal of Earth Sciences and Engineering (IJEE),4(6):801-804.

265. Panda, K. C., Bhattacharyya, S. K., and Barai, S. V. (2011b). "Strengthening of RC T-beams with shear deficiencies using GFRP strips." Journal of Civil Engineering and Architecture,5, 1, pp. 56-67.

266. Park, R., Priestly, M. J. N. and Gill, W. D. (1982), "Ductility of square confined concrete columns", Journal of Structural Division ASCE, 108(4), pp. 929-951.

267. Paramasivam, Ong, K. C. G. and Lim, C. T. E., (1994). "Ferrocement Laminate for Strengthening of RC T-Beams" Cement and Concrete Composite, 16, pp 143-152,

268. Pautre, P., Eid, R., Langlois, Y. and Levesque, Y. (2010), "Behaviour of Steel fibre reinforced high strength concrete columns under uni-axial compression", Journal of Structural Engineering ASCE, 136(10), pp. 1225-1235.

269. Peng, G. F. (2000), "Evaluation of fire damage to high performance concrete", Ph.D. Thesis, Departments of Civil Engineering and Structural Engineering, The Hong Kong Polytechnic University Hong Kong, pp.213.

270. Peng, G. F., Bian, S. H., Guo, Z. Q., Zhao, J., Peng, X. L. and Jiang, Y. C. (2008), "Effect of thermal shock due to rapid cooling on residual mechanical properties of fibre concrete exposed to high temperatures", Construction and Building Materials 22, pp. 948-955.

271. Peng, G. F., Bian, S. H., Zhao, Z. L., and Yl, Q. X. (2006), "Effect of Cooling Regimes on Mechanical Properties of Fibre-Toughened High-Performance Concrete", Key Engineering Materials, pp.603-609.

272. Pellegrino, C., and Modena, C. (2002). "Fiber reinforced polymer shear strengthening of reinforced concrete beams with transverse steel reinforcement." Journal of Composites for Construction, 6, 104.

273. Phan L.T., Carino N.J., (1998), "Review of mechanical properties of HSC at elevated temperature," ASCE J Mater Civil Eng, 10(1):58-64.

274. Phan, L. T. and Carino, N. J. (1998), "Review of mechanical Properties of high strength concrete at elevated temperature", Journal of Materials in Civil Engineering ASCE, 10(1), pp. 58-64.

275. Phan, L. T. and Carino, N. J. (2002), "Effects of test conditions and mixture proportions on behaviour of high-strength concrete exposed to high temperatures", ACI Materials Journal, 99 (1), pp. 54–66.

276. Phan, L.T. (1996). "Fire performance of high-strength concrete: A report of the state-of-the art, Building and Fire Research Laboratory", National Institute of Standards and Technology, NISTIR 5934, Maryland, Dec.

277. Phani Prasad, D. M. S., Sharma, U. K. and Bhargava, P. (2009), "Effect of elevated temperature on the properties of reinforcing steel bar", Journal of the Institution of Engineers (India), 99, Nov 2009, pp. 3-6.

278. Poon, C. S., Shui, Z. H. and Lam, L. (2004), "Compressive behaviour of fibre reinforced high-performance concrete subjected to elevated temperatures", Cement and Concrete Research, 34, pp. 2215-2222.

279. Purkiss, J. A. and Dougill, J. W. (1973), "Apparatus for compression tests on concrete at high temperatures", Magazine of Concrete Research, 25(83), pp. 102-108.

280. Quiertant, M. and Clement, J. L., (2011). "Behavior of RC columns strengthened with different CFRP systems under eccentric loading" Construction and Building Materials, 25, pp.452–460.

281. Rafi, M. M., Nadjai, A. and Ali, F., (2008), "Finite Element Modeling of Carbon Fiber-Reinforced Polymer Reinforced Concrete Beams under Elevated Temperatures", ACI Structural Journal, V. 105, No. 6, pp.701-710.

282. Raju, M. P., Rao, K. S. and Raju, P. S. N. (2007), "Compressive strength of heated high strength concrete", Magazine of Concrete Research, 59(2), pp. 79-85.

283. Ramkrishna Dandapat, Arghya Deb and Bhattacharyya, S. K. (2012) "Localised failure in Fibre-Reinforced-Polymer wrapped cylindrical concrete columns" Journal of ACI, Structural Engg., 109, Issue.4.

284. Raut, N. K. and Kodur, V. K. R., (2011), "Response of High-Strength Concrete Columns under Design Fire Exposure", ASCE, Journal of Structural Engineering, 137, 1, pp. 69-79.

285. Rathish Kumar. P, Oshima, T, Mikami S. and Yamazaki, T. (2007), "Studies n RC and Ferrocement Jacketed Columns Subjected to Simulated Seismic Loading", Asian Journal of Civil Engineering 8(2): 215-225.

286. Rathish Kumar. P, Rao C. B. K. (2006). "Constitutive behavior of high-performance ferrocement under axial compression. Magazine Concrete Research, 58(10), 647–56.

287. Raithby. K. D, (1982). "Strengthening of concrete bridges decks with epoxy bonded steel plates. International journal Adhesion and adhesives, pp 115-118.

288. Reddy D. V. Sobhan. K. and Young. J. (2006). "Effect Of Fire On Structural Elements Retrofitted By Carbon Fiber Reinforced Polymer Composites". 31st Conference On Our World In Concrete & Structures.

289. Repair of concrete structures with reference to BS EN 1504. The Concrete Society: Technical Report No.69.

290. Reparability of fire damaged structures CIB W14 Report. Fire Safety Journal, 1990, 16(4), pp. 251-336.

291. Rennesund K. E. and Halden J., (1985). "Strengthening of bridges by glued steel plates. pp 48.

292. Rini, D. and Lamont, S., (2008), "Performance Based Structural Fire Engineering for Modern Building Design", ASCE, Structures 2008: Crossing Borders.

293. Saad, M., El-Enein, S. A. A., Hanna, G. B. and Kotkata, M. F. (1996), "Effect of temperature on physical and mechanical properties of concrete containing silica fume", Cement and Concrete Research, 26 (5), pp. 669-675.

294. Saatcioglu, M. and Razvi, S. R. (1992), "Strength and ductility of confined concrete", Journal of Structural Engineering ASCE, 118(6), pp. 1590-1607.

295. Saatcioglu. M, Ozbakkaloglu. T and Elnabelsy. G, (2008) "Seismic behaviour and design of reinforced concrete columns confined with FRP stay-in-place formwork. ACI Structural Journal, 257(09): 149-170.

296. Saadatmanesh, H., and Ehsani, M. R. (1991). "RC beams strengthened with GFRP plates. I: Experimental study." Journal of Structural Engineering, 117(11), 3417-3433.

297. Sargin, M. (1971), "Stress-strain relationship for concrete and analysis of structural concrete sections", Study No.4, Solid Mech. Div. University of Water Loo On, Canada, pp.167.

298. Schneider U, editor, RILEM, (1985), "Properties of material at high temperature: Concrete" Germany: Department of Civil Engineering, University of Kassel, 131 pp.

299. Schneider, U. (1985), "Properties of material at high temperatures-concrete", RILEM-Committee 44-PHT, Department of Civil Engineering, University of Kassel.

300. Schneider, U. (1990) "Repairability of fire damaged structures," CIB W14 Rep., Fire Safety Journal.

301. Scott, D. W., Lai, J. S., and Zureick, A. H. (1995). "Creep behavior of fiber-reinforced polymeric composites: a review of the technical literature." Journal of Reinforced Plastics and Composites, 14(6), 588-617.

302. Seshu, D. R. (2000). "Flexural Behaviour of Ferrocement Confined Reinforced Concrete (FCRC) Simply Supported Beams", Journal of Ferrocement. 30(3): 261-274.

303. Sezen, H., Asce, M., & Miller, E. A., (2011),"Experimental Evaluation of Axial Behavior of Strengthened Circular Reinforced-Concrete Columns". Journal of Bridge Engineering, 16(2), 238-247.

304. Shannag, M.J., (2002), "High-Performance Cementitious Grouts for Structural Repair". Cement and Concrete Research, 2002, 32, 803-808.

305. Shannag. M.J and Alhassan, M. A. (2005). "Seismic Upgrade of Interior Beam-Column Sub assemblages with High-Performance Fiber-Reinforced Concrete Jackets" ACI Structural Journal, 102, 1, pp. 131-138

306. Sheikh. S. A, and Li, Y, (2006). "Design of FRP confinement for square concrete columns". Engineering Structures 29, pp. 1074–1083.

307. Sheikh. S. A, (2002). "Performance of concrete structures retrofitted with fibre reinforced polymers". Engineering Structures, 24(7): 869-879.

308. Sheikh, S. A. and Toklucu, M. A. (1993), "Reinforced concrete columns confined by circular spirals and hoops", ACI Structural Journal, 90(5), pp. 542-553.

309. Sideris, K. K., Manita P. and Chaniotakis, E. (2009), "Performance of thermally damaged fibre reinforced concretes", Construction and Building Materials, 23, pp. 1232-1239.

310. Singh K. K and Kaushik S. K (1997), "Behaviour of Ferrocement Composite Columns in Compression", ACI International Conference on High Performance Concrete, design and Materials and recent advances in concrete technology.

311. Skazlic. M, Bjegovic. D. and Serda. M. (2009). "Utilization of high performance fiber-reinforced micro-concrete as a repair material" Concrete Repair, Rehabilitation and Retrofitting II – Alexander et al. pp 859-862.

312. Sorelli, L., Meda, A., Plizzari, G., Rossi, B. (2004): "Experimental investigation of slabs on grade: steel fibres vs. conventional reinforcement", in 6th Rilem Symposium on Fibre Reinforced Concrete (BEFIB 2004), pp. 1083-1093.

313. Spadea, G., Bencardino, F. and Swamy, R. N., (1998) "Structural Behavior of Composite RC Beams with Externally Bonded CFRP," Journal of Composites for Construction, ASCE, 2(3), pp. 132-137.

314. Subhash C. Yaragal., Babu Narayan K. S., and Adari S. (2012) "Strength characteristics of concrete exposed to elevated temperatures and cooled under different regimes", International Journal of Structural Fire Engineering, United Kingdom, 3, 4, pp.301-310

315. Suresh, N. (2002), "Flexural Strength of Concrete subjected to sustained elevated temperature", Indian Concrete Institute Journal, India.

316. Swamy R. N., and Jones R. (1980)." Behaviour of plated reinforced concrete beams subjected to cyclic loading during glue hardening" The International Journal of Cement Composites. 2(4), pp. 233-234.

317. Swamy R. N., Jones R. and Bloxham J. W., (1987). "Structural Behaviour of reinforced concrete beams strengthened by epoxy bonded steel plates." The Structural Engineer. 65(2).

318. Takeuchi, M., Hiramoto, M., Kamagai, N., Yamazaki, N., Kodaira, A. and Sugiyama (1993), "Material properties of concrete and steel bars at elevated temperatures" SMiRT-12/K. Kussmaul (Editor), Elsever Science Publishers B.V. H04/4, pp. 133-138.

319. Takiguchi, K. and Abdullah (2000). "Experimental Investigations on Ferrocement as an Alternative Material to Strengthen Reinforced Concrete Columns". Journal of Ferrocement. 30(2): 177-190.

320. Takiguchi K and Abdullah, (2001), "Shear Strengthening of Reinforced Concrete Columns using Ferrocement Jackets". ACI Structural Journal, 98(5): 696–704.

321. Takeda, K., Mitsui, Y., Murakami, K., Sakai, H., and Nakamura, M. (1996). "Flexural behaviour of Reinforced Concrete Beams Strengthened with Carbon Fiber Sheets." Composites Part (A), 27, 981-987.

322. Taljsten B., (1990). "Strengthening of concrete structures by adhesively bonded steel plates external bonded reinforcement." TULEA 06, pp 212.

323. Täljsten B., 1997, "Strengthening of Beams by Plate Bonding", Journal of Materials in Civil Engineering, November 1997, pp. 206-212.

324. Täljsten B. FRP Strengthening of Existing Concrete Structures, Design Guidelines. Luleå University Printing Office: Luleå, Sweden, 2002

325. Talukdar. S., and Borsaikia A., (2005), An assessment of the progrssive failure of concrete using pulse velocity measurements", Indian Concrete Journal,79 (2), February, pp 61-64.

326. Tao, Z, and Yu, Q. (2008). Behaviour of CFRP-strengthened slender square RC columns. Magazine of Concrete Research, 60(7): 523-533.

327. Teng J. G, Chen J. F, Smith S. T, Lam L. (2002). "FRP Strengthened RC Structures", John Wiley & Sons Ltd, UK.

328. Teng, J. G., Lam, L., and Chen, J. F. (2004). "Shear strengthening of RC beams with FRP composites." Progress in Structural Engineering and Materials, 6(3), 173-184.

329. Terro, M. J. and Hamoush, S. A. (1997), "Effect of confinement on siliceous aggregate concrete subjected to elevated temperatures and cyclic heating", ACI Materials Journal, 94(2), pp. 83-89.

330. Tim J Stratford, Martin Gillie, Chen J. F, Usmani A.S.,(2009). "Bonded fibre reinforced polymer strengthening in a real fire" Advances in Structural Engineering ,12,6, 867-878.

331. Toutanji, H. A., and Gomez, W. (1997). "Durability characteristics of concrete beams externally bonded with FRP composite sheets." Cement and Concrete Composites, 19(4), 351-358.

332. Toutanji, H. A., (1999) "Stress-Strain Characteristics of Concrete Columns Externally Confined with Advanced Fiber Composite Sheets", ACI Materials Journal, Vol. 96, No. 3, pp. 394-404.

333. Tucker. D. M. and Read. R. E. H, (1981). "Assessment of fire-damaged structures. BRE Information Paper IP 24/81, Building Research Establishment, Watford.

334. Turgay. T, Polat. Z, Koksal. H. O, Doran. B and Karakoc. C, (2010), "Compressive behavior of large-scale square reinforced concrete columns confined with carbon fiber reinforced polymer jackets". Materials and Design 2010; 31(8): pp.357–364.

335. Triantafillou, T. C. (1998). "Strengthening of structures with advanced FRPs." Progress in Structural Engineering and Materials, 1(2), 126-134.

336. Tsonos. G. A, (2008). "Effectiveness of CFRP-jackets and RC-jackets in post-earthquake and pre-earthquake retrofitting of beam-column sub assemblages". Engineering Structures, 30(3): 777-793.

337. Udaya Kumar, P. M. V.., Raju, M. P., and Rao, K. S. (2009). "Performance of repaired fire affected RC beams". *Current Science*, *96*(3), 398-402.

338. Ueda Dai, J., T., Sato, Y. (2005). "Development of the nonlinear bond stress-slip model of fiber reinforced plastics sheet-concrete interfaces with a simple method." Journal of Composites for Construction, 9(1), 52-62

339. Usmani, A. S., Rotter, J. M., Lamont, S., Sanad, A.M. and Gillie, M. (2001), "Fundamental principles of structural behaviour under thermal effects", Fire Safety Journal. 36, pp. 721-744.

340. Van Gemert D. and Van Den Bosch M., (1983). "Renovation of reinforced concrete structures by epoxy bonded steel plates, Proceeding International Kolloqium, pp 237-243.

341. Van Gemert D. (1990). "Force transfer in epoxy bonded steel/ concrete joints". International Journal Adhesion and Adhesives, pp 67-73.

342. Vidya Sagar. R., Raghu Prasad B.K., Singh R.K., (2013) "Laboratory Investigations on Concrete Fracture Using Acoustic Emission Technique" VIII International Conference on Fracture Mechanics of Concrete and Concrete Structures FraMCoS-8

343. Walliuidin A. M & Rafeeqi S. F. A (1994), "Study of Behaviour of Plain Concrete Confined with Ferrocement", Journal of Ferrocement, 24(2): 139–145

344. Wang, H., Zha, X. and Ye, J., (2009), "Fire Resistance Performance of FRP Rebar Reinforced Concrete Columns", International Journal of Concrete Structures and Materials Vol.3, No.2, pp. 111-117.

345. Wang, Y. C., and Hsu, K. (2009). "Design recommendations for the strengthening of reinforced concrete beams with externally bonded composite plates." Composite Structures, 88(2), 323-332.

346. Wang. Y. C, Hsu. K, (2008). "Design of FRP-wrapped reinforced concrete columns for enhancing axial load carrying capacity. Composite Structures Composite Structures 2008; 82(1): p. 132-139.

347. Williams, B., Bisby, L., Kodur, V. K. R., Green, M., and Chowdhury, E. (2006). "Fire insulation schemes for FRP-strengthened concrete slabs." Composites Part A, 37(8), 1151-1160

348. Williams, B., Kodur, V. K. R., Green, M. F., and Bisby, L. (2008). "Fire endurance of fiber-reinforced polymer strengthened concrete T-Beams." ACI Structural Journal, 105(1), 60-67.

349. Woo. S. K and Yen Lee, (2010). "Experimental study on Interfacial behavior of CFRP – bonded concrete". KSCE journal of Civil Engineering, 14, 385- 393

350. Wu, B., Su, X. P., Li, H. and Yuan, J. (2002), "Effects of high temperature on residual mechanical properties of confined and unconfined high strength concrete", ACI Material Journal, pp. 399-407.

351. Wu Y. F, Yan J. H, Zhou Y. W, Xiao Y. (2010). "Ultimate strength of reinforced concrete beams retrofitted with hybrid bonded fiber-reinforced polymer", ACI structural journal, 107(4): 451-460.

352. Wu, Z. S., Iwashita, K., Yagashiro, S., Ishikawa, T., and Hamaguchi, Y."(2005). "Temperature effect on bonding and debonding behavior between FRP sheets and concrete." Journal Social. Material. Science, 54(5), 474 –480.

353. Xanthakos, P.P., (1996), "Bridge strengthening and rehabilitation". Prentice-Hall, Eaglewood Cliffs, N.J.

354. Xiong, G. J., Wu, X. Y., Li, F. F., & Yan, Z., (2011), "Load carrying capacity and ductility of circular concrete columns confined by ferrocement including steel bars". Construction and Building Materials, 25, 2263–2268.

355. Xiao. J., Jie Li and Quanfan Zha. (2004). "Experimental study on bond behavior between FRP and concrete" Construction and Building Materials 18, 745–752.

356. Yang, X., and Nanni, A. (2002). "Lap Splice Length and Fatigue Performance of FRP Laminates." ACI Materials Journal, 99(4), 386-392.

357. Yao J, Teng J. G, Chen J. F. (2005). "Experimental study on FRP-to-concrete bonded joints. Composites: Part B, 36: 99-113.

358. Yaqub, M., & Bailey, C. G., (2011) "Repair of fire damaged circular reinforced concrete columns with FRP composites". Construction and Building Materials, 25(1), 359-370.

359. Yaqub, M., Bailey, C. G., Nedwell, P., Q.U.Z. Khan, Q.U.Z., & Javed, I., (2013) "Strength and stiffness of post-heated columns repaired with ferrocement and fibre reinforced polymer jackets", Composites: Part B, 44, 200–211

360. Yaqub, M., & Bailey, C. G., (2011), "Cross sectional shape effects on the performance of post-heated reinforced concrete columns wrapped with FRP composites. Composite Structures, 93(3), 1103-1117.

361. Yaqub, M., Bailey, C. G., & Nedwell, P., (2011), "Axial capacity of post-heated square columns wrapped with FRP composites. Cement and Concrete Composites", 33(6), 694-701.

362. Youssef, M.A. and Moftah, M. (2007), "General stress-strain relationship for concrete at elevated temperatures", Engineering Structures, 29, pp. 2618-2634.

363. Yousef. A, Salloum.Al, (2007) "Influence of edge sharpness on the strength of square concrete columns confined with FRP composite laminates. Composites Part B: Engineering 2007; 640-650(5-6): p. 38.

364. Yuan, H., Wu, Z., and Yoshizawa, H. (2001). "Theoretical Solutions on Interfacial Stress Transfer of Externally Bonded Steel/Composite Plates, Journal Structural. Mechanism Earthquake Engineeering. 18(1), 27-39.

365. Yuan H, Teng J. G, Seracino R, Wu Z. S and Yao J. (2004). "Full-range behavior of FRP-to-concrete bonded joints. Enginerering Structures, 26(5): 553-564.

366. Zaidi, K.A., Sharma, U.K. and Bhandari, (2012), "Effect on uni-axial compressive behaviour of confined concrete" Fire Safety Journal, V. 48, pp. 58-68.

367. Zaidi, S.K.A (2011), "Residual compressive behaviour of confined concrete subjected to elevated temperature", Ph.D. Thesis, Department of Civil Engineering, Indian Institute of Technology Roorkee, Roorkee, India, 219pp.

368. Zhang, B. (2011), "Effect of moisture evaporation (weight loss) on fracture properties of high performance concrete subjected to high temperatures", Fire Safety Journal, V. 46, pp. 543-549.

369. Zhang, Z., Hsu, C. T. T., and Moren, J. (2004). "Shear strengthening of reinforced concrete deep beams using carbon fiber reinforced polymer laminates." Journal of Composites for Construction, 8, 403.

LIST OF PUBLICATIONS

1. Danie Roy, A.B., Sharma, U.K., & Bhargava, P., Strengthening of Heat Damaged Reinforced Concrete Cylinders, International Conference on Applications of Structural Fire Engineering. Prague, 19-20 April 2013.pp 486-492

2. Danie Roy, A.B., Sharma, U.K., & Bhargava, P A Study on Different Techniques of Restoration of Heat Damaged R.C. Beams. 8th International Conference on Structures in Fire, Shanghai, China, June 11-13, 2014, pp 1015-1022.

3. Danie Roy, A.B., Sharma, U.K., & Bhargava, P, Behavior of Square And Circular Heat Damaged Reinforced Concrete Column Strengthened With Different Composites Tested Under Axial Compression. The 8th International Conference on Asian Concrete Federation, Seoul, Korea, September 17-19, 2014.

4. Danie Roy, A.B., Sharma, U.K., & Bhargava, P., Strengthening of Heat Damaged Reinforced Concrete Short Columns, Journal Structural Fire Engineering.5 (4), pp. 381-398.

5. Danie Roy, A.B., Sharma, U.K., & Bhargava, P., Confinement Strengthening of Heat Damaged Reinforced Concrete Short Columns, Construction & Building Materials. (Under Review)